



University of Kentucky  
UKnowledge

---

Theses and Dissertations--Chemistry

Chemistry

---

2017

## TOWARDS THE TOTAL SYNTHESIS OF 7-EPI-CLUSIANONE

Shubhankar Dutta

University of Kentucky, sdu224@uky.edu

Digital Object Identifier: <https://doi.org/10.13023/ETD.2017.266>

[Right click to open a feedback form in a new tab to let us know how this document benefits you.](#)

---

### Recommended Citation

Dutta, Shubhankar, "TOWARDS THE TOTAL SYNTHESIS OF 7-EPI-CLUSIANONE" (2017). *Theses and Dissertations--Chemistry*. 79.

[https://uknowledge.uky.edu/chemistry\\_etds/79](https://uknowledge.uky.edu/chemistry_etds/79)

This Doctoral Dissertation is brought to you for free and open access by the Chemistry at UKnowledge. It has been accepted for inclusion in Theses and Dissertations--Chemistry by an authorized administrator of UKnowledge. For more information, please contact [UKnowledge@lsv.uky.edu](mailto:UKnowledge@lsv.uky.edu).

## **STUDENT AGREEMENT:**

I represent that my thesis or dissertation and abstract are my original work. Proper attribution has been given to all outside sources. I understand that I am solely responsible for obtaining any needed copyright permissions. I have obtained needed written permission statement(s) from the owner(s) of each third-party copyrighted matter to be included in my work, allowing electronic distribution (if such use is not permitted by the fair use doctrine) which will be submitted to UKnowledge as Additional File.

I hereby grant to The University of Kentucky and its agents the irrevocable, non-exclusive, and royalty-free license to archive and make accessible my work in whole or in part in all forms of media, now or hereafter known. I agree that the document mentioned above may be made available immediately for worldwide access unless an embargo applies.

I retain all other ownership rights to the copyright of my work. I also retain the right to use in future works (such as articles or books) all or part of my work. I understand that I am free to register the copyright to my work.

## **REVIEW, APPROVAL AND ACCEPTANCE**

The document mentioned above has been reviewed and accepted by the student's advisor, on behalf of the advisory committee, and by the Director of Graduate Studies (DGS), on behalf of the program; we verify that this is the final, approved version of the student's thesis including all changes required by the advisory committee. The undersigned agree to abide by the statements above.

Shubhankar Dutta, Student

Dr. Robert B. Grossman, Major Professor

Dr. Mark A. Lovell, Director of Graduate Studies

TOWARDS THE TOTAL SYNTHESIS OF 7-*EPI*-CLUSIANONE

---

DISSERTATION

---

A dissertation submitted in partial fulfilment of the requirements for the degree of  
Doctor of Philosophy in the College of Arts and Sciences at the University of Kentucky

By  
Shubhankar Dutta  
Lexington, Kentucky

Director: Dr. Robert B. Grossman, Professor of Chemistry  
Lexington, Kentucky  
2017

Copyright © Shubhankar Dutta 2017

## ABSTRACT OF DISSERTATION

### TOWARDS THE TOTAL SYNTHESIS OF 7-*EPI*-CLUSIANONE

Polycyclic polyprenylated acylphloroglucinols (PPAPs) are plant- (Guttiferae) derived natural products. They have fascinating bicyclo[3.3.1]nonane-2,4,9-trione or [3.2.1]nonane-2,4,8-trione cores decorated with prenyl or geranyl groups. More than 200 PPAPs have been isolated, but only a few of them have been synthesized, although most of the synthesized PPAPs are of type A and have an exo substituent at C (7). Here, we are trying to make a type B 7-endo PPAP, 7-*epi*-clusianone. The synthetic plan involves an alkynylation–aldol strategy to construct the bicyclic core. Having established the bicyclic core, the synthesis presents a new challenge: the oxidation of a very hindered 2-alkenone to the  $\beta$ -hydroxy 2-alkenone.

**KEYWORDS:** Polycyclic polyprenylated acylphloroglucinols, 7-*epi*-clusianone, bicyclo[3.3.1]nonane, 2-alkenone,  $\beta$ -hydroxy 2-alkenone

---

Shubhankar Dutta

---

07/10/2017

---

TOWARDS THE TOTAL SYNTHESIS OF 7-*EPI*-CLUSIANONE

By

Shubhankar Dutta

Dr. Robert B. Grossman

---

Director of Dissertation

Dr. Mark A. Lovell

---

Director of Graduate studies

07/10/2017

---

Date

Dedicated to My Mother, Sumita Dutta

## Acknowledgements

Born in a family of lawyers, where every household member is destined to become a gen-next lawyer to carry forward the legacy of the family business, a ‘renegade’ appeared—who never thought of studying in the United States, let alone dreaming about a Ph.D. in Chemistry. I owe this incredible feat to some extraordinary people, or perhaps better to say some pristine minds, who have left an impression on me.

First and foremost, I shall start with Dr. Robert B. Grossman, my research advisor, whom I admire and thank for providing me with the opportunity to research in his group. He gave me hope and restored my confidence that I could be a research scientist when my career hit rock-bottom. His stoic endurance has always spellbound me and he never discouraged me from discussing ideas, no matter how puerile they may be. In many ways, he is, I believe, reminiscent of great Napoléon, who once said, there are no bad soldiers, only bad generals.

I express my sincere gratitude to my committee member, Dr. Cammers, who always inspired me to push the boundaries of knowledge. Dr. Selegue and Dr. Röhr from the UK College of Pharmacy have always enriched my knowledge by offering insightful thoughts during committee meetings and discussions. I cordially thank them for accepting my request to be on my research committee. John Layton and Art Sebesta are the other two pillars of my research. John always helped me understand NMR, while Art has provided me with assistance fixing the instruments in the lab, even on Saturdays. Dr. Patwardhan was instrumental in guiding me through difficult times. Thank you, Dr. Patwardhan.

My friends at UK also deserve credit. Subbu, Aman, Nikhil, and Rahul have always ‘tolerated’ me and helped me to grow as a scientist. I am grateful to them. I am also grateful to my lab mates, especially Meenakshi for her support and encouragements.

Life is full of subtle moments, and each moment tells a story that might not have a logical conclusion at the time when it was told, but it altered my course. I solemnly bow my head to those people who were the center of those moments. Dr. Subhabrata Sen was one of such persons who laid the ‘seed’ for me to pursue a Ph.D. Without him, I could not have reached the US to continue my journey as a student. Dr. Debasis Chakraborty was instrumental in nurturing the plant that sprouted from that early seed. I am grateful to the late Bires Chandra Bose, whom I revered because of his memory and command of English literature. He would be happy today to know that I have written 250 pages of a dissertation in English, which is not my native language. And I am thankful to all those teachers who have enlightened my young mind in times of confusion.

Here, I cannot forget Debiprasad Chakraborty who compelled me to switch to Chemistry from English for some unknown reason. Now, I feel that it was ‘destined’ to happen—a term scientists always have avoided. My math teacher, Paresh Govinda Sinha, needs a special mention since he sent an application form for Chemistry for me, and I did not know that fact. And Chand aunt, who is no more, used to be a tutor till my seventh grade and subconsciously taught me that there is no alternative to hard work.

Charity begins at home, the adage says. Everyone has first teachers in the form of parents. My mother, Sumita Dutta, is my first teacher who has been the bedrock of my character, ever since I got a conscience. She did not complete her bachelor's, but she always surprises me with her intellect and poses to me a question—what does education mean? My father, Soumyen Dutta, has been a great teacher without losing his temper—keeping his calm in dire situations indicating how astute a lawyer he is, and teaching me how to live a peaceful life. He always tells me how to fight back after a defeat. Without my parents'



support, I could not be here. My only little sister, Soumi, has supported me through these years by taking care of my parents. I am very much thankful to her.

Last but not least, Sayantani Guha, my wife, my lady love, I say, thank you for your unconditional support. She has suffered the most because of me, a capricious husband, and it was not easy to take care of a graduate student like me, although she has never complained about it. Thank you.

## Table of Contents

Acknowledgements.....	iii
List of Figures.....	x
List of Tables.....	xii
List of Schemes.....	xiii
1 Introduction to natural products.....	18
1.1 Introduction.....	18
1.2 Introduction to PPAPs.....	20
1.3 Classification of PPAPs.....	22
1.4 History of PPAPs.....	24
1.5 Revisiting some structures of type B endo PPAPs.....	29
1.6 Biosynthesis of MPAPs.....	34
1.7 Biosynthesis of PPAPs.....	38
1.8 Sources and structures of type B endo PPAPs.....	42
1.9 Medicinal properties of type B endo PPAPs.....	50
1.9.1 Garcinol and its derivatives.....	51
1.9.2 Guttiferone A-F, K, O, P.....	53
1.9.3 Clusianone and 7- <i>epi</i> -clusianone.....	56
1.9.4 Coccinones A-H.....	60
1.9.5 Symphonones A-I.....	61
1.10 SAR (structure-activity relationship) studies in type B PPAPs.....	61
2 Synthetic endeavors towards type B endo-PPAPs.....	65
2.1 Introduction.....	65
2.2 Some newer synthetic strategies for constructing bicyclo [3.3.1] nonane.....	67

2.2.1	Annulation approach of allenyl sulphonate esters to make bicyclo nonane by Bhat et al.	67
2.2.2	Metathesis-acylation approach to construct bicyclo [3.3.1] nonane.....	70
2.3	Domino Michael-aldol approach by Alexakis .....	72
2.4	Syntheses of (+)-30- <i>epi</i> , (-)-6- <i>epi</i> , and (±)-6,30- <i>diepi</i> -13,14-didehydroxyisogarcinol by Porco et al.....	74
2.4.1	Retrosynthetic analysis of <i>epi</i> -didehydroxyisogarcinols .....	76
2.5	Synthesis of (+)-6- <i>epi</i> , (+)-30- <i>epi</i> -13, 14-didehydroxyisogarcinols .....	78
2.6	Total synthesis of natural analogs of (+)-clusianone by Coltart et al.....	82
2.7	Total synthesis of (±)-hyperforin by Shair .....	85
2.8	Biomimetic approach to hyperforin by Maimone .....	89
2.9	Hyperforin and papuaforin A-C, and formal synthesis of nemorosone by Barriault et al.	93
2.9.1	Retrosynthetic approach of Barriault .....	94
2.9.2	Synthesis of hyperforin, nemorosone, and papuaforin A-C by Barriault et al. ....	96
2.10	Total synthesis of 7- <i>epi</i> -nemorosone by Porco .....	100
2.11	Plietker's divergent approach for the total syntheses of type B endo PPAPs .....	104
2.11.1	Synthesis of 7- <i>epi</i> -clusianone, oblongifolin, hyperibone L, hyperpapuanone, and regio-hyperpapuanone.....	104
2.11.2	Retrosynthetic analysis of type B endo PPAPs .....	105
2.11.3	Total synthesis of 7- <i>epi</i> -clusianone .....	106
2.12	Total synthesis of oblongifolin.....	110
2.13	Total synthesis of hyperpapuanone .....	111
2.14	Total synthesis of hyperibone L and regio-hyperpapuanone .....	112
2.15	Total syntheses of sampsonione P and hyperibone I by Plietker et al. ....	114
2.15.1	End of synthesis of sampsonione P .....	117
2.15.2	End of the synthesis of hyperibone I .....	118
2.16	Total syntheses of guttiferone A and 6- <i>epi</i> -guttiferone A by Plietker et al. ....	119

2.16.1	Retrosynthetic approach of guttiferone A and 6- <i>epi</i> -guttiferone A.....	120
2.16.2	Synthesis of 6- <i>epi</i> -guttiferone A .....	121
2.16.3	Synthesis of guttiferone A .....	123
2.17	Total synthesis of garcinol and isogarcinol.....	126
2.18	Grossman's approach to the synthesis of PPAPs .....	131
3	Our strategy for 7- <i>epi</i> -clusianone .....	134
3.1	Introduction .....	134
3.2	Initial retrosynthetic strategy.....	135
3.3	Synthesis of 7- <i>epi</i> -clusianone .....	136
3.4	Revised retrosynthetic strategy .....	137
3.5	Enol ether formation and allylation followed by methylation .....	138
3.6	Methylation and hydrolysis .....	139
3.7	Synthesis of $\beta$ -keto ester .....	139
3.8	Allylation and enol ether synthesis .....	140
3.9	Determination of stereochemistry of major diastereomer .....	142
3.10	Conversion of ester to aldehyde .....	147
3.11	Alkynylation and allyl–methyl exchange.....	147
3.12	Carboxymethylation and reduction .....	149
3.13	Claisen rearrangement and oxidation of alcohol.....	151
3.14	Stereoselective reduction of alkynal to <i>Z</i> -alkenal, and intramolecular aldol reaction	151
3.15	Oxidation of C4 in bicyclo[3.3.1]nonane: a dilemma or enigma? .....	154
3.16	Plan for the oxidation of C4 in 310 .....	154
3.16.1	Desaturation followed by oxidation .....	154
3.16.2	Reduction and enol ether formation followed by oxidation .....	156
3.16.3	Epoxidation and nucleophilic ring opening.....	162
3.16.4	Conjugate addition–oxidation .....	163

3.17	New plan for C4 oxidation .....	163
3.18	The revised plan for oxidation of C4 .....	164
3.18.1	Hydrosilylation and C–H activation .....	168
3.19	Co-promoted hydrosilylation .....	170
	Experimental .....	172
	Conclusion .....	181
	Appendix .....	182
	References .....	197
	Vita .....	209

## List of Figures

Figure 1.1.1. Some important natural products.....	19
Figure 1.1.2. % Natural products/year (the figure has been taken from Newman and Cragg's recent article). <sup>13</sup> .....	20
Figure 1.2.1. Representative PPAP .....	21
Figure 1.3.1. Core structures of PPAPs .....	22
Figure 1.3.2. Classification of PPAPs.....	23
Figure 1.3.3. Unusual PPAPs.....	24
Figure 1.4.1. History of some PPAPs .....	26
Figure 1.4.2. Clusianone and 7- <i>epi</i> -clusianone.....	28
Figure 1.4.3. Lalibinones A-E and laxifloranone .....	29
Figure 1.5.1. Structural diversity among PPAPs .....	30
Figure 1.5.2. Structural conundrum: guttiferone E and isoxanthochymol.....	31
Figure 1.5.3. Guttiferones I and G .....	33
Figure 1.5.4. hyperibone I and sampsonione P .....	34
Figure 1.6.1. Diverse arrays of PPAPs from benzophenone.....	35
Figure 1.6.2. $\alpha$ and $\beta$ -acids.....	37
Figure 1.9.1. Garcinol and derivatives .....	52
Figure 1.9.2. Guttiferones A, E, C, D .....	54
Figure 1.9.3. Mechanism of transcription regulation by LXR triggered by guttiferone I <sup>88</sup> .....	56
Figure 1.9.4. Diagram for cell death mechanism induced by guttiferone A.....	56
Figure 1.9.5. Clusianone and 7- <i>epi</i> -clusianone.....	57
Figure 1.9.6. Possible mechanism of action of clusianone .....	60

Figure 1.10.1. Structure activity relationship of PPAPs .....	63
Figure 2.3.1. PPAPs family having bicyclo [3.2.1] octane cores .....	72
Figure 2.3.2. Bifunctional catalysts .....	74
Figure 2.4.1. Several target didehydroxyisogarcinols .....	75
Figure 2.5.1. Transition state model for cyclization .....	81
Figure 2.9.1. Target molecules for Barriault's group .....	94
Figure 2.11.1. Rationale for diastereoselection of allylic substitution .....	109
Figure 2.11.2. Dieckman condensation to construct the bicyclo [3.3.1] nonane .....	109
Figure 2.13.1. Hyperpapuanone, regio-hyperpapuanone, and 7- <i>epi</i> -clusianone .....	111
Figure 2.15.1. Sampsonione P and hyperibone I .....	115
Figure 2.16.1. Substrate similarity comparison .....	119
Figure 2.17.1. Garcinol and isogarcinol.....	127
Figure 3.8.1 Transition state model for the diastereoselectivity.....	142
Figure 3.9.1. <sup>1</sup> H NMR spectrum of 325 in C <sub>6</sub> D <sub>6</sub> .....	143
Figure 3.9.2. COSY spectrum of 325 .....	145
Figure 3.9.3. NOESY spectrum of 325 .....	146
Figure 3.9.4 NOE interactions in 325 and <i>epi</i> -325 .....	147
Figure 3.12.1. X-ray Structure of 329B .....	150
Figure 3.14.1. Possible intermediate in syn reduction .....	152
Figure 3.14.2. Bicyclic structure of 310 .....	154
Figure 3.16.1. Crystal structure of 343 .....	160
Figure 3.19.1 H NMR of 343.....	182
Figure 3.19.2 C NMR of 343.....	183

## List of Tables

Table 1.3.1. List of earlier works on <i>Garcinia mangosta</i> .....	25
Table 1.5.1. Different $\alpha$ -acids and $\beta$ -acids.....	37
Table 1.7.1. Type B endo PPAPs.....	42
Table 1.8.1. Bioactivity of guttiferone A against different virus.....	53
Table 1.8.2. IC <sub>50</sub> values on different cell lines of guttiferone F.....	55
Table 1.8.3. Cytotoxicity against cancer cell lines.....	58
Table 1.8.4. Biological activity of coccinones A-H.....	61
Table 2.2.1. Substrate Scope for annulation.....	68



## List of Schemes

Scheme 1.5.1. Biosynthesis of MPAPs.....	36
Scheme 1.5.2. Synthesis of $\alpha$ and $\beta$ -acids from MPAP .....	37
Scheme 1.6.1. Precursors to type A, B, and C PPAPs .....	39
Scheme 1.6.2. Mechanistic pathway for type A, B and C .....	40
Scheme 1.6.3. Mechanistic rationale for two unusual PPAPs .....	41
Scheme 2.2.1. Synthesis of bicyclo[3. <i>n</i> .1]nonane by Bhat et al. ....	68
Scheme 2.2.2. Mechanism of annulation strategy .....	69
Scheme 2.2.3. Retrosynthetic analysis of bicyclo[3.3.1]nonane by Schmitt et al. ....	70
Scheme 2.2.4. Synthesis of bicyclo [3.3.1] nonane by Schmitt et al. ....	71
Scheme 2.2.5. Modified approach to bicyclononane by Schmitt .....	72
Scheme 2.3.1. Synthetic scheme for domino Michael–aldol reaction by Alexakis et al. ..	73
Scheme 2.3.2. Probable mechanism for domino Michael–aldol reaction.....	73
Scheme 2.4.1. Retrosynthetic analysis of (–)-6- <i>epi</i> and (+)-30- <i>epi</i> -13,14- didehydroxyisogarcinols .....	76
Scheme 2.4.2. Syntheses of bisalkylated didehydrobenzopyrans .....	78
Scheme 2.5.1. Finishing the total synthesis of (+)-6- <i>epi</i> - and 30- <i>epi</i> -13,14- didehydroxyisogarcinol.....	80
Scheme 2.5.2. By-product formation .....	82
Scheme 2.6.1. Retrosynthesis of (+)-clusianone by Coltart.....	83
Scheme 2.6.2. Synthesis using enantioselective alkylation .....	83
Scheme 2.6.3. Finishing the total synthesis of (+)-clusianone .....	84
Scheme 2.7.1. Retrosynthetic analysis of hyperforin by Shair’s group .....	85
Scheme 2.7.2. Matt Shair’s biomimetic approach .....	86

Scheme 2.7.3. Hyperforin synthesis by Shair .....	87
Scheme 2.7.4. The origin of diastereoselectivity .....	88
Scheme 2.7.5. Finishing synthesis of hyperforin by Shair et al.....	89
Scheme 2.8.1. Retrosynthesis of hyperforin by Maimone .....	90
Scheme 2.8.2. Synthesis of hyperforin by Maimone .....	91
Scheme 2.8.3. Proposed mechanism of oxidative rearrangement .....	92
Scheme 2.9.1. Synthesis of PPAP core by gold catalysis .....	95
Scheme 2.9.2. Retrosynthesis of type A PPAPs by Barriault .....	96
Scheme 2.9.3. Syntheses of the silyl ketones.....	97
Scheme 2.9.4. Synthesis of bromoalkyne for cyclization .....	98
Scheme 2.9.5. Finishing the total synthesis of nemorosone .....	99
<b>Scheme 2.9.6.</b> Finishing the syntheses of papuaforins A–C .....	100
Scheme 2.10.1. Retrosynthetic scheme of 7- <i>epi</i> -nemorosone by Porco.....	101
Scheme 2.10.2. Synthesis of 7- <i>epi</i> -nemorosone by Porco et al. ....	102
<b>Scheme 2.10.3.</b> The mechanism of formation of adamantane alcohol.....	102
<b>Scheme 2.10.4.</b> Mechanistic rationale for unusual rearrangement.....	103
<b>Scheme 2.10.5.</b> Finishing the synthesis of 7- <i>epi</i> -nemorosone .....	104
Scheme 2.11.1. Retrosynthetic analysis of Plietker’s synthesis of type B endo PPAP ...	106
Scheme 2.11.2. Synthesis of 7- <i>epi</i> -clusianone.....	107
Scheme 2.12.1. Synthesis of oblongifolin .....	110
Scheme 2.13.1. Synthesis of hyperpapuanone .....	112
Scheme 2.14.1. Synthesis of regio-hyperpapuanone and hyperibone L .....	113
Scheme 2.15.1. Retrosynthetic analysis of sampsonione P and hyperibone I .....	116
Scheme 2.15.2. Synthesis of sampsonione P and hyperibone I .....	117

Scheme 2.15.3. Syntheses of sampsonione P .....	118
Scheme 2.15.4. Finishing the synthesis of hyperibone I.....	119
Scheme 2.16.1. Retrosynthetic analysis of guttiferone A and 6- <i>epi</i> -guttiferone A .....	120
Scheme 2.16.2. Synthesis of 6- <i>epi</i> -guttiferone A .....	122
Scheme 2.16.3. Synthesis of 6- <i>epi</i> -guttiferone A .....	123
Scheme 2.16.4. Beginning of the synthesis of guttiferone A.....	124
Scheme 2.16.5. New diastereoselectivity problem in the synthesis of guttiferone A.....	125
Scheme 2.16.6. Synthesis of guttiferone A.....	126
Scheme 2.17.1. Retrosynthetic analysis of garcinol and isogarcinol.....	128
Scheme 2.17.2. Syntheses of garcinol and isogarcinol.....	129
Scheme 2.17.3. Stereochemistry of the exchange reaction.....	130
Scheme 2.17.4. Synthesis of isogarcinol .....	131
Scheme 2.18.1. Retrosynthetic analysis of nemorosone by Grossman et. al.....	132
Scheme 2.18.2. Model study by Grossman et al.....	133
Scheme 3.2.1. First retrosynthetic strategy.....	136
Scheme 3.3.1. A <sup>1,2</sup> -strain .....	137
Scheme 3.4.1. Revised retrosynthetic strategy for 7- <i>epi</i> -clusianone .....	138
Scheme 3.5.1. Synthesis of allyl enone 315.....	139
Scheme 3.6.1. Methylation and hydrolysis.....	139
Scheme 3.7.1. Synthesis of $\beta$ -ketoesters 318 and 318B .....	140
Scheme 3.8.1. <i>O</i> -allylation and Claisen rearrangement and enol ether synthesis .....	141
Scheme 3.10.1. Synthesis of aldehyde before alkynylation.....	147
Scheme 3.11.1. Synthesis of alkyne and <i>O</i> -allyl vinyl ether .....	148
Scheme 3.11.2. Mechanism of Colvin rearrangement.....	148

Scheme 3.12.1. One-carbon homologation–methoxycarbonylation.....	150
Scheme 3.13.1. Synthesis of the alkynal.....	151
Scheme 3.14.1. Reduction of alkynal to cis alkenal .....	152
Scheme 3.14.2. Synthesis of bicyclo[3.3.1]nonane via aldol reaction .....	153
Scheme 3.15.1. Ultimate roadblock to the success!.....	154
Scheme 3.16.1. Proposed synthetic scheme for the oxidation of C4 in 310.....	155
Scheme 3.16.2. Failed allylic transposition .....	156
Scheme 3.16.3. Strategy for C4 oxidation via Corey-Yu’s method .....	157
Scheme 3.16.4. Attempts to reduce the $\alpha$ , $\beta$ -unsaturated ketone in bicyclic enone 310..	158
<b>Scheme 3.16.5.</b> Trials for dissolved metal reduction .....	159
<b>Scheme 3.16.6.</b> An unusual reaction of <b>310</b> with Mg in methanol .....	160
Scheme 3.16.7. An alternate reaction mechanism for the bicyclo[4.3.0]nonane.....	161
Scheme 3.16.8. Mechanistic rationale for an unexpected rearrangement.....	161
Scheme 3.16.9. C4 oxidation: epoxidation and nucleophilic ring opening .....	162
Scheme 3.16.10. Addition of sulfur nucleophile to bicyclic enone .....	163
Scheme 3.17.1. Rationale for the failure of the oxidation at C4 in 310.....	164
Scheme 3.18.1. Addition of PhSH to 332.....	165
Scheme 3.18.2. Strategy for C4 oxidation via propanedithiol reaction .....	166
Scheme 3.18.3. Addition of 1,2 or 1,3-dithiol to alkynal .....	166
Scheme 3.18.4. Proposed mechanism for the deformylation of 332 .....	167
Scheme 3.18.5. Azidation and oxidation strategy for C4 oxidation .....	167
Scheme 3.18.6. Hydrosilylation–C–H activation route for C4 oxidation.....	168
Scheme 3.18.7. Attempts to hydrosilylate 332 with 2-pyridylsilane .....	170
Scheme 3.19.1. Co-promoted hydrosilylation of alkynal 332 with HSiEt <sub>3</sub> .....	170

Scheme 3.19.2. Co-promoted hydrosilylation with 2-pyridyldimethyl silane .....171

# 1 Introduction to natural products

## 1.1 Introduction

According to Wikipedia, natural products (NPs) are defined as compounds or substances that are produced by any living organism.<sup>1,2</sup> Scientifically speaking, however, secondary metabolites are referred to as NPs. Their source may come from plants, marine organisms, or animals. From the beginning of time, NPs have been the main source of sustenance for civilization. Moreover, the NPs enriched with medicinal properties, in particular—obtained from various plants, marine organism, and animals—have been fighting diseases over several millennia.<sup>3-5</sup> Mesopotamian inhabitants used to take clay tablets as medicines to cure several diseases 4000 years ago.<sup>4,6</sup> Ancient manuscripts found in India, China, and North Africa revealed that the inhabitants of those areas were aware of distinct medicinal properties of various plants. In early Egypt, scientists knew about the properties of different NPs that preserved mummies for ages without any decomposition. Those scientists most likely drew pictures of various usages of medicinal plants on the walls of pyramids.<sup>7</sup> From folklore, there were traditional medicines, which are still common in modern households, used to fight minor illnesses all over the world. For example, mandrake helps ease pain, turmeric is used as a medicine for lowering blood pressure, and garlic is used to reduce the cholesterols in blood. Likewise, a Chinese herb, artemisinin, also known as qinghaosu, has been used to treat malaria for ages. Youyu Tu won the Nobel Prize for medicine in 2015 for her discovery of this herb's usages. NPs not only aid in medicine but have also influenced civilizations across the globe. Because of them, some cities were built to cater the need of NPs for foreign traders. Romans and Greeks knew about one of the properties of red chilies in preserving meat from rotting. They sailed to Muziris port, now in Cochin, India, in search of red chilies. Indigo played a

significant role in the Peasant Movement in India back in 1870. Indigo, a plant that grows in mostly river deltas, was used for dyeing clothes and was in high demand by mills across England in the 1870s when the Industrial Revolution was at its peak. In other words, NPs have influenced human civilization in many ways, but most prominently, via medicinal benefits that are the primary source of their relevance today.

In the 19<sup>th</sup> century, when experimental science was making advances, Friedrich Sertürner, a 20-years old German chemist, first isolated morphine (1) from opium and studied its effects on humans and dogs (Figure 1.1.1).<sup>8</sup>

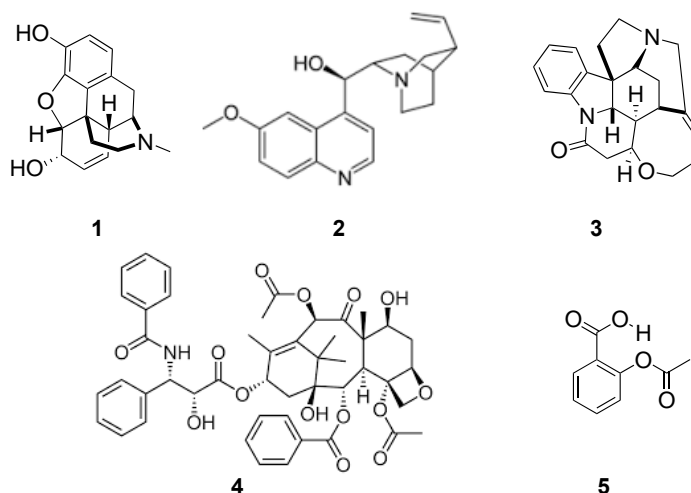


**Figure 1.1.1.** Some important natural products

Then it followed that other NPs were discovered such as atropine (2),<sup>9</sup> strychnine (3), a ‘Bitter Nemesis’,<sup>10</sup> and most recently, taxol (4).<sup>11</sup> The most common anti-inflammatory drug, aspirin (5), was derived from salicin, a natural product extracted from the bark of the willow tree. Even in the present age of chemical biology, NPs are still the best source of life-saving drugs and inspiration for the new drug molecules. Many pharmaceutical companies, however, have reduced their research on NPs because of HAT screening and combinatorial drug research. Despite that, since 1940, out of 175 anticancer drugs, 141

small molecules were either directly taken from NPs or inspired by NPs. From 1981 until now, 75% of the small molecules and anti-cancer drugs were directly related to NPs.<sup>12</sup> In 2010; twenty new drug molecules came to the market, and half of them were from NPs.<sup>13</sup> According to WHO report, 80% of the world's population still relies on plant-based materials for minor illnesses. Recently, Newman and Cragg published a review article in *J. Nat. Prod.*, where they presented 34 years of data showing that one-third of the prescribed drugs are directly related to NPs, which reiterates the point: NPs are still a source of major drug discovery (Figure 1.1.2).<sup>13</sup>

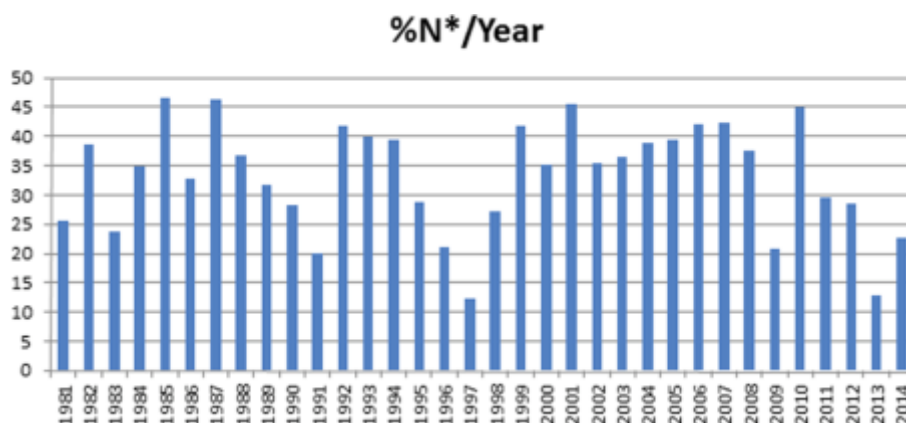


**Figure 1.1.2.** % Natural products/year (the figure has been taken from Newman and Cragg's recent article).<sup>13</sup>

## 1.2 Introduction to PPAPs

Plants from *Clusiaceae* (Guttiferae) and related families, namely, *Symphonia*, *Allanblackia*, *Ochrocarpos*, and *Moronobea*, are known for their traditional medicinal uses across the globe.<sup>14-16</sup> Since prehistoric times, people have been using these plants as a source of medicine for treatment of various diseases, like fever, diarrhea, and fungal infections. In general, Guttiferae plants are found all over the world, but in particular, in tropical regions. Fruits, flowers, and barks of the timber from this family of plants have been major sources in folklore medicine. Ancient Greeks used Saint John's wort (SJW) as



a remedy for depression. It was also effective in treating small burn and skin injuries.<sup>17</sup> SJW is a small- to medium-height herbaceous plant with yellow flowers. It is widespread in the northern part of Europe, and it is cultivated in North America. It is harvested and dried in late summer.

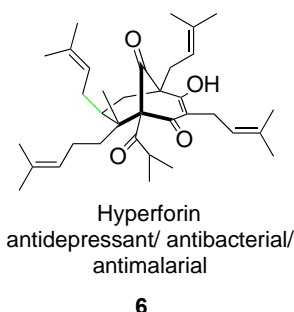


**Figure 1.2.1.** Representative PPAP

The dried herbs consist of a considerable number of phenolic derivatives of flavonoids, hypericin (about 0.1%) and pseudohypericin (about 0.2%). It is naphthodiathone, however, that is responsible for the antidepressant activity. The famous Greek philosopher, Aristotle, advised Spartans to use propolis—a complex material produced by honeybees, containing primarily wax and resins collected from different buds or plant secretions—to heal wounds. Aristotle probably got inspiration from honeybees, which use resin and latex to construct hives. After killing intruders, honeybees keep the corpses of the intruders in the hives, which normally would cause bacterial infection in the bees. To avoid this, they use propolis to preserve the corpses. Studies have revealed that propolis contains nearly 200 compounds.<sup>18, 19</sup> The composition of propolis differs from region to region because of the biodiversity in Guttiferae plants. Propolis and hive extracts have shown a wide range of biological and medicinal attributes, such as anticancer,<sup>20</sup> antioxidant, antiinflammatory,<sup>21</sup> and antimicrobial properties.<sup>22</sup> Nemorosone was identified as one of the active ingredients in propolis. In the western part of India, especially the coastal region of Maharashtra, the

dried rind of the fruits from Garcinia, a plant from *Clusiaceae* family, is used to garnish the flavor and color of a curry. In turn, the famous kokum curry has been very effective in treating gastric ulcers.<sup>23</sup>

### 1.3 Classification of PPAPs

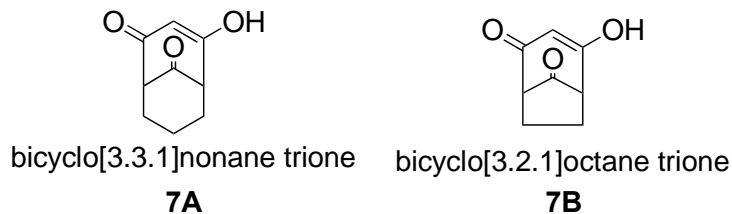


**Figure 1.3.1.** Core structures of PPAPs

Recently, organic chemists have become more interested in secondary metabolites produced by these plants from the Guttiferae family. This is due in large part to the antidepressant activity of *Hypericum perforatum*, popularly known as St. John's wort. Research data have shown that plants from these families contain a novel class of compounds, polycyclic polyprenylated acylphloroglucinols (PPAPs). Until now, more than 200 PPAPs have been identified. After much rigorous analysis of these isolated PPAPs, researchers have found that they feature either bicyclo[3.3.1]nonane-2,4,9-trione or bicyclo[3.2.1]octane-2,4,8-trione core (Figure 1.3.1). These scaffolds are decorated with prenyl or geranyl group and sometimes also with lavandulyl or isolavandulyl side chains. Depending on unique structural patterns, PPAPs are broadly classified into two categories, namely, type A, type B (Figure 1.3.2). The classification is based on the spatial arrangement of prenyl and acyl groups on in the main scaffold. Type A has an acyl group at C1 and an alkyl group at C3. C1 is next to a quaternary center at C8, whereas, in the case of type B, the acyl group is at C3.<sup>7</sup>

Recently, some unusual structural patterns, which do not fall in the above classification, have been found in PPAPs.<sup>24,25</sup> Often, PPAPs can undergo further oxidation in prenyl or geranyl side chains to add more structural complexity, like in garsubellin A,<sup>26</sup> where the prenyl group undergoes further oxidative addition of C2 oxygen or C4 oxygen to form a tetrahydrofuran type ring in the molecule.<sup>27</sup> Adamantane is also a common structural core, found in PPAPs, due to secondary cyclization.<sup>28</sup>

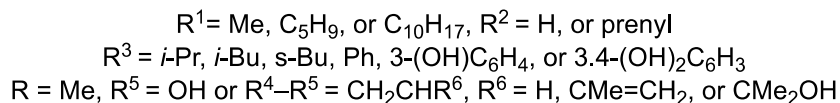
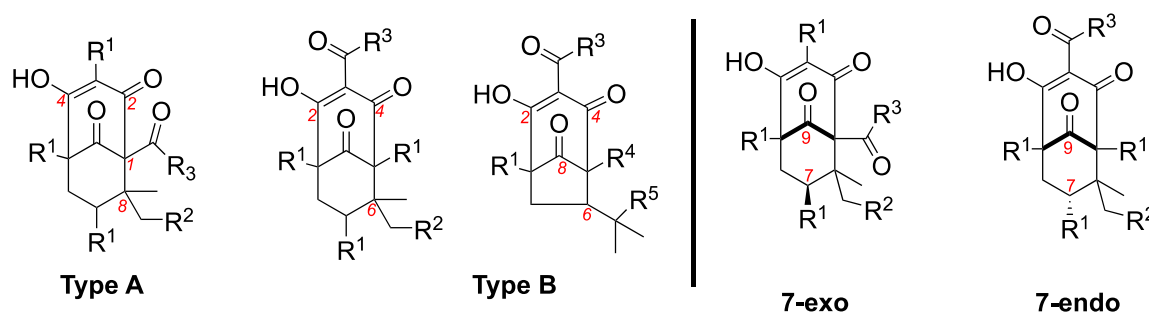


**Figure 1.3.2.** Classification of PPAPs

Type A and type B can be further classified into exo and endo. Therefore, type A can be both exo and endo; similarly, type B can be both exo and endo. However, most type A PPAPs are exo, while most type B PPAPs are endo. Exo and endo nomenclature are made by the orientation of C7 prenyl or geranyl group with respect to C9 keto group. If C7 prenyl or geranyl appendage is cis to C9 keto group, it is termed as exo; in the case of trans, it is called endo (Figure 1.3.2).

Recently, Xiao-Jiang Hao et al. isolated two unusual PPAPs from *Garcinia multiflora*.<sup>29</sup> The detailed spectroscopic analysis revealed that these molecules contained an unusual caged type structure. The Hao group isolated two compounds, namely,

garcimulin A and B. The molecule contains tetracyclo [5.4.1.<sup>11,5,0<sup>9,13</sup></sup>] tridecane skeleton (Figure 1.3.3), which calls for an explanation in PPAPs biosynthesis.

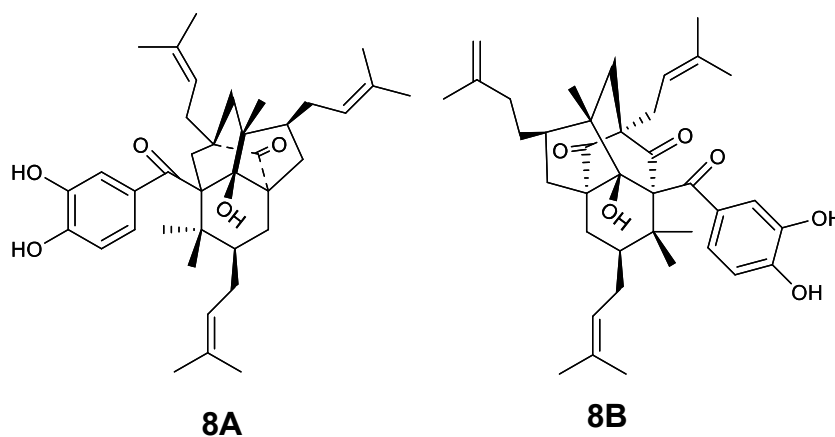


**Figure 1.3.3.** Unusual PPAPs

#### 1.4 History of PPAPs

In modern PPAP history, a German scientist, W. Schmid, was probably the first to isolate a yellow crystalline compound from the plant *Garcinia mangosta* in 1855.<sup>30</sup> Later, there were eight other scientists, after Schmid who isolated the same yellow crystalline substance from the *Garcinia mangosta* (Table 1.4.1).<sup>31</sup> The structures proposed by the scientists were vividly different from each other. In 1932, a Japanese natural product scientist, J. Murakami, worked on the same yellow crystalline solid compound and proposed several structures. Five years later, in 1937, an Indian scientist, Sanjiva B. Rao, isolated a yellow crystalline product from the seeds from *Garcinia morella*. He termed it as morelline. The isolated compound was levorotatory, but

**Table 1.4.1.** List of earlier works on *Garcinia mangosta*

Scientists	Formula	Year of Publication
W. Schmid	C <sub>40</sub> H <sub>44</sub> O <sub>10</sub>	1855
R. Hill	C <sub>23</sub> H <sub>24</sub> O <sub>4</sub>	1915
J. Dekker	C <sub>16</sub> H <sub>22</sub> O <sub>5</sub>	1924
S. Yamashiro	C <sub>20</sub> H <sub>22</sub> O <sub>5</sub>	1930
O. Dragendorff	C <sub>18</sub> H <sub>18</sub> O <sub>4</sub>	1930

Rao could not figure out the exact structure of morelline. He, however, proposed that morelline might have a chemical formula of C<sub>30</sub>H<sub>34</sub>O<sub>6</sub> and might contain four phenolic OH groups.<sup>32</sup> He also suggested that morelline might possess a structure very similar to the same compound that was extracted from *Garcinia mangosta* by Schmid and the other scientists.

After World War II, science and technology were leapfrogging because of numerous inventions, and chemistry benefited a lot, thanks to X-ray and NMR spectroscopy. At the beginning of the 1960s, almost 20 different PPAPs were isolated from various Guttiferae plants. Surprisingly, most of them were xanthenes, and a few were phloroglucinols.

While working on morelline structure determination, in 1962, Kartha and his group proposed that morelline might contain a bicyclo[2.2.1]octane ring.<sup>33</sup> Kartha's group used NMR and crystallographic data to reach the conclusion that morelline contains prenyl appendages and a  $\alpha,\beta$ -unsaturated aldehyde group with a chromone ring. Hyperforin was the first PPAP whose structure was determined after isolation by Koloso's group in 1975. Later, his group also defined the absolute stereochemistry.

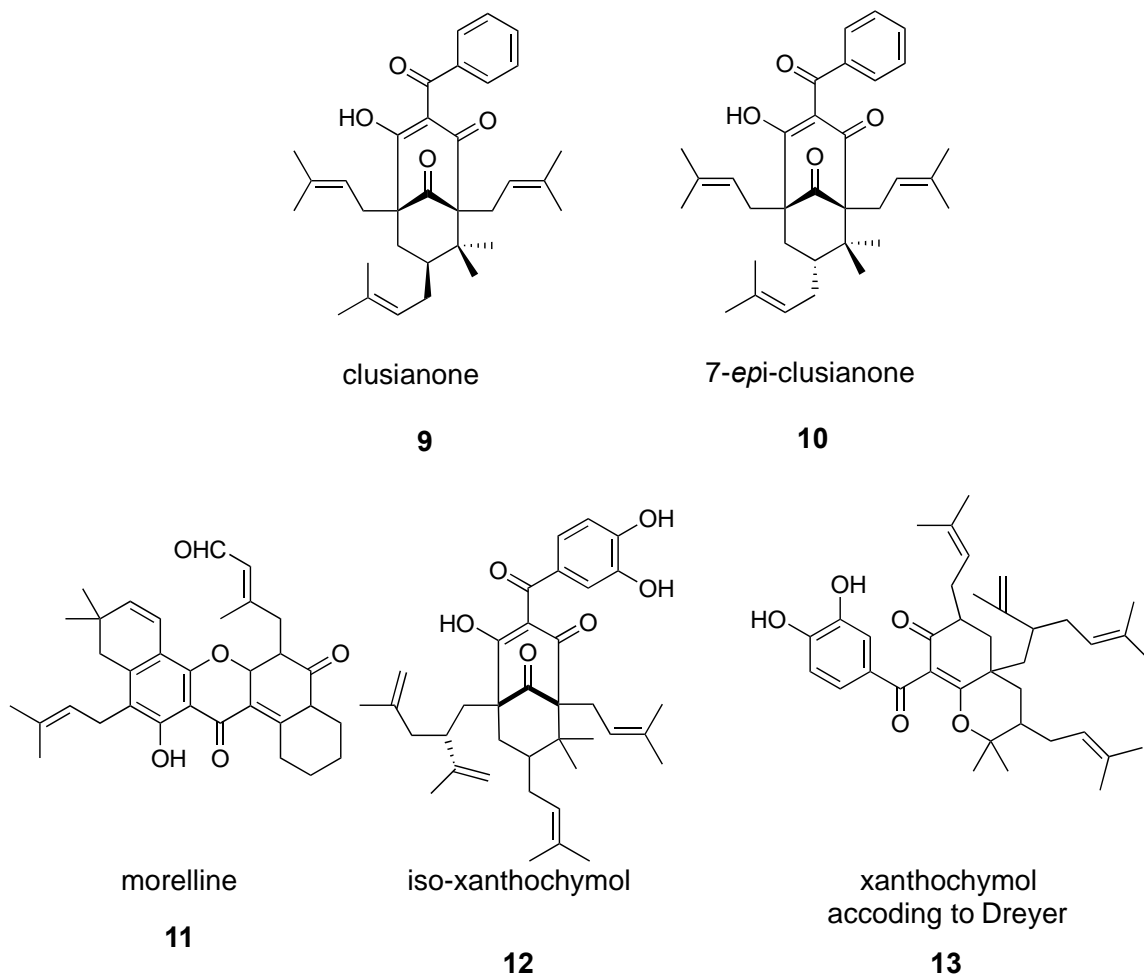


**Figure 1.4.1.** History of some PPAPs

For type B PPAPs, xanthochymol and isoxanthochymol were isolated in 1970 by Karanjoakar *et al.* in a collaboration with Western Regional Research Laboratory, Berkeley.<sup>34</sup> They proposed a bicyclic structure for isoxanthochymol based on the derivative of the naturally occurring crystals (Figure 1.4.1). Rao, however, could not figure out the xanthochymol structure. A year later in 1971, Dreyer predicted a very similar structure that was proposed by Rao *et al.*—a monocyclic structure of xanthochymol—after extracting it from an autograph tree (*Clusia rosea*).<sup>35</sup> Dreyer, however, proved that there were three aromatic protons, three vinyl groups, and a disubstituted C=C bond in the molecule, but he

was not sure about vinyl C-methyl groups in the molecule. Moreover, overlapping integrals at  $\delta$  2.8 rendered him undecided on the structure of xanthochymol.

In 1976, Blount and William revisited the structure of xanthochymol and isoxanthochymol.<sup>36</sup> Relying on X-ray and <sup>1</sup>H NMR data, the duo proposed the structures shown in Figure 1.4. To continue the research, they extracted xanthochymol and isoxanthochymol from *Garcinia xanthochymus*. The structure of isoxanthochymol was determined from a bromo derivative of **8**.<sup>36</sup> The lack of a sufficient number of H atoms in the bicyclic scaffold misled Dreyer to deduce the incorrect structure of xanthochymol. Blount and William assigned the correct structure of xanthochymol with the help of X-ray crystallography.

Clusianone (**9**) and 7-*epi*-clusianone (**10**) remained enigmas for several years so far as their structures were concerned. Clusianone was first isolated from *Clusia congestiflora*, a plant from Guttiferae, which comprises of 40 genre and 1200 species,<sup>37</sup> in 1976. X-ray analysis firmly established the structure of clusianone and showed that the C7 prenyl group is *exo*. In 1991, Dalle *et al.* reported clusianone—extracted from fruits of *Clusia sandinesis*—in the form of a white crystal.<sup>38</sup> In 1996, De Oliveira isolated clusianone from the floral resin of *Clusia spiritu-santensis* after diazomethane treatment.<sup>39</sup> The structures of clusianone and 7-*epi*-clusianone were markedly different from one another. Later, Santos *et al.* isolated 7-*epi*-clusianone from *Raheedia gardneriana*. NMR and X-ray analysis showed that the C7 prenyl group in 7-*epi*-clusianone is *endo*, thereby confirming the structure of 7-*epi*-clusianone (Figure 1.4.2).<sup>40</sup>

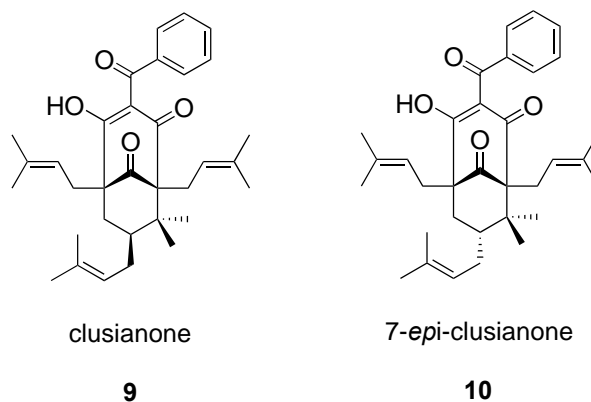


**Figure 1.4.2.** Clusianone and 7-*epi*-clusianone

Lalibinone and its analogs, A–E (**14–18**), were isolated from *Hypericum papuanum*.<sup>41</sup> It is a woody plant from the Guttiferae family and grows widely in mountains of Papua New Guinea. In folklore medicine, this tree's leaves were used in treating sores. In 1999, Winlemann et al. isolated five different compounds from the aerial part of *H. papuanum* in the form of a hexane extract.<sup>42</sup> Detailed structural analyzes—based on <sup>1</sup>H NMR, <sup>13</sup>C NMR, HMBS, and HSQC—of these isolated five compounds revealed that the molecules contain a tricyclic structure with a bicyclo[2.3.1] octane-2,4,8-trione core (Figure 1.4.3)

Laxifloranone (**19**) is a unique PPAP. It was isolated from an organic extract of *Marila laxiflora* Rusby.<sup>43</sup> The plant belongs to the Clusiaceae family. Bokesch et al. determined its structure in 1999.<sup>44</sup> The molecule is rich with aromatic rings. Structural analysis showed that the molecule has a hydrocinnamic acid side chain, instead of a prenyl group. In that respect, the molecule is different than other PPAPs. It belongs to the type B endo PPAP family.



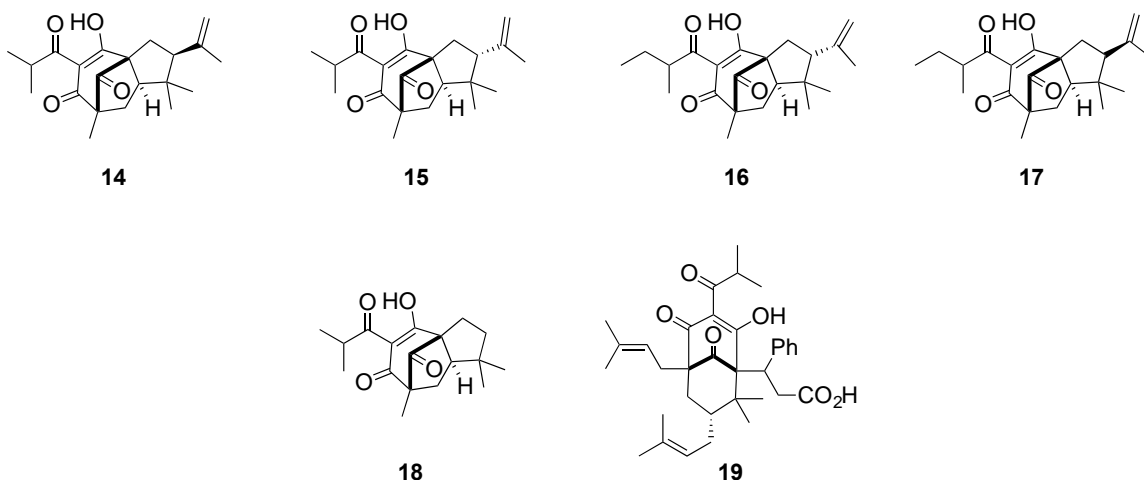


**Figure 1.4.3.** Lalinones A-E and laxifloranone

### 1.5 Revisiting some structures of type B endo PPAPs

Along with medicinal properties and architectural diversity of NPs, the third reason for the total synthesis is to confirm whether existing structures in the literature are correct or not. This has been the case similarly with PPAPs. The correct structure determination of PPAPs has been a problem for years because of the relative stereochemistry at the C7 appendage, which specifically categorizes a PPAP as endo or exo. In some cases, however, scientists were successful in isolating PPAPs from plants as crystalline solids. Consequently, X-ray analysis of those PPAPs unambiguously established their structures, including exo or endo stereochemistry of C7.<sup>40</sup> In this section, I will revisit some of such stories related to the endo type B PPAPs, whose structures were corrected after they had been reported.

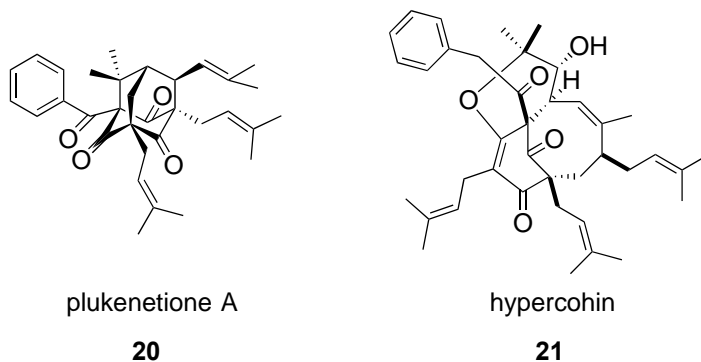


**Figure 1.5.1.** Structural diversity among PPAPs

Although the overlapping peaks in  $^1\text{H}$  NMR spectra make the identification of PPAPs difficult, high-temperature NMR, nearly at  $60\text{ }^\circ\text{C}$ , resolves some of the issues, such as finding the 1,3-diketone framework in the molecule and the C3 substituent.<sup>41</sup> The real problem, however, is the determination of exo or endo stereochemistry of the molecule concerned. Grossman and Jacob have demonstrated that  $^1\text{H}$  NMR and  $^{13}\text{C}$  NMR are very helpful in categorizing the PPAPs as exo or endo based on the chemical shifts of certain protons and carbons.<sup>45-47</sup> They proposed that if the difference of chemical shifts between the two H atoms at C6 in the  $^1\text{H}$  NMR spectrum is 0.3 to 1.2 ppm, and the C7 chemical shift in the  $^{13}\text{C}$  NMR spectrum is 41 to 44 ppm, the PPAP is exo, whereas if the difference of chemical shifts between the two H atoms at C8 in the  $^1\text{H}$  NMR spectrum is 0.0 to 0.2 ppm, and the C7 chemical shift in the  $^{13}\text{C}$  NMR spectrum is 45 to 49 ppm, the PPAP is endo. I shall utilize these observations to consider some endo PPAPs where the discrepancies were found in previous reports (Figure 1.5.2).

Initially, there were doubts in assigning the stereochemistry of some endo type B PPAPs like garcinol (**22**) ( $[\alpha]_D -138$  (0.1)) and isogarcinol (**23**) ( $[\alpha]_D +224$  (MeOH, 0.1)), and some endo PPAPs have different C(7)  $\delta$  or H(6) or H(8) chemical shifts, which were not consistent with endo PPAPs of the same configuration.<sup>5</sup> The enantiomers of garcinol

and isogarcinol were named differently: (+)-garcinol (**62**) was given the name of guttiferone E (**24**) ( $[\alpha]_D -101$  (0.1)), and (+)-isogarcinol (**23**) was given the name of isoxanthochymol (**25**) ( $[\alpha]_D +181$  (EtOH, 0.6)) (Figure 1.5.2). Assigning the absolute configuration to these compounds becomes tough by various names and optical rotations. Moreover, the chemical shifts of C7 or hydrogens at C6 or C8 were not as per the general rule proposed by Grossman and Jacob.<sup>45</sup> For isogarcinol and isoxanthochymol (Figure 1.5.2), the values are within the range of exo compounds: C6 hydrogen in isogarcinol or C8 hydrogen in xanthochymol has a chemical shift of 0.75 or 0.70 ppm in HNMR respectively. Plietker and Socolsky noticed the discrepancies and attempted to resolve it via chemical synthesis.

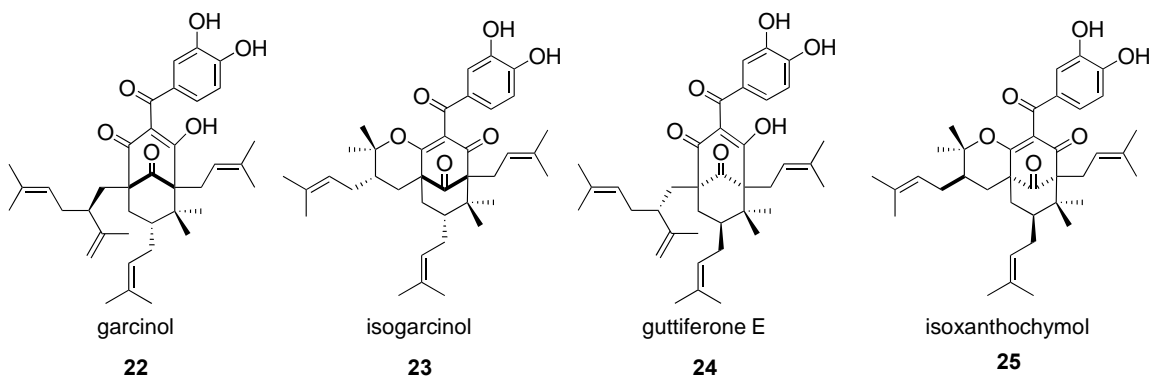


**Figure 1.5.2.** Structural conundrum: guttiferone E and isoxanthochymol

The previously recorded X-ray crystallographic analyses of these compounds were confirmed with the crystals obtained from Plietker's work. The crystal analysis of both compounds showed that the tetrahydropyran ring is at lowest energy conformation: in a twist boat form. Because of that, the isoprenyl substituent became equatorial. Socolsky and Plietker not only relied on chemical syntheses but also utilized TURBOMOLE6.5 in conjunction with the graphical interface Tmole 3.4. They also used TD-DFT (Time Dependent Density Functional Theory) to calculate the excitation energy and find out the

combinations of a possible number of allowed spins in excited states. They converted these data into simulated CD (circular dichroism) spectra that gave a theoretical graph. Then, they compared these simulated CD spectrum with the natural products (garcinol and isogarcinol) that Plietker's group had synthesized. The theoretical CD spectrum of isogarcinol—where the relative configuration of C30 is S—showed both positive and negative Cotton effect at 220 and 265 nm respectively. That was agreeing with the experimental value obtained with chemically synthesized isogarcinol. This result proved that they synthesized the naturally occurring enantiomer of isogarcinol and garcinol. A similar result was observed with isoxanthochymol. Thereby, Socolsky and Plietker concluded that isoxanthochymol and isogarcinol are enantiomers. Previously, Grossman and Ciochina proposed the same observation in their review article.<sup>7</sup> Socolsky and Plietker's article reiterated the importance of chemical syntheses of NPs: to correct a structure of a natural product.

There were also some discrepancies about the correct structures of guttiferone G (**74**) and guttiferone I (**66**) (Figure 1.5.3). These two compounds were isolated from the same source, *G. hummulis*, by Herath et al. NMR analysis, UV, and IR data showed that both molecules contain a dihydroxy phenol group. Nevertheless, there was confusion about the assignment of the C7 prenyl group. Initially it was thought that both compounds were endo type B. The specific rotation, however, of both compounds were different; guttiferone I has a specific rotation of  $+8.7^\circ$  in  $\text{CHCl}_3$ , while guttiferone G showed a rotation of  $-25^\circ$  in  $\text{CHCl}_3$  also. The J-coupling value for H atoms at C6-C8 in guttiferone I was 13.0 Hz, which is quite high among the all other type B endo PPAPs. 2D-NOE gave an indication that guttiferone I is a type B endo, but the experiment did not negate the possibility of type B exo either. Later, Nilar et al. attempted to assign the absolute

stereochemistry of guttiferone G–I, and because of conflicting data, they could not assign it.<sup>48</sup>

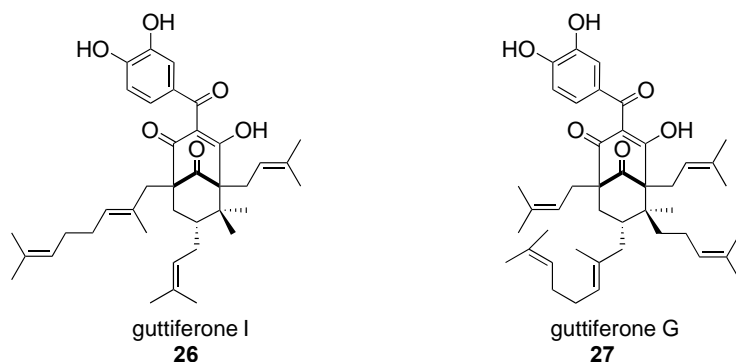


**Figure 1.5.3.** Guttiferones I and G

Another interesting revelation was determination of sampsonione P (**26**) and hyperibone I (**28**). Initially, scientists proposed that sampsonione P has an endo configuration and its isomer, hyperibone I, has an exo configuration. Grossman and Ciochina, however, predicted that hyperibone might be endo type B.<sup>7</sup> Plietker and his group synthesized both the molecules and carried out 2D NOE to assign the absolute stereochemistry at C7. They observed a strong correlation between C7 H and C6 H<sub>ax</sub>. Moreover, there were two other strong correlations—firstly, between C6 axial hydrogen and an axial methyl group; secondly, C7 equatorial hydrogen and a C6 equatorial methyl group. In consideration of this evidence, the duo proposed the following structure (Figure 1.5.4), proving Grossman’s hypothesis on hyperibone I correct. Similarly, they concluded the same relative configuration—type B endo PPAP predicted by Grossman and Ciochina—with sampsonione P.

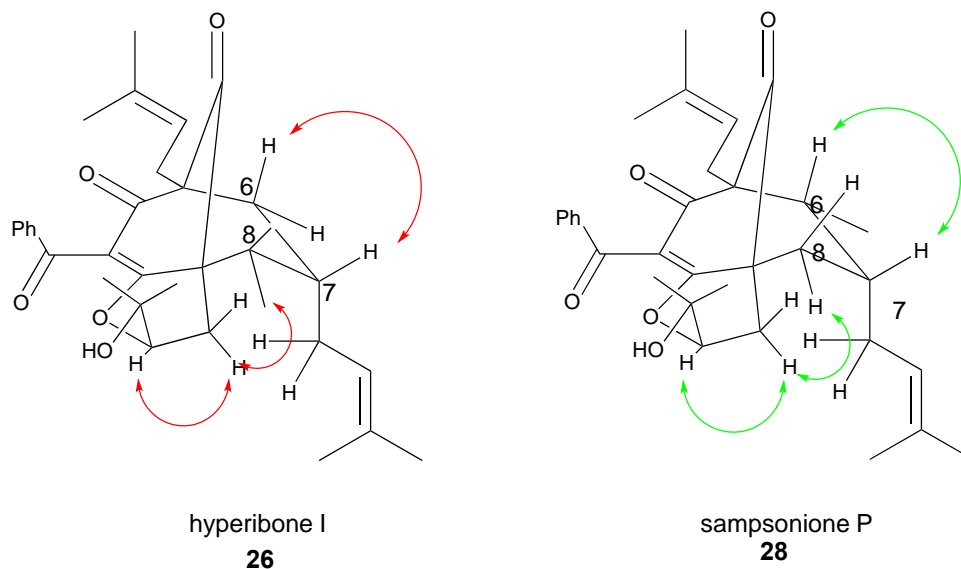


**Figure 1.5.4.** hyperibone I and sampsonione P

## 1.6 Biosynthesis of MPAPs

The recent advances in labeling experiments have provided a deep insight into the biological pathways. Several research studies have shown enough evidence that PPAPs are products of two important biological pathways—shikimate and acetate-isoprenoid. The shikimate pathway contributes the phenol part to the overall molecule and the acetate-malonate pathway provides side chains and carbocycle.<sup>49</sup> Plants synthesize PPAPs from MPAPs, which are products from the acetate pathway. Three malonyl-CoA and an acetate unit combine in Claisen condensation to make a  $\beta$ -polyketoester. The poly ketoester can fold in two ways—one way goes to orselinic acid and the other to phloroglucinols (Scheme 1.6.1), which are the starting unit of many MPAPs. An enzyme complex carries out the whole sequence of reactions without any detectable intermediates.<sup>50</sup> From the organic chemist's point of view, the formation of acylphloroglucinols from poly  $\beta$ -keto-esters is a result of Claisen condensation.

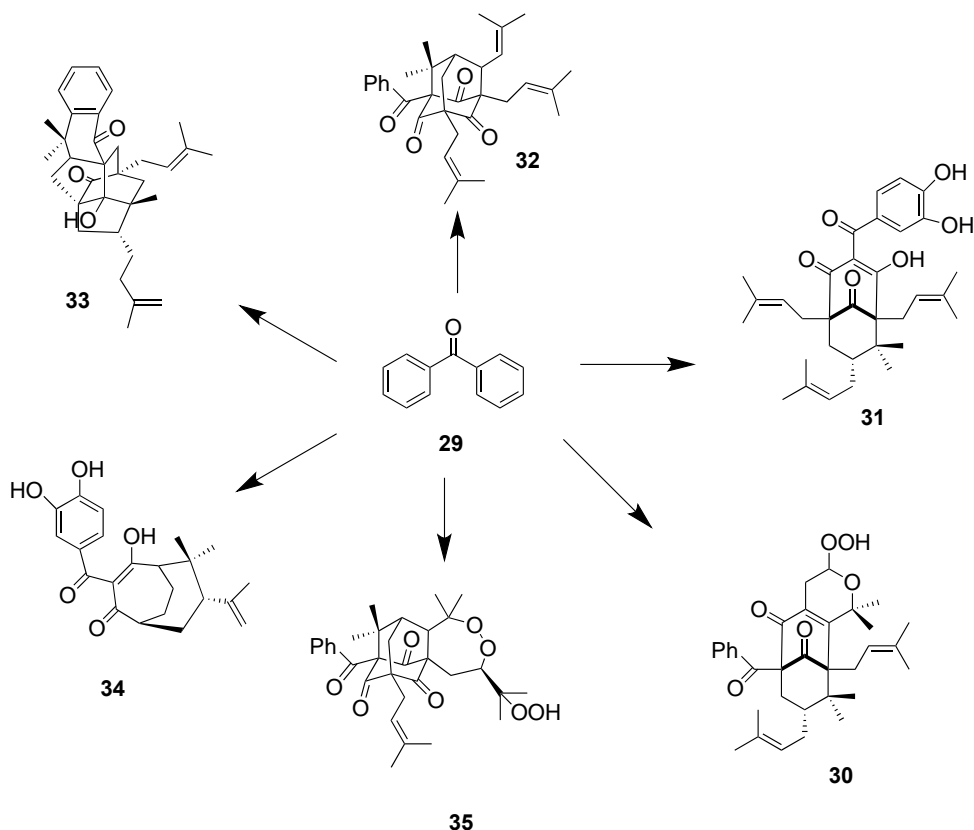
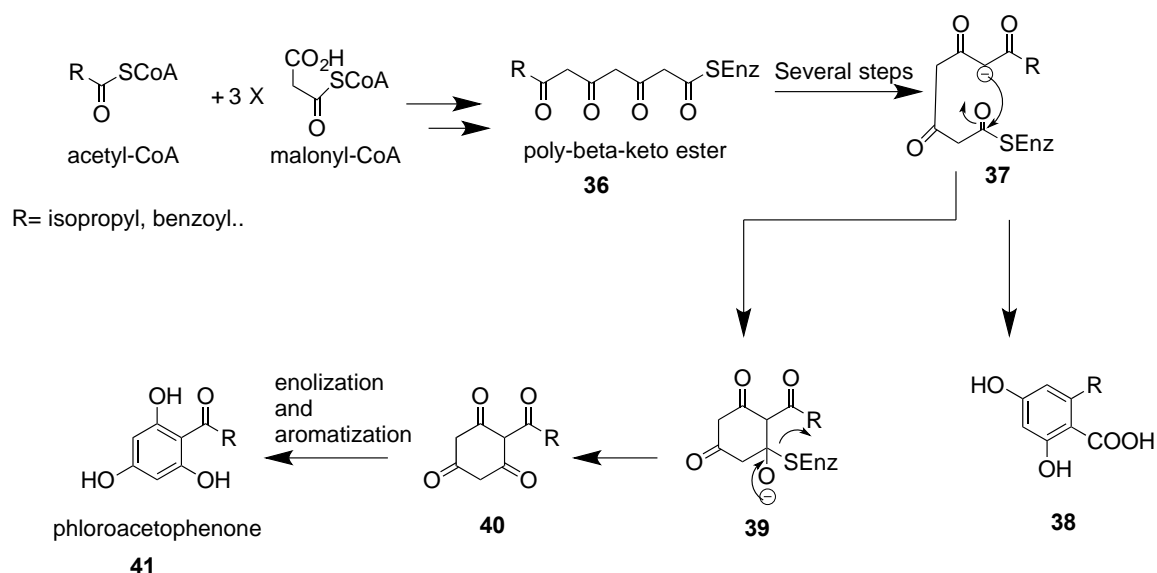


**Figure 1.6.1.** Diverse arrays of PPAPs from benzophenone

The polyketide synthase and polyketide catalase are two enzymes responsible for Dieckman condensation in this case. The enzymes have structural resemblance with fatty acid synthase. The distinctive feature of this pathway is that the oxygenation pattern is *meta*, and even after the formation of the final product, the meta-oxygenation pattern is retained. The MPAPs can undergo various transformations further, and one of the transformations is prenylation with DMAPP (dimethyl allyl pyrophosphate) or GMAPP (geranyl pyrophosphate). The prenyl transferase catalyzes these reactions, leading to other MPAPs. The labeling experiments have shown that the prenylation goes via a non-concerted way. Out of different MPAPs, cohulolones and colupulones are noteworthy since they have some commercial values.

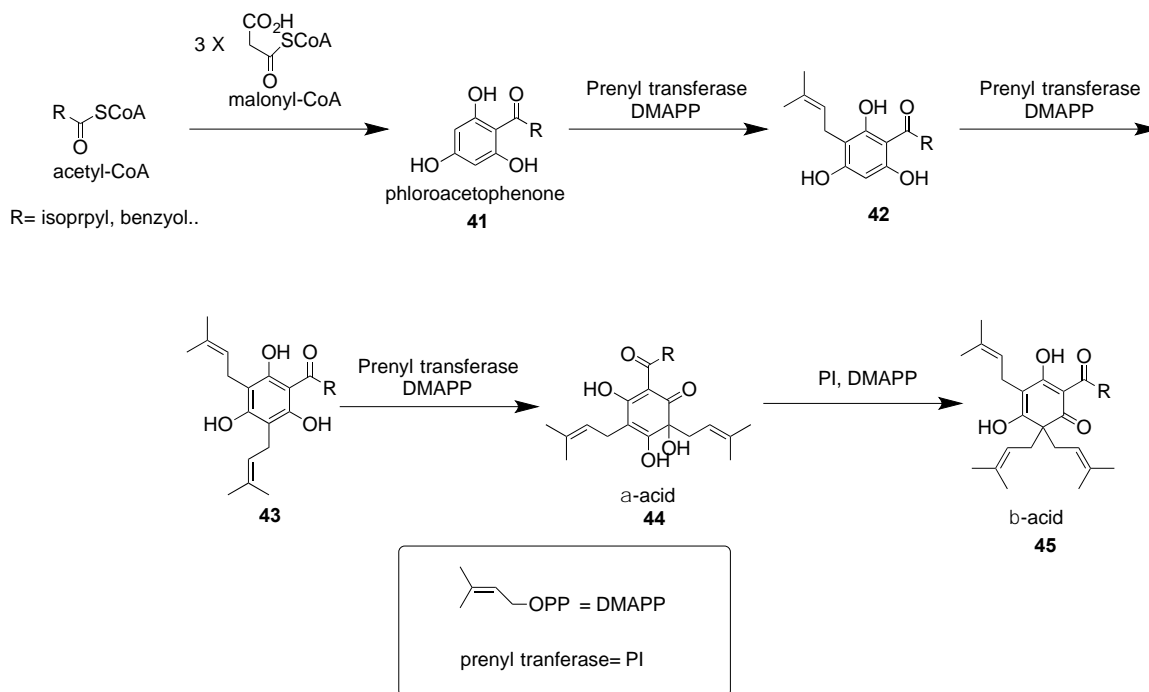


**Scheme 1.6.1.** Biosynthesis of MPAPs

The polyketide synthase and polyketide catalase are two enzymes responsible for Dieckman condensation in this case. The enzymes have structural resemblance with fatty acid synthase. The distinctive feature of this pathway is that the oxygenation pattern is *meta*, and even after the formation of the final product, the meta-oxygenation pattern is retained (Scheme 1.6.1). The MPAPs can undergo various transformations further, and one of the transformations is prenylation with DMAPP (dimethyl allyl pyrophosphate) or GMAPP (geranyl pyrophosphate). The prenyl transferase catalyzes these reactions, leading to other MPAPs (Scheme 1.6.2). The labeling experiments have shown that the prenylation goes via a non-concerted way. Out of different MPAPs, cohulolones and colupulones are noteworthy since they have some commercial values. MPAPs have shown anti-fungal, anti-bacterial, and antifeedant properties. Hops—scientifically known as *Humulus lupulus*—have been in use in folklore medicine as an anti-bacterial agent, tranquilizer, and healing the symptoms of menopause.<sup>51</sup> The most significant hops are female inflorescences, which are used in beer production. Interestingly, MPAPs have shown anti-fungal, anti-bacterial, and antifeedant properties. Interestingly, it is the  $\alpha$ -acid, which adds flavor and bitter taste



to the beer. The  $\beta$ - acids act as a radical scavenger and have shown anti-bacterial properties. it is the  $\alpha$ -acid, which adds flavor and bitter taste to the beer (Figure 1.6.2). The  $\beta$ - acids act as a radical scavenger and have shown antibacterial properties (Table 1.6.1).



**Scheme 1.6.2.** Synthesis of  $\alpha$  and  $\beta$ -acids from MPAP

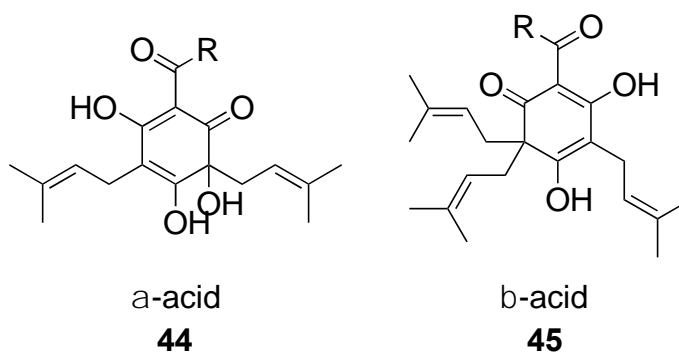


**Figure 1.6.2.**  $\alpha$  and  $\beta$ -acids

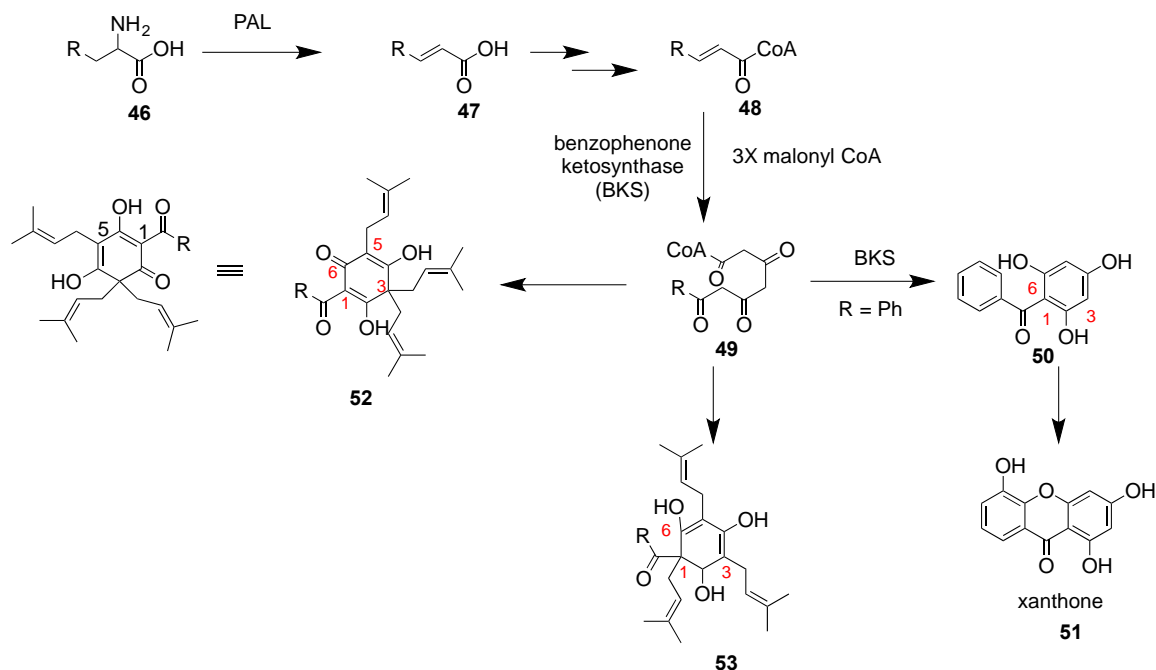
**Table 1.6.1.** Different  $\alpha$ -acids and  $\beta$ -acids

R	$\alpha$ -acids	$\beta$ -acids
<i>i</i> -Pr	Cohumulone	Colupulone
<i>i</i> -Bu	Humulone	Lupulone

## 1.7 Biosynthesis of PPAPs

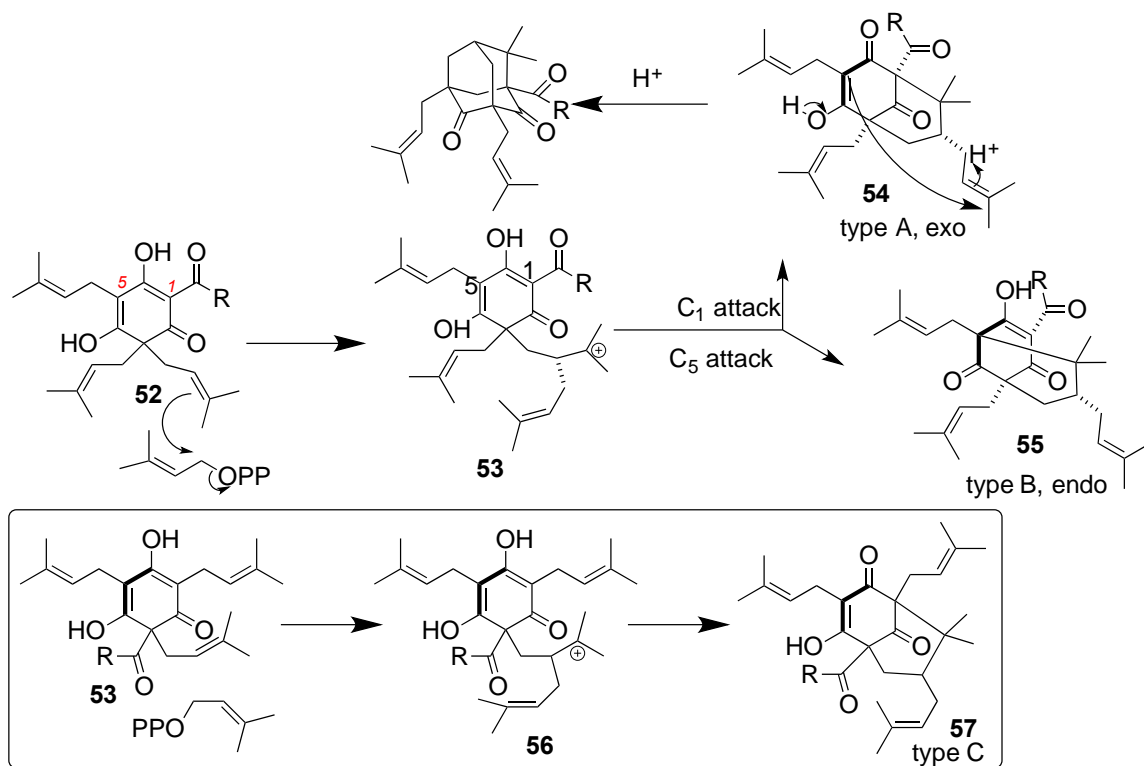
PPAPs are synthesized from MPAPs that could undergo further modifications in the presence of prenyl transferase to construct the bicyclo[3.3.1]nonane. Type A, B and C PPAPs originate from acylphloroglucinols through a series of carbocationic rearrangements (Scheme 1.7.1). The chemoselective bond formation in the enzymatic pathway leads either type A, B or C. According to Cuesta-Rubio, MAPPs cyclize in the presence of prenyl transferase to type A and type B from the same precursor **52**. The mechanism needs an  $S_N2$  type attack on DMAPP by one of the enantiotopic prenyl groups, giving rise to a carbocation intermediate that could make a bond either to C1 or C5 in the aromatic ring. Attack from C1 end leads to a type A; while the C5 attack leads to a type B.

Type C PPAPs are rare, and it can be explained by a mechanism mentioned in Scheme 1.7.2. To make a type C PPAP, C1 must have a quaternary center and to synthesize it naturally is not simple, possibly because of the steric factor.



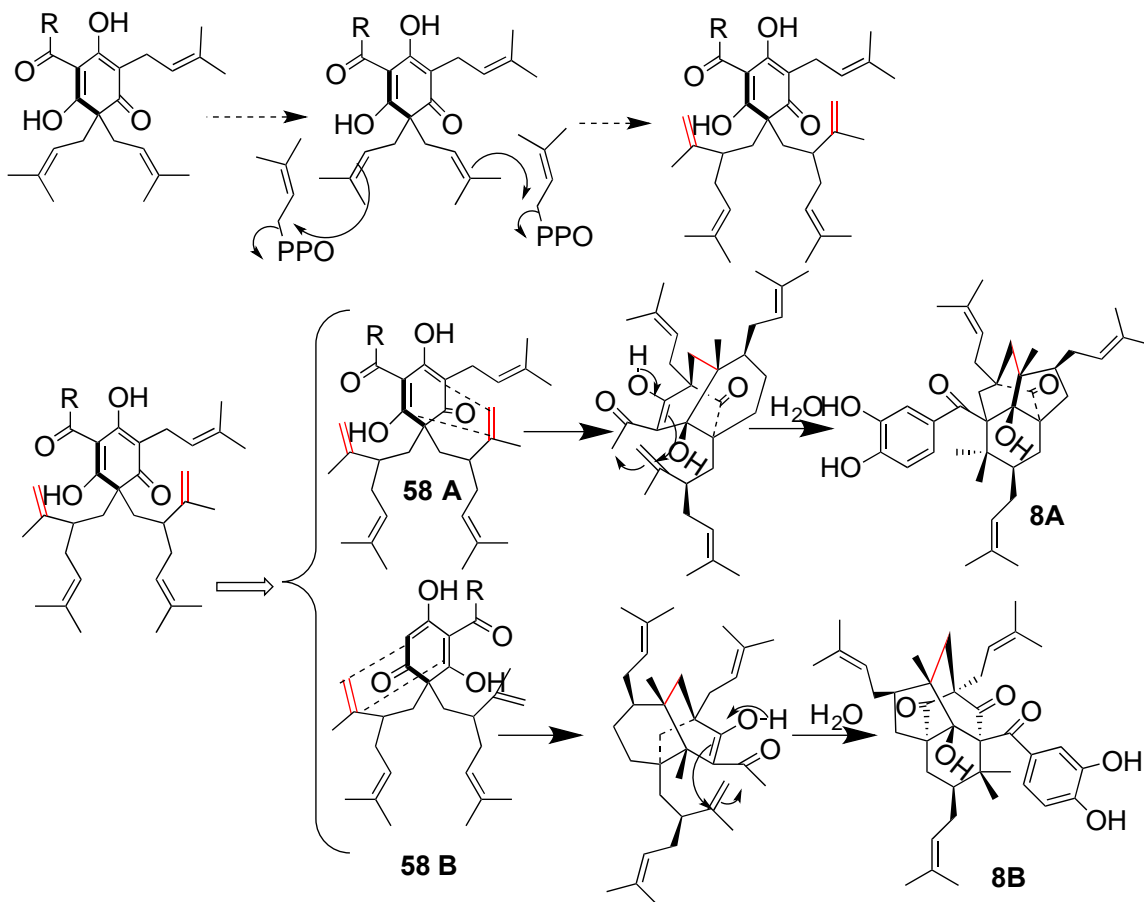
**Scheme 1.7.1.** Precursors to type A, B, and C PPAPs

In the previous section, we have said that MAPPs are synthesized from acetyl or malonyl-CoA via a series of Dieckman condensations.<sup>52</sup> If we consider the detail of the mechanism, we find that benzoyl-CoA is derived from the shikimate pathway. L-Phenylalanine undergoes a series of reactions, namely, deamination and decarboxylation to produce benzoyl-CoA (Scheme 1.7.1). Then benzoyl-CoA again undergoes a series of reactions, namely, Dieckman condensation, and alkylation, to produce type A, B, and C PPAPs. PPAPs can undergo further cyclization that adds more complexity to the overall structure of the PPAP. For example, the type A PPAPs may react with another molecule of DMAPP, and consequently, PPAP with an adamantane is formed. Plukenetione A **32** is an example of such a PPAP.



**Scheme 1.7.2.** Mechanistic pathway for type A, B and C

In section 1.1.2, I mentioned two unusual PPAPs (**17**, **18**) that contained a tetracyclotridecane skeleton. The formation of such an unusual skeleton can be explained based on [4+2] cycloaddition followed by a keto-enol tautomerism (Scheme 1.7.3).

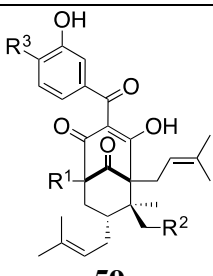


**Scheme 1.7.3.** Mechanistic rationale for two unusual PPAPs

## 1.8 Sources and structures of type B endo PPAPs

Until now, we know many things about PPAPs, including type A, B, and C, namely, their structure and biological activities. My predecessors, Roxana Ciochina and M. P. Suresh Jayasekara, have given a detailed account of biological importance and the sources of PPAPs in their dissertations.<sup>5, 53</sup> Therefore, there is no point in going over the same PPAPs again, here. In past several years, however, natural product scientists have isolated many new PPAPs that were not talked about neither in Ciochina nor in Jayasekara's dissertation. In this section, I will focus on endo type B PPAPs whose structures have been known or discovered recently. Nearly 23 new PPAPs have been identified between 2006 to 2013. There will be a separate section where I will place some new type B and some unusual type A PPAPs, which cannot be avoided because of structure and medicinal properties associated with them. However, focus of my research remains on type B endo PPAPs.

**Table 1.8.1.** Type B endo PPAPs

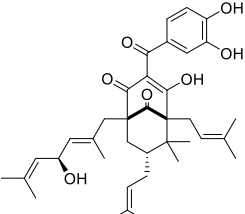
No.	R group or structure.	Name	Source	$[\alpha]_D^{25}$ (°)
 <p><b>59</b></p>	R <sup>1</sup> , R <sup>2</sup> = prenyl, R <sup>3</sup> = OH,	guttiferone A	<i>S. globulifera</i> <sup>2</sup> <i>G. livingstonei</i> <sup>3</sup> <i>G. humils</i>	+34 (c <sup>4</sup> 1.7)

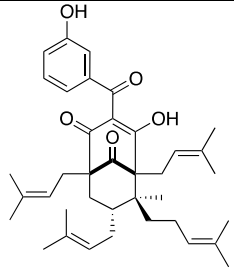
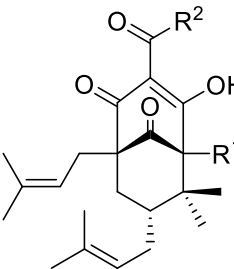
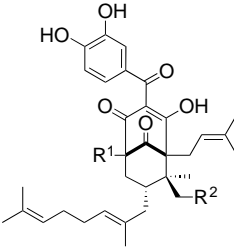
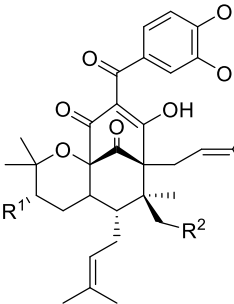
<sup>1</sup> OMe or OAc indicates the specific rotation was measured for that derivative

<sup>2</sup> S= *Symphonia*

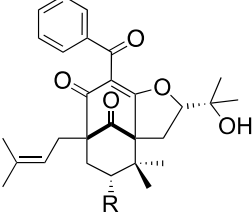
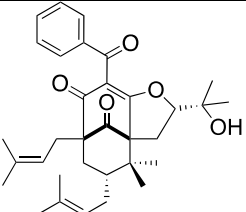
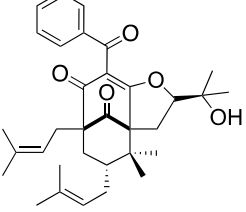
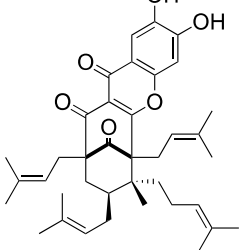
<sup>3</sup> G = *Garcinia*

<sup>4</sup> not all of the stereocenters' configuration have been assigned

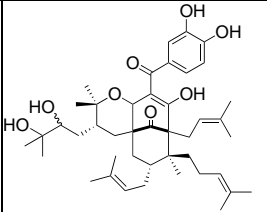
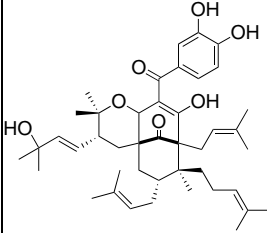
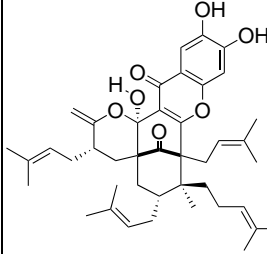
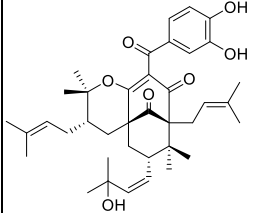
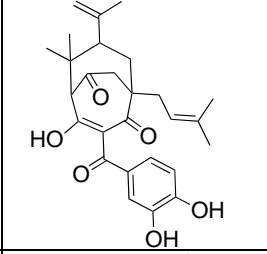
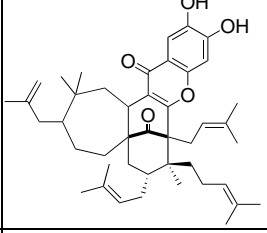
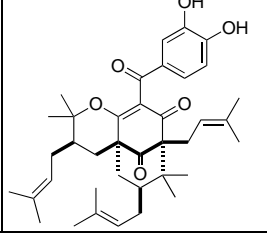
<b>60</b>	R <sup>2</sup> = prenyl; R <sup>3</sup> = OH, R <sup>1</sup> = ω- lavandulyl	guttiferone C	<i>S. globulifera</i>	mixed with <b>61</b> +92 (c 0.9)
<b>61</b>	R <sup>1</sup> = lavandulyl R <sup>2</sup> = prenyl, R <sup>3</sup> = OH	guttiferone D	<i>S. globulifera</i>	mixed with <b>60</b> +92 (c 0.9)
<b>62</b>	R <sup>1</sup> = ( <i>S</i> ) lavandulyl; R <sup>2</sup> = prenyl, R <sup>3</sup> = OH	guttiferone E	Cuban propolis <i>C.rosea</i> <i>G.ovafolia</i>	+101 (c 0.5)
<b>63</b>	R <sup>1</sup> = ( <i>S</i> )-lavandulyl; R <sup>2</sup> =H (enantiomer), R <sup>3</sup> = OH	garcinol (camboginol)	<i>G.cambogia</i> <i>G.indica</i>	-138 (c 0.1)
<b>64</b>	R <sup>1</sup> = 3,4-(OH) <sub>2</sub> C <sub>6</sub> H <sub>3</sub> R <sup>2</sup> = prenyl; R <sup>3</sup> = ( <i>R</i> )-isogeranyl, R <sup>4</sup> = H	guttiferone F	<i>Allanblackia</i> <i>stuhlmannii</i>	293 (c 0.4)
<b>65</b>	R <sup>1</sup> = prenyl, R <sup>2</sup> = H; R <sup>3</sup> = OH	aristophenone	<i>G.xanthochymus</i>	+58 (c 0.1) OAc: +53 (c 0.1) +54 (c 0.1)
<b>66</b>	R <sup>1</sup> = geranyl; R <sup>2</sup> = H, R <sup>3</sup> = OH	guttiferone I	<i>G. griffithii</i> Cuban propolis, <i>G.xanthochymus</i>	-68 (c 1.2)
<b>67</b>	R <sup>1</sup> = ( <i>S</i> )-ω- lavandulyl; R <sup>2</sup> = H, R <sup>3</sup> = OH	xanthochymol	<i>G.mannii</i> <i>G.staudtti</i> <i>G.subelliptica</i> <i>R. madrunno</i>	+138 (c 0.1)
<b>68</b>	R <sup>1</sup> = ( <i>S</i> )-lavandulyl, R <sup>2</sup> = H, R <sup>3</sup> = H	14- deoxygarcinol	<i>M. coccinea</i>	+41 (c 0.3)
 <b>69</b>	32-hydroxy-ent- guttiferone	guttiferone M	<i>Rheedia edulis</i>	[α] <sub>D</sub> <sup>25</sup> = +9.6 (c 0.1, MeOH)

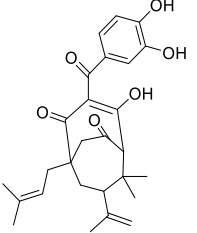
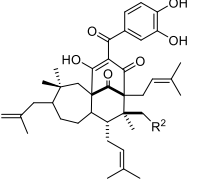
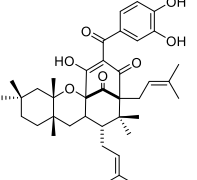
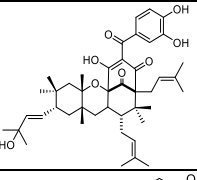
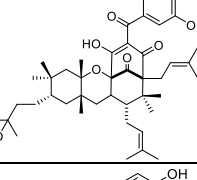
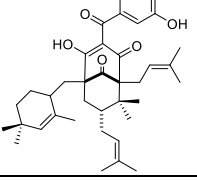
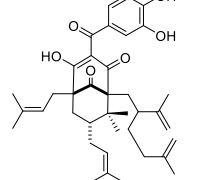
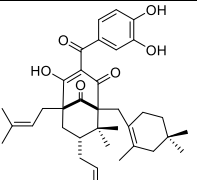
 <p><b>70</b></p>		6- <i>epi</i> -guttiferone J	<i>Rheedia edulis</i>	$[\alpha]_D^{25} = +10.8$ (c 0.1, MeOH)
 <p><b>71</b></p>	$R^1 = \text{Me}; R^2 = \text{Ph}$	hyperibone L	<i>H. scabrum</i>	+69.5 (c 0.2)
<b>72</b>	$R^1 = \text{prenyl}; R^2 = \text{Ph}$	7- <i>epi</i> -clusianone	<i>Rheedia gardeneriana</i>	+62 (c 1.1)
<b>73</b>	$R^1 = \text{Me}; R^2 = i\text{-Pr}$	hyperpapuanone	<i>H. papuanum</i>	+15 (c 0.1, MeOH)
 <p><b>74</b></p>				
<b>74</b>	$R^1 = R^2 = \text{prenyl}$	guttiferone G	<i>G. humilis</i> <i>G. macrophylla</i>	-25 (c 0.04)
<b>75</b>	$R^1 = \text{prenyl}; R^2 = \text{H}$	oblongifolin C	<i>G. oblongifolia</i>	+23 (c 0.35)
<b>76</b>	$R^1 = \text{geranyl}; R^2 = \text{H}$	oblongifolin D <sup>54</sup>	<i>G. oblongifolia</i>	+44.6 (c 0.21)
 <p><b>76</b></p>				

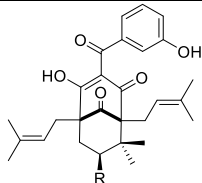
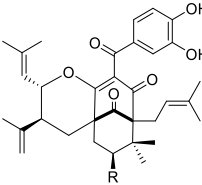
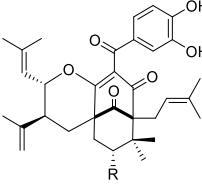
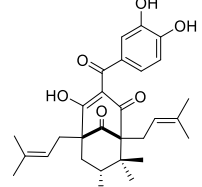
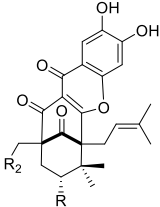
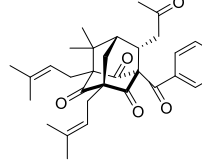
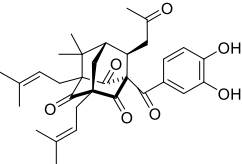


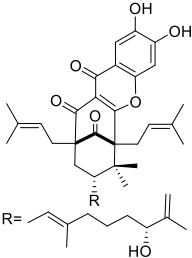
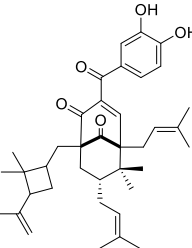
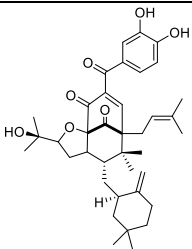
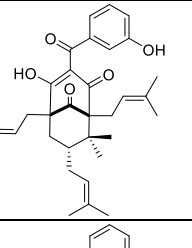
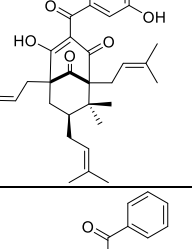
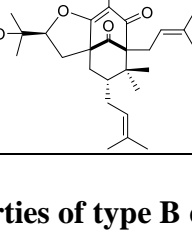
<b>77</b>	R <sup>2</sup> = H, R <sup>1</sup> = prenyl	isogarcinol <sup>55, 56</sup>	<i>G. indica</i> <i>G. pedunculata</i> <i>G. cambogia</i> <i>G. pyrifera</i> <i>G. subelliptica</i>	+224 (c 0.1, MeOH)
<b>78</b>	R <sup>2</sup> = H; R <sup>1</sup> = prenyl	isoxanthochymo l <sup>55, 56</sup> (enantiomer)	<i>G. xanthochymus</i> <i>G. ovafolin</i>	+181 (c 0.6, EtOH)
<b>79</b>	R <sup>2</sup> = H, R <sup>1</sup> = isoprenyl	(-) cycloxanthochy mol <sup>57</sup>	<i>G. subelline</i>	+80.5 (c 2.20, MeOH)
				
<b>80</b>	R = ( <i>E</i> )-CH= CHCMe <sub>2</sub> OH	hyperibone H	<i>H. scabrum</i>	+12.4 (c 0.4)
<b>81</b>	R = prenyl	hyperibone I	<i>H. scabrum</i>	+13.3 (c 0.3)
<b>82</b>		sampsonione P	<i>H. samsonii</i>	+18.6 (c 0.022)
				
<b>83</b>		hyperibone I	<i>Hypericum scabrum</i>	N/A
				
<b>84</b>		1,16- oxyguttiferone A <sup>58</sup>  or oxyguttiferone K1	<i>S. globulifera</i>	[α] <sub>D</sub> <sup>20</sup> = +53 (c 1, MeOH)
				

85		hyperattenin J <sup>59</sup>	<i>H. attenuatum</i>	$[\alpha]_D^{25} = +23.8$ (c 0.3, MeOH)
86		attenuatumione E <sup>60</sup>	<i>H. attenuatumn</i>	$[\alpha]_D^{25} = +39.7$ (c 0.13, CHCl <sub>3</sub> )
87		attenuatumione F <sup>60</sup>	<i>H. attenuatum</i>	$[\alpha]_D^{25} = +19.6$ (c 0.18, CHCl <sub>3</sub> )
88		spiranthenones B <sup>61</sup>	<i>Spiranthera odoratissim</i>	$[\alpha]_D^{30} = +13$ (c 0.17, CHCl <sub>3</sub> )
89		guttiferone O <sup>62</sup>	<i>Garcinia afzelli</i>	N/A
90		guttiferone P <sup>62</sup>	<i>Garcinia afzelli</i>	N/A
91		7-epi-coccinone B <sup>63</sup>	<i>Symphonia globulifera</i>	N/A

92		symphonone E <sup>15</sup>	<i>Symphonia globulifera</i>	+50 (c 0.4, CHCl <sub>3</sub> )
93		symphonone B <sup>15</sup>	<i>Symphonia globulifera</i>	-50 (c 0.9, CHCl <sub>3</sub> )
94		symphonone I <sup>15</sup>	<i>Symphonia globulifera</i>	-22 (c 0.4, CHCl <sub>3</sub> )
95		symphonone C <sup>15</sup>	<i>Symphonia globulifera</i>	-67 (c 1.0, CHCl <sub>3</sub> )
96		guttiferone H <sup>64, 65</sup>	<i>G. xanthochymus</i>	N/A
97		gambogeneone <sup>64</sup>	<i>G. xanthochymus</i>	N/A
98		7-epi-isogarcinol	<i>G. multiflora</i>	N/A

<b>99</b>		guttiferone H <sup>64,65</sup>	<i>G. xanthochymus</i>	N/A
<b>100</b>		gambogone <sup>64</sup>	<i>G. xanthochymus</i>	N/A
<b>101</b>		coccinone A <sup>63</sup>	<i>Moronobea coccinea</i>	+28 (c 1.0, CHCl <sub>3</sub> )
<b>102</b>		coccinone B <sup>66</sup>	<i>Moronobea coccinea</i>	-55 (c 0.3, CHCl <sub>3</sub> )
<b>103</b>		coccinone C <sup>15</sup>	<i>Moronobea coccinea</i>	-55 (c 0.2, CHCl <sub>3</sub> )
<b>104</b>		coccinone F <sup>63</sup>	<i>Moronobea coccinea</i>	-32 (c 0.7, CHCl <sub>3</sub> )
<b>105</b>		coccinone G <sup>63</sup>	<i>Moronobea coccinea</i>	-16 (c 1.0, CHCl <sub>3</sub> )
<b>106</b>		coccinone H <sup>63</sup>	<i>Moronobea coccinea</i>	+2 (c 1.0, CHCl <sub>3</sub> )

107	 <p>R = prenyl</p>	garcicowin B <sup>56</sup>	<i>Garcinia cowa</i>	N/A
108	 <p>R = prenyl</p>	garcicowin C <sup>56</sup>	<i>Garcinia cowa</i>	N/A
109	 <p>R = prenyl</p>	garcicowin D <sup>56</sup>	<i>Garcinia cowa</i>	N/A
110	 <p>R = prenyl</p>	garcimultifloron e H <sup>67</sup>	<i>G. multiflora</i>	$[\alpha]_D^{20} = +29.8$ (c 0.62, MeOH)
				
111	R = prenyl; R <sub>2</sub> = lavandulyl	multiflorone J <sup>67</sup>	<i>G. multiflora</i>	$[\alpha]_D^{20} = +11.1$ (c 0.44, MeOH)
112		oblongifolin J	<i>G. oblongifolia</i>	$[\alpha]_D^{25} = +8.6$ (c 0.03, MeOH)
113		oblongifolin K	<i>G. oblongifolia</i>	$[\alpha]_D^{25} = +55.4$ (c 0.07, MeOH)

114		oblongifolin T	<i>G. oblongifolia</i>	$[\alpha]_D^{20} = +10.8$ (c 0.05, MeOH)
115		eugeniaphenon <sup>68</sup>	<i>G. eugeniaefolia</i>	$[\alpha]_D^{27} = +41.6$ (c 0.11, MeOH)
116		paucinone D <sup>69</sup>	<i>G. paucinervis</i>	$[\alpha]_D^{27} = +41.6$ (c 0.11, MeOH)
117		18-hydroxy-7- <i>epi</i> -clusianone <sup>70</sup>	<i>H. hypericoides</i>	N/A
118		18-hydroxy-clusianone <sup>70</sup>	<i>H. hypericoides</i>	N/A
119		sampsonione P	<i>H. sampsonii</i>	$[\alpha]_D^{20} = +18.6$ (c 0.022, CHCl <sub>3</sub> )

### 1.9 Medicinal properties of type B endo PPAPs

Until today, many type B PPAPs have been isolated from nature, and most of them have shown potential biological activities. Diseases such as leishmaniasis and

trypanosomiasis caused by parasites are on the rise. In the case of malaria alone, this tropical disease affects more than 300 million people all over the world and this has led to the death of a population of more than 429,000 people in the world in 2015. These diseases are becoming more lethal because of inefficient therapies, the toxicity of drugs, and growing resistance to current therapeutic drugs. For last few years, World Health Organization, WHO, has resorted to combinatorial therapy to deal with malaria because of increasing drug resistance. Artemisinin has been a champion drug for several years to treat malaria.<sup>71</sup> Despite this, there are some evidence that mosquitos are moving toward resistance to artemisinin.<sup>52, 72</sup> Therefore, new drugs are sought in order to win over these diseases, and type B PPAPs could be the ideal candidates. Here, we are giving of account some of them that have drawn the attention of the both biologists and organic chemists.

### 1.9.1 Garcinol and its derivatives

Garcinol and its epimer, isogarcinol, also known as camboginol and isocamboginol, are typical representatives of type B PPAPs (Figure 1.9.1) They are obtained from *Garcinia indica*, a tropical, medium- or small-sized tree with shiny dark green leaves and ovoid fruits, which are red or yellow in color with six to eight seeds embedded in a juicy rind. The plant is abundant on the west coast of India.<sup>73</sup> The dried fruit's rind is used as a gourmet item, kokum curry. Garcinols and its related members like isogarcinol (**70**), cycloxanthochymol, 30-*epi*-cambogin A, and 7-*epi*-garcinols (**98**) have shown very wide rgane of biological activity. Isogarcinol is very interrsting compound because of its wide range of therapeutic index, ranging from colon cancer, leukemia,<sup>74</sup> HIV,<sup>75</sup> medullablastoma,<sup>76</sup> antioxidant,<sup>77</sup> antimicrobial,<sup>75, 78</sup> transplant rejection, autoimmune

diseases like collagen-induced rheumatoid arthritis<sup>79, 80</sup> to breast cancer and Parkinson's disease.<sup>80</sup> Both garcinol and isogarcinol have shown promising biological activities.

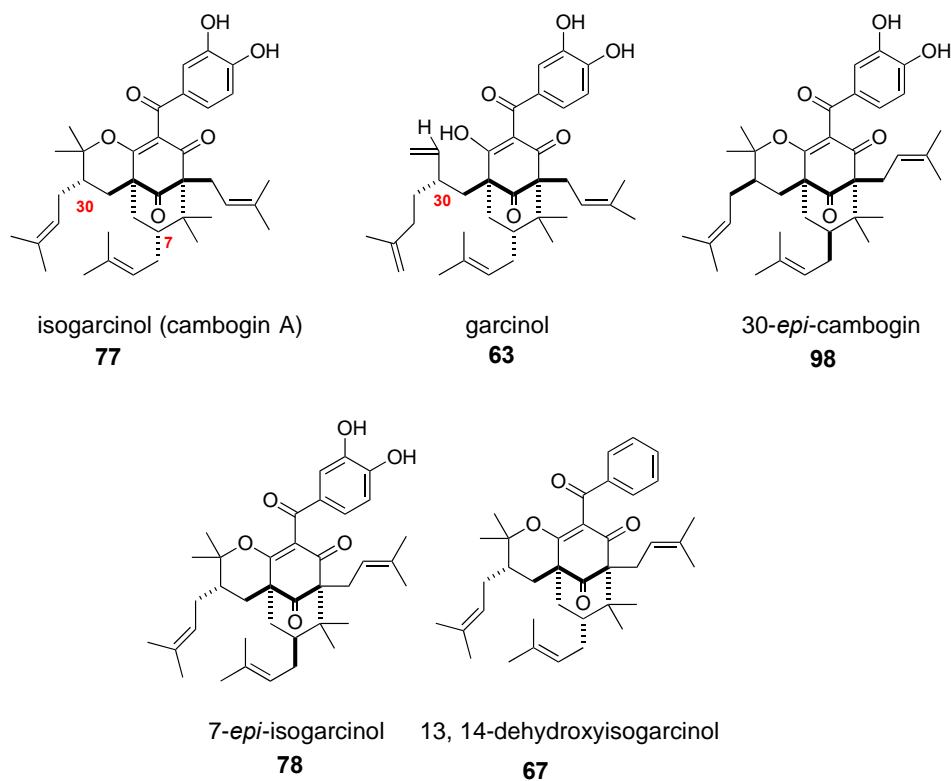


**Figure 1.9.1.** Garcinol and derivatives

Traditionally, fruit rinds of garcinol have been in use for years to treat bowel problems and rheumatism and also available for human consumption in the form of mangosteen drink. Garcinol and isogarcinol are very effective against the methicillin-resistant bacteria *S. aureus* with a comparison to vancomycin. It inhibits the topoisomerase I and II in a concentration comparable to etoposide.<sup>81</sup> It has been known to suppress colonic aberrant crypt foci formation by acting as HATs inhibitors, inducing apoptosis through cytochrome c release, and activating caspases in the human leukemia HL-60 cell. Its antioxidant property is noteworthy. Several experiments have shown that garcinol suppresses superoxide anion, hydroxyl radical, and a methyl radical in H<sub>2</sub>O<sub>2</sub>-NaOH-



DMSO. In spite of an unknown mechanism of the antioxidant property, garcinol is three times more potent than the 2,2-diphenyl-1-picrylhydrazyl (DPPH) and DL- $\alpha$ -tocopherol scavenging activity by weight. Garcinol and its epimer have been shown to inhibit NF- $\kappa$ B activation and a COX-2 expression. In addition, it decreases the iNOS expression and NO release from the LPS-stimulated macrophase by inhibition of the signal transducer and activator of transcription-I. Garcinol and isogarcinol have interesting antiulcer and antibiotic activities against methicillin-resistant *staphylococcus aureus* (MRSA). Garcinol has been shown to inhibit histone acetyltransferase and p300/PCB, a well-known gene regulator<sup>6</sup>.

### 1.9.2 Guttiferone A-F, K, O, P

Guttiferone and its analogs (Figure 1.9.2) are derived from *Garcinia aristata* in the form of a hexane extract from fruit rinds. They show very promising medicinal properties. For example, it has shown anti-HIV, cytotoxic, trypanocidal, antiplasmodial, leishmanicidal,<sup>82</sup> and antibacterial activity.<sup>83, 84</sup> Most recent studies have revealed its substantial neuronal quality and the permeability of the mitochondrial membrane. Guttiferone has shown moderate activity against gram-positive bacterium *S.aureus* but has not demonstrated any discernable activity against *E. coli*, fungi *T. rubrum*, and *C. albicans* in vivo studies as manifested by IC<sub>50</sub>  $\pm$  SD values in  $\mu$ M (Table 1.8.1).<sup>82</sup>

**Table 1.9.1.** Bioactivity of guttiferone A against different virus

	<i>S. aureus</i>	<i>E. coli</i>	<i>T. rubrum</i>	<i>C. albicans</i>
Guttiferone A	7.5 $\pm$ 0.8	>64	19.6 $\pm$ 17.5	64.0

But more interesting results are found in the fight against protozoa, *P. falciparum*—the prime reason for malaria—with IC<sub>50</sub> values lower than 1  $\mu$ M. The

cytotoxicity on the MRC-5 cell showed  $IC_{50}$  value in the range of 1.2  $\mu$ M where the SI value is 24. Although the *in vivo* mechanism of this action has not been discovered for guttiferone A, *in vitro* studies have revealed that it can inhibit cysteine proteases B, papain, serine peptidase cathepsins G, and trypsin because these are present in plasmodium parasites for the development of the host cell. This explains why guttiferone A is lethal in fighting against malaria.

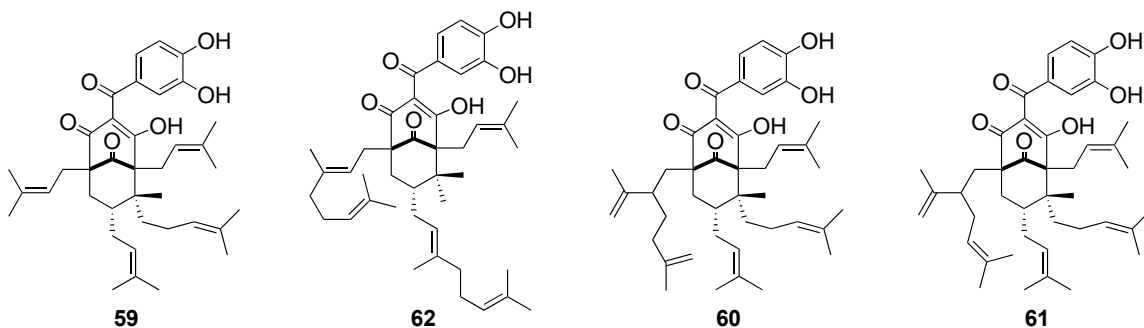


**Figure 1.9.2.** Guttiferones A, E, C, D

In a different study, guttiferone A revealed its role as antineurodegenerative agent by scavenging ROS and thereby protecting the cell against oxidative stress .<sup>85</sup>

Recently, Xin Li's study<sup>84</sup> has demonstrated that guttiferone F (GF) can inhibit the growth of prostate cancer cell lines under serum starvation by inducing the increase in a sub-G1 fraction and DNA fragmentation. By controlling the Bcl-2 protein family, GF promotes the apoptosis targeting mitochondria. It also reduces the expression of an androgen receptor and the phosphorylation of ERK $\frac{1}{2}$  protein, and increases JNK protein phosphorylation and Ca<sup>2+</sup> influx. Therefore, controlling the caloric restriction, GF could be lethal against prostate cancer without much toxicity although the viability of *in vivo* caloric restriction has been a subject of debate. In a different study, guttiferone K (0.1-25  $\mu$ g/mL), like guttiferone A, has revealed its power in protecting protein and lipid degradation by reducing the formation of the carbonyl group and TBARS.<sup>86</sup>

**Table 1.9.2.** IC<sub>50</sub> values on different cell lines of guttiferone F

Cell line	Cell type	IC <sub>50</sub> (μM)
Ln Cap	Prostate cancer	5.17±0.20
Hep G2	Hepatocellular carcinoma	32.92±1.56
HeLa	Cervical cancer	13.13±1,32
CNE	Nasopharyngeal carcinoma	17.97±1.30
PC 3	Prostate cancer	12.64±3.01

Ligand-controlled transcriptional factors are members of a nuclear receptor family that controls embryogenesis, calcium homeostasis, and lipid and glucose metabolism. Guttiferone I has inhibited the binding activity selectively to the LXR  $\alpha$  receptor with an IC<sub>50</sub> at 3.4-nM in a binding assay.<sup>87</sup> Guttiferone O and P have shown inhibitory effects on phosphorylation of the synthetic biotinylated peptide substrate KKLNRTLSVA. These two PPAPs stop this process by the serine/threonine protein kinase MAPKAPK-2 (Figure 1.9.3). The IC<sub>50</sub> value is 22 mM. As a result, these two PPAPs could be potential drugs for inflammatory diseases and cancer.<sup>62</sup>

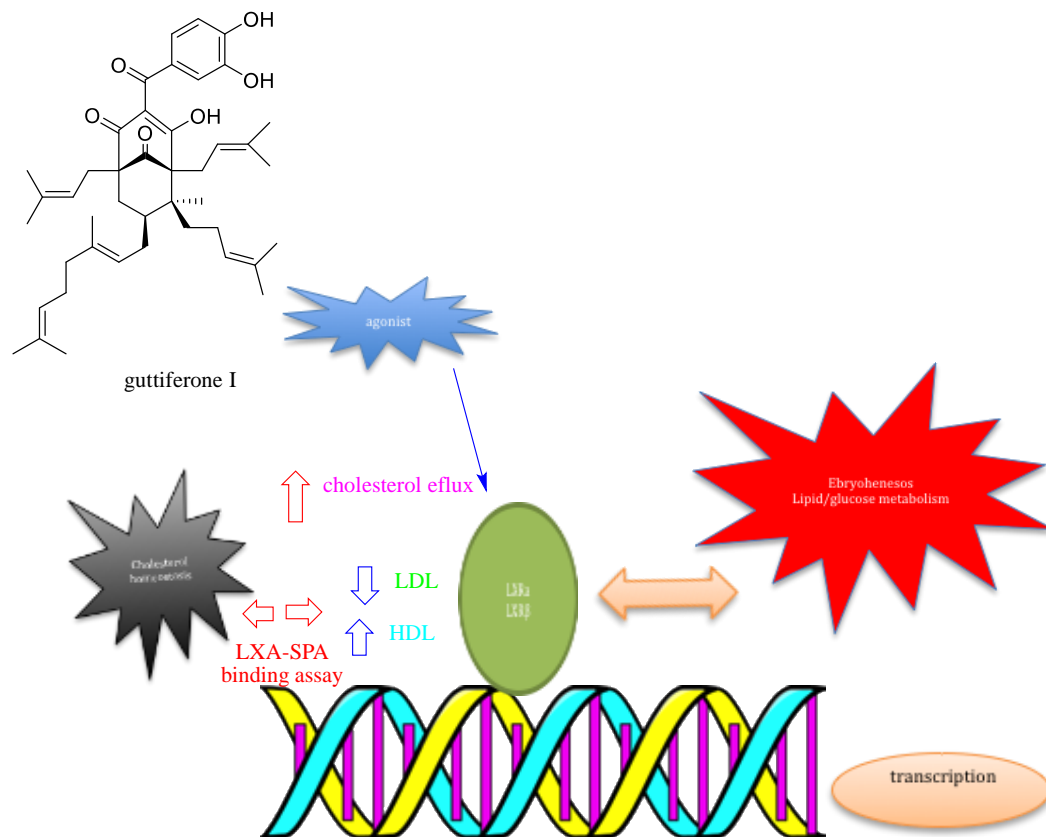


**Figure 1.9.3.** Mechanism of transcription regulation by LXR triggered by guttiferone I<sup>88</sup>

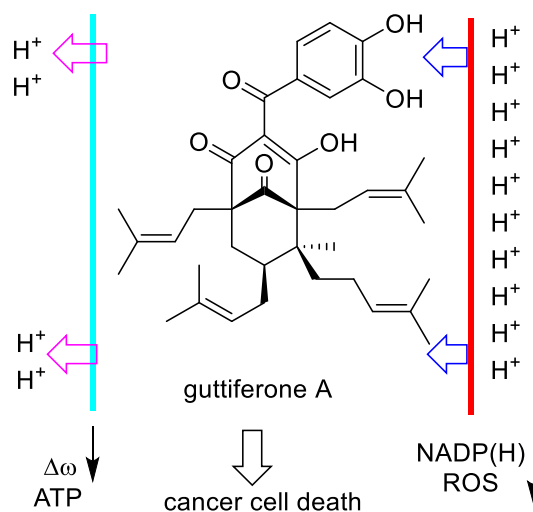


**Figure 1.9.4.** Diagram for cell death mechanism induced by guttiferone A

### 1.9.3 Clusianone and 7-*epi*-clusianone

Clusianone (**9**) is a member of the PPAP family with a wide biologically active profile. It is extracted from the roots of *Clusia congestiflora*. Clusianone, a type B exo

PPAP, and its 7-endo epimer have drawn the attention of scientists because of their extensive medicinal properties, namely, anti-HIV, anti-Epstein-Barr virus, being cytotoxic against HD-MY-Z, K-562, KE-37 tumor cell lines, antimicrobial, antinociceptive, and anti-inflammatories.<sup>89-95</sup>

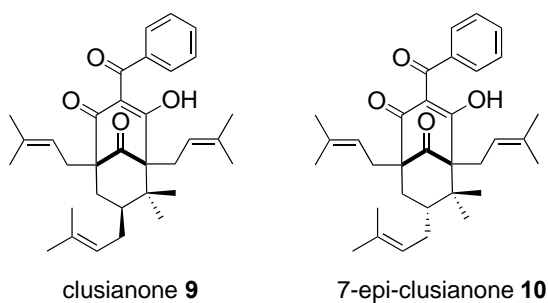


**Figure 1.9.5.** Clusianone and 7-*epi*-clusianone

In the past several years, chemotherapeutic drugs have been in use for treating cancer, and one of the problems of these drugs is that competent cancer cells develop resistance to them, leading to an increase in dose and, ultimately, failure of the treatment. Therefore, scientists are in urgent need to find new types of drugs. Clusianone (**9**) and 7-*epi*-clusianone (**10**) could be alternatives to current therapeutics.

Biologists have shown that 7-*epi*-clusianone could be used to cure lung cancer, which is one of the largest causes of death worldwide. Despite its antiproliferative effects against several tumor cells, 7-*epi*-clusianone's activity against lung cancer cell lines is very promising. Cell lines A549 derived from lung cancer tumors are under investigation in several studies against the activity of 7-*epi*-clusianone. In *in vitro* studies, these results have demonstrated a new understanding of how 7-*epi*-clusianone acts as a potent antiproliferative agent.

Studies done by Marisa Ionta *et al.*<sup>96</sup> showed that 7-*epi*-clusianone has been very effective in arresting the cell cycle in the G1/S transition and promotes apoptosis.

Generally, healthy cells that have wild type P53 arrest the cell cycle in the G1 phase because of the G1 phase check point activation. Conversely, the cells that have mutated or impaired P53 arrest the cell cycle in the G2 phase.

The research conducted by Marisa Inota et al. has shown that *7-epi-clusianone* can activate the G1 check point to arrest the cell cycle of the cancer cells. The results showed that the cell viability was reduced drastically, in a concentration-dependent manner, after 48-hour incubation, indicating an IC<sub>50</sub> value of 16.13 ± 1.12 μM. *7-epi-clusianone* has shown better potency than cisplatin (IC<sub>50</sub> value of 21.71 ± 1.17 μM), the most commonly used chemotherapeutic drug. In a similar study, cytotoxicity of *7-epi-clusianone* was tested against several cancer cell lines like KE-37 (T-cell-leukaemia), K-652 (chronic myeloid leukaemia) and HD-MY-Z (Hodgkin's lymphoma) and daunorubicin was taken as a reference. The result was promising and *7-epi-clusianone* has shown cytotoxicity against these cancer cell lines (Table 1.9.3).

**Table 1.9.3.** Cytotoxicity against cancer cell lines

IC <sub>50</sub> (μmol)			
Compound	KE-37	K-652	HD-MY-Z
<i>7-epi-clusianone</i>	13.6 ± 1.5	11.8 ± 1.3	9.8 ± 1.4
Daunorubicin	0.6 ± 0.01	1.5 ± 0.1	2.1 ± 0.11

Like guttiferone A, *7-epi-clusianone* has shown promising activity against trypomastigotes of *T. cruzi* in vitro with a dose of IC<sub>50</sub> at 518 mM. The result was not very encouraging in the mouse model study because of the ineffectiveness of the drug in vivo. *7-epi-clusianone* has indicated an activity against *Leishmania amazonensis* with an IC<sub>50</sub> value of 19.13 M. The drug, however, has been toxic to mammalian cells.<sup>97</sup> The role of *7-epi-clusianone* as a vasodilator has been known since 1998. The effect of the molecule was

studied on rat model by Cortes and his colleagues. The research group observed an endothelium-dependent vasodilating response at a lower concentration but induced a vasocontractile effect at higher concentrations.<sup>98</sup>

Obesity is a growing concern in the modern world. A current estimation has shown that 30% or more world population are either obese or overweight.<sup>99</sup> *7-epi-clusianone* has revealed its promise to be an alternative to Rosiglitazone, an antidiabetic drug, because of its high hydrophobicity, electrostatic,  $\pi$ -stacking interaction, and hydrogen bonding capacity because of keto functionality. The conclusion was drawn from SAR studies with Rosiglitazone which possesses akin structure to *7-epi-clusianone*, although the latter has fewer OH groups than are essential to potency, as revealed by the docking studies.<sup>100</sup>

Piccinelli et al. have shown that clusianone is active at very low concentration ( $EC_{50} = 0.02 \mu\text{M}$ ) with a reduced therapeutic index, whereas its *7-epimer* has better anti-HIV ( $EC_{50} = 2.0 \mu\text{M}$ ) properties, with an enhanced therapeutic index of 10.<sup>37</sup> The difference between these values is contingent upon the orientation of the C7 prenyl group.

The exact mechanism of action of these two molecule are debated, but Reis et al. demonstrated how the cytotoxicity of clusianone against Hep2 cells ultimately led to apoptosis by specifically targeting the mitochondrial membrane potential (Figure 1.9.6).<sup>101</sup> Their studies indicated that the free enolic OH played an instrumental part in targeting the mitochondrial potential.<sup>89</sup> When the enolic OH was protected as a methyl enol ether, it lost potency.<sup>7</sup> Therefore, it was concluded that the free enolic OH was important to target the mitochondria. The study also showed that the apoptosis was related to the depletion of ATP, which ultimately triggered the cell death (Figure 1.9.6). The similar argument could be put forward in the context of *7-epi-clusianone*, which is a known topoisomerase II inhibitor.

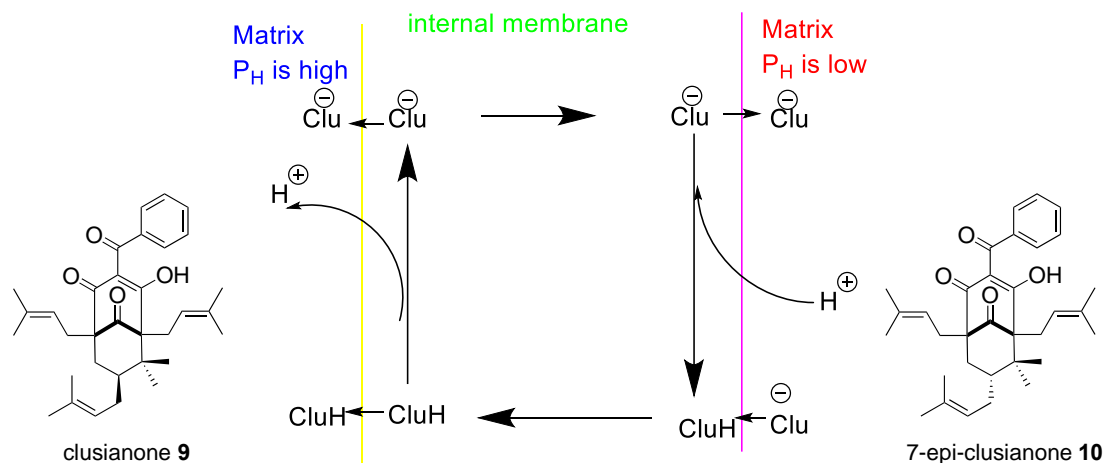


**Figure 1.9.6.** Possible mechanism of action of clusianone

#### 1.9.4 Coccinones A-H

Coccinones A-H were extracted from the latex of *Moronobeia coccinea*. Extracts from the trunk bark and fruit of this tree have revealed encouraging antiplasmodial activity. Coccinone A through H have shown effective activity against chloroquine-resistant *P. falciparum* and have been proven to be cytotoxic to human MRC-5. However, all the coccinones were not equally effective; coccinones A through E were proved to be effective with an IC<sub>50</sub> value in the range of 3.3 to 9 μM. The value surprisingly indicated a typical pattern in the structure of coccinones A-E; all five PPAPs contain a tetrahydropyran ring fused to the bicyclo [3.3.1] nonane. However, coccinones F through H showed a reduced antiplasmodial activity toward *P. falciparum*, having an IC<sub>50</sub> value of more than 10 μM, and these three PPAPs have a free enolic hydroxyl group. On the other hand, in case of cytotoxicity, coccinones that have a free enolic hydroxyl group were noteworthy.<sup>63</sup>



**Table 1.9.4.** Biological activity of coccinones A-H

Coccinone	IC <sub>50</sub> p.f.FcB1 (μM)± SD3	IC <sub>50</sub> MRC 5(μM)
A	4.3±1.3	3.3±0.8
B	5.5±0.4	11.7±0.6
C	9.0±1.2	9.3±1.1
D	7.0±0.9	10.9±0.3
E	4.9±0.7	9.1±1.3
F	17.0±9.4	21.3±2.8
G	19.2±5.9	11.5±0.4
H	16.6±6.1	10.5±0.6
chloroquine	0.078±0.006	25±3.8

### 1.9.5 Symphonones A-I

Symphonones A-I were derived from *Symphonia globulifera* by Marti et al. in a continuing research aimed at finding a better PPAP for treating malaria, a leading cause of death in the developing world. They observed a very similar trend mentioned in the previous section, during their study towards the activity of coccinones against *P. falciparum*. The research group carried out a similar study as they performed with coccinones. Symphonones A through E, and G— which contain either a fused tetrahydropyran or a tetrahydrofuran ring—gave better anti-plasmodium activity than symphonones F, H, and I—have a free enolic hydroxyl group—with IC<sub>50</sub> values ranging from 2.1 to 10.1 μM. The trend was reversed in the case of cytotoxicity; the PPAPs with a free enolic hydroxyl group gave better cytotoxic responses than those PPAPs containing a fused ring attached to the bicyclo[3.3.1]nonane framework.<sup>15</sup>

### 1.10 SAR (structure-activity relationship) studies in type B PPAPs

The wide range of biological activities of PPAPs has inspired several scientists to study SAR on these molecules (Figure 1.10.1). The results from these experiments are

interesting and can lead to new drug discoveries in the future. Several research studies have debated over the importance of a phenyl ring or a phenol moiety in PPAPs for the potency. It is no doubt that presence of the phenyl ring affects the cytotoxicity of PPAP to cancer cell lines. In 2010, Kuo published an article on the cytotoxicity of different PPAPs, namely, garcinialiptone A (a type A), garcinialiptone B, cycloxanthochymol (a type B), and garcinialiptone C (a type C), xanthochymol (a type B), and isoxanthochymol (a type B), having a 2,3-dihydroxy-phenol moiety common in all of them. These compounds were tested against HeLa and WiDr cells. Paclitaxel (Taxol) was used as a positive control in the experiment. The cytotoxic study revealed that all the compounds have a moderate to a borderline activity ( $IC_{50}$  4-5  $\mu\text{g/mL}$  range); interestingly, garsubellin A—which does not have an aromatic ring—has no cytotoxic effect on the cancer cell lines. Although these molecules were less active than paclitaxel but were active against the MDR subline, it was concluded that these six molecules could be potential anticancer agents.<sup>102</sup>

Phenolic compounds are known for their antioxidant activity. The research carried out by Saputri et al. demonstrated that the number of OH groups at the benzene ring influences the antioxidant activity because the phenolic OH groups stabilize the radicals, which are essential for antioxidant activity.<sup>103</sup>

Keto-enol tautomerism is an important phenomenon in PPAPs, which influences cytotoxicity activity of the NPs. The comparative studies repeatedly demonstrated that etherification or cyclization of enolic oxygen diminishes the antioxidant activity.<sup>81</sup> However, the etherification of the phenolic oxygen also reduces the antioxidant activity. If there is more than one phenolic OH, etherification of one the phenolic OH has less impact on the antioxidant activity.<sup>104</sup>

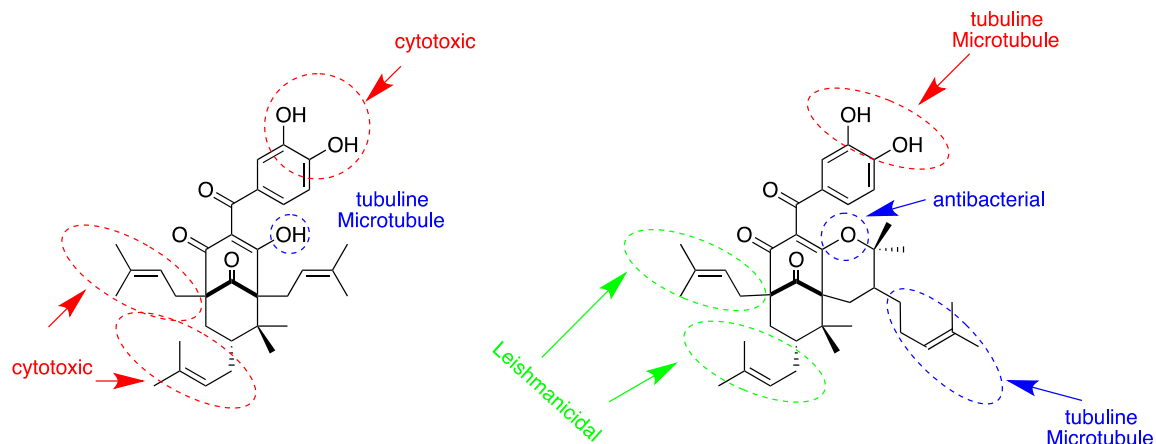


**Figure 1.10.1.** Structure activity relationship of PPAPs

Prenyl groups also play a significant role in SAR.<sup>65</sup> Some research data show that the presence of more prenyl groups increases the potency of the PPAPs against leishmanicidal activity.<sup>105</sup> Pereira's study demonstrated a direct correlation between lipophilic character and leishmanicidal activity of some PPAPs.<sup>97</sup>

The importance of the enolic hydroxyl group in PPAPs has been debated over last decade.<sup>106</sup> In an interesting study, Iinuma established that the presence of an enolic hydroxyl group was necessary for the cytotoxicity against the methicillin-resistant *Staphylococcus aureus*.<sup>107</sup> In that research, the scientists studied five different PPAPs, namely, garcinol, isogarcinol, xanthochymol, isoxanthochymol, and cycloxanthochymol that were obtained from the pericarps of *G. subellipta*. Out of the five PPAPs, only garcinol, and xanthochymol showed strong anti-MRSA activity. The minimum inhibitory concentration or MIC for xanthochymol showed a range of 3.13 to 12.5  $\mu\text{g/mL}$  against MRSA, which was equal to vancomycin, 6.25  $\mu\text{g/mL}$ . Isogarcinol, isoxanthochymol and cycloxanthochymol were found to be less reactive compared to xanthochymol and garcinol. This result suggested that the chelation of the hydroxyl group is necessary for inhibitory activity.<sup>107</sup>

The side chains, like geranyl or lavandulyl or isolavandulyl, and fused rings, like tetrahydropyran and tetrahydrofuran, in PPAPs, also play a significant role in antiplasmodial activities (Fig. 1.10.1).<sup>66</sup> Marti et al. have proposed that the presence of nonpolar side chains contributes to antiplasmodial activity against falciparum FcB1 and cytotoxicity on the human fibroblast cell line MRC5. The studies on symphonones A-I and coccinones A-H have demonstrated a strong correlation in activities with the presence of fused side rings.

Surprisingly, the free enolic hydroxyl group reduced the antispasmodic activity. For symphonones A-H, the IC<sub>50</sub> values ranged from 2.11 to 10.1 μM, which were close to the result obtained on a similar study on *M. coccinea* by the same research group, Marti et al.<sup>71</sup> The result concluded that the presence of a fused ring with the bicyclo[3.3.1]nonane slightly increases the antiplasmodial activity, whereas 7-*epi*-garcinol (**98**), with no fused ring to bicyclo[3.3.1]nonane, showed a reduced potency. These studies show that the presence of an enolic hydroxyl group plays a significant role in the cytotoxicity of the cancer cells, whereas a fused ring attached to bicyclo[3.3.1]nonane is required for antiplasmodial activity.<sup>88</sup>

## 2 Synthetic endeavors towards type B endo-PPAPs

### 2.1 Introduction

Organic chemists have always been impelled by the total synthesis of natural products. This is not only because of the fascinating architectural design of many natural products but also the fact that they provide numerous medicinal benefits. Almost 70% of drugs in the market, for example, have been derived from natural products.<sup>108</sup> Total synthesis also prods synthetic organic chemists, particularly regarding structural revision.<sup>37, 109</sup> For the last six decades, synthetic organic chemists have been learning from and utilizing quintessential works of Woodward, Overman, Corey, Nicolaou, Baran, Stoltz, Sarpong, and numerous others. PPAPs meet the criteria noted above. In some parts of the world, they are used as food garnishing material, while in others they are found in folklore medicine. PPAPs have shown very potent biological activities:

Nemorosone - antibacterial;

Clusianone - antimicrobial and antiproliferative;

Garsubellin A - antineurodegenerative;

Hyperforin - antidepressant (signature member of all PPAPs, popularly known as Saint John's wort).

It is highly encouraging that hyperforin is on the market and sold as Saint John's wort. However, hyperforin has developed some problem because of drug-drug interaction. It has manifested itself by the total number of syntheses reported. Less than 20 of the nearly 200 PPAPs have been synthesized to date. Many research groups were investigating the process of developing a method to construct PPAPs synthetically. In 1999, Nicolaou and his group at Scripps first published a methodology to construct bicyclo[3.3.1]nonane core for garsubellin.<sup>110</sup> Seven years later, Danishefsky's group published the total synthesis of

garsubellin A,<sup>111</sup> and subsequently, a classic divergent synthesis of nemorosone and clusianone.<sup>112</sup> Then came Shibasaki's *ent*-hyperforin synthesis in 2010,<sup>113</sup> which consisted of nearly 55 steps.<sup>114</sup> That was the first enantioselective synthesis of any known PPAP. Since then, numerous research groups have focused on synthesizing different PPAPs or trying to find new, shorter routes to construct these molecules. A few years ago, Maimone's and Shair's groups synthesized hyperforin independently.<sup>115, 116</sup> Recently, Barriault's group also synthesized hyperforin, papuaforin, and nemorosone using gold catalysis. These remarkable syntheses reiterate the importance of total synthesis of PPAPs even today. In all of these cases, the number of steps continued to decrease to less than twelve. There is a commonality in the previously mentioned syntheses: all the molecules are *exo* type A PPAP, except Porco's seminal work on *7-epi*-nemorosone, which was the only *endo* type A PPAP synthetically reported until today.

Much progress towards the total synthesis of PPAPs was made for type A *exo* PPAPs, but syntheses of type B *endo* PPAPs were elusive until 2011. In that year, Plietker's synthesis of an *endo* type B PPAP<sup>117</sup> was the first of this kind and, since then, his group has published the synthesis of several type B *endo* PPAPs.

My research centers on finding a viable route for the total synthesis of *7-epi*-clusianone (**10**), a type B *endo* PPAP. Therefore, syntheses of some type B *endo* PPAPs will be summarized in this section. Although my research focuses on type B *endo* PPAPs, some of the notable syntheses of type A PPAPs, published between 2012–2015, will also be discussed.

My predecessors, Jayasekara and Ciochina, who had worked on the PPAP project before me, wrote elaborately about the syntheses of type A compounds before 2009 in their dissertations.<sup>5, 118</sup> There is no point in rehearsing these details here. At the same time, it is

very tough to resist talking about some of the recently published (post 2010) total syntheses, because these are state-of-the-art. As far as our knowledge of this topic goes, no group has yet reported the synthesis of any type C PPAP. Finally, each of the syntheses is unique, and it will also be interesting to see how these syntheses have resolved the issue of C4 oxidation to install a 1,3-funtionality in the respective molecules.

Organic chemists approach a total synthesis in two ways: one is strategy derived where an organic chemist prudently disconnects a molecule so that they could use the chemistry available to them; the other think of developing a new methodology of a key reaction in the scheme, which could lead to the final target. In the recent years, mostly after 2010, we came across some new interesting methodology developments to synthesize PPAPs. I have summarized some of them here.

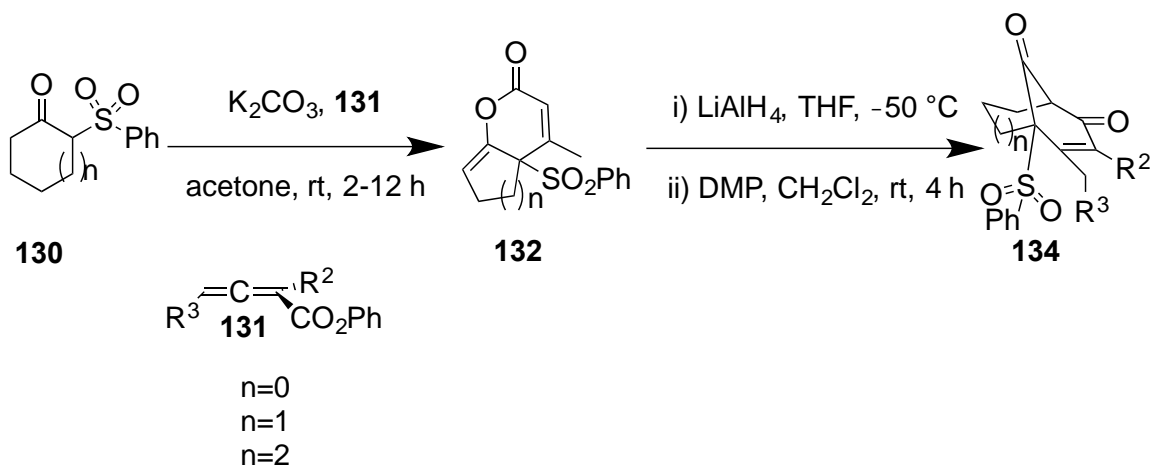
## **2.2 Some newer synthetic strategies for constructing bicyclo [3.3.1] nonane**

In this section, I discuss some new synthetic methodologies that were published in recent years for synthesizing the bicyclo nonane functionality in PPAPs.

### **2.2.1 Annulation approach of allenyl sulphonate esters to make bicyclo nonane by Bhat et al.**

To synthesize bicyclo[3.3.1]nonane, Bhat et al. proposed an annulation of allenyl sulphonate esters (Scheme 2.2.1).<sup>119</sup> Synthetically speaking, the reaction is nothing but an addition to an *sp* carbon atom of an allenyl ester **131**, followed by a reductive aldol condensation. The reaction looks apparently straightforward; however, it proceeds via an enol-lactone intermediate **132**, instead of a bicyclic diketone, which Bhat et al. did not expect. Fortunately, they realized the enol-lactone could be transformed into a

bicyclo[3.3.1]nonane in two-step process via the reductive-aldol reaction. Finally, the aldol product could be oxidized to the bicyclic diketone with an excellent yield.<sup>119</sup>



**Scheme 2.2.1.** Synthesis of bicyclo[3.*n*.1]nonane by Bhat et al.

The research group attempted the methodology over several substrates and found out that the viability of the synthetic route was acceptable. The diastereomeric ratios, however, in some cases, were not excellent, merely an average of 5:3 (Table 2.2.1).

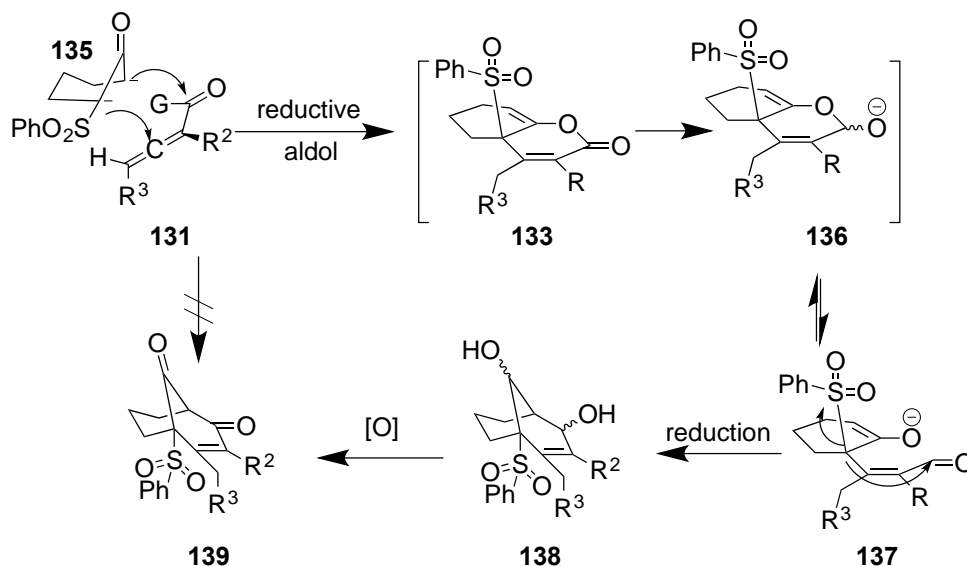
**Table 2.2.1.** Substrate Scope for annulation

Sulphonate ester	Bridged bicycle	Yield
<p style="text-align: center;"><b>133a</b></p>	<p style="text-align: center;"><b>137a</b></p>	45%
<p style="text-align: center;"><b>133b</b></p>	<p style="text-align: center;"><b>137b</b></p>	54%
<p style="text-align: center;"><b>133c</b></p>	<p style="text-align: center;"><b>137c</b></p>	20%



The reaction Scheme 2.2.1 might look promising in constructing a bridged bicyclic compound, the main motif in PPAPs; however, one of the shortcomings is that the construction of a 1,3-diketone functionality that was not addressed in the article. The synthesis of 1,3-diketone functionality could be achieved by oxidizing the vinyl methyl group to carboxylic acid, followed by converting the resulting acid to acid azide which would lead to diketone functionality, thanks to Curtius rearrangement. This strategy can only be applied in the substrate with  $\beta$ -vinyl methyl group, and not the substrates with both  $\alpha$  and  $\beta$  vinyl dimethyl groups. Another problem with the synthesis is that diastereomeric ratio in annulation step is not very high, which might prove to be the Achilles' heel of the scheme.

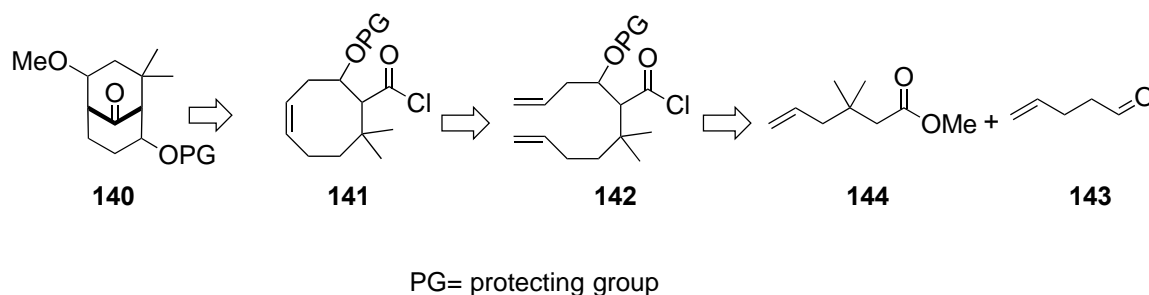
The reaction mechanism for the formation of the bridge bicycle was absorbing and shown below (Scheme 2.2.2). It started off with the nucleophilic attack of sp carbon of allenyl ester **131** by the enolate from **135** via a reductive aldol fashion. The reaction ultimately furnished enolate **137** that kicked off the sulphonate group, and then reduction to generate the diol **138**. The final oxidation of **138** brought forth the bridge bicycle **139**.



**Scheme 2.2.2.** Mechanism of annulation strategy

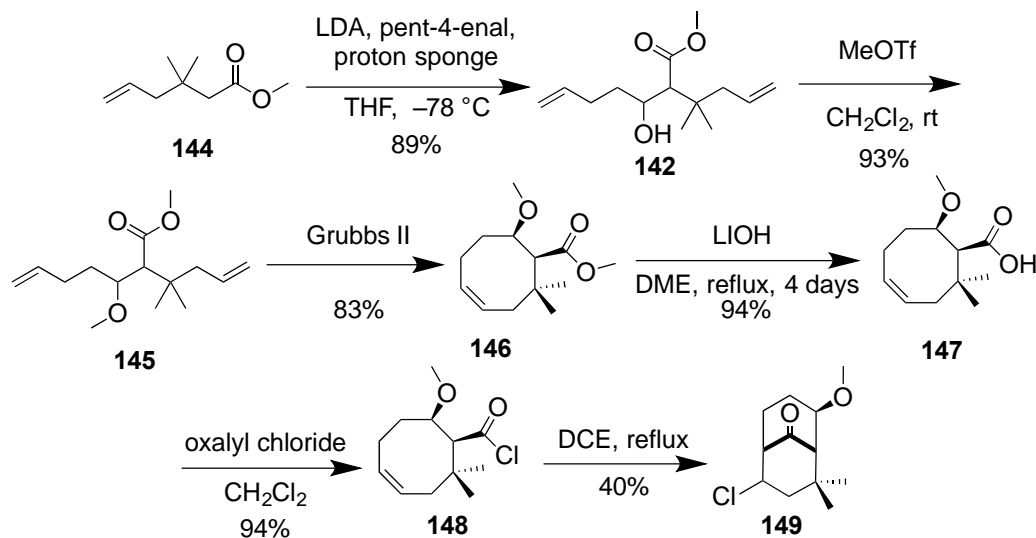
## 2.2.2 Metathesis-acylation approach to construct bicyclo [3.3.1] nonane

In 2014, S. Schmitt et al. proposed a new synthetic methodology for constructing a bicyclic core of PPAPs using a ring-closing metathesis and a transannular cyclization of the acid chloride.<sup>120</sup> According to Schmitt et al. plan (Scheme 2.2.3) that compound **140**



**Scheme 2.2.3.** Retrosynthetic analysis of bicyclo[3.3.1]nonane by Schmitt et al.

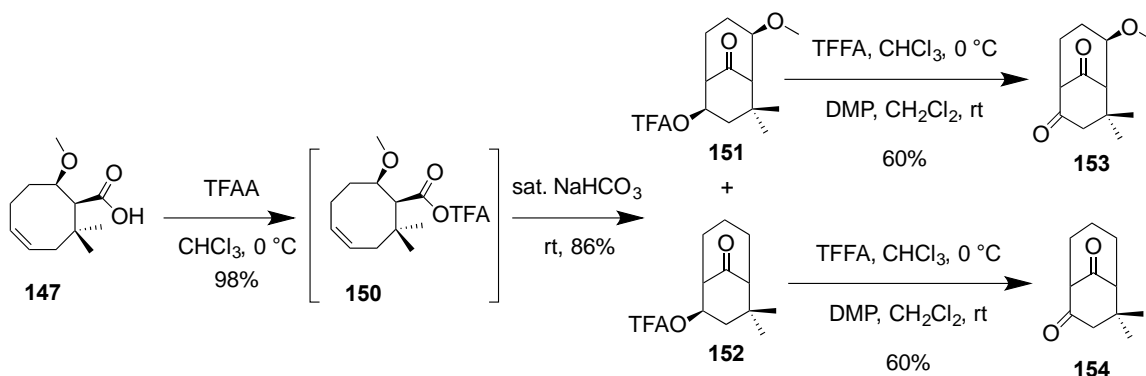
envisioned, retrosynthetically, by a disconnection from cyclooctene acid chloride **141**, which could be synthesized by Grubbs' metathesis of the ester compound **145**, furnished by a  $\text{TiCl}_4$ -catalyzed Sakurai reaction between pent-4-enal **143** and 4-methyl-2-oxo-3-pentenitrile **144**. Sakurai reaction yielded an ester **142** with an 89% yield. The resulting alcohol was protected as methyl ether **145** with an excellent yield of 93%. The protected methyl ether set the stage for Grubbs' metathesis, which underwent with an impressive, thanks to the gem-dimethyl effect. For a transannular ring closer of an acid chloride, cyclooctenemethyl ester **146** was required to be hydrolyzed to acid **147**, and this reaction was proved to be tough to accomplish because of the gem-dimethyl group next to the tetrahedral carbon.



**Scheme 2.2.4.** Synthesis of bicyclo [3.3.1] nonane by Schmitt et al.

However, the research group found a harsh condition: refluxing ester **146** in DME, in the presence of LiOH and water, for four days yielded the acid, which was converted into acid chloride **148**. This acid chloride then set the transannular ring closer that furnished **149** with a poor yield in the presence of  $\text{AlCl}_3$ ; however, the corresponding acid chloride in DME at 21 hours of reflux yielded the required bridge bicycle. The reaction yielded both exo and endo diastereomers in an 18:1 ratio (Scheme 2.2.4). The current plan unambiguously showed that the reaction had some problem, and Schmitt et al. realized that instead of acid chloride, the acid anhydride would better serve the purpose for the transannular ring closer. Moreover, it turned out as per expectation; the mixed anhydride of the TFA salt of the acid, in situ, furnished the exo diastereomer exclusively at  $0\text{ }^\circ\text{C}$ , and the yield of the reaction increased to a 98% (Scheme 2.2.5). The next task was to complete the synthesis of the model compound and therefore, the TFA compound was cleaved into two diastereomeric alcohols that were treated with  $\text{NaHCO}_3$  to remove TFA, and then oxidation of the resulting alcohol yielded **152**. The next challenge was to install 1,3-diketone functionality in the molecule to finish the synthesis. Schmitt et al. have not offered

such a route in their present scheme. This might be a major problem for the applicability of the route.



**Scheme 2.2.5.** Modified approach to bicyclononane by Schmitt

### 2.3 Domino Michael-aldol approach by Alexakis

We have seen many PPAPs with a bicyclo[3.2.1]octane core. Lalibinone A, enaimeone A, and liliflodione are few examples of such PPAPs that contain a bicyclo[3.2.1]octane scaffold (Figure 2.3.1). This was the inspiration for Alexakis et al. to propose a domino Michael–aldol reaction strategy to construct a bicyclooctane motif.

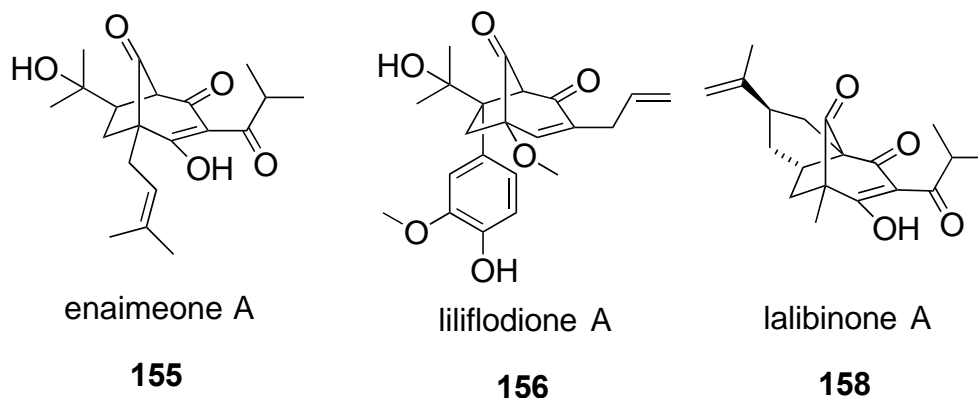
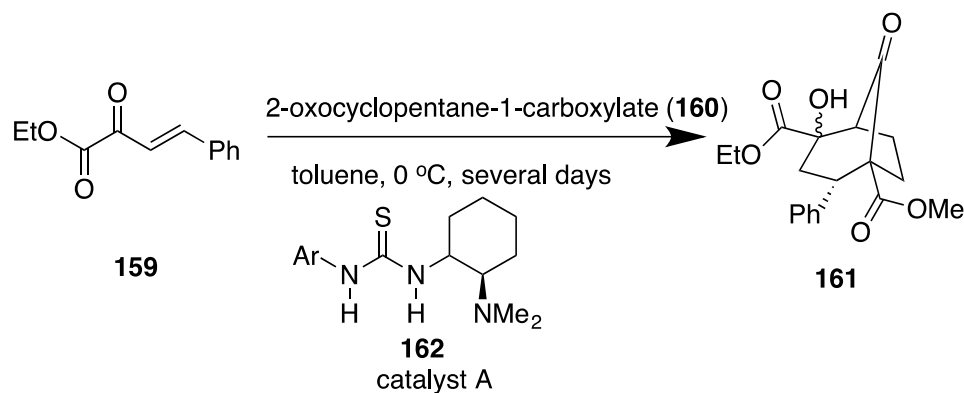


**Figure 2.3.1.** PPAPs family having bicyclo [3.2.1] octane cores

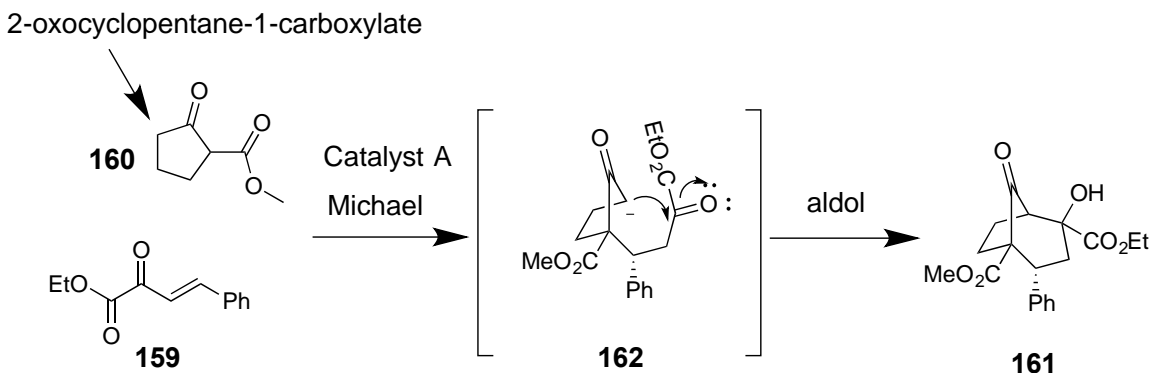
Alexakis et al. planned to accomplish a bicyclo[3.2.1]octane core in a step using tandem Michael/aldol reaction (Scheme 2.3.1). They chose a bifunctional catalyst **160** after screening cinchona alkaloid and urea derivatives. However, to make an octane scaffold,

they needed a five-carbon unit, which came from a cyclopentanone derivative, and a three-carbon unit, which came from ethyl (3E)-2-oxo-4-phenyl-3-butenate **159**.



**Scheme 2.3.1.** Synthetic scheme for domino Michael–aldol reaction by Alexakis et al.

With this plan in mind, they applied the condition of domino Michael–aldol reaction to ethyl (3E)-2-oxo-4-phenyl-3-butenate **159** and methyl 2-oxocyclopentane-1-carboxylate **160** catalyzed by urea-based bifunctional catalyst (Figure 2.3.2). The reaction yielded the bicyclo[3.2.1]octane with four stereocenters with an excellent diastereoselectivity; however, the enantioselectivity was not impressive (Scheme 2.3.2). Using other bifunctional catalysts, namely, **163**, **164**, and **165**, the improvement in enantioselectivity did not increase, even using a 20 mol% catalyst in the reaction.



**Scheme 2.3.2.** Probable mechanism for domino Michael–aldol reaction

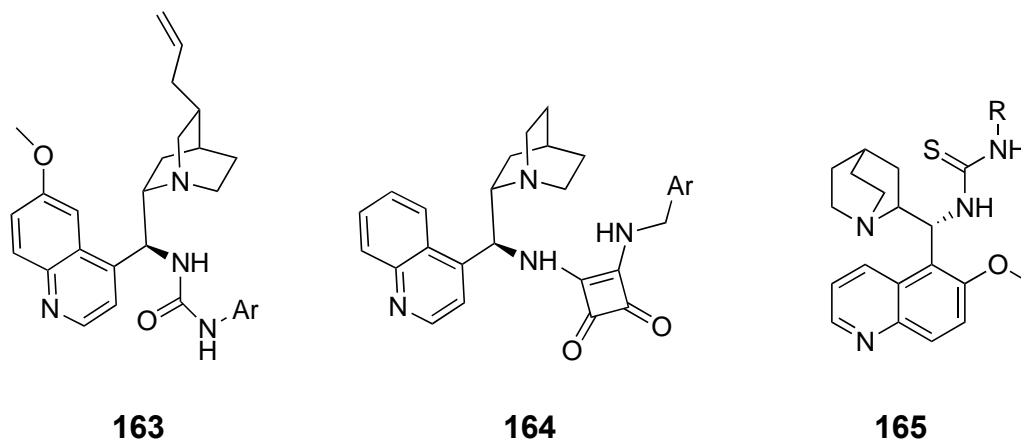


**Figure 2.3.2.** Bifunctional catalysts

With this plan in mind, they applied the condition of domino Michael–aldol reaction to ethyl (3*E*)-2-oxo-4-phenyl-3-butenolate **159** and methyl 2-oxocyclopentane-1-carboxylate **160**. The catalyst used in the reaction was a urea-based bifunctional catalyst (Figure 2.3.2). The reaction yielded the bicyclo[3.2.1]octane with four stereocenters with an excellent diastereoselectivity; however, the enantioselectivity was not impressive. Using other bifunctional catalysts, namely, **163**, **164**, and **165**, the enantioselectivity did not increase, even using a 20 mol% catalyst in the reaction.

#### 2.4 Syntheses of (+)-30-*epi*, (–)-6-*epi*, and (±)-6,30-*diepi*-13,14-didehydroxy-isogarcinol by Porco et al.

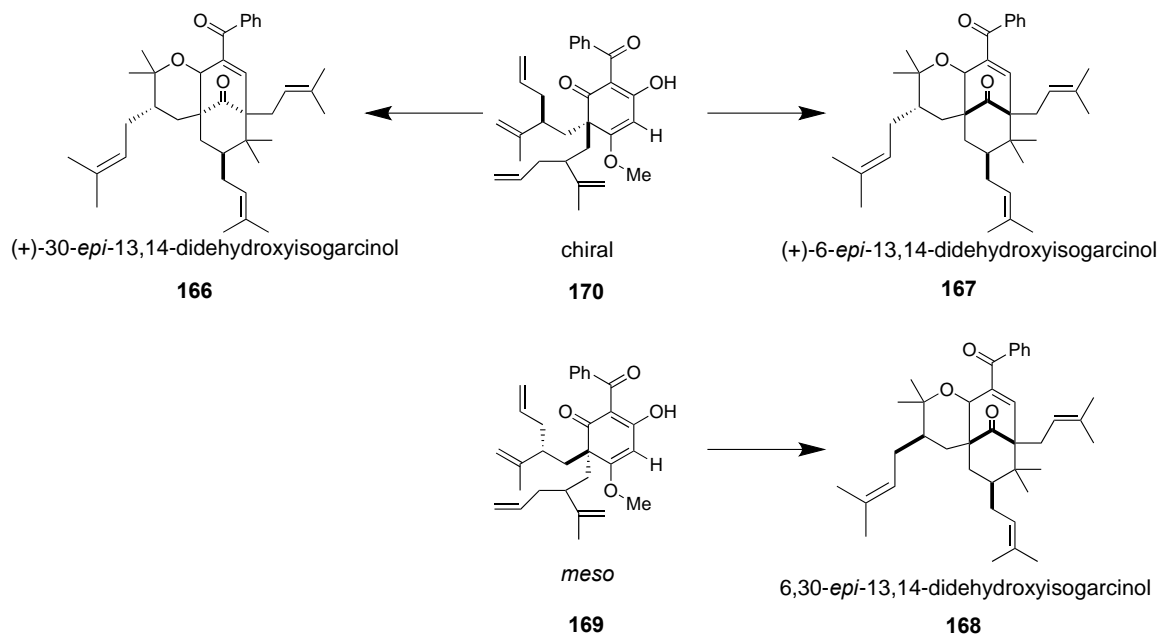
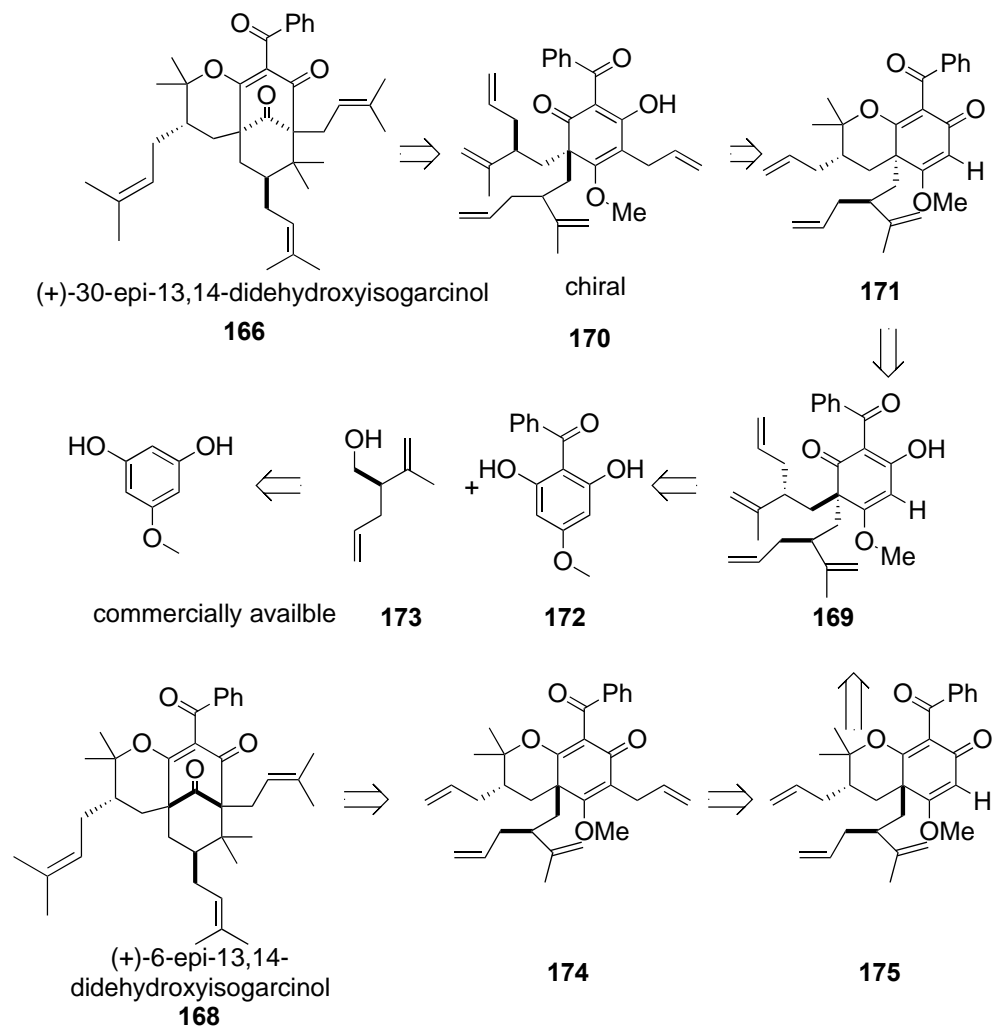


**Figure 2.4.1.** Several target didehydroxyisogarcinols

Impressed by the therapeutic index of 13,14-didehydroxyisogarcinol, namely, potent against leukemia, colon cancer, HIV, medulloblastoma, autoimmune disease, Porco and his research team devised a scheme to synthesize different series of nonnatural diastereomers of 13,14-didehydroxyisogarcinols.<sup>121</sup> His group is famous for dearomatizing annulation, a thoughtfully crafted strategy that had already delivered some remarkable syntheses.<sup>122-124</sup> However, he wanted to synthesize three different molecules, (+) 30-*epi*-, (–)-6-*epi*-, and (+)-6,30-*diepi*-13,14-didehydroxyisogarcinols, from a common intermediate, either **170** or **169**, and to achieve that he needed another strategy—that could fulfill his goal—which is called diastereoselective, Lewis-acid-controlled cyclization. In many ways, the approach is partly reminiscent of Nature’s strategy to synthesize PPAP molecules from a common intermediate; that is, we see Nature manufactures type A and type B PPAPs from a common cationic intermediate via a diastereoselective carbocationic cyclization (Scheme 2.4.1).



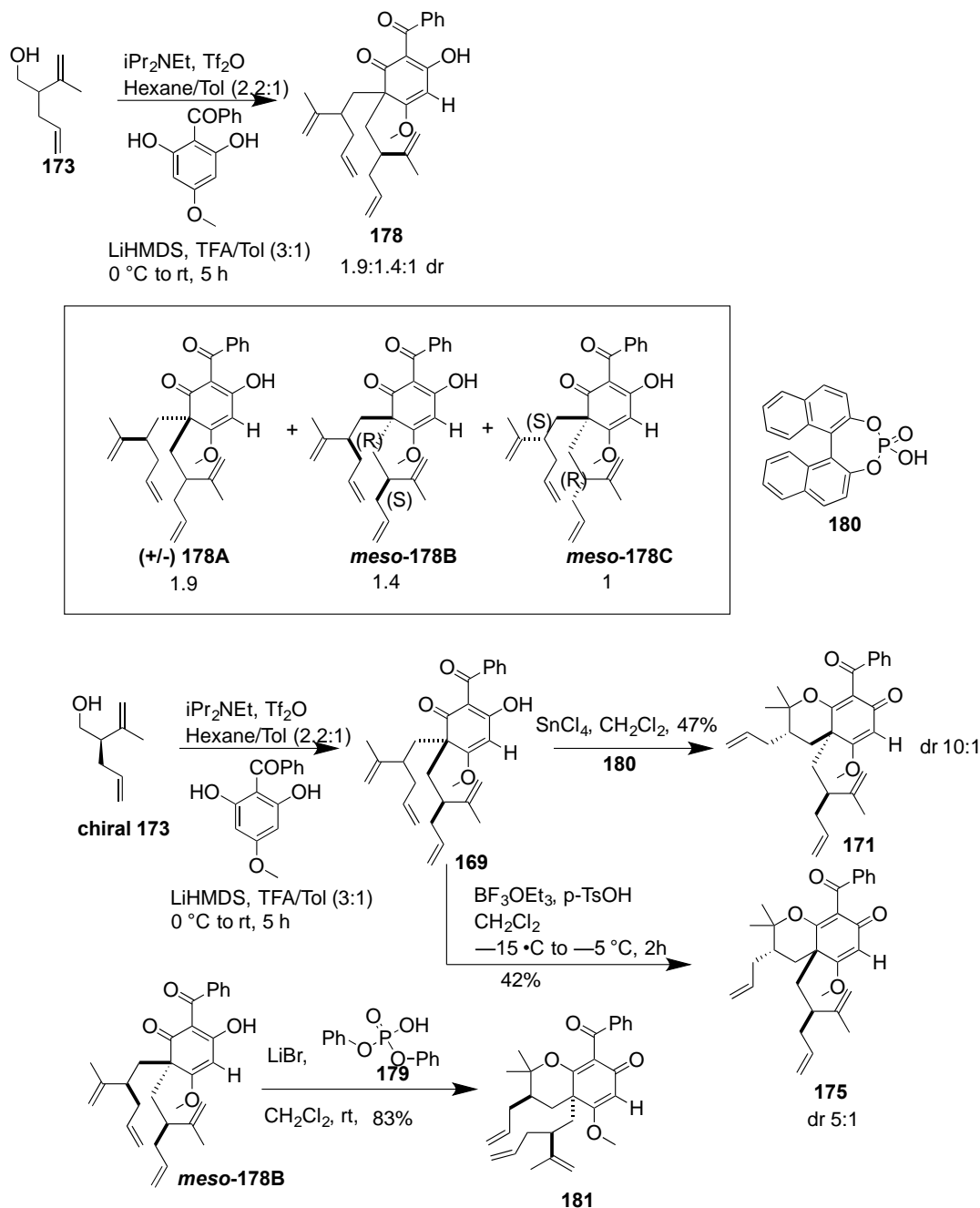
**Scheme 2.4.1.** Retrosynthetic analysis of (-)-6-*epi* and (+)-30-*epi*-13,14-didehydroxyisogarcinols

### 2.4.1 Retrosynthetic analysis of *epi*-didehydroxyisogarcinols

The retrosynthetic analysis (Scheme 2.4.1) of **166** and **168** started from a diastereoselective cationic cyclization and metathesis from chiral intermediates **170** and **174** respectively.<sup>125</sup> Compounds **170** and **174** could be synthesized from **171** and **175** respectively via vinylic alkylation using higher order cuprate chemistry. **171** and **175** could be accessed from a common intermediate **169** via a diastereoselective cationic O-cyclization, which is the crucial step in the whole total synthesis, because (+)-30-*epi*- and



(-)-6-*epi*-13,14-didehydroxyisogarcinol diverged from this intermediate, **169**. Regioselective dearomative cyclization of **172** with alcohol **173** would provide **169**, and on the other hand, alcohol **173** could be synthesized from a commercially available starting material, ethyl 3-methyl-2-butenate, whereas **172** could be prepared from commercially available phloroglucinol **174** via Friedel-Crafts acylation.



**Scheme 2.4.2.** Syntheses of bisalkylated didehydrobenzopyrans

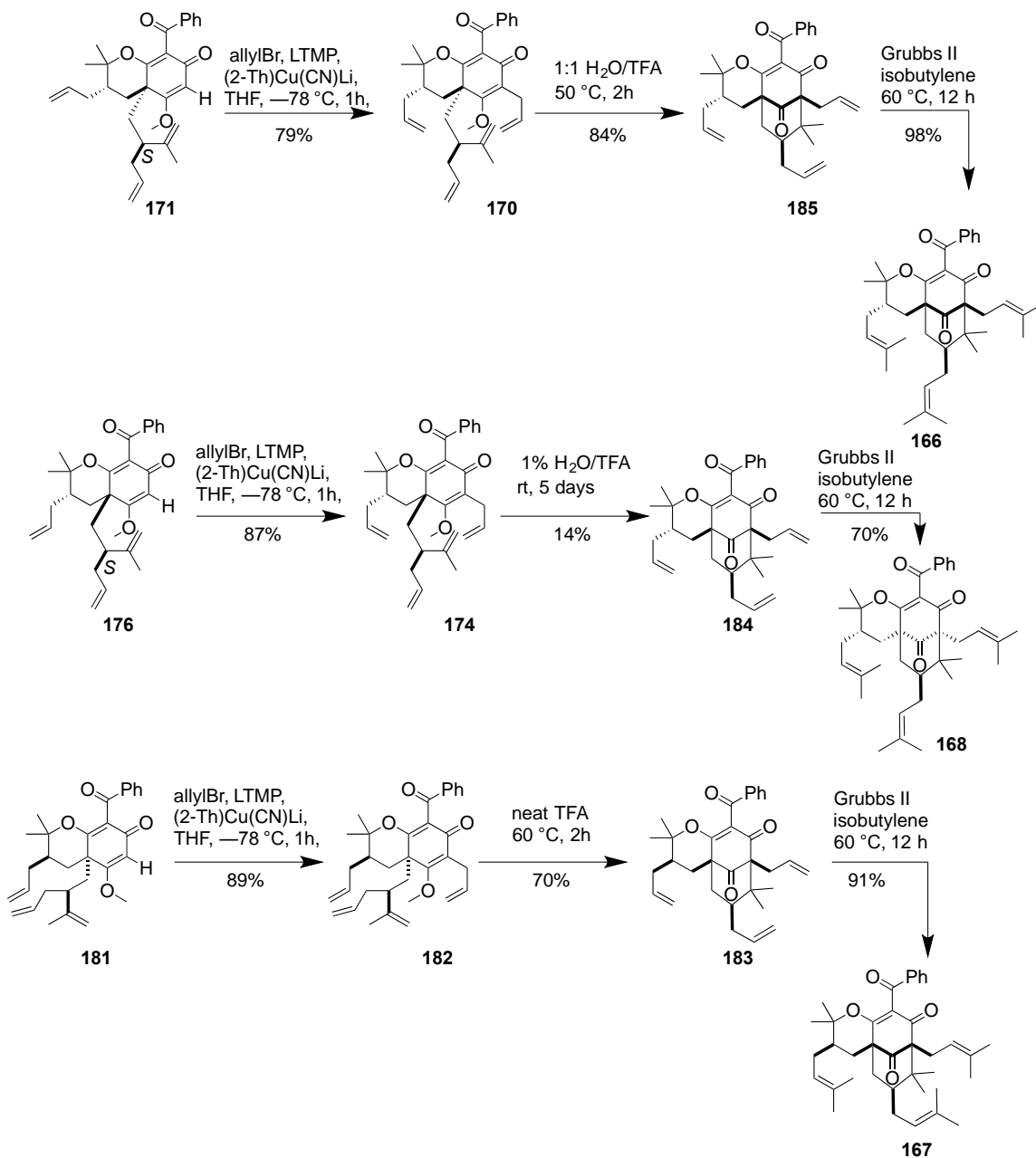
## 2.5 Synthesis of (+)-6-*epi*, (+)-30-*epi*-13, 14-didehydroxyisogarcinols

The synthesis started with the regioselective alkylation of **172** with the triflate derivative of racemic alcohol **173** in the presence of LiHMDS (Scheme 2.4.2). The reaction produced three dearomatized enols, namely, **178A**, **178B** and **178C** in a diastereomeric

ratio of 1.9:1.4:1. Out of these three enols, **178A** is a racemic enol, whereas **178B** and **C** are *meso*/ achiral, and their structures were confirmed by X-ray crystallography. From pure enantiopure alcohol of **173**, after regioselective alkylation, the reaction brought forth enantiopure **169**. Intermediate **169** then set the stage for diastereoselective Brønsted/Lewis acid-base carbocyclization. Porco and his group found the right conditions to get the desired diastereomers from the same intermediate. Use of SnCl<sub>4</sub>/phosphoric acid combination produced a single enantiomer, **171**, with a 10:1 dr, whereas BF<sub>3</sub>-OEt<sub>3</sub> furnished **175** with a 5:1 dr. To get two different enantiomerically pure single diastereomers from an enantiomerically pure single diastereomer, Porco needed a reagent that could differentiate between two diastereomeric alkenyl appendages in **169**, based on the rate of protonation. In one case, he found that **169** reacted with SbCl<sub>5</sub>/ phosphoric acid and produced **171** that would lead to (+)-6-*epi*-13,14-dehydroisogarcinol, whereas BF<sub>3</sub>-OEt<sub>3</sub> combination reacted with **169** to produce **175**, which would lead to (+)-30-*epi*-13,14-dehydroisogarcinol.

The acidity of a Brønsted acid increases upon the addition of a Lewis acid, and this increased acidity also restricts the release of H<sup>+</sup>, depending on the accessibility of a protonating center. This property was exploited in this cyclization reaction for the construction of the pyran ring. Authors gave a detailed account of computational studies to explain this result with the help of several reaction trials, using different Brønsted/ Lewis acid combination. Deprotonation of the pyranodienones α-H in **171**, **175** and **181** with Li (2-Th)<sub>2</sub>Cu(CN)Li and then, reacting with allyl bromide furnished **170**, **174** and **182** in a good yield. The next critical step was to convert pyradienones, **170**, **174**, and **182**, into bicyclo[3.3.1]nonane trione cores **185**, **184** and **183** respectively. The formation of (–)-6-*epi*-13,14-didehydroisogarcinol from **185**, and similarly, (±)-6,30-*epi*-13,14-

didehydroxyisogarcinol from **183** did not pose as much of a challenge as for (+)-30-*epi*-13,14-didehydroxyisogarcinol from **184**. In the previous two cases, TFA/H<sub>2</sub>O in a 1:1 ratio at 60°C smoothly converted the pyradinones to bicyclo[3.3.1]nonane, giving rise to **166** and **168** in impressive yields (Scheme 2.5.1).



**Scheme 2.5.1.** Finishing the total synthesis of (+)-6-*epi*- and 30-*epi*-13,14-didehydroxyisogarcinol

The axially oriented allyl group at C6, generated from **174**, increases the energy of the transition state as shown in (Figure 2.5.1) by clashing with benzoyl group in **T<sub>1A</sub>**. There is no such unfavorable interaction in **T<sub>2A</sub>**, leading to product **183**. In neat TFA, compound **174** produced O-alkylated product **184A** as a major product in addition to the required C-alkylated product. However, in the presence of water, the diastereomeric cationic carbocyclization favored C-alkylation product with a low yield. The amount of water was very critical for this transformation, which could favor the reaction toward either **184A** or **184** (Figure 2.5.1). Fortunately, 1% water in TFA proved to be the ideal condition for the reaction, which gave the correct diastereomer **184**, with a low yield of 14%. Surprisingly, the reaction took 5 days to complete, and the prolong reaction time could be another reason to the increased amount of O-alkylated product **184A** (Scheme 2.5.2).

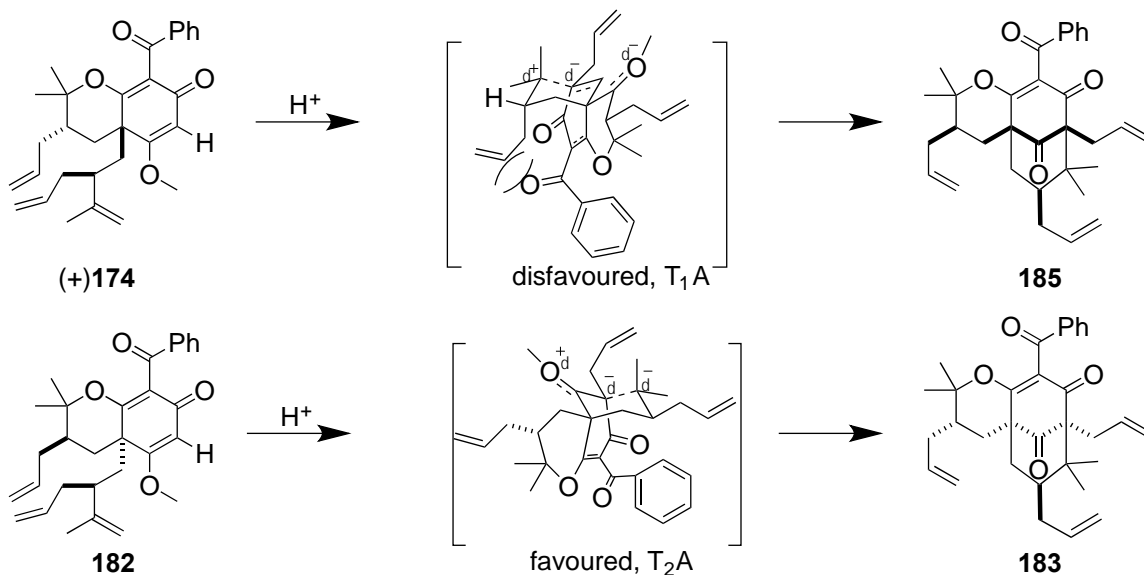
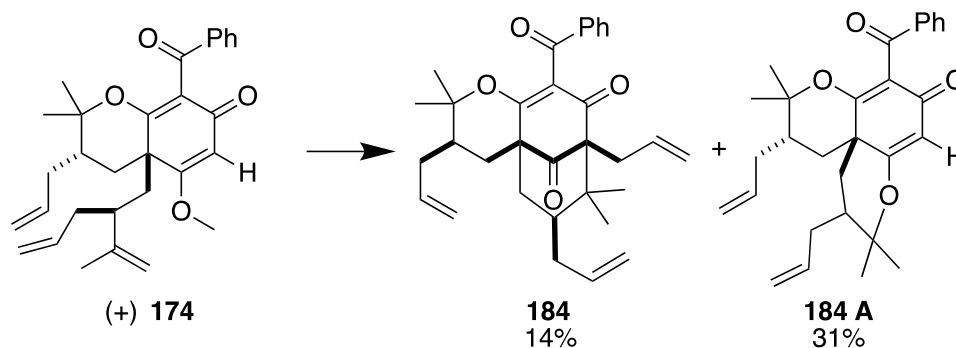


**Figure 2.5.1.** Transition state model for cyclization

The axially oriented allyl group at C6 in **T<sub>1A</sub>** (Fig. 2.5.1), generated from **174**, increases the energy of the transition state by clashing with benzoyl group. There is no such unfavorable interaction in **T<sub>2A</sub>**, leading to product **183**. In neat TFA, compound **174**

produced O-alkylated product **184A** as a major product in addition to the required C-alkylated product. However, in the presence of water, the diastereomeric cationic carbocyclization favored the C-alkylation product with a low yield (Scheme 2.5.2).



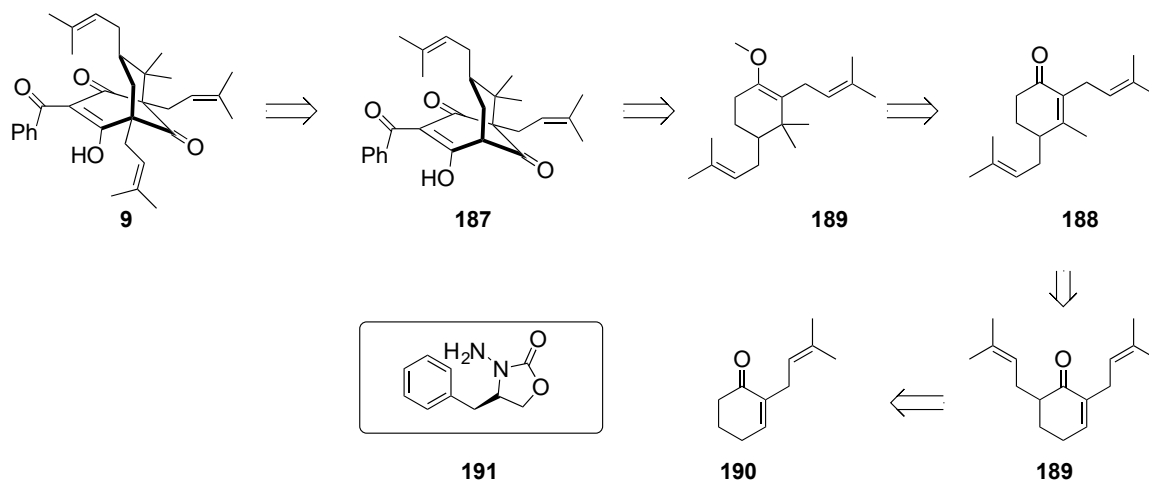
**Scheme 2.5.2.** By-product formation

Finally, global Grubbs' metathesis of **185**, **184** and **183** produced **166**, **168** and **166** with an excellent yield of 98%, 70% and 91% respectively.

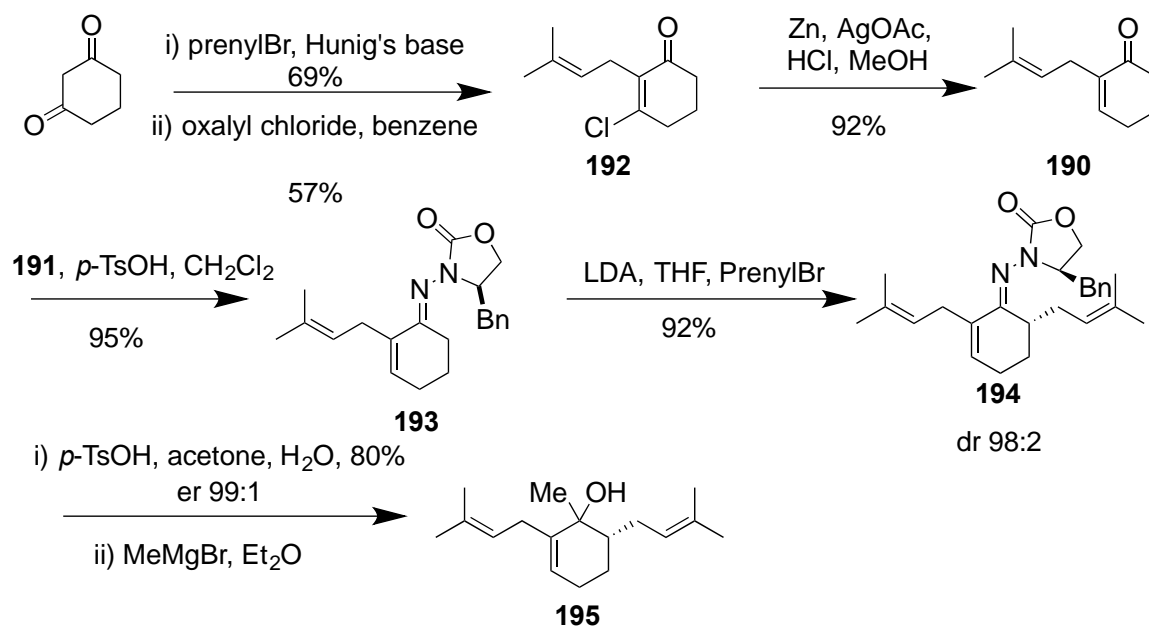
## 2.6 Total synthesis of natural analogs of (+)-clusianone by Coltart et al.

Coltart and his research group at Duke University were intrigued by PPAPs because of its synthetic challenges and medicinal properties. Subsequently, his group came up with  $\alpha$ -alkylation of chiral *N*-aminocarbamate derived hydrazones **191** strategy to synthesize enantiomerically pure  $\alpha$ -alkyl cyclohexanones **187** to synthesize some of the PPAPs.<sup>126</sup> The idea behind the route was that chiral auxiliary would react rapidly with ketones to furnish corresponding hydrazones, which later would undergo deprotonation by the strong base to an *aza* enolate to install prenyl group at  $\alpha$  to the ketone and this  $\alpha$ -ketone would, then cyclize with malonyl dichloride to construct bicyclo[3.3.1]nonane. With this idea in mind, the group disconnected the  $\alpha$ -prenyl group at C3 from **9** to produce **187** (Scheme 2.6.1). The reason behind this disconnection was that Danishefsky showed that the late stage bridgehead alkylation was possible. **187** could be obtained from **189** by a base-

mediated ring closer with malonyl dichloride. **189** could be synthesized from **188** by 1,4-Michael addition to the  $\alpha, \beta$ -unsaturated double bond followed by a methyl enol formation. The conjugated ketone **188** could be furnished from **189** with a LDA mediated prenylation of hydrazone of **190** in good yield.



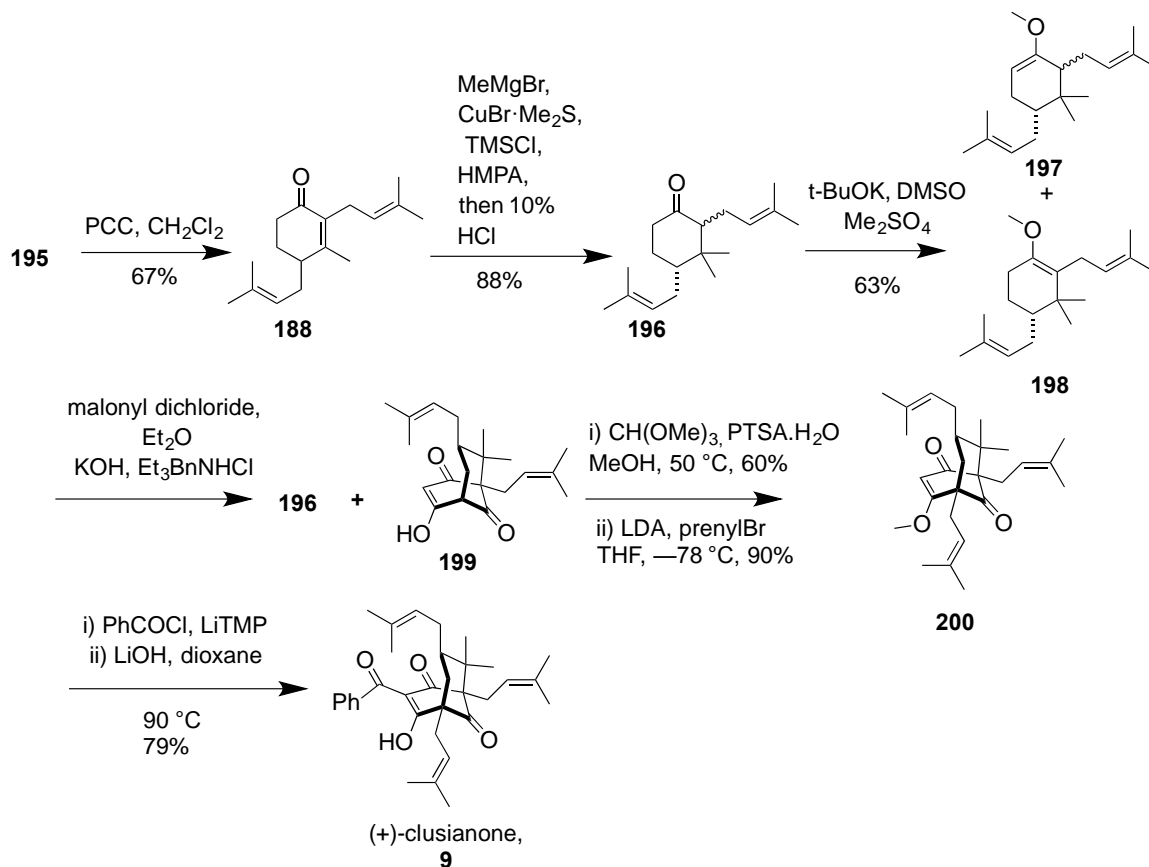
**Scheme 2.6.1.** Retrosynthesis of (+)-clusianone by Coltart



**Scheme 2.6.2.** Synthesis using enantioselective alkylation

Synthesis commenced with a mono-alkylation of 1,3-cyclohexanedione with prenyl bromide in the presence of a Hunig's Base, affording a prenylated enol ether (**Scheme**

2.6.2). Oxalyl chloride converted to vinyl chloride **192**. **192** was dechlorinated with Zn in AcOH in the presence of AgOAc to **190**. The ketone, **190**, formed a hydrazone **193** with **191** and alkylated with prenyl bromide by LDA to yield **194** with a high chiral induction of 98:2 dr. The removal of the chiral auxiliary with *P*-TsOH produced **195** with a high er of 99:1.



**Scheme 2.6.3.** Finishing the total synthesis of (+)-clusianone

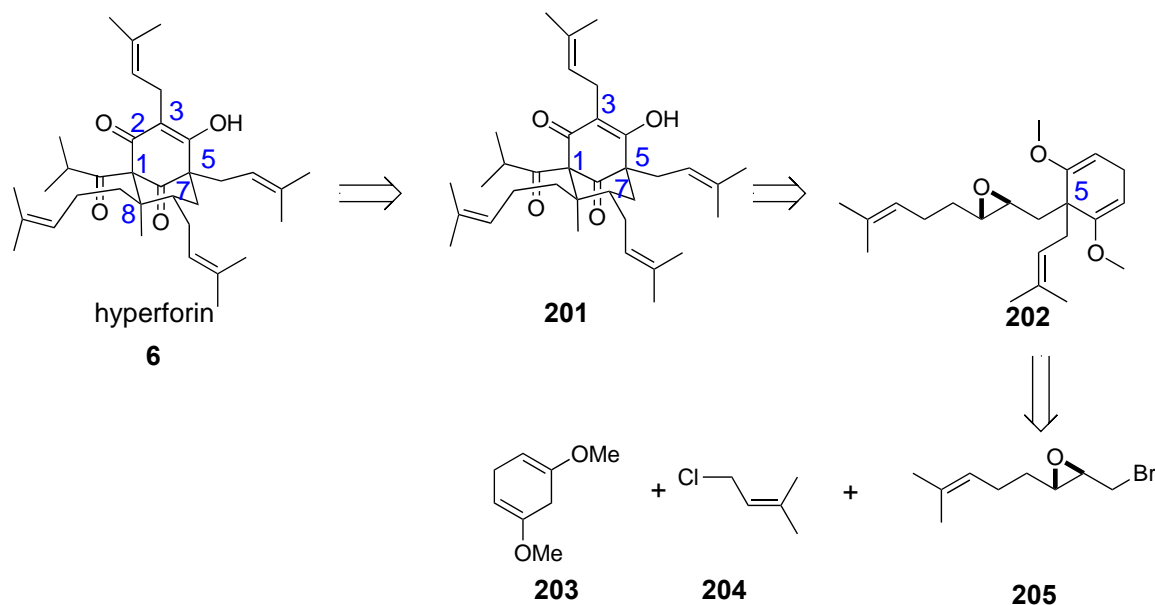
The next two steps were the nucleophilic addition of MeMgBr to the product from **194** to produce alcohol **195** and subsequent allylic rearrangement of that alcohol catalyzed by PCC to furnish **188** (Scheme 2.6.3). Methylmagnesium bromide added a methyl group to **188** in the presence of CuBr·Me<sub>2</sub>S to provide **196** with an impressive yield of 85%. The base mediated methylation of **196** resulted in isomeric enol ethers, **197** and **198**, and



subsequently the ring closing by Effenberger cyclization, with malonyl dichloride PTC, and benzyl triethyl ammonium chloride, afforded the desired bicyclo[3.3.1]nonane **199** plus **196**. Compound **199** was converted into its methyl enol ether in two steps. A bridgehead allylation with LDA and allyl bromide produced **200**. Finally, acylation at C3 with benzoyl chloride, LiTMP, and hydrolysis of the methyl enol ether with LiOH in dioxane built a natural analog of (+)-clusianone **9**, in 79% yield in the final step (Scheme 2.6.3).

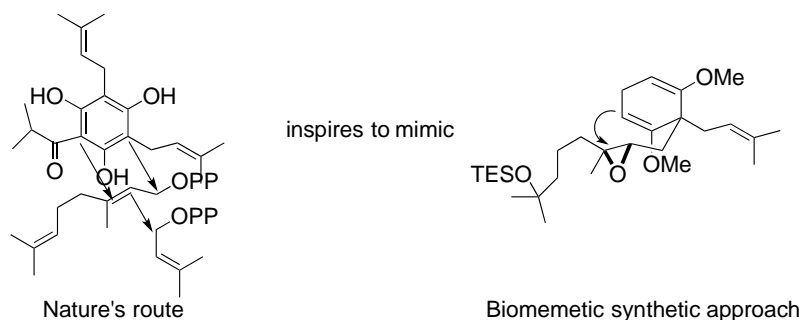
## 2.7 Total synthesis of (±)-hyperforin by Shair

Two years after Shibasaki's hyperforin synthesis, in the year of 2012, Matt Shair's group proposed a biomimetic approach towards hyperforin<sup>116</sup> and a successful synthetic route comprised of 18 steps, bringing it down 33 steps from Shibasaki's synthesis, which required 51 steps.



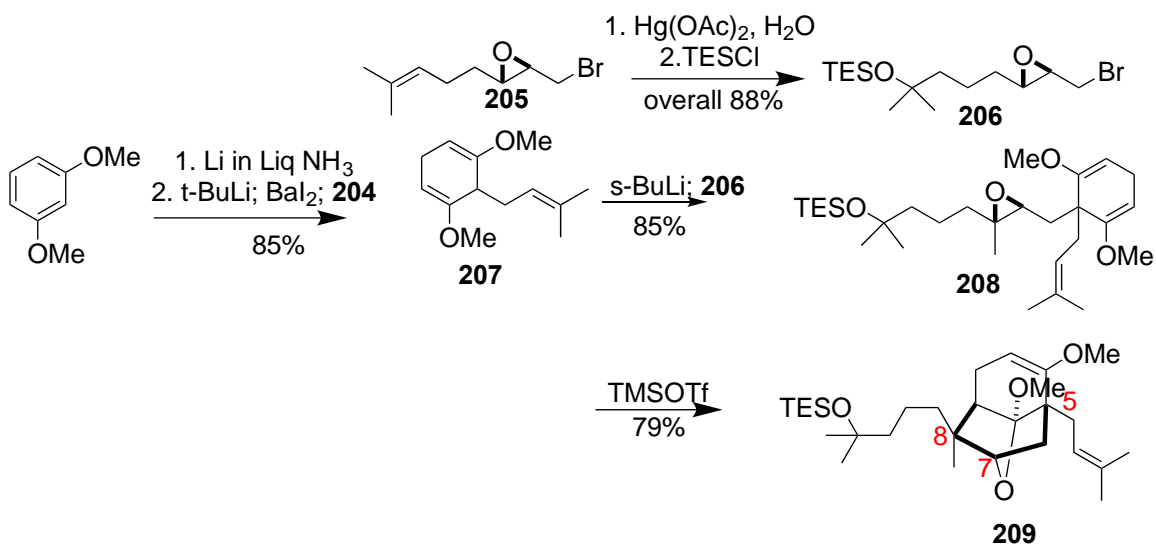
**Scheme 2.7.1.** Retrosynthetic analysis of hyperforin by Shair's group

Retrosynthetically, hyperforin **6** (Scheme 2.7.1) could be obtained by assembling six chemicals. Therefore, he envisaged that hyperforin could be obtained by bridgehead alkylation of alcohol **201**, and alcohol **201** could be made from stereoselective and chemoselective Lewis acid mediated epoxide ring opening of **202**. This cyclohexene containing epoxide could be synthesized regioselectively from the reaction of 1,5-dimethoxy-1,4-cyclohexadiene **203** with prenyl chloride **204** and epoxy geranyl bromide **205**. Although the route was inspired by nature's robust mechanistic artillery, known as an enzyme, Shair's group had no such luxury (Scheme 2.7.2); as a result, they thought that epoxide moiety might be placed in such a way that stereochemical information could be passed on to construct **201**, and the selective choice of Lewis acid would do the job. However, the issue was concerned with diastereoselectivity, the stereochemistry of C7 in **201**, and whether OH would occupy axial or equatorial position based on the transition state (TS). Thus, the boat TS was disfavored over the chair TS (Scheme 2.7.4). The boat-like TS, however, led to 5-(enol-*endo*)-tet cyclization to form a bicyclo[3.3.1]nonane, and this cyclization is unfavorable; therefore, the reaction follows the 6-(enol *endo*)-tet cyclization. This watershed reaction ultimately took care of three major issues: formed the bicyclo[3.3.1]nonane scaffold, established the C5 stereochemistry, and also defined the stereochemistry at C8.



**Scheme 2.7.2.** Matt Shair's biomimetic approach

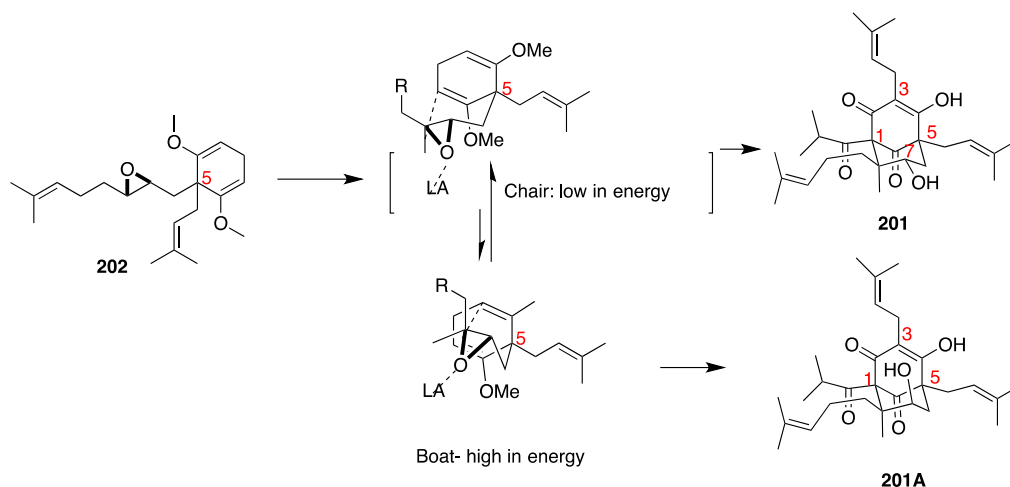
Based on these findings, Shair's group set out to synthesize the target molecule, hyperforin. The synthesis (Scheme 2.7.3) began with enantioselective epoxidation of geraniol and bromination, which yielded **205** (91% *ee*). Oxymercuration–hydration of **205**, and then protection of the concomitant alcohol with TESCl gave **206** in 88% yield. 1,3-Dimethoxycyclohexadiene—obtained from 1,3-dimethoxybenzene by Birch reduction—was subjected to prenylation with the help of ortho-lithiation and mediated by freshly synthesized BaI<sub>2</sub>, giving **207** in 85% yield.



**Scheme 2.7.3.** Hyperforin synthesis by Shair

The next goal was to install a geranyl moiety into the molecule for building the bicyclic motif. Again, with the help of ortholithiation mediated by *s*-BuLi, the allyl anion generated from **207** reacted in S<sub>N</sub>2 fashion with **206**. Then, **208** underwent cyclization in the presence of TMSOTf to produce ketal **209** in a decent yield. This step accomplished three tasks: establishing the stereochemistry at C5 and C8 and construction of the bicyclic motif. The next step was the allylic oxidation of C2, which was accomplished by the treatment of TBHP, PhI(O<sub>2</sub>CCF<sub>3</sub>), and O<sub>2</sub>. The reaction yielded **210** in 55% yield. This

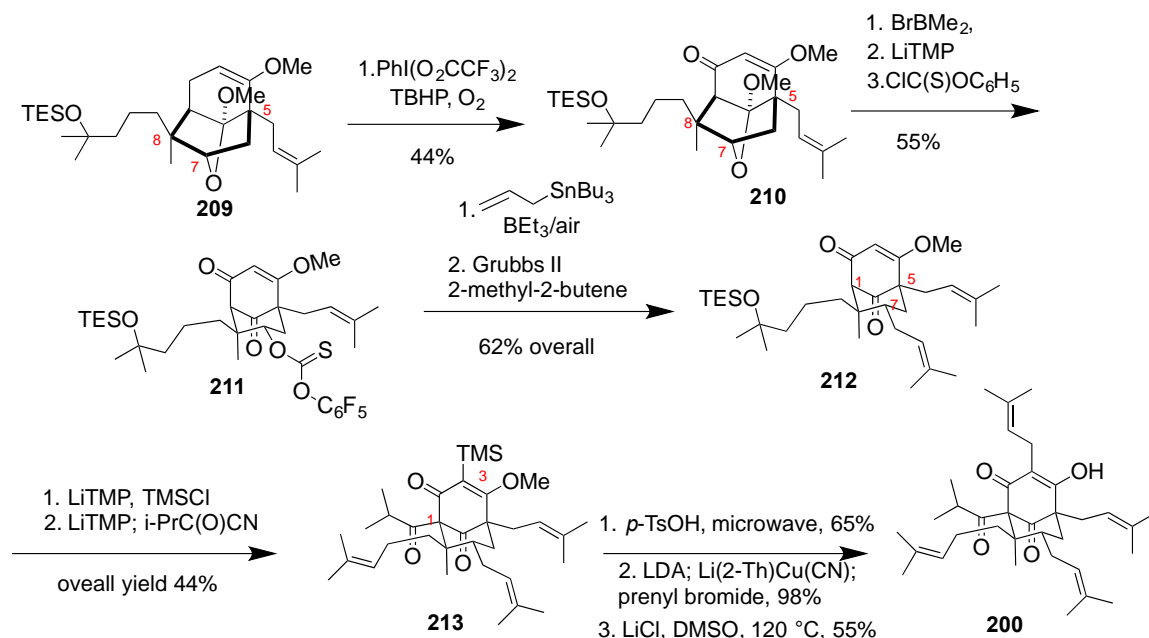
oxidation was challenging and has been a bottleneck for many PPAP syntheses, given the stereoelectronic environment around carbon.



**Scheme 2.7.4.** The origin of diastereoselectivity

The Lewis acid,  $\text{BrBMe}_2$ , opened the epoxide ring of **210** via a chair TS, leading to alcohol, which was converted to thiocarbonate **211** in 72% yield in three steps.  $\text{BEt}_3/\text{air}$  worked to initiate a free radical prenylation reaction with allyl tributyltin in 62% yield. The reaction was famously known as Keck allylation. This reaction was followed by metathesis with 2-methyl-2-butene in the presence of Grubbs II catalyst (Scheme 2.7.5).

Bridgehead acylation with isopropyl cyanofornate, using LiTMP as a hindered base, installed the isopropyl ketone moiety at C1, and microwave-assisted desilylation went smoothly. Then deprotonation of C3 by LDA, transmetalation with  $\text{Li}(2\text{-Th})\text{CuCN}$ , and trapping the resulting vinyl anion with prenyl bromide installed the last prenyl group on C3. Finally, heating **213** in DMSO-LiCl mixture unmasked the hydroxyl group and brought forth hyperforin. Thereby, after 18 steps, the total synthetic scheme yielded 40 mg of hyperforin (Scheme 2.7.5).

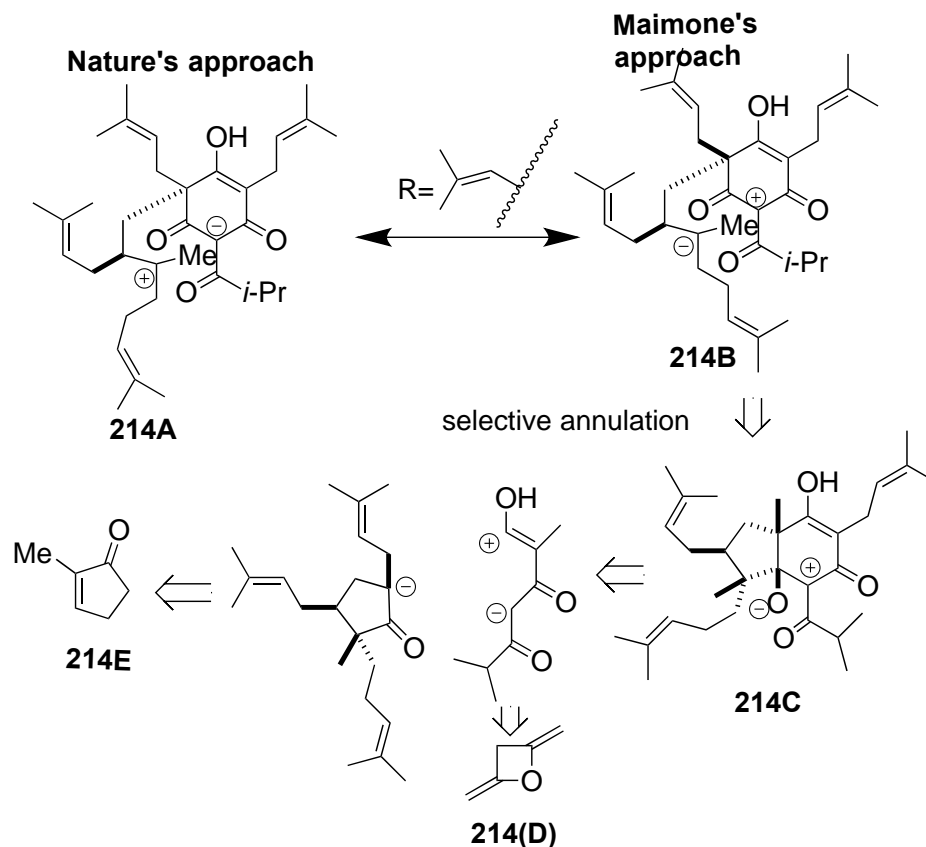


**Scheme 2.7.5.** Finishing synthesis of hyperforin by Shair et al.

The key features of the synthesis were: 1) desymmetrization of the hidden symmetry of the molecule; 2) the attaching of a geranyl epoxide appendage to 1,4-cyclohexadiene; and, 3) an enantiotopic double bond was made diastereotopic for the preferential attack of pro-R-enol to the epoxide via chair TS. It is also interesting to notice that Shair and his group resorted to late stage oxidation of C2 in hyperforin in their approach (Scheme 2.7.4).

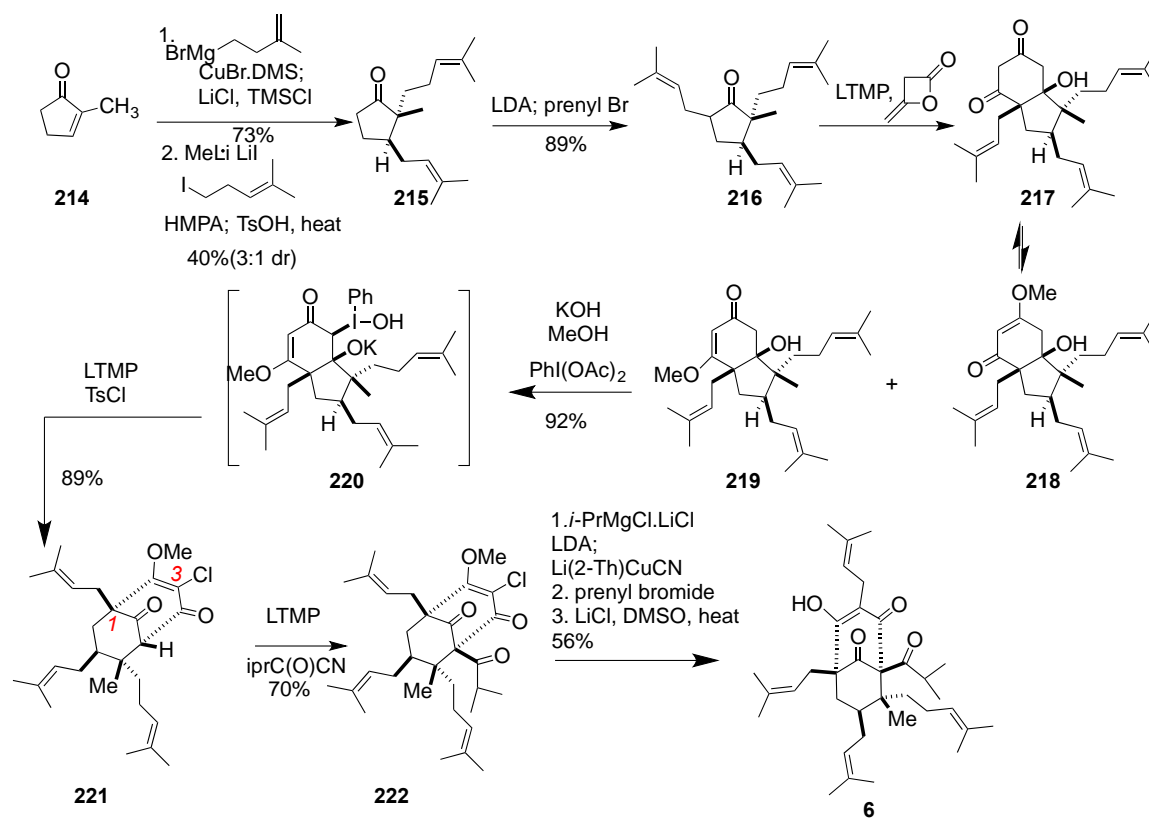
## 2.8 Biomimetic approach to hyperforin by Maimone

In 2015, Maimone published an enantioselective synthesis of hyperforin,<sup>115</sup> reducing the number of steps in the synthesis to **10**. To the best of our knowledge, it has the least number of steps involved in any PPAP synthesis to date. The key feature of the synthesis was the oxidative rearrangement that constructed the bicyclo[3.3.1]nonane motif with the correct stereochemistry at C8.



**Scheme 2.8.1.** Retrosynthesis of hyperforin by Maimone

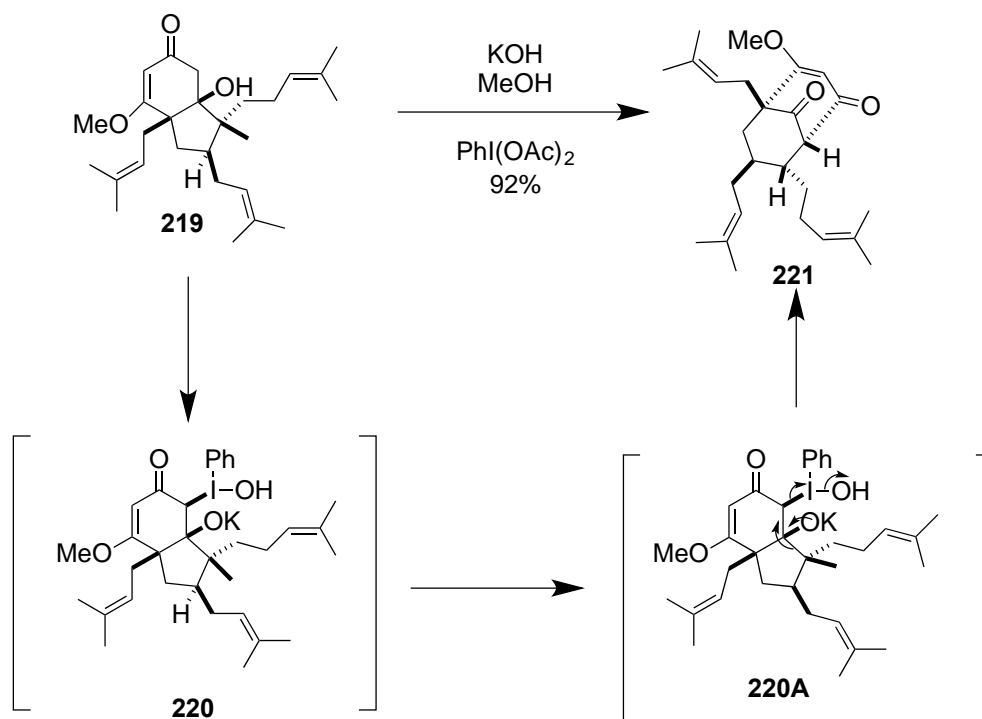
Nature's synthetic approach toward hyperforin relies on the attack of an enol to a carbocationic intermediate **214A**, which is involved in the crucial bond formation reaction to construct the bicyclic scaffold (Scheme 2.8.1). Drawing his inspiration from nature, Maimone resorted to a polarity-reversed approach to decipher the molecule of his interest: hyperforin. He thought of creating an intermediate **214C**, which might rearrange to bicyclic motif via the [1,2] alkyl shift. The idea of proposing the reversal of polarity in intermediate **214C** stems from **214B**, where the polarities of C1 and C8 were opposite in **214A**, which was connected to the biosynthetic pathway. Now, the strategic disconnection of **214C** showed that the intermediated **214C** could be achieved from **214D** and **214E** via a series of reactions.



**Scheme 2.8.2.** Synthesis of hyperforin by Maimone

Based on the retrosynthetic principle mentioned above, Maimone's synthesis started off from the conjugated addition to **214**, mediated by CuI, of (3-methyl-3-buten-1-yl)magnesium bromide and trapping the concomitant enolate by homoprenyl bromide (Scheme 2.8.2). The product from this reaction underwent isomerization, catalyzed by TsOH and heat, to generate to convert the terminal, disubstituted alkene to an internal, trisubstituted one. The reaction gave a 40% yield of **215** with 3:1 dr. LDA-promoted prenylation of **215** gave an excellent yield of **216** and set the stage for the annulation reaction. Using a highly hindered and strong base like LiTMP, the enolate anion, generated from **216**, underwent acylation and annulation with diketene to furnish 5,6-*cis*-fused bicycle **217** as a single diastereomer. In spite of this spectacular transformation, the yield of the reaction was not impressive, merely 45%, and calculated based on the recovered

starting material. This step might prove to be an Achilles' heel for the overall synthetic scheme. They, however, did not consider this low yielding step and proceeded with the scheme. Compound **217** was converted into regioisomeric vinylogous esters, **218** and **219**, in 1:1 ratio by the action of TMS-diazomethane. These esters were separable, and later, after a rigorous analysis, compound **219** was found to be the requisite intermediary for the synthesis of hyperforin. Compound **219** was a milestone in the hyperforin synthesis and set the stage for an oxidative rearrangement, which is the unique selling point of this total synthesis (Scheme 2.8.3).



**Scheme 2.8.3.** Proposed mechanism of oxidative rearrangement

After a lot of screening of stoichiometric oxidants, they found PhI(OAc)<sub>2</sub> was the ultimate choice. The mechanism of the reaction is interesting (Scheme 2.8.3). It showed that hypervalent iodine oxidizes the resulting enolate to **220**, which then began to expel the iodobenzene, leading to a 1,2-alkyl shift: reminiscent of Favorski-like rearrangement. This step added a new dimension to the synthesis by locking the stereochemistry at C8 with

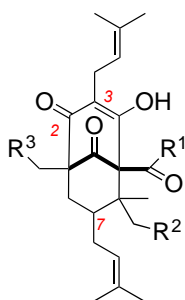


an excellent yield of 92%. LiTMP-mediated deprotonation of the C3 proton, followed by chlorination with TMSCl, gave a good yield of **221**. The halogen-metal exchange has not been effective for vinyl chloride. Using Li(2-Th)CuCN, however, they performed a halogen metal exchange with vinyl chloride **222** and which underwent a reaction with prenyl chloride resulting in **200**. Finally, LiCl in DMSO removed the methoxy group and installed the OH group leading to 1,3-diketone functionality in the molecule.

In a nutshell, the focus on the synthesis was an Umpolung-derived oxidative rearrangement of an intermediate **217** to construct the bicyclic motif in **221**. This approach, regarding synthesis, resembles the biosynthetic pathway. It is also interesting to note that C4 in the molecule (in the case of a type A PPAP) is already in a right oxidation state from the beginning of the synthesis. Thus, chemists need not think about the intricacies of a late stage oxidation.

## **2.9 Hyperforin and papuaforin A-C, and formal synthesis of nemorosone by Barriault et al.**

In 2014, Louis Barriault and his group developed a gold-catalyzed carbocyclization approach to construct PPAPs (Figure 2.9.1) and published the synthesis of hyperforin, papuaforin A-C, and nemorosone from a common intermediate (Figure 2.9.1).<sup>127</sup> In many ways, this synthesis reminds researchers of Danishefsky's seminal work on the total synthesis of clusianone and nemorosone,<sup>111</sup> where the latter resorted to a common precursor, which was en route to two different PPAPs via a series of riveting chemical transformations.

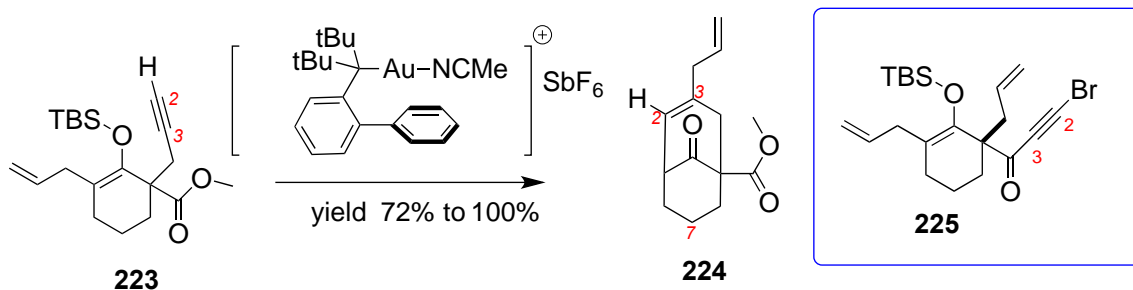


if  $R^1 = \text{CH}(\text{Me})_2$ ,  $R^2 = \text{geranyl}$ ,  $R^3 = \text{isoprenyl}$ , the molecule is hyperforin  
 if  $R^1 = \text{phenyl}$ ,  $R^2 = \text{isoprenyl}$ ,  $R^3 = \text{isoprenyl}$ , the molecule is nemorosone  
 if  $R^1 = \text{isopropyl}$ ,  $R^2 = \text{isoprenyl}$ ,  $R^3 = \text{substituted pyran}$ , the molecule is papuaforin

**Figure 2.9.1.** Target molecules for Barriault's group

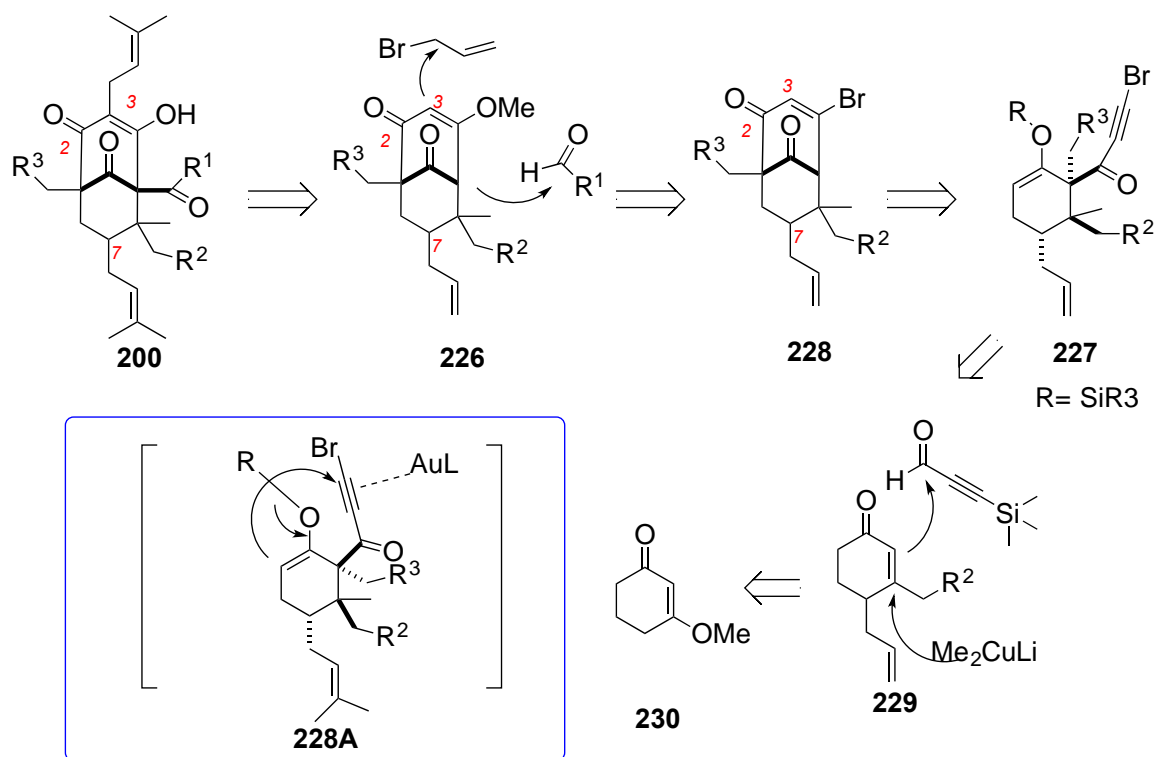
### 2.9.1 Retrosynthetic approach of Barriault

Chemoselectivity of gold (I) phosphine carbene complexes have been well addressed in synthetic chemistry for decades.<sup>128-131</sup> Inspired by the fascinating gold (I) carbene chemistry, Barriault's group proposed a gold-catalyzed carbo-cyclization of an alkyne to set up a bicyclo [3.3.1] motif via the 6-*endo-dig* mechanism. They hypothesized that the carbocyclization of an enoether catalyzed by the gold carbene complex would lead to the required bicyclic motif via the 6-*endo-dig* instead of the 5-*exo-dig* pathway. Moreover, to achieve the carbo- cyclization, the group used a special gold catalyst with suitable ancillary ligands. They published a detailed study of ancillary ligands used for this type of transformation in 2009 and, based on their findings, C4 carbon was not in the proper oxidation state.<sup>132, 133</sup> They struggled over the years to figure out the solution of oxidation at C4. Eventually, they choose bromo alkyne **225** so that bromine could be replaced to oxidize C4.



**Scheme 2.9.1.** Synthesis of PPAP core by gold catalysis

Retrosynthetically speaking, all allyl groups replaced the prenyl groups in **200** (Scheme 2.9.2). Compound **226** could be obtained from the alkylation of C3 by a sterically hindered base, and **227** could be converted to **226** by bridgehead acylation following Danishefsky's method, which he adopted in synthesizing clusianone and nemorosone.<sup>111</sup> Compound **228** could be obtained by the 6-*endo-dig* cyclization of silyl enol ether **227**, thanks to [(JohnPhos)Au(NCMe)][SbF<sub>6</sub>]. Compound **227** could be easily traced back to a commercially available 3-methoxycyclohex-2-en-1-one, **230**.

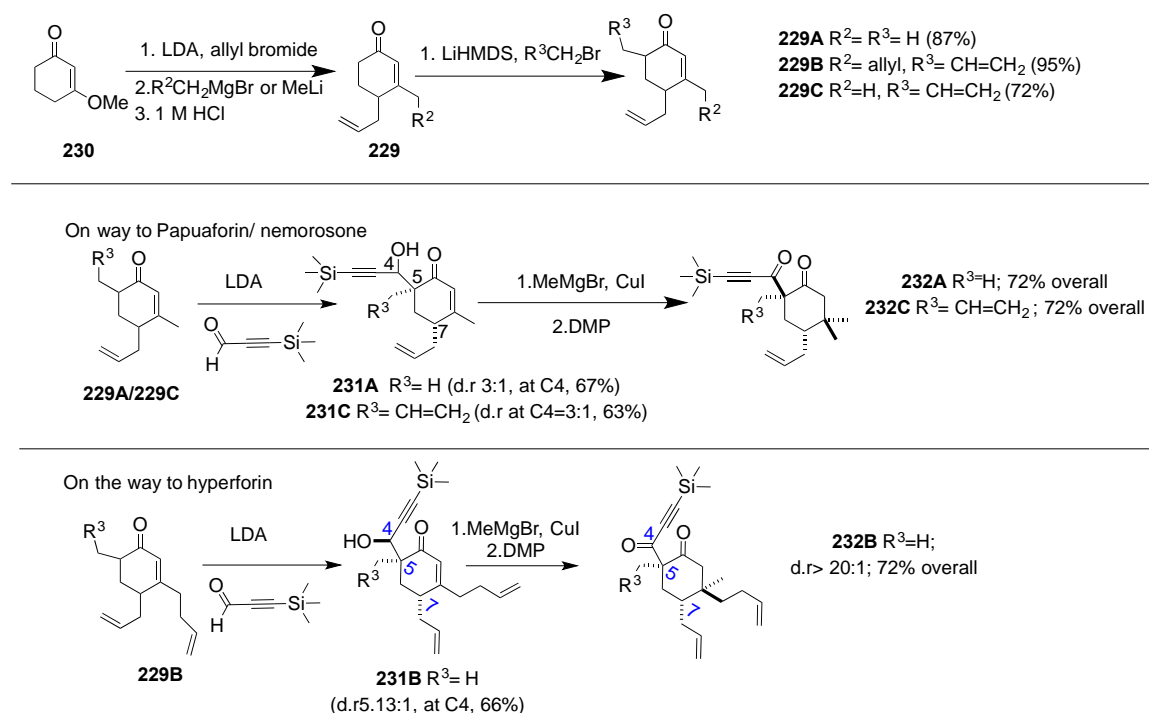


**Scheme 2.9.2.** Retrosynthesis of type A PPAPs by Barriault

## 2.9.2 Synthesis of hyperforin, nemorosone, and papuaforin A-C by Barriault et al.

With the retrosynthetic scheme in mind, Barriault's group started by alkylating **230** with allyl bromide and LDA (Scheme 2.9.3). The resulting compound from the previous reaction underwent a Grignard reaction that depended upon the final target compound (Figure 2.9.1). For example, for hyperforin, the group used (but-3-en-1-yl) magnesium as a Grignard reagent. Yet, for nemorosone, they chose MeLi. Subsequently, hydrolysis with 1 M HCl, depending on target compound, furnished **229** in a decent yield (>80%, depending on the Scheme). LiHMDS-mediated alkylation of **229** gave a decent yield. Deprotonation of the C5 hydrogen from **229A**, **229B**, or **229C** and then, treating the resulting enolate with the 3-(TMSCl)-2-propynal. The reaction yielded **232** in alkyne with a variety of diastereomeric ratios, which was dependent on the synthesis of the target PPAP (Figure 2.9.1)

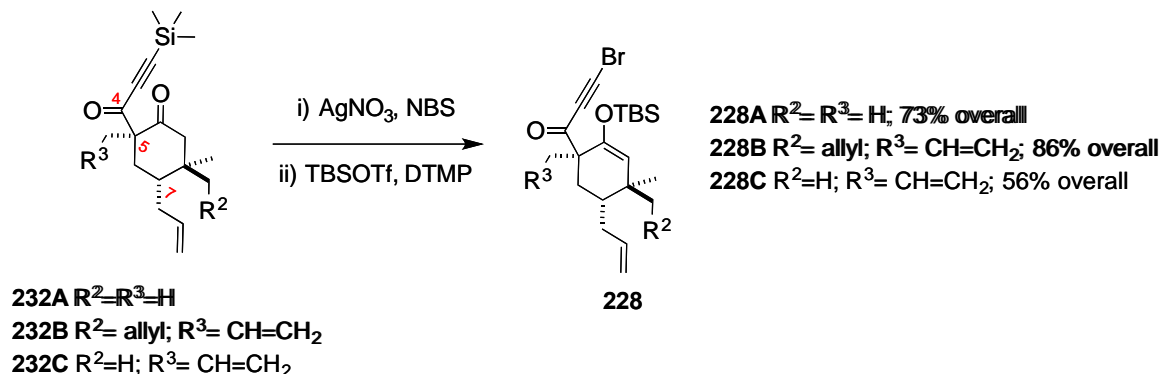
The next step was very interesting regarding setting up the stereochemistry at C8. The conjugate addition to **232** was tricky since substrate **232**—a  $\delta$  substituted cyclohexenone—was prone to an anti-addition but, fortunately, Barriault's group observed a syn-addition (Scheme 2.9.3). Magnesium makes a chelate on the top face of the double bond and, thereby, facilitates the nucleophile to approach to the double bond by syn fashion; this was a steric approach control that determined the outcome of the stereochemistry.



**Scheme 2.9.3.** Syntheses of the silyl ketones

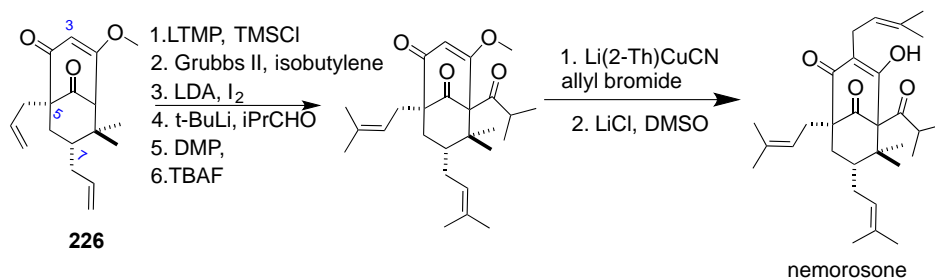
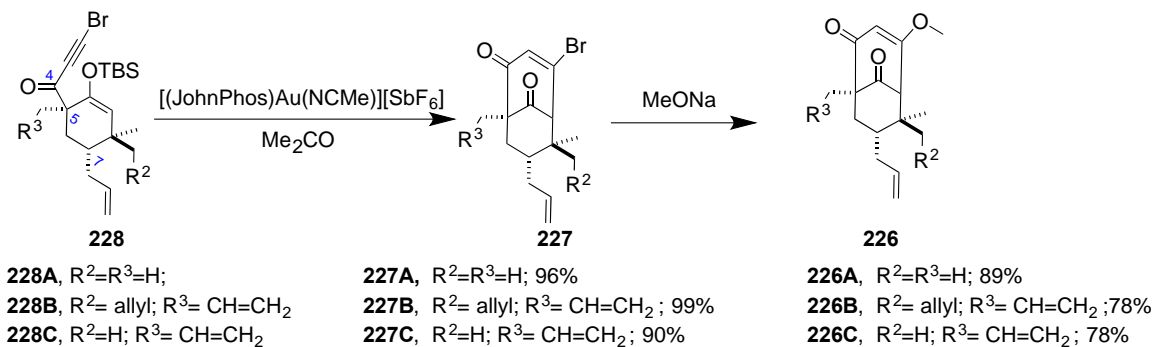
Next, oxidizing the propargyl alcohol to the ketone and deprotecting the silane group, followed by bromination with AgNO<sub>3</sub> and NBS, furnished **232**. The ketone was protected with TBSOTf to produce enol ether, **228**. This step set the stage for the most important reaction of the entire synthetic scheme: a gold(I)-catalyzed carbocyclization for the construction of a [3.3.1] bicyclo nonane motif, **227A-C**. The bromo-bicyclic enone was converted to methoxy enone, **226A-C** with a good yield.

The step was critical for finishing the synthesis of the PPAPs because of the steric and electronic encumbrance around the C4 carbon, which has been a red herring in numerous trials for successful PPAP synthesis. Compounds **226 A-C** were important stopping points in the syntheses. Hyperforin and papuaforin A-C, along with the synthesis of nemorosone, took different routes.



**Scheme 2.9.4.** Synthesis of bromoalkyne for cyclization

In other words, compounds **226A-C** proved to be an important junction in the whole synthetic endeavor. Nemorosone was synthesized from **226A** within five steps (Scheme 2.9.5) by following Simpkin's method.<sup>134, 135</sup> The Barriault-group needed to take precautions for the synthesis of hyperforin and papuaforin because of bridgehead acylation. It was surprising from the synthetic point of view because there was literary precedent for such acylation.<sup>136</sup> Danishefsky's solution of bridgehead acylation saved their day.

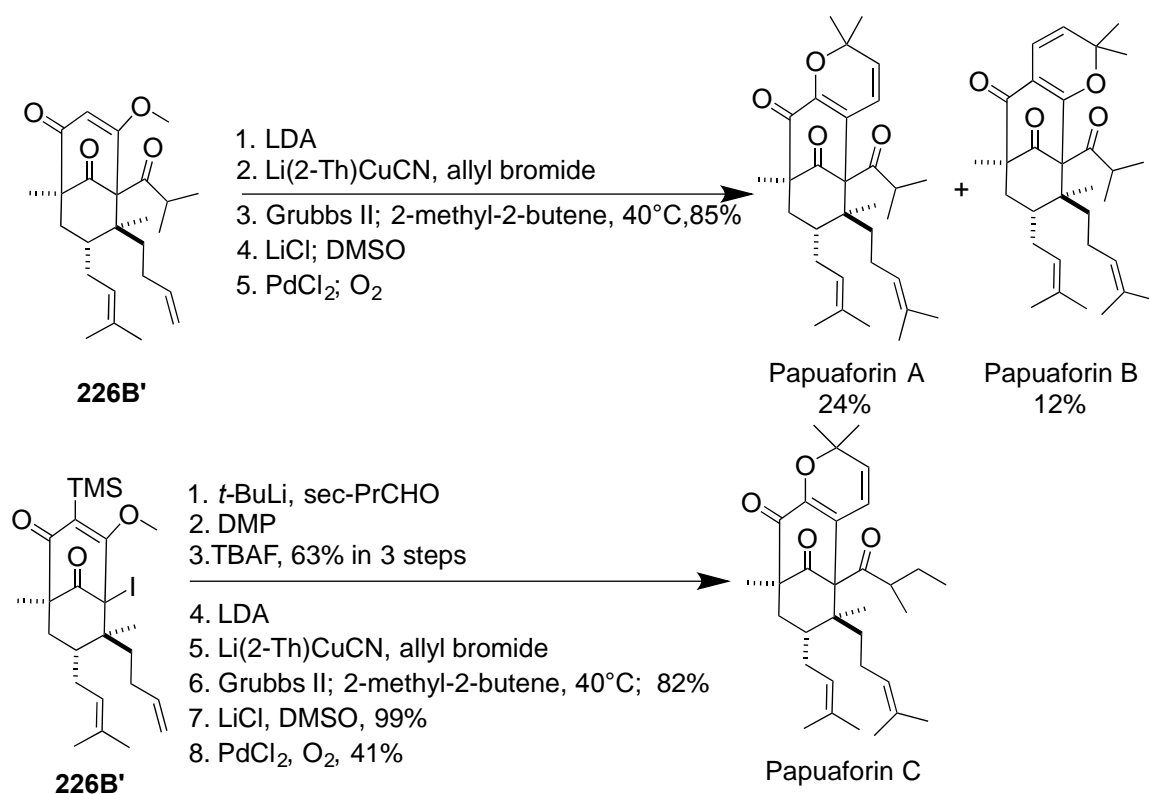


**Scheme 2.9.5.** Finishing the total synthesis of nemorosone

The LDA-mediated iodination of the bridgehead carbon (C1), not touching the other double bonds, as well as an I/Li exchange using *t*-BuLi, installed the isopropyl ketone in all the final molecules; namely, nemorosone, hyperforin, and papuaforin A-B. Although bridgehead acylation helped the group reach their targets, the yields were not satisfactory, ranging between 18% to 29%.

Once the bridgehead acylation was done in **226A-C**, depending on the end molecule, they set out to finish the synthesis, and the next few steps—alkylation of C3 with hindered Li-Cu salt, Grubbs' metathesis, and demethylation with LiCl in DMSO—were uneventful (**Scheme 2.9.6**). Papuaforin A-C, however, contains an extra dihydropyran ring, which is a further modification because the C3 prenyl group underwent an acid-catalyzed carbocyclization. Using PdCl<sub>2</sub> and molecular O<sub>2</sub>, the dihydropyran ring was installed diastereoselectively leading to papuaforin A and B.

The mechanism for the formation of the ring is very simple: Wacker type oxidation. Since the 1,3-diketone functionality is in equilibrium with two different mesomeric forms, both the keto oxygen at C2 and C4 act as nucleophilic centers, resulting in papuaforin A and B (Scheme 2.9.6).



**Scheme 2.9.6.** Finishing the syntheses of papuaforins A–C

Key points from this synthetic research are the formation of a bicyclo[3.3.1]nonane motif by gold catalysis from bromoalkyne (**228**), and the subsequent replacement of the Br-group in **227** with an OMe group to circumvent the problem of oxidation at C4.

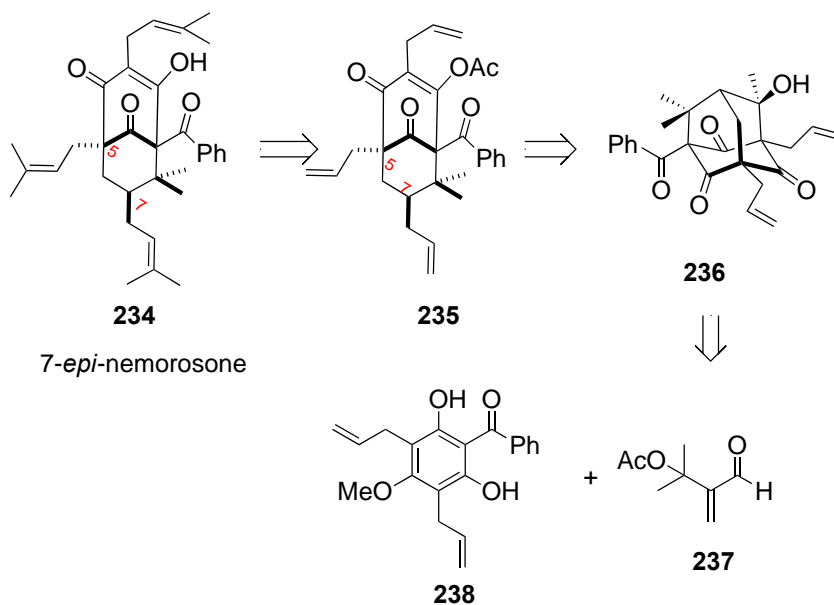
## 2.10 Total synthesis of 7-*epi*-nemorosone by Porco

John A. Porco was the first to devise a synthetic scheme for a type A endo PPAP, 7-*epi*-nemorosone, after successful synthesis of some type B endo PPAPs by Plietker.<sup>117</sup>



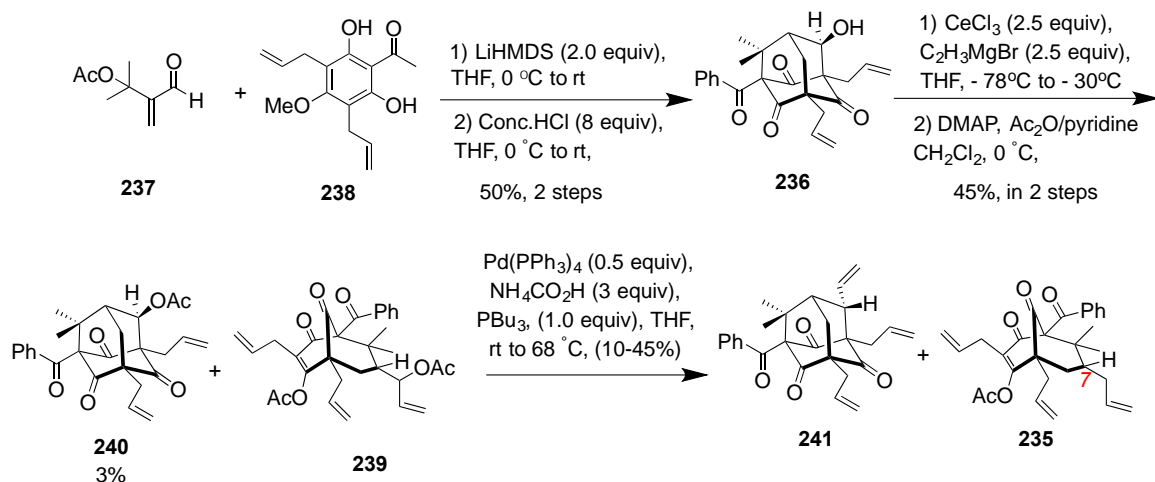
Porco's approach to these types of compounds is known as dearomatization-annulation.

Using this method, his group synthesized ( $\pm$ )-clusianone.<sup>123</sup>



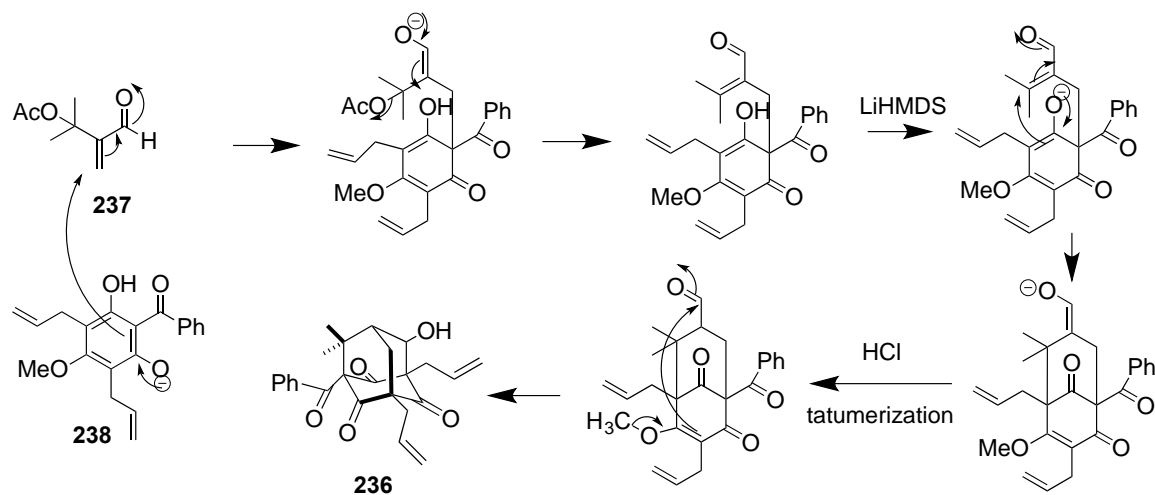
**Scheme 2.10.1.** Retrosynthetic scheme of 7-epi-nemorosone by Porco

With the help of metathesis, all the prenyl groups could be introduced easily; this thought led retrosynthetically to **235**, which could be obtained from **236** by a retro-aldol reaction (Scheme 2.10.1). Interestingly, this adamantane core was not necessarily needed to synthesize these kinds of molecules; in other words, he could have avoided this scheme, which proceeds via an adamantane motif. He and his group, however, prudently devised such a scheme so they could access the PPAPs that contain an adamantane core. Adamantane alcohol **236** could be accessed in one step from aldehyde, **237**, and phenol, **238**, via a Michael–aldol reaction.



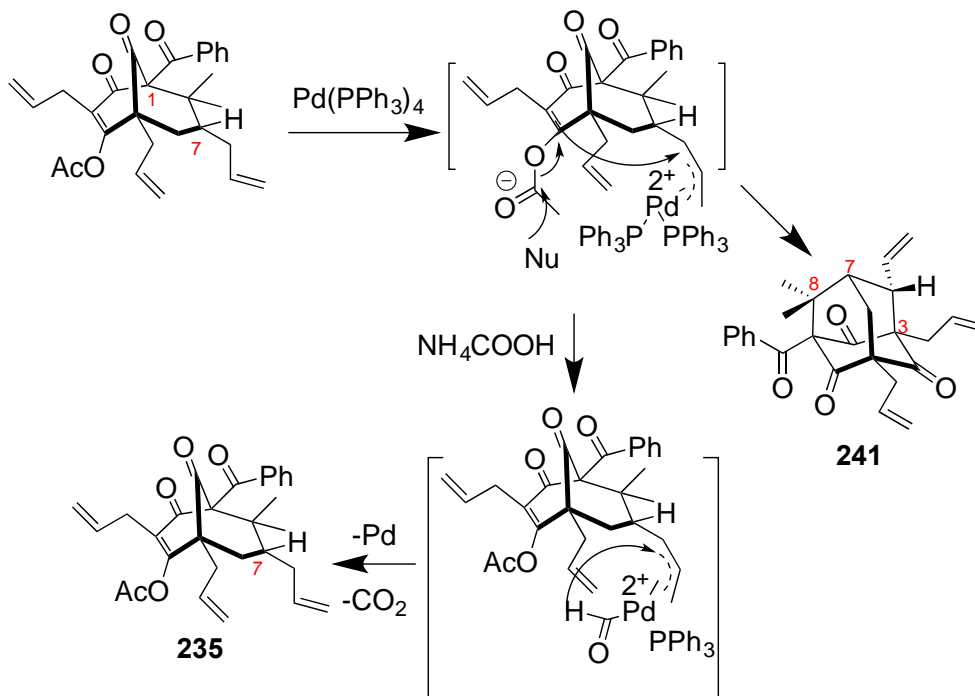
**Scheme 2.10.2.** Synthesis of 7-*epi*-nemorosone by Porco et al.

The synthesis (Scheme 2.10.2) started off with deprotonation of phenolic hydrogen of **238** by one equivalent of LiHMDS; the resulting phenoxide underwent 1,4-addition to **237**, at which point the nascent enolate anion expelled acetate. The second equivalent of LiHMDS generated phenoxide again, and this resulting phenoxide anion underwent Michael addition followed by aldol condensation to generate adamantane alcohol **236** (Scheme 2.10.3).



**Scheme 2.10.3.** The mechanism of formation of adamantane alcohol

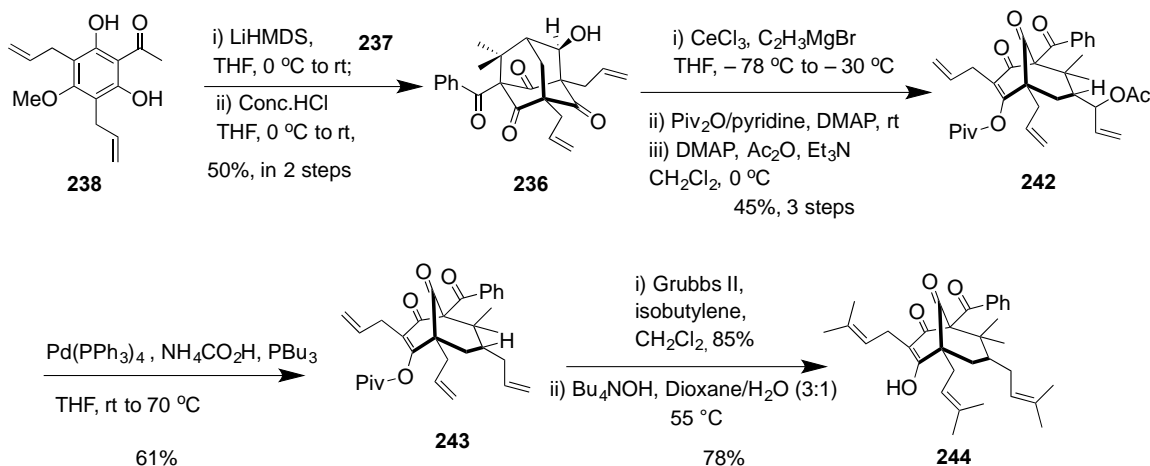
Using steric congestion around the adamantane core in **236**, a  $\text{CeCl}_3$  / vinyl magnesium-mediated tandem retro-aldol condensation was followed by a Grignard reaction. It furnished two alcohols esterified by  $\text{Ac}_2\text{O}$  and pyridine. The deacylation of **239** catalyzed by  $\text{Pd}(\text{PPh}_3)_4$ , however, proved problematic because of an unusual rearrangement to adamantane core **241** as a major product.



**Scheme 2.10.4.** Mechanistic rationale for unusual rearrangement

Detailed mechanistic analysis (**Scheme 2.10.4**) showed that there were two competitive mechanisms in place: one was a nucleophilic attack on the C4 acyl group followed by deacylation, resulting in **241**; the other was expected, namely, a deacylation reaction that led to **235**. Porco and his team quickly figured out the issue: using a larger protecting group for the 1,3-diketone. Thus, they replaced acetate with pivalate (**Scheme 2.10.5**), and the issue was resolved. Once adamantane alcohol **236** was esterified with  $\text{Piv}_2\text{O}$  in pyridine and carried out the same reaction sequence like in **Scheme 2.9.5**, they secured an exclusive pivalate derivative of **236** with a 61% yield. The remaining steps went

smoothly; **242** was reductively de-acylated with ammonium formate with the help of Pd(PPh<sub>3</sub>)<sub>4</sub> and Grubbs (II) catalyst replaced all the allyl groups with prenyl groups. Finally, Bu<sub>4</sub>NOH, in a 1,4-dioxane-H<sub>2</sub>O mixture, deprotected the pivalate ester **243**, resulting in 7-*epi*-nemorosone in an impressive 78% yield.



**Scheme 2.10.5.** Finishing the synthesis of 7-*epi*-nemorosone

Key points from this synthesis are dearomative/cyclization and a CeCl<sub>3</sub>-catalyzed vinyl magnesium-mediated ring opening to bicyclo [3.3.1] nonane (**Scheme 2.10.5**). Although the synthesis is unique in the sense that it was the first synthesis of type A endo, the final purification step was cumbersome, leading to purification via prep HPLC. Finally, the construction of a 1,3-diketone functionality was clearly not a problem here since Porco and his group started with 2-benzoyl-5-methoxy-4, 6-bis(prop-2-en-1-yl)benzene-1, 3-diol, which has the 1,3 diketone already built in; thus, there was no oxidation problem.

## 2.11 Plietker's divergent approach for the total syntheses of type B endo PPAPs

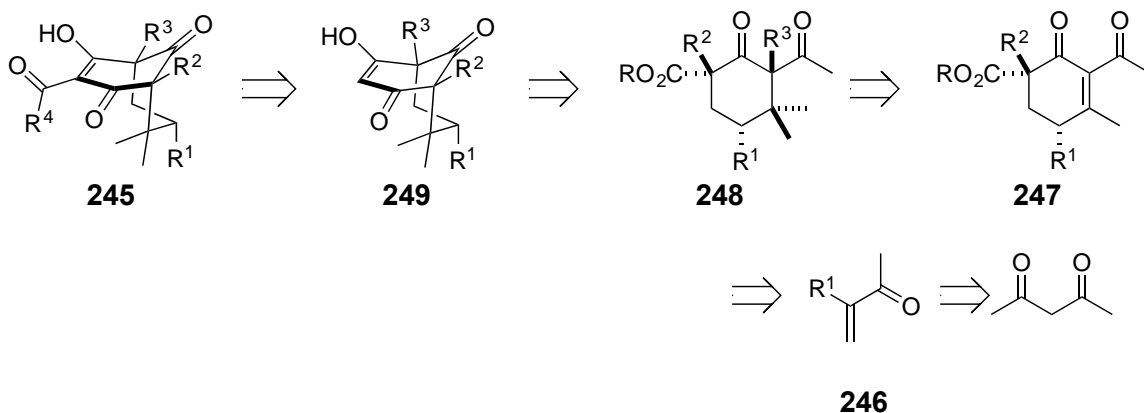
### 2.11.1 Synthesis of 7-*epi*-clusianone, oblongifolin, hyperibone L, hyperpapuanone, and regio-hyperpapuanone

Until 2011, most of the successful total syntheses of PPAPs had been exo type A, except clusianone, which is a type B *exo*. There were multiple research groups trying to synthesize

type B endo PPAPs because of their unique structure and a wide range of medicinal properties, but success was elusive. From my perspective, the geometry of type B endo compounds was the main reason behind the long list of unsuccessful synthetic attempts by organic chemists. The type B endo PPAPs exist in a boat conformation rather than a chair, which is common to type an exo PPAPs. Things changed in 2011—when Bernd Plietker and his group developed a unique approach to addressing these challenges for the type B endo synthesis.<sup>117</sup> This led to the total synthesis of *7-epi*-Clusinone, oblongifolin, hyperibone L, hyperpapuanone, and regio-hyperpapuanone. As far as our knowledge goes in this field, his group is the only one that has been synthesizing type B endo compounds successfully. Here, I will provide an account of his method and decipher the philosophy of these state-of-the-art syntheses. Since his approach to this synthetic challenge is the same for all five compounds, I shall only discuss *7-epi*-Clusinone, which is also the molecule of my interest, in more detail. The remaining four compounds will be discussed briefly.

### 2.11.2 Retrosynthetic analysis of type B endo PPAPs

Plietker's group decided to approach the synthetic challenge using simple chemistry without a protecting group strategy (Scheme 2.11.1). Plietker envisioned developing a common module that would deliver a diverse array of type B endo PPAPs. Accordingly, he proposed that target **245** could be achieved from **248** via Dieckman condensation, which would be applied here for the first time to synthesize type B endo PPAPs. Compound **248** could be obtained from **247** by tandem conjugate addition and  $\alpha$ -alkylation. Compound **247** could be made from 3-methyl-3-buten-2-one derivative **246** via a tandem Michael–Knoevenagel reaction. Finally, compound **246** could be synthesized by alkylation of acetyl acetone followed by aldol condensation with formaldehyde.



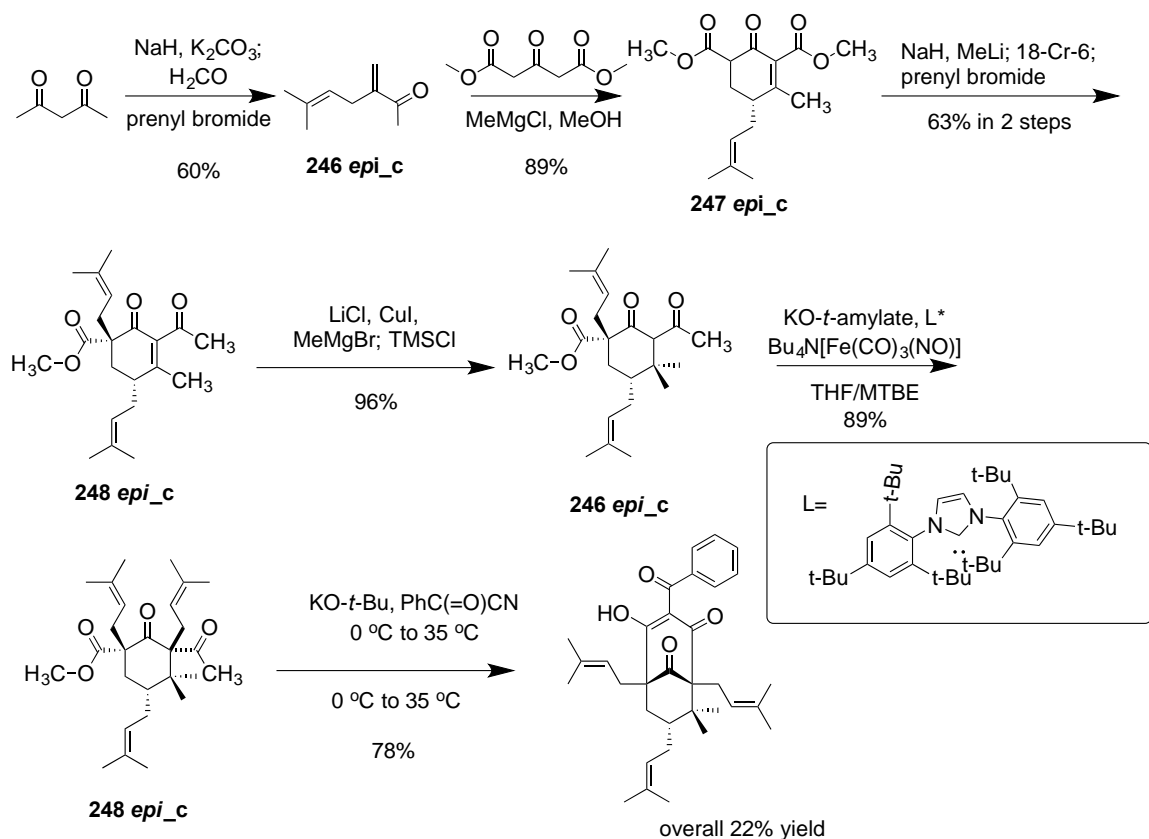
R<sup>1</sup>, R<sup>2</sup>, R<sup>3</sup>, and R<sup>4</sup> = alkyl or alkenyl group depending upon the final molecule

**Scheme 2.11.1.** Retrosynthetic analysis of Plietker's synthesis of type B endo PPAP

### 2.11.3 Total synthesis of 7-*epi*-clusianone

Keeping in mind the diversification of the synthetic route, acetyl acetone was the starting point and suitable alkylating reagent. For 7-*epi*-clusianone, prenyl bromide was used. NaH-mediated alkylation was followed by an aldol-type methylation and an extrusion of acetate anion, giving the desired enone, **246 *epi*\_c** (since we are discussing 7-*epi*-clusianone) (Scheme 2.10.1). MeMgCl-promoted conjugate addition of dimethyl-1,3-acetonedicarboxylate to **247 *epi*\_c**, followed by a tandem Michael-Knoevenegal reaction, furnished cyclohexenone **247 *epi*\_c** (Scheme 2.35). Once the cyclohexenone ring was constructed, the aim was to install the prenyl group at C1 with the correct stereochemistry. Deprotonation of **247 *epi*\_c** with NaH, followed by addition of MeLi, 18-crown-6, and prenyl bromide converted the C5 ester group to a methyl ketone and successfully installed the second prenyl group at C1 with the correct stereochemistry, trans to the C7 prenyl group. Interestingly, only one of the two ester groups in **247 *epi*\_c** was converted into a methyl ketone by the action of MeLi (Scheme 2.11.2).

The question that arose here, inevitably, was: which reaction should go first, alkylation at C1 or MeLi addition at C5 ester carbonyl carbon? The molecule, being a  $\beta$ -keto ester, has the option to distinguish between two esters. Thus, NaH first deprotonates the C1 proton because of its low  $pK_a$ . Subsequently, the ester group at C1 becomes poorly electrophilic since the negative charge on C1 can now be delocalized between C1 ester and C9 carbonyl. MeLi could now be added easily to C5 ester carbonyl, converting it into a methyl ketone. Once the conversion of the ester into ketone was successful, the addition of prenyl bromide added the second prenyl group at C1 with the correct stereochemistry. The yield was 62% in this step. This step also fixed the oxidation state of C4.



**Scheme 2.11.2.** Synthesis of 7-*epi*-clusianone

The next goal was to construct a gem-dimethyl group at C6 in **248\_epi\_c** (Scheme 2.11.2). To do so, the group resorted to a Lewis acid-promoted conjugate addition of

MeMgBr at  $-78\text{ }^{\circ}\text{C}$ . The reaction yielded the desired product, **246 epi\_c**. Having established a gem dimethyl group at C6, there were three more steps to accomplish the total synthesis of 7-*epi*-clusianone: (I) installing the last prenyl group at C5 with a correct stereochemistry; (II) making bicyclo[3.3.1]nonane; and the last, (III) putting the phenacyl group at C3. When the group tried to install the prenyl group at C5 by alkylation using NaH, they faced steric congestion at C6 because of the gem-dimethyl group. This led to failure in seeding the prenyl appendage at C5. After deliberations, they decided to rely on the allylic alkylation method,<sup>137</sup> which they had developed in their lab, using a  $\text{Bu}_4\text{N}[\text{Fe}(\text{CO})_3(\text{NO})]$  catalyst. The reaction demanded putting the prenyl group at C5 trans to C7 prenyl with an acceptable dr. Fortunately, they succeeded in installing the prenyl group at C5 with an acceptable dr with a high yield of 90%. This allylic alkylation deserves some deliberation regarding diastereocontrol. Two equivalents of KO-*t*-amylate were used. One was used to deprotonate C5 in **246 epi\_c**, the  $\text{pK}_a$  of which is very low, near 10, and the second equivalent was used to prevent acetate anion from picking up an  $\alpha$ -proton. The enolate anion from the deprotonation created flattened chair conformation, where the bottom face was covered by carboethoxy and Me group, because of the chelation by the iron between C9 carbonyl oxygen and C5 methyl ketone oxygen. Now, the incoming electrophile,  $\pi$ -allyl complex, had no option but to approach the reactive center other than from the top face (Figure 2.11.1).



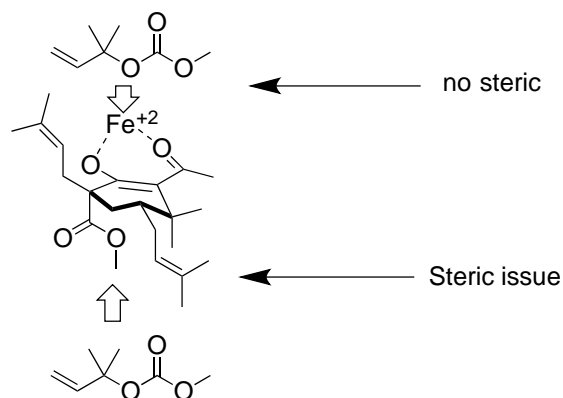


**Figure 2.11.1.** Rationale for diastereoselection of allylic substitution

The next step was to construct a bicyclo [3.3.1] nonane in **249 epi\_c**. They envisioned making a C2–C3 bond by Dieckman condensation and, to do that, compound **249 epi\_c** needed to switch from a chair conformation to a boat one, which is energetically unfavorable (Figure 2.11.1). However, the formation of a C–C  $\sigma$  bond and deprotonation of the product 1,3-diketone provide sufficient driving force in this reaction; this led to the construction of a bicyclo [3.3.1] nonane.

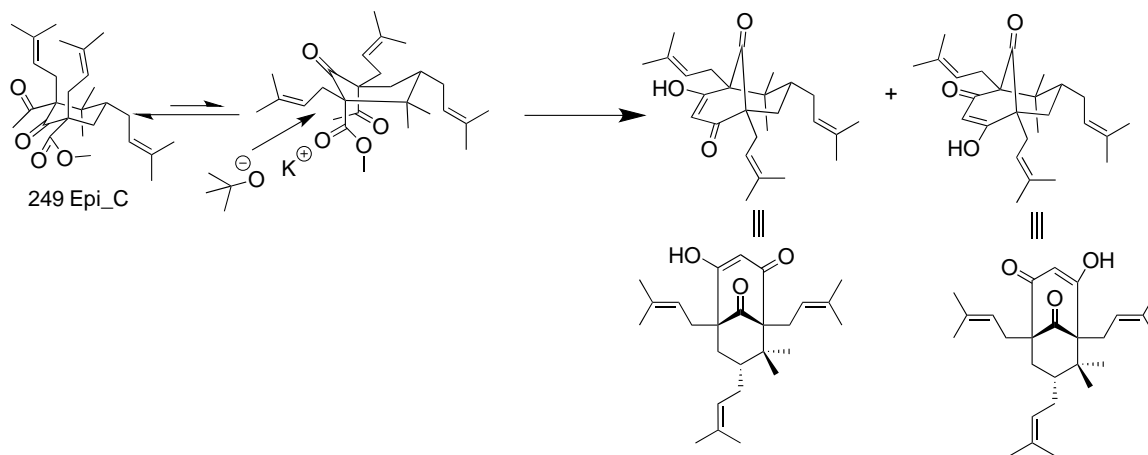
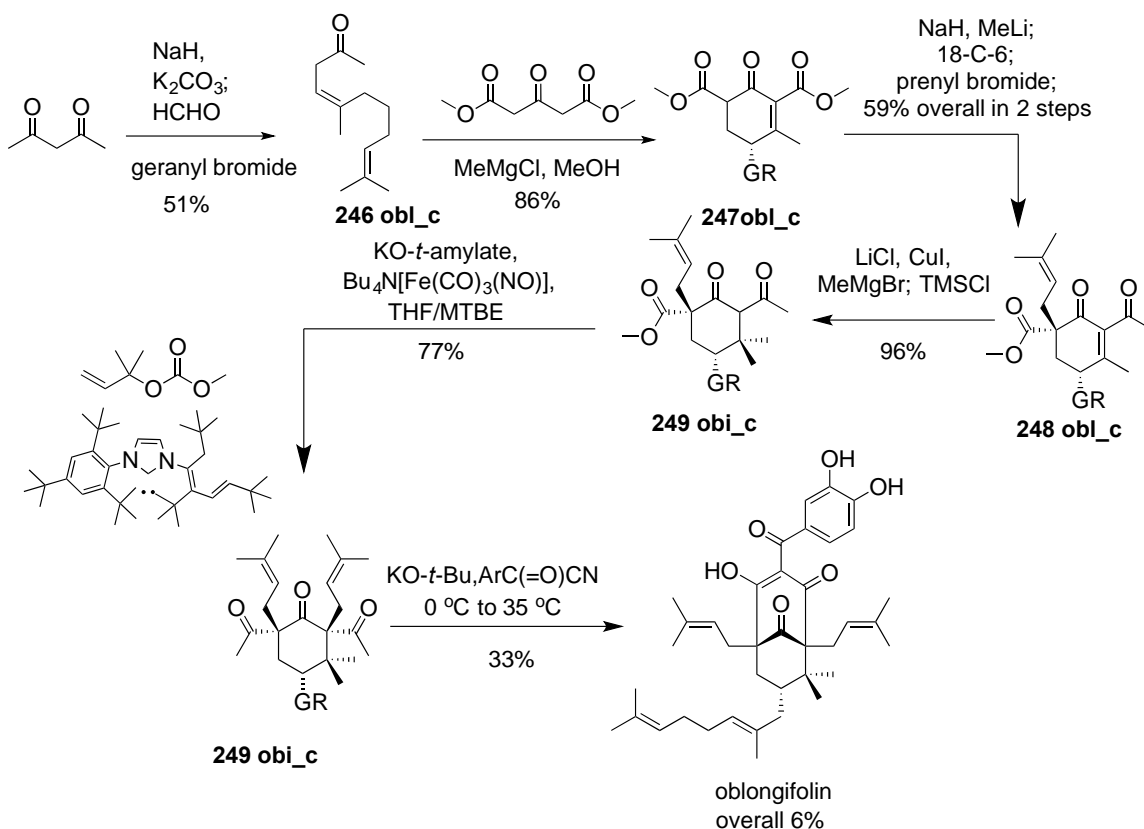


**Figure 2.11.2.** Dieckman condensation to construct the bicyclo [3.3.1] nonane

The resulting enolate from the Dieckman reaction, which was trapped by benzoyl chloride for C-acylation at C3, resulted in a mixture of tautomers in a 72% yield. Finally, after the base treatment, the reaction furnished 7-*epi*-clusianone (**10**) with an overall yield of 22%.

## 2.12 Total synthesis of oblongifolin

Oblongifolin is another type B endo PPAP.<sup>117</sup> It has the same structure as *7-epi-clusianone*, but includes the C7 appendage, which is a geranyl rather than a prenyl group. So, the overall scheme remains the same.



Scheme 2.12.1. Synthesis of oblongifolin

Since the retrosynthetic approach towards the molecule was the same as *7-epi-clusianone* (Scheme 2.11.2), Plietker's group accomplished the total synthesis of oblongifolin with the same methodology (Scheme 2.11.2). In the first step, acetyl acetone underwent alkylation with geranyl bromide, followed by aldol type methylenation, to set the stage for the Michael–aldol reaction. The last step, the acylation at C3 with 3,4-dihydroxybenzoyl cyanide, resulted in oblongifolin in 33% yield (Scheme 2.12.1). The yields in each step were very much on par with *7-epi-clusianone* **10**.

### 2.13 Total synthesis of hyperpapuanone

Hyperpapuanone (**73**) is a type B endo PPAP and structurally very similar to 7-*epi*-clusianone (**10**), but with two minor differences: first, there is a methyl group at C1 instead of a prenyl group; and second, there is an isobutyryl substituent at C3 instead of a benzoyl group (Figure 2.13.1).<sup>117</sup>

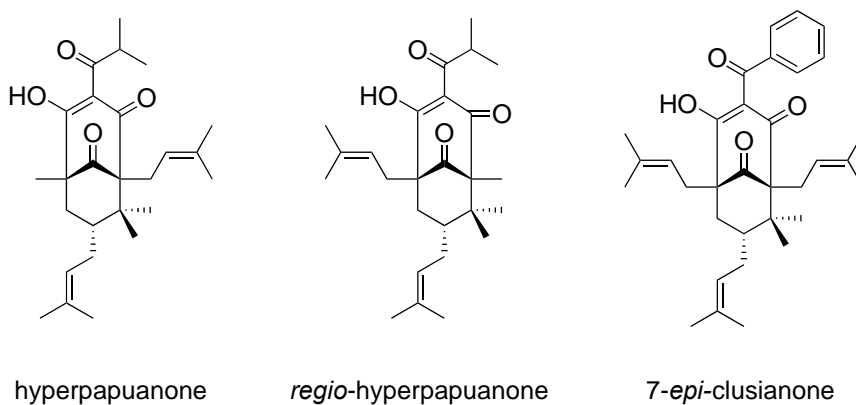
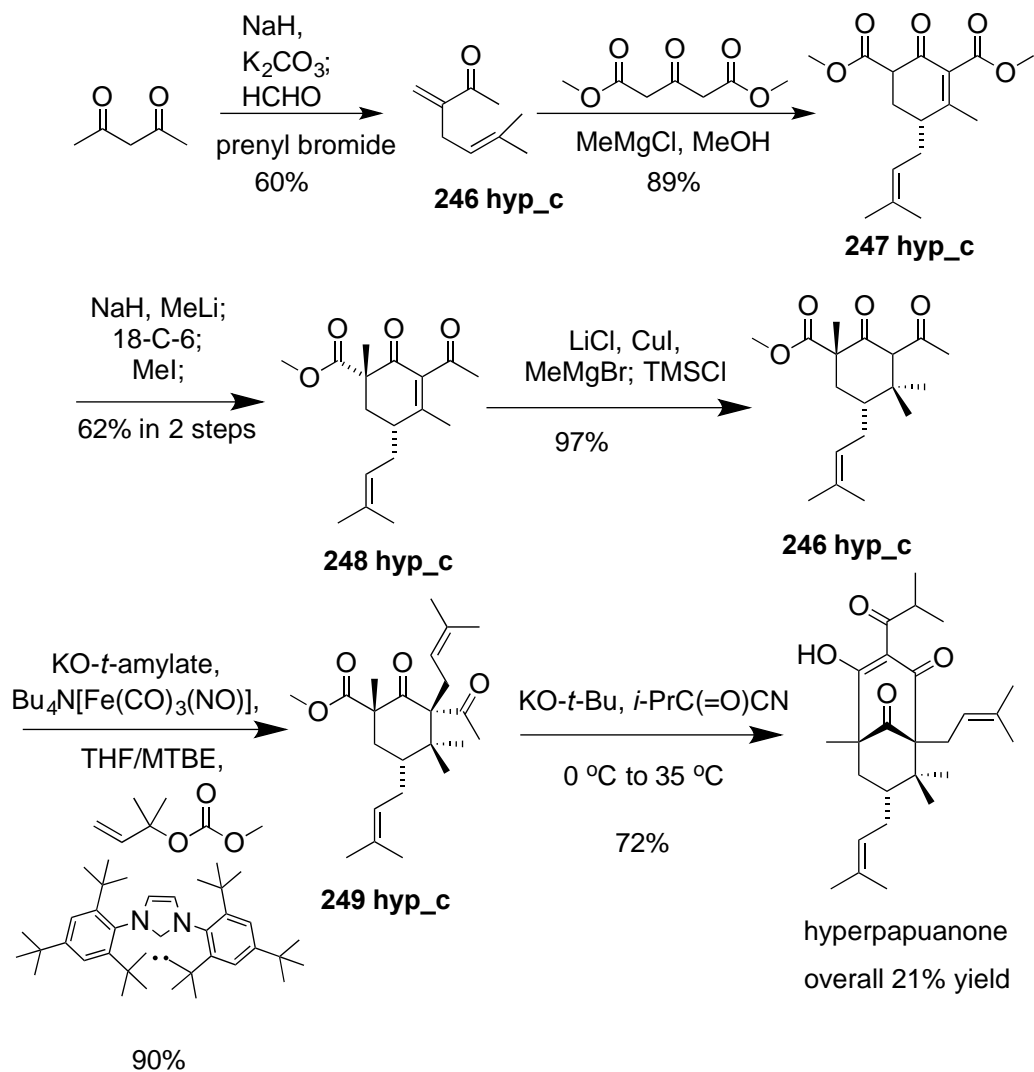


**Figure 2.13.1.** Hyperpapuanone, regio-hyperpapuanone, and 7-*epi*-clusianone

Since the retrosynthetic approach towards the hyperpapuanone was the same as 7-*epi*-clusianone (Scheme 2.13.1), Plietker's group approached the total synthesis of hyperpapuanone with the same methodology. In the process, the second alkylation step where a NaH/MeI combination methylated C1, the transformation of **247 hyp\_c** into **248 hyp\_c**, as well as acylation at C3 with 2-methylpropanoyl cyanide, were the only two different reactions in the entire total synthetic scheme (Scheme 2.13.1). The yields in each step were very much at par with 7-*epi*-clusianone, along with the overall 21% yield.

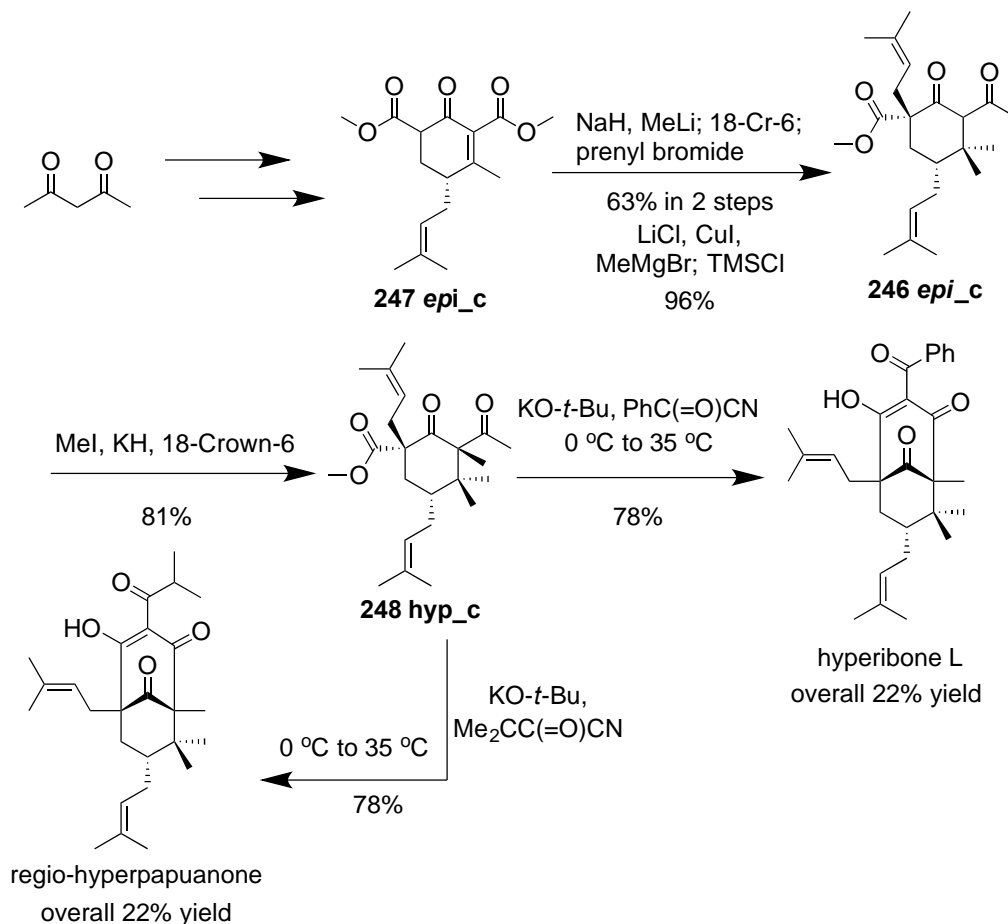


**Scheme 2.13.1.** Synthesis of hyperpapuanone

## 2.14 Total synthesis of hyperibone L and regio-hyperpapuanone

Structurally, hyperibone L and regio-hyperpapuanone are very much like one another. The C3 substituent in hyperibone L contains a benzoyl; by contrast, regio-hyperpapuanone has an isobutyryl group at C3. Plietker's group approached the total synthesis of hyperibone L and regio-hyperpapuanone with the same methodology as they used to prepare *7-epi-clusianone*.<sup>117</sup> The approach to hyperibone L and regio-hyperpapuanone (Scheme 2.14.1) differed from the approach to *7-epi-clusianone* only

when the last alkylation step was reached, where a KH/MeI combination methylated C5, which resulted in the transformation of **246 epi-c** into **249 hyp-c**. The last step, acylation at C3 with isobutyryl cyanide and benzoyl cyanide respectively, was the only step that differentiated the syntheses of hyperibone L and regio-hyperpapuanone. The overall yields were quite on par with 7-*epi*-clusianone at 22% and 14%, respectively.



**Scheme 2.14.1.** Synthesis of regio-hyperpapuanone and hyperibone L

There are many noteworthy aspects of these total syntheses. This strategy was effectively executed to make five compounds from a common precursor with moderate to good yields in less than seven steps. Last, but not least, Plietker et al. realized the importance of C4 oxidation for the success of their synthetic plan. Thus, they did not rely

upon late stage oxidation; rather, they devised a strategy where the C4 was at the desired oxidation state from the very beginning, and they took care of this step in the Michael–aldol tandem reaction. Perhaps the structure of the final molecules, which exist in a boat conformation rather than a chair—a common feature among endo PPAPs, led to this kind of approach. They envisioned constructing the bicyclo[3.3.1]nonane via Dieckman condensation from the precursor, which was in a chair conformation but was required to transform into a boat form. The explanation was the same what I have proposed in the case of clusianone (Scheme 2.11.1).

### **2.15 Total syntheses of sampsonione P and hyperibone I by Plietker et al.**

After his seminal work in 2011, Plietker and his group did not stop there; they continued exploring additional type B endo PPAPs employing their established methodology. In this process of exploration, the group published a total synthesis of sampsonione P (**81**) and hyperibone I (**82**) in 2013 (Figure 2.15.1).<sup>109</sup> These are two unique type B endo PPAPs with tetrahydrofuran side chains. Plietker and his group were not only fascinated by the unique structures of these PPAPs, but also intrigued with determining them correctly and differentiating their useful biological properties. Sampsonione P was isolated from *Hypericum sampsonii*, a family of Hypericaceae, in 2007, and hyperibone I was obtained from *Hypericum scabrum* in 2002.<sup>138</sup> There was confusion about the correct structure of both PPAPs; initially, it was thought that hyperibone I and sampsonione P were isomers, differing only at the C7 appendage orientation; that is, hyperibone I was thought to be an exo type B PPAP, while sampsonione P was assigned to be an endo type B PPAP. Dr. Grossman et al. had proposed a type B endo structure for hyperibone I in 2006 based on the available data.<sup>7</sup>

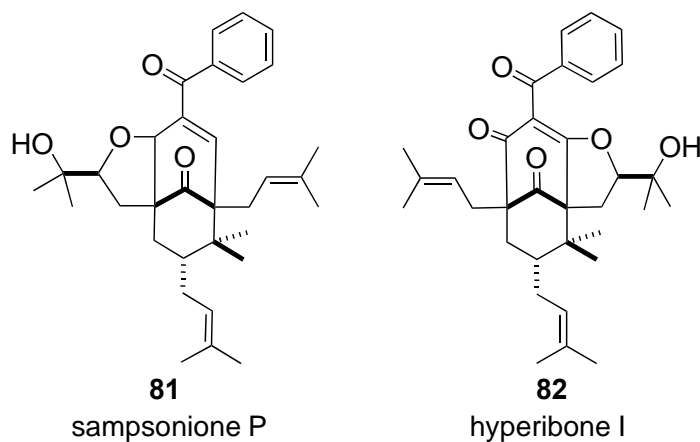
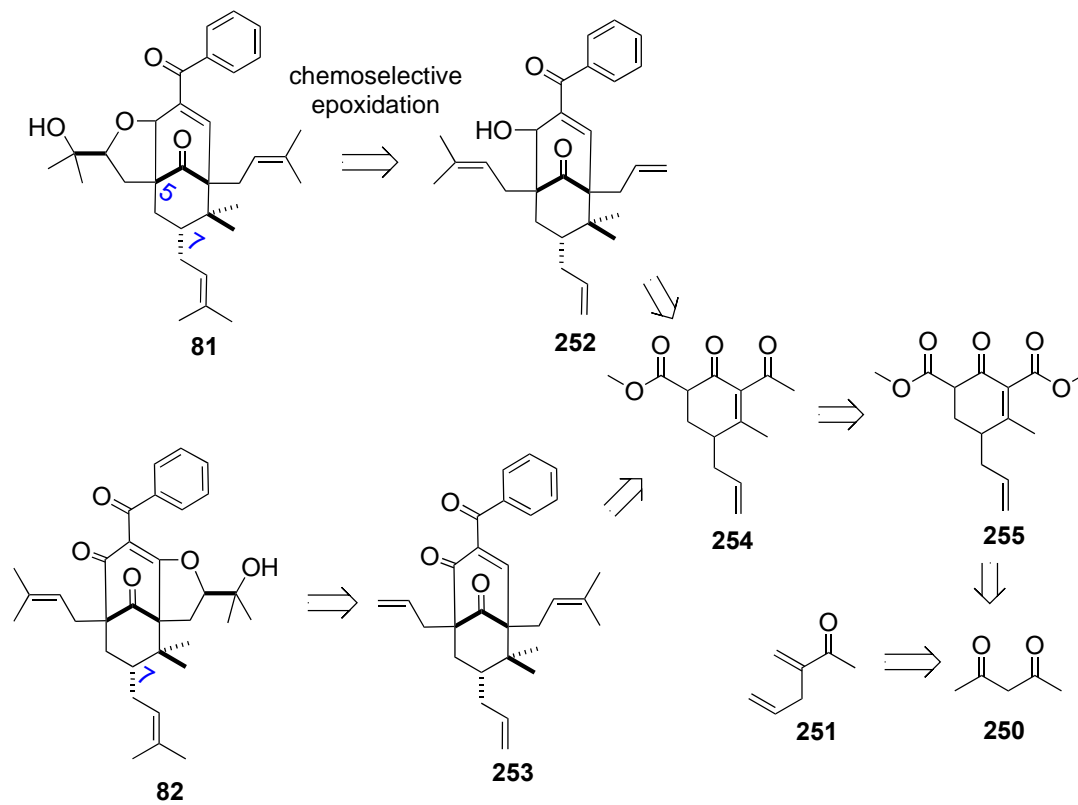


**Figure 2.15.1.** Sampsonione P and hyperibone I

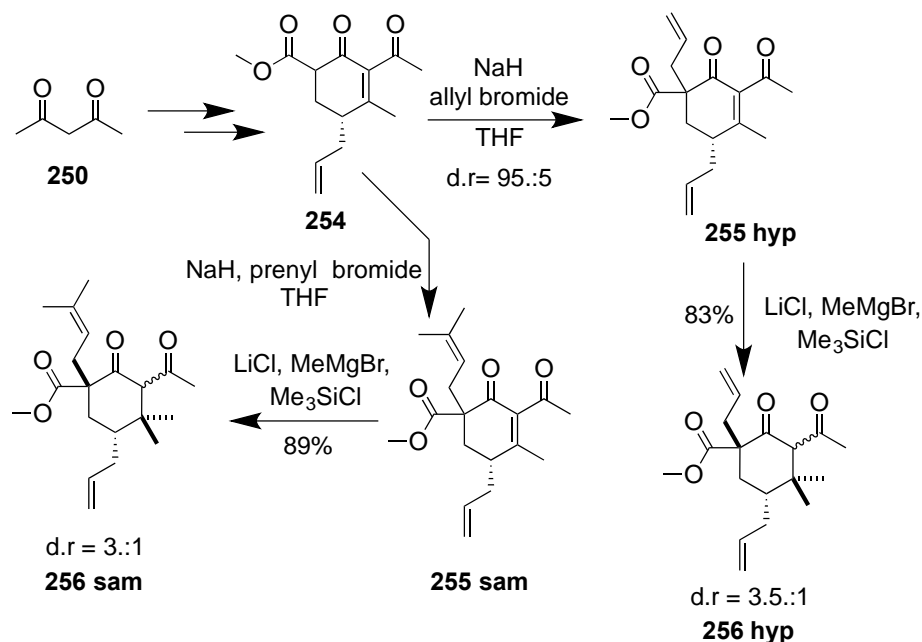
To confirm Grossman's proposal, Plietker and his group set out to synthesize these two molecules. They relied on the same strategy that was published in 2011,<sup>117</sup> which was discussed in detail in previous sections. Retrosynthetically speaking, **81** and **82** are the same as *7-epi*-clusinanone, hyperpapuanone, and hyperibone L, but there is an extra tetrahydrofuran ring present in hyperibone I (**82**) and sampsonione P (**81**) (Scheme 2.15.1). This tetrahydrofuran ring is the result of further oxidation and cyclization of one of the prenyl side chains. The strategy was to install prenyl and allyl groups regioselectively in **254** to give regioisomers **252** and **253**, and then to execute a chemoselective epoxidation of the prenyl group to construct the tetrahydrofuran rings in **81** and **82** (Figure 2.15.1).



**Scheme 2.15.1.** Retrosynthetic analysis of sampsonione P and hyperibone I

The synthesis began with acetylacetone (Scheme 2.15.2) and was the same as 7-*epi*-clusianone in both cases. Therefore, only noteworthy steps will be discussed here.



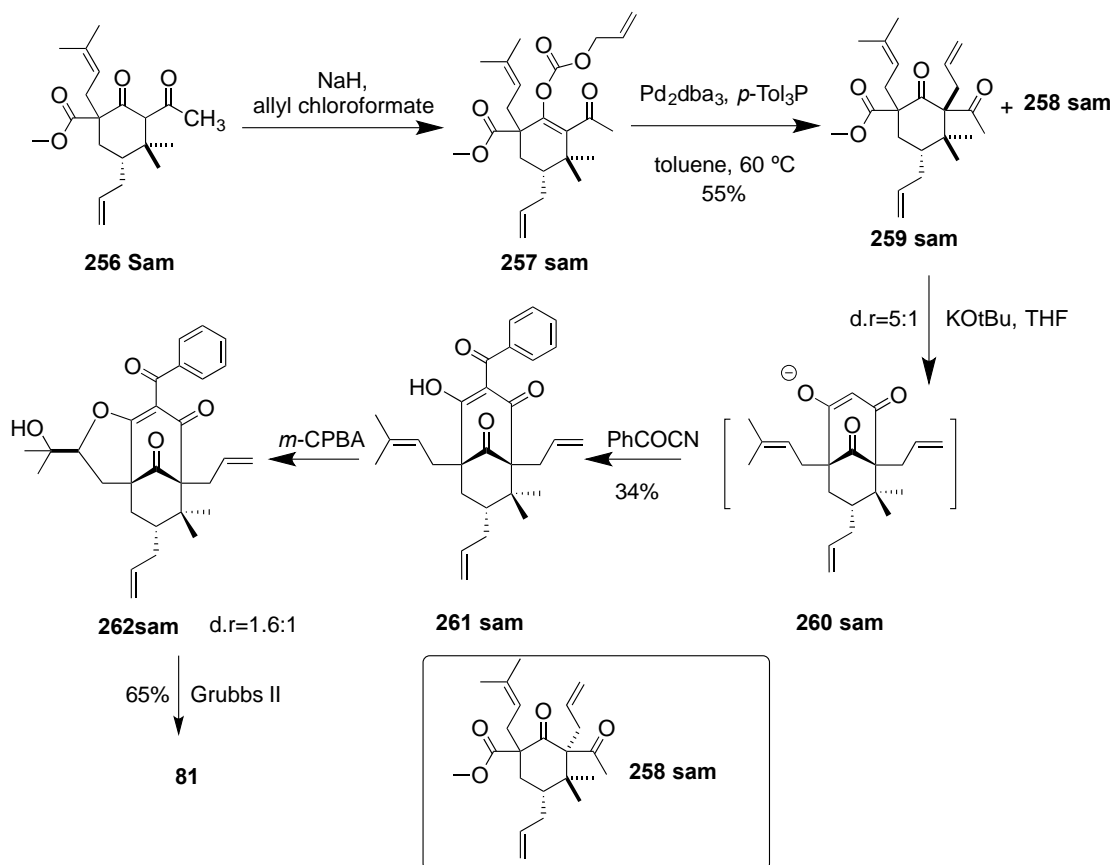


**Scheme 2.15.2.** Synthesis of sampsonione P and hyperibone I

### 2.15.1 End of synthesis of sampsonione P

Sampsonione P necessitated an installation of a prenyl group at the C5. To install a prenyl group required an allyl group in **256 sam** at C5, but NaH-mediated C5-allylation was tough because of the C6 quaternary center. Therefore, **256 sam** was converted to an O-allyl carbonate, **257 sam**, with allyl chloroformate and NaH, and **257 sam** then underwent a Pd-catalyzed intramolecular allylation to furnish two diastereomers in a 5:1 ratio, **258 sam** being a non-required diastereomer, and required being **259 sam**. The required diastereomer, **259 sam**, where the C1 and C7 allyl groups were trans to each other, was directly utilized for Dieckman condensation catalyzed by potassium *t*-butoxide. The intramolecular Dieckman condensation generated an enolate, **260 sam**, which was trapped by PhCOCN in situ to furnish **261 sam**. The C1 prenyl group was converted into an epoxide regioselectively over the less electron-rich allyl group but with low diastereoselectivity, and this step was followed by epoxide ring opening via a nucleophilic attack of OH at the

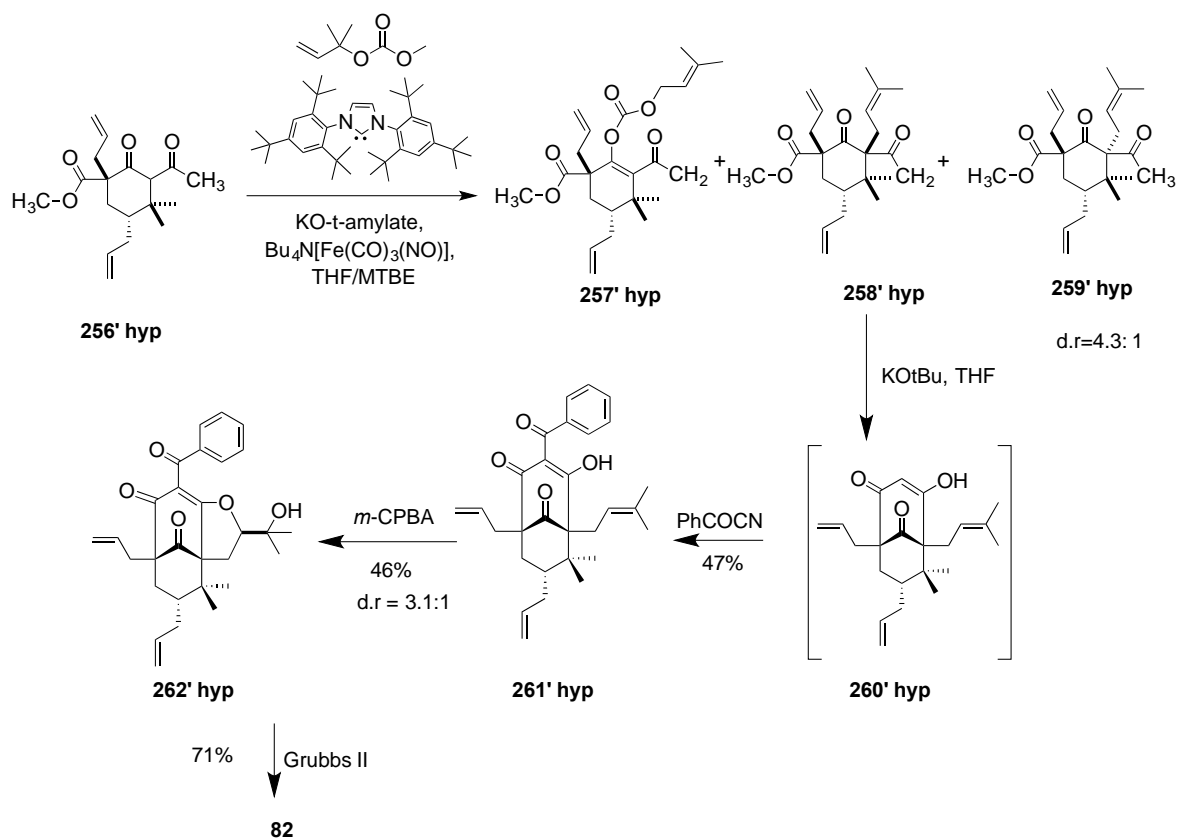
C2. This reaction installed the tetrahydrofuran ring in **262 sam**. Finally, the stage was set for Grubbs metathesis to convert the two allyl groups into prenyl groups; this was accomplished to give sampsonione P (**81**) in 65% yield (Scheme 2.15.3).



**Scheme 2.15.3.** Syntheses of sampsonione P

### 2.15.2 End of the synthesis of hyperibone I

The total synthesis of hyperibone I (Scheme 2.15.4) was problematic since the installation of the prenyl group at C5 proved to be difficult. Therefore, they decided to implement the same idea, which was used in 7-*epi*-clusianone, namely, an iron-catalyzed allylic substitution. The yield was not satisfactory; they also recovered O-prenyl **257' hyp**, which yielded 17%. The remaining steps were the same as in the synthesis of sampsonione P; repeating them led to hyperibone I, **82**.



**Scheme 2.15.4.** Finishing the synthesis of hyperibone I

## 2.16 Total syntheses of guttiferone A and 6-*epi*-guttiferone A by Plietker et al.

In 2014, Plietker's group published another article on the total synthesis of guttiferone A and 6-*epi*-guttiferone A.<sup>139</sup>

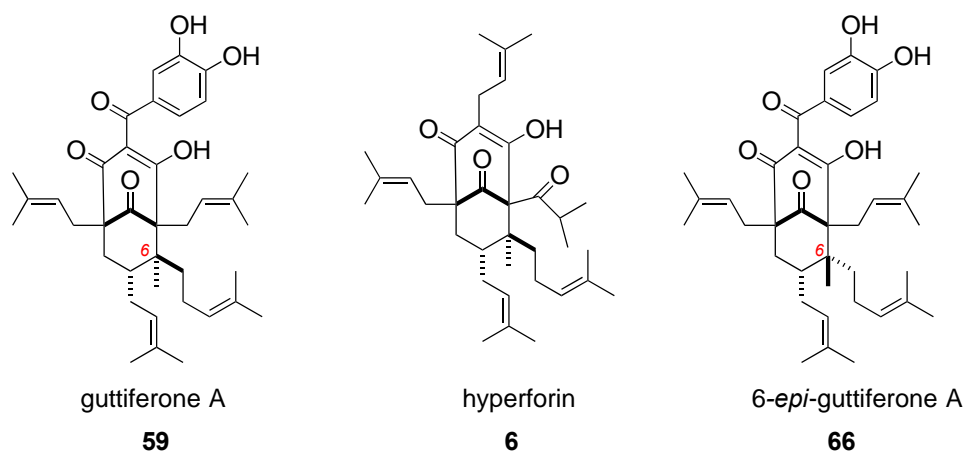
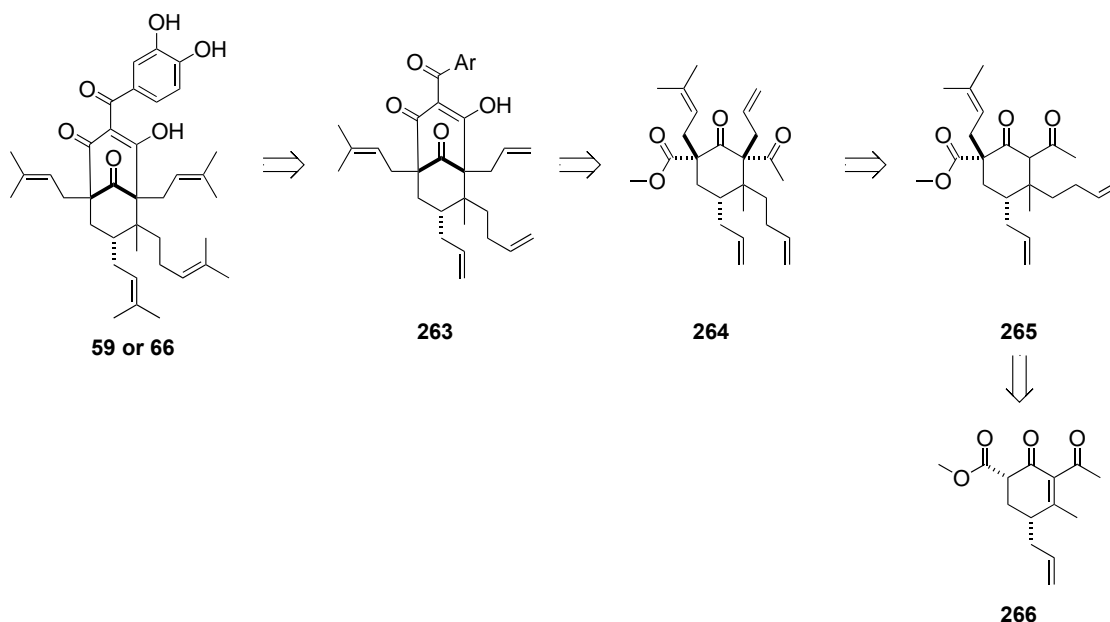


**Figure 2.16.1.** Substrate similarity comparison

Structurally, guttiferone A is an endo type B PPAP (Figure 2.16.1) and contains geranyl appendage at C6. If we compare hyperforin and guttiferone A, it is quite clear that they both possess the same structure, differing in C3 substituents, where guttiferone A has a phenacyl group at C3 and hyperforin has an isopropyl ketone at C5. Guttiferone and epi-guttiferone are epimers. The stereochemistry only differs at C6.

### 2.16.1 Retrosynthetic approach of guttiferone A and 6-*epi*-guttiferone A

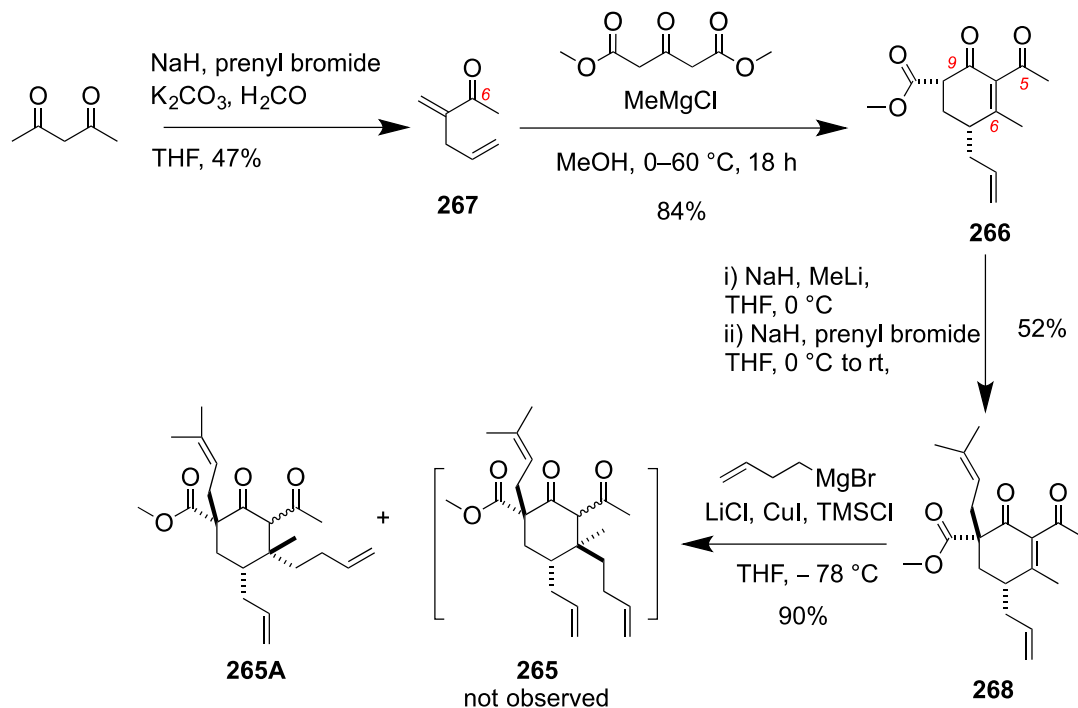
Based on the retrosynthetic strategy (*vide supra*), they delivered a couple of successful endo type B PPAPs beforehand. Therefore, they envisaged that dimethyl cuprate type addition to an enone Scheme 2.16.1 (Scheme 2.16.1) would establish the quaternary center at C6 with the correct stereochemistry. The geranyl appendage must be *cis* to the allyl group in **264** in guttiferone A, while *trans* in epi-guttiferone A. This was the prime challenge in the total synthesis. The remaining steps in the syntheses were the same as the other type B endo PPAP syntheses, which were discussed in depth in the previous sections, beginning with the alkylation of acetyl acetone with allyl bromide.



**Scheme 2.16.1.** Retrosynthetic analysis of guttiferone A and 6-*epi*-guttiferone A

### 2.16.2 Synthesis of 6-*epi*-guttiferone A

The Plietker began their synthesis of guttiferone A by alkylating acetylacetone with allyl bromide, followed by aldol-type demethylation to generate **267** in 47% yield. Then, **267** was allowed to react with dimethyl-1,3-acetonedicarboxyate in the presence of MeMgCl at low temperature to furnish cyclohexenone **266** in an 84% yield. This reaction was a tandem Michael-Knoevenegal reaction, which brought two ester groups in a molecule, separated by a ketone. Compound **266** was first treated with MeLi to convert C5 ester to methyl ketone and was then prenylated in the same pot at C1 using NaH stereoselectively. After this, the most interesting step of the sequence was performed: the installation of a 3-buten-1-yl group at C6 to construct the quaternary center. Following Yamamoto protocol, compound **268** was added to a cuprate, generated from the action of CuI and 3-buten-1-ylmagnesium bromide, gave **265A** as a single diastereomer at C6 (but an inconsequential 1:1 mixture of stereoisomers at C5, between the two ketones). This result was unexpected, and it caused the group to change the target of their synthesis from guttiferone A to 6-*epi*-guttiferone A.

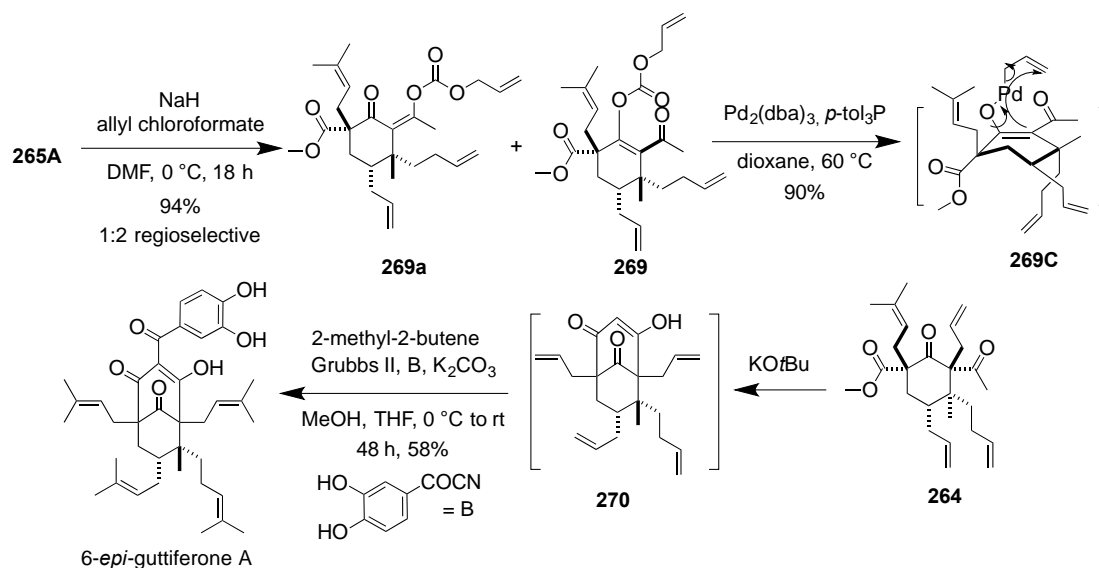


**Scheme 2.16.2.** Synthesis of 6-*epi*-guttiferone A

The next challenge was to install an allyl group at C5, which would be trans to the butenyl group at C6.  $Bu_4N[Fe(CO)_3(NO)]$  was the initial catalyst of choice for *C*-allylation, but it did not bring forth the desired result. Thus, they resorted to a palladium-catalyzed decarboxylative allylation, which was quite an effective method for Plietker's group in previous schemes. To execute the plan, they allowed **266** to react with allyl carbonate and NaH. The reaction yielded two regioisomers in a 1:2 ratio. Heating induced a Claisen rearrangement of the allyl vinyl carbonates. The diastereocontrol of the Claisen rearrangement was excellent, 95:5.

Once the construction of the quaternary center at C5 was accomplished, the next aim was to generate the bicyclo[3.3.1]nonane that was furnished by Dieckman condensation using potassium *tert*-butoxide. Global Grubbs metathesis replaced all the allyl groups with the prenyl groups and, finally,  $K_2CO_3$  deprotonated a C3 proton, and the

resulting enolate reacted with 3,4-bis-acetoxybenzoyl to accomplish the total synthesis of 6-*epi*-guttiferone (**59**) (Scheme 2.16.3).



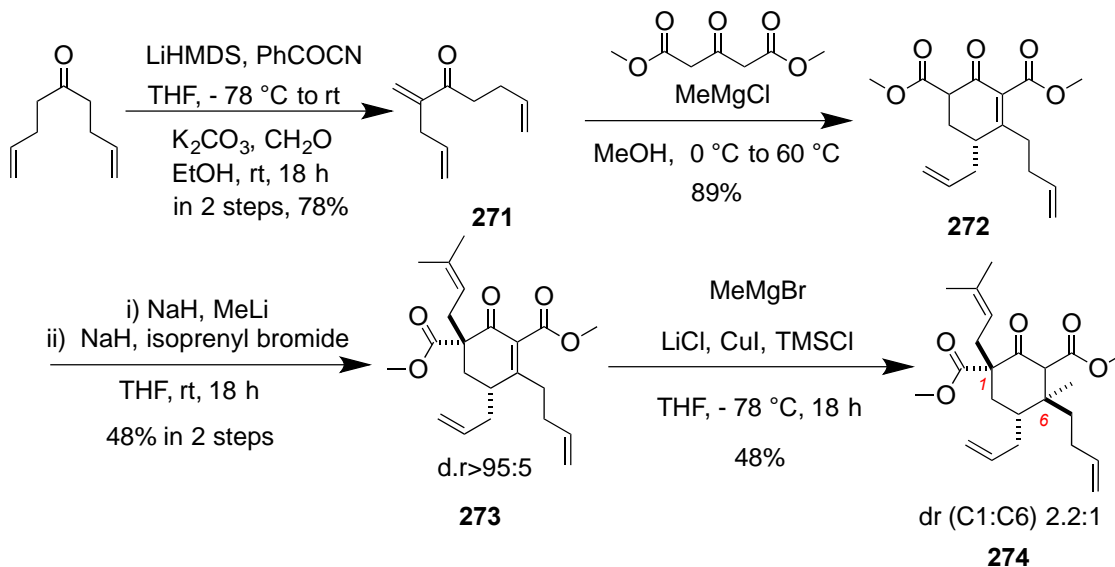
**Scheme 2.16.3.** Synthesis of 6-*epi*-guttiferone A

### 2.16.3 Synthesis of guttiferone A

After completing the total synthesis of 6-*epi*-guttiferone A, Plietker *et al.* decided to revisit the challenge of the synthesis of guttiferone A. They realized that C6 stereochemistry would hold the key for the success of the synthesis. Remember that the 1,4-addition reaction, following modified Yamamoto's condition, gave an unexpected product, **265A**, when they envisioned getting **265** (Scheme 2.16.3). Therefore, they needed to devise a plan in such a way that it could establish a geranyl substituent on C6 and make the Dieckman condensation route feasible. The research group planned to introduce the 3-buten-1-yl moiety at the very beginning of the synthesis so they could induce the diastereoselection later via suitable reagents.

Based on this idea, they set out to synthesize guttiferone A (Scheme 2.16.4). The synthetic scheme began by acylation of 1,8-nonadien-5-one by LiHMDS and was followed by the methylenation with formaldehyde. Then, as usual, a tandem Michael–aldol

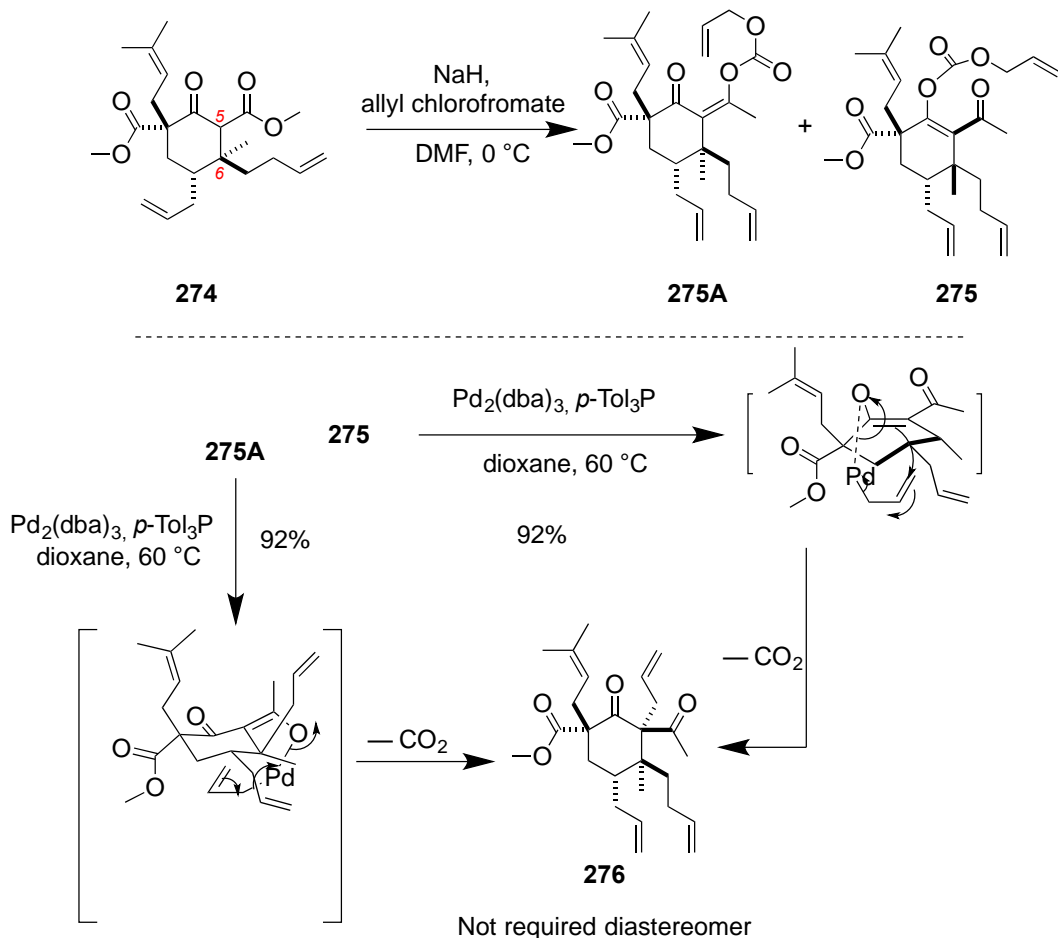
condensation of **271** with dimethyl acetonedicarboxylate constructed cyclohexene **272**. Prenylation of **272** gave enedione **273**. Then, conjugate addition of a methyl cuprate to **273** went exclusively cis to the allyl group at C7 to give **274**, as desired and expected from the 6-*epi*-guttiferone synthesis.



**Scheme 2.16.4.** Beginning of the synthesis of guttiferone A

Fe-catalyzed allylic substitution at C5 of **274** was not possible in this case because of the steric demand, and this led them to consider palladium-catalyzed decarboxylative allylation. The action of NaH and allyl chloroformate on **274** yielded both **275** and **275A** (Scheme 2.16.5). The decarboxylative allylation of either compound by Pd(II), however, gave **276** as a major product, which had the undesired stereochemistry. The ester groups on C1 and the keto methyl group on C5 were trans to each other, which was not a correct geometric requirement for Dieckman condensation to construct the bicyclo[3.3.1]nonane motif.

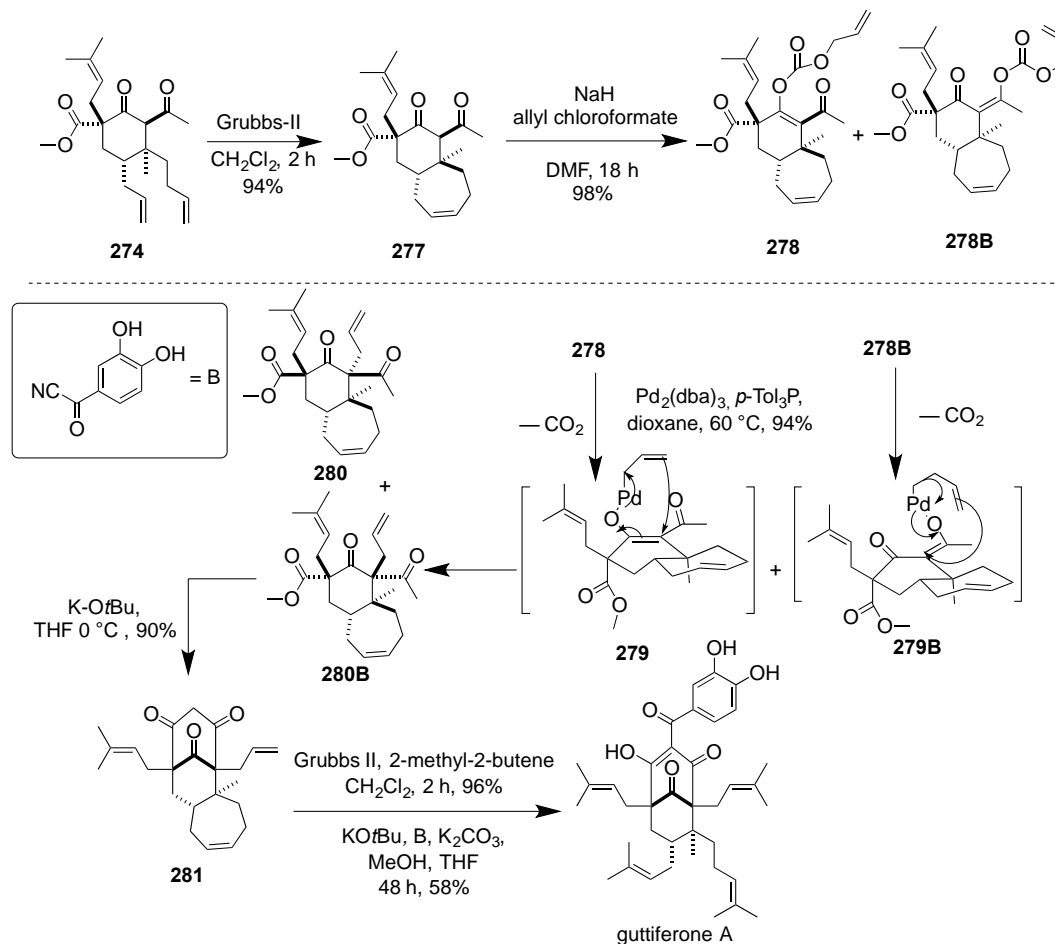




**Scheme 2.16.5.** New diastereoselectivity problem in the synthesis of guttiferone A

Therefore, they thought of an alternative plan: the introduction of a cyclic group from the two unsaturated appendages in **274** would enhance the formation of the required diastereomer. Thus, they converted **274** into **277** using Grubbs-II in 94% yield (Scheme 2.16.6). After that, they tried NaH-mediated allylation of **277** with allyl chloroformate and the reaction produced **278** and **278B**, which was followed by Pd-catalyzed decarboxylative allylation to furnish **280** and **280B**. The yield of the reaction was impressive, nearly 94%, and the diastereomeric excess ratio was 95:5 with respect to the desired isomer, **280B**. Compound **280B** was treated with potassium *t*-butoxide to construct the bicyclo[3.3.1]nonane **281**. Finally, global Grubbs' metathesis of **281** and acylation with

3,4-bis-acetoxybenzoyl cyanide yielded guttiferone A in 58% yield in 13 steps (Scheme 2.16.6). The most important points from this synthetic plan are: I) developing a route to install the correct geometry at C1 and C5 so that Dieckman condensation could take place; and, II) starting from a precursor with the correct oxidation state at C4 so that late stage oxidation would not pose any threat to the new route.



**Scheme 2.16.6.** Synthesis of guttiferone A

## 2.17 Total synthesis of garcinol and isogarcinol

Socolsky and Plietker published an article in 2015 showing the total synthesis of garcinol and isogarcinol. The purpose of this paper was not only to devise a route to endo PPAPs but also to ascertain the relative configuration of the molecules correctly. There

were discrepancies in secondary literature concerning the relative configuration of garcinol and isogarcinol (Figure 2.17.1. Garcinol and isogarcinol).<sup>140</sup>

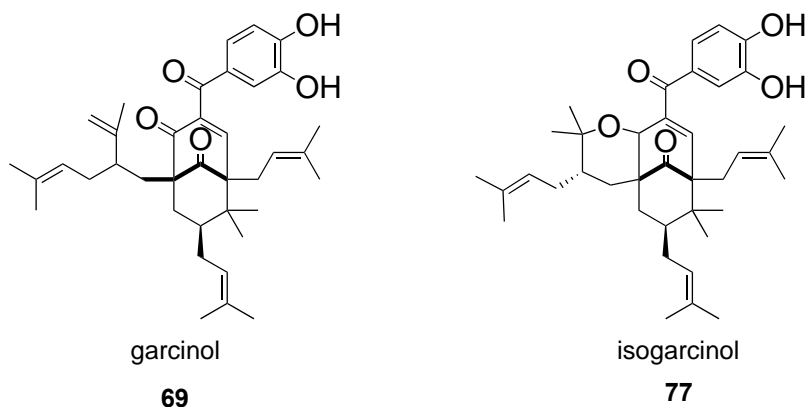
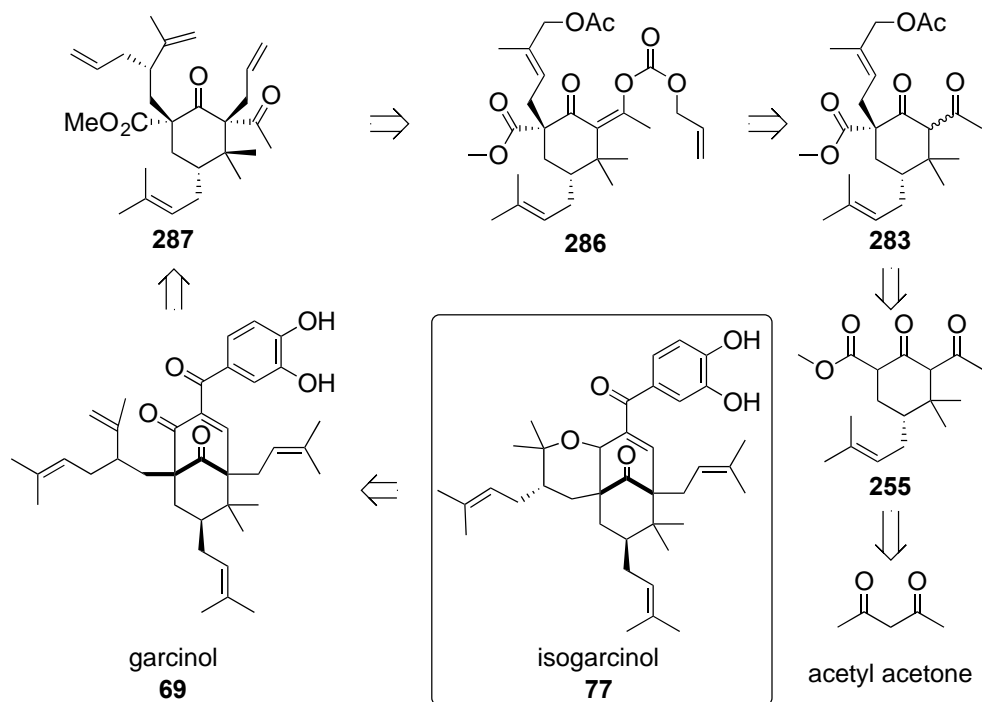


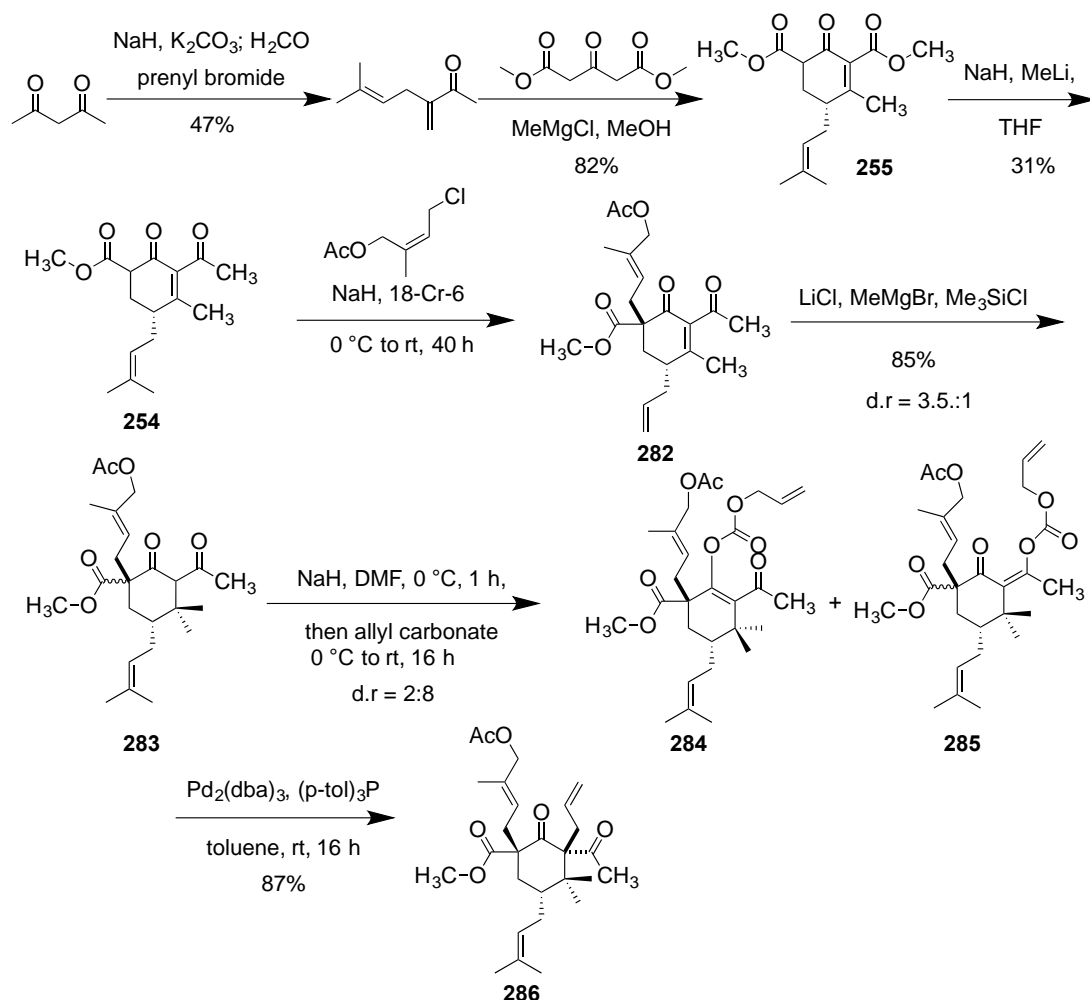
**Figure 2.17.1.** Garcinol and isogarcinol

In 2011, Plietker and his group published a seminal work on the total synthesis of endo type B molecules. The 2015 article is a continuation of their earlier work. The retrosynthesis started from the removal of all the prenyl groups from the molecule and replacing them with allyl groups (Scheme 2.17.1). They relied as usual upon an internal Dieckman condensation to set up a bicyclo[3.3.1]nonane trione core. The key challenge, however, in the whole synthetic scheme was to affix a lavandulyl side chain on the carbon C5. That step involved a lot of fascinating chemistry, which I explain later.



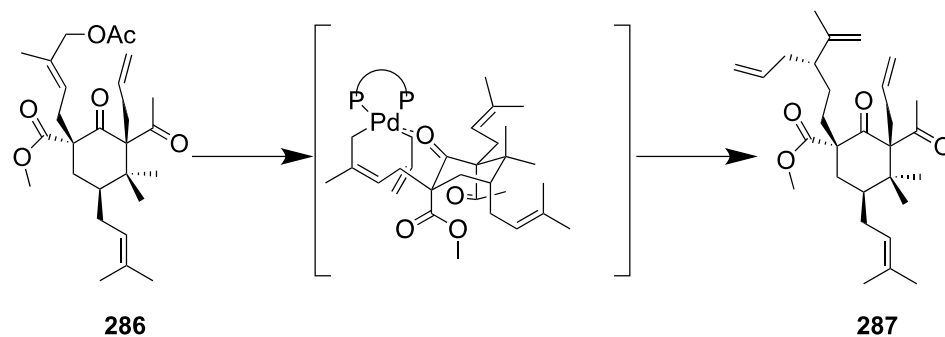
**Scheme 2.17.1.** Retrosynthetic analysis of garcinol and isogarcinol

The synthesis started from acetyl acetone (Scheme 2.17.2), which underwent alkylation with prenyl bromide followed by extrusion of acetate via aldol reaction, to furnish the prenylated ketone. The prenylated ketone underwent tandem Michael/Knoevenegal reaction to construct the cyclohexenone, **255**. Next, **255**, a keto-diester, was made a keto-monoester **254** by using NaH and MeLi under standard conditions, which the group employed several times. The C-5 allylation with (2E)-4-chloro-3-methylbut-2-en-1-yl acetate went smoothly without complication. The reaction produced **282** with a decent yield. Allylation at C1 proved to be a roadblock for the synthesis since Trost-Tsuji allylation did not work, presumably because of the gem dimethyl group. Therefore, they resorted to formation of the allyl carbonates. Two *O*-allyl carbonates formed, **284** and **285**, but both yielded the required diastereomer of **286** after Claisen rearrangement.



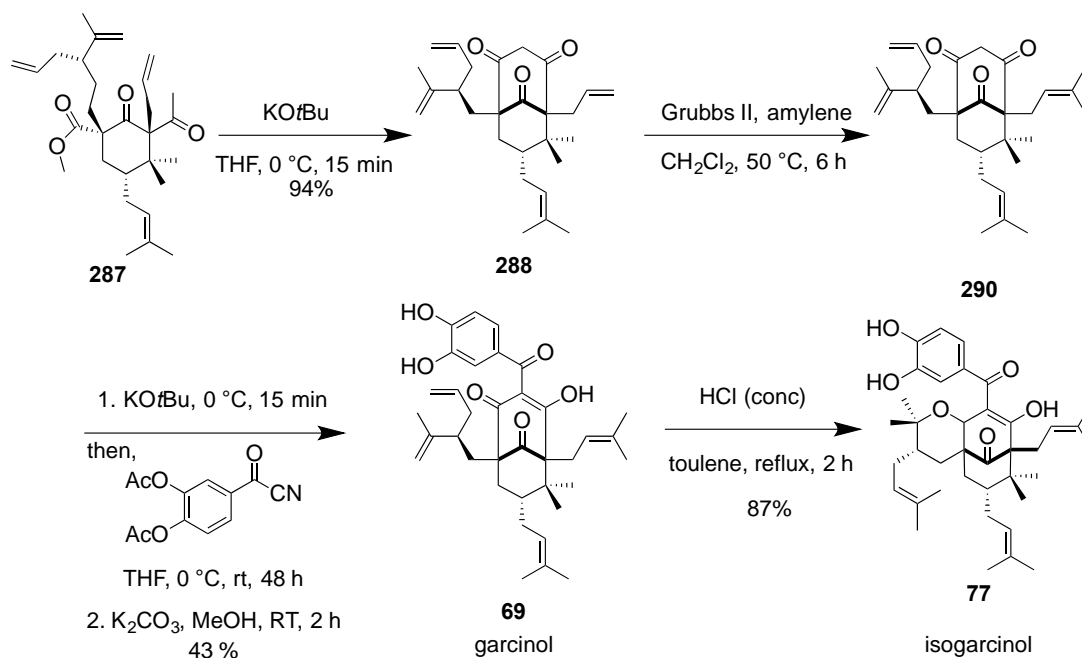
**Scheme 2.17.2.** Syntheses of garcinol and isogarcinol

The conversion of the acetoxyprenyl group at C5 of compound **286** to a lavandulyl group was challenging, since a palladium catalyzed allyl–allyl exchange reaction could result in a simple  $S_N2$  substitution with hydrogen and  $\beta$ -elimination (Scheme 2.17.2). After screening many ligands and bases, they found that  $[Pd_2(dba)_3]$ , dppe, allyl(pinacol)borane, and CsF gave the best result of the exchange reaction, although they recovered some  $\beta$ -elimination product (Scheme 2.17.2). The stereochemical outcome could be explained by the TS model (Scheme 2.17.3), where Pd coordinated to the carbonyl group in cyclohexane ring by forming a palladacycle that prevented the allyl transfer from the other direction, leading to the stereoselective fixation of the allyl group on the prenyl moiety.



**Scheme 2.17.3.** Stereochemistry of the exchange reaction

After installing the lavandulyl moiety at C5, Dieckmann condensation of **287** promoted by KO-*t*-Bu was followed by Grubbs metathesis (Scheme 2.17.4). The 1,3-diketone was again deprotonated and trapped by 3,4-dihydroxybenzoyl cyanide. Garcinol, **69**, was produced in 43% yield over the two steps. Isogarcinol, **77**, was made from garcinol by the action of concentrated HCl. The reaction yielded isogarcinol in 87% yield. Overall, there were 13 steps in the garcinol synthesis and 14 in the isogarcinol one. Plietker's group separated the two compounds by chiral HPLC along with possible four enantiomers, and each of them was identified by an arduous characterization process, namely  $^1\text{H}$  NMR,  $^{13}\text{C}$  NMR, and 2D correlation spectroscopy. After data analysis, they reached the conclusion that guttiferone E and garcinol were enantiomers, as were isogarcinol and isoxanthochymol. How they reached such a conclusion was discussed in detail in Chapter 1.



**Scheme 2.17.4.** Synthesis of isogarcinol

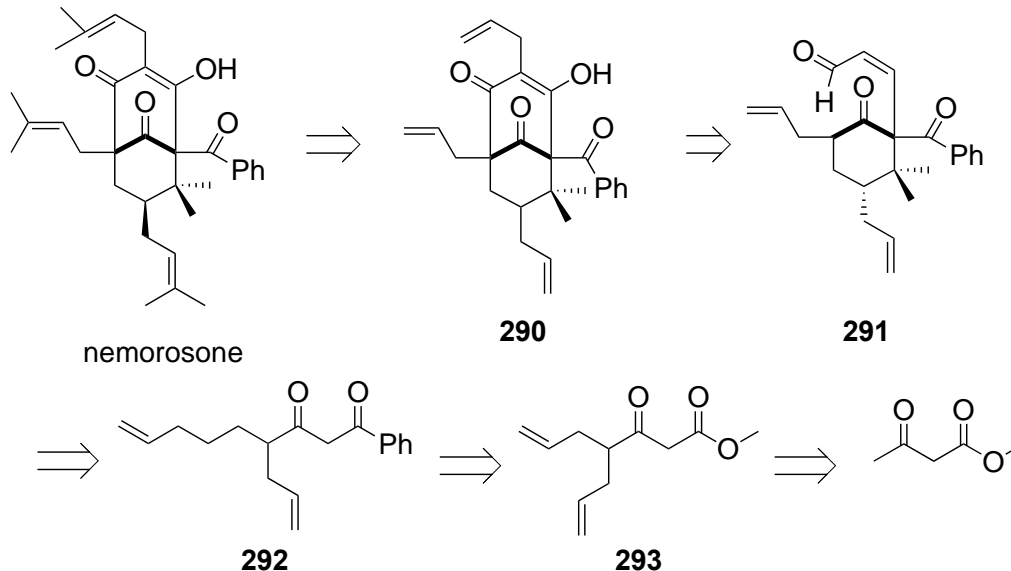
Plietker's group separated two compounds by chiral HPLC along with possible four enantiomers, and each of them was identified by arduous characterization process, namely  $^1\text{H NMR}$ ,  $^{13}\text{C NMR}$ , 2D-correlation spectroscopy. After data analysis, they reached the conclusion that guttiferone E and garcinol are enantiomers, as are isogarcinol and isoxanthochymol. How they reached such conclusion was discussed in detail in chapter 1.

## 2.18 Grossman's approach to the synthesis of PPAPs

Dr. Grossman's group has a longstanding interest in this field. They have contributed by devising a synthetic route to construct a bicyclo[3.3.1]nonane,<sup>7, 141</sup> which is known as the 'alkynylation–aldol approach.' They envisioned developing a scheme that would work as a model for the synthesis of any PPAPs irrespective of their classification. The scheme was initially designed for nemorosone, a type A PPAP, but later, they realized that the newly devised scheme would also be effective for type B endo PPAPs with some minor modifications. They envisioned replacing the prenyl groups with robust allyl groups

(Scheme 2.18.1), which would make the reactions simpler. When decoration around the bicyclic core was needed, prenyl groups would be introduced by global metathesis in **290**. Compound **290**, on the other hand, could be constructed from **291** by an aldol followed by oxidation. The most interesting point about **291** is that it is a *Z*-alkenal and, to construct **291**, it was necessary for the aldol condensation. Here, they thought about making a model system to synthesize **291** without the gem-dimethyl next to the benzoyl group in **291**. Therefore, they redrew their retrosynthetic scheme without the gem-dimethyl group and **291** could be deconstructed to **292**, which did not contain a gem-dimethyl group.

Grossman et al. thought to reduce the alkynal chemoselectively using cobalt catalyst. They decided on a model study to examine if the route proposed could be realistic. Therefore, **292** was replaced by **293**, which could be synthesized via a double alkylation from ethyl acetoacetate, **294**.

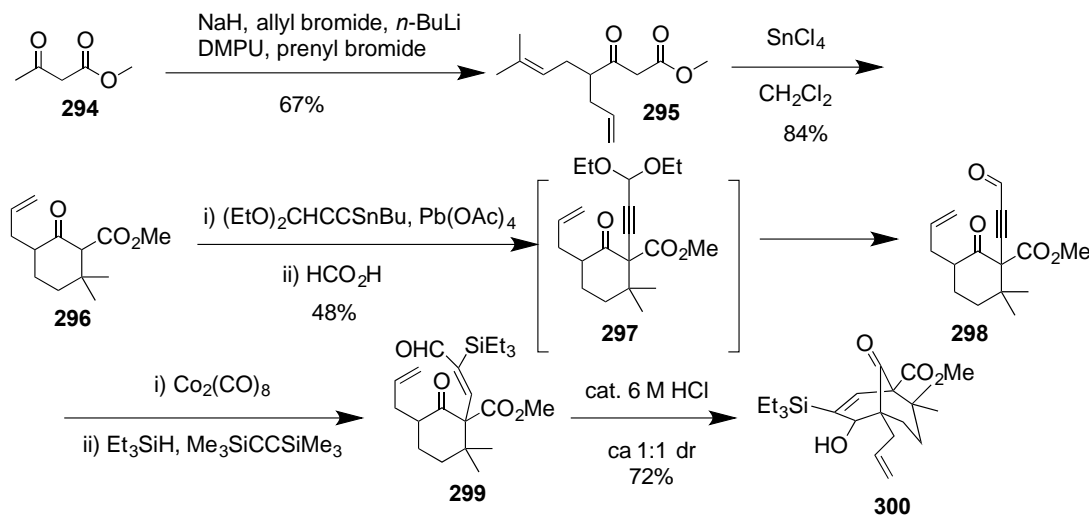


**Scheme 2.18.1.** Retrosynthetic analysis of nemorosone by Grossman et. al.

They began with ethyl acetoacetate **294**, which was first alkylated with allyl bromide (Scheme 2.18.2) to **295**. The addition of prenyl bromide to the dianion of methyl 3-oxo-6-heptanoate furnished **296** with an overall yield of 67%.  $\text{SnCl}_4$ -promoted 6-*endo*-



*dig* cyclization of **296** converted it into **298** via a radical mechanism. The cyclic  $\beta$ -keto ester **296** was then converted to dimethoxy compound **297** by  $\text{Pb}(\text{OAc})_4$  and subsequent hydrolysis yielded **298**.



**Scheme 2.18.2.** Model study by Grossman et al.

Alkynal **298** was hydrosilylated to alkenal **299** by  $\text{Co}_2(\text{CO})_8$  and  $\text{Et}_3\text{SiH}$ . One of the interesting aspects of this chemistry is that the triple bond was reduced to a *cis* double bond. The *Z*-geometry of the double bond is essential for closing the ring by aldol condensation. An  $\text{HCl}$ -mediated aldol reaction led to bicyclic compound **300**. The real challenge was to install a 1,3-diketone functionality in **300** by oxidizing the C4 carbon. It appeared from their model study that C4 carbon was too reluctant to undergo  $\text{sp}^2$  to  $\text{sp}^3$  hybridization. All the methods to put any oxygen-containing group at C4 failed, presumably because of the gem-dimethyl groups at C8. Although the route did not deliver the result, and the synthesis of nemorosone was not accomplished, the route would be exploited with some modifications in the synthesis of 7-*epi*-clusianone **10**.

### 3 Our strategy for 7-*epi*-clusianone

#### 3.1 Introduction

In chapter 1, I have discussed the medicinal properties of PPAPs in detail.<sup>27, 142</sup> Frankly speaking, they are one of the prime reasons for chemists to synthesize these molecules. My reasons for synthesizing these molecules are not different. These molecules are fascinating, partly because of the wide range of therapeutic properties in their initial trials. Initial studies of these molecules hint towards this direction—garsubellin A shows antineurodegenerative activity,<sup>26</sup> hyperforin shows antidepressant activity,<sup>101, 142, 143</sup> and clusianone shows antibacterial activity.<sup>88, 101</sup> There is another aspect of PPAPs—endo and exo epimers differ quite substantially,<sup>98</sup> as far as their medicinal properties are concerned. However, these results are not conclusive enough that these molecules could be marketed for fighting diseases. For these reasons, we need to have enough of these molecules on hand to carry out conclusive research.

On the other hand, we are synthetic organic chemists, and therapeutic details of a compound cannot be the only goal of our research; there must be another dimension to it. The architectural design acts as an added flavor to our research. In particular, 7-endo type B PPAPs exist in a boat conformation, and this makes their synthesis more challenging. Furthermore, many total syntheses of 7-exo type A PPAPs have been reported, but the syntheses of type A endo, except 7-*epi*-nemorosone, and type B endo, with the exception of Plietker's seminal works, have not been well addressed.<sup>117, 144</sup> Therefore, we have striven to find a viable method to synthesize type B 7-endo PPAPs so that we could develop a model that would work for many PPAPs.

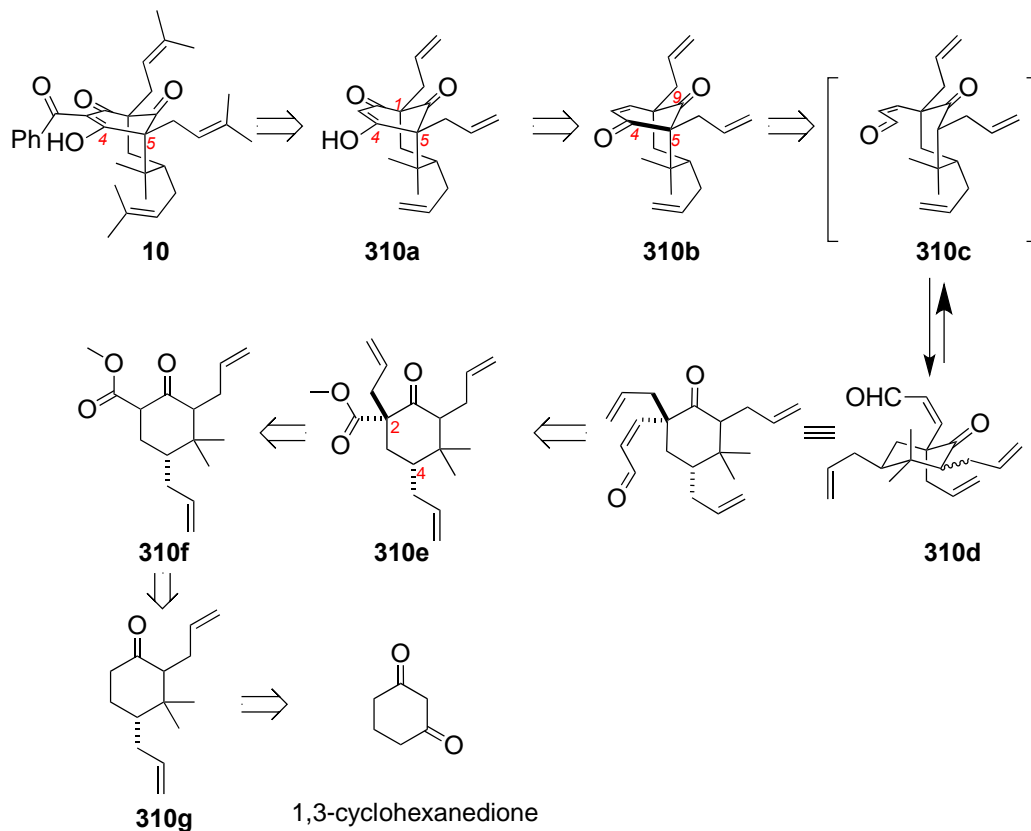
We chose 7-*epi*-clusianone as our target compound. There are two reasons for this selection: one, its wide range of biological activity—anticancer,<sup>89</sup> antiplasmodic,<sup>71</sup>

vasorelaxant,<sup>145</sup> and antibacterial<sup>91, 96, 146</sup>—and the second, its unique structure, which exists in the boat conformation.<sup>37</sup> When we started this project back in 2011, no one had published a total synthesis of a type B 7-endo PPAP. However, in 2011, a research group in Germany led by Bernd Plietker published the first total synthesis of 7-*epi*-clusianone.<sup>117</sup> Since then, to the best of our knowledge, no group has reported any total synthesis of the molecule using a different route. Herein, we have sought to devise a path for the total synthesis of 7-*epi*-clusianone **10** following the alkynylation-aldol method.

### 3.2 Initial retrosynthetic strategy

The first approach to synthesize 7-*epi*-clusianone **10** came from a joint venture led by my predecessor, M. P. Suresh Jayasekara, and Dr. Grossman. They approached the retrosynthesis of the molecule differently; initially, they realized that compound **10** might be synthesized from 1,3-diketone **310a** by an acylation of C3, followed by a global Grubbs' metathesis (Scheme 3.2.1). They believed that they could prepare 1,3-diketone **310a** by oxidation of the enone in **310b**. They envisaged constructing the bicyclic system by making a bond between the C4 and the C5 carbon (dark bond) in **310b**. Therefore, diketone **310b** might be accessed from **310c**, in equilibrium with **310d**, by an intramolecular aldol condensation followed by oxidation of the diastereomeric alcohols. They believed that the equilibrium between **310c** and **310d** would favor **310d**, but they postulated that enough **310c** would be produced at equilibrium to allow the aldol reaction. Cis enal **310d**, they thought, could be synthesized from **310e** by Still-Gennari reaction. The trans relationship of the C2 and C4 allyl appendages in **310e** was crucial for the synthesis of the desired 7-*epi*-clusianone **10**. They assumed that **310e** could effectively be obtained from by Trost-

Tsuji allylation of  $\beta$ -keto ester **310f**, which could ultimately be synthesized from cyclohexanone **310g** and thence 1,3-cyclohexanedione in six steps.

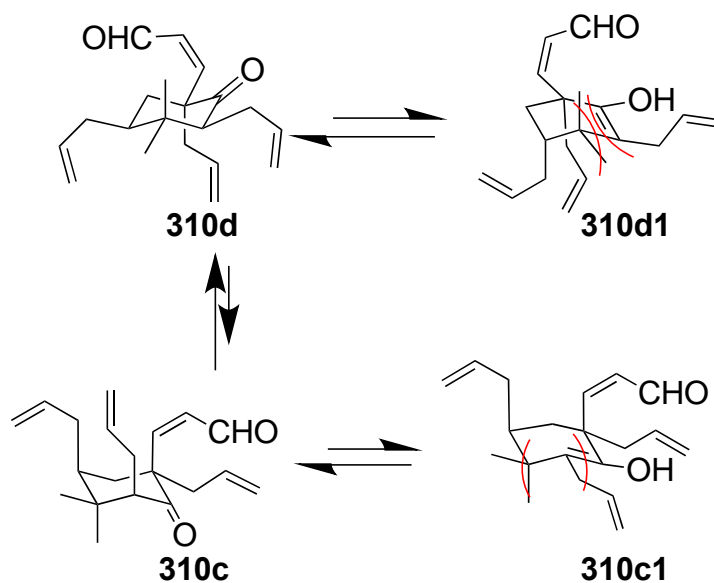


**Scheme 3.2.1.** First retrosynthetic strategy

### 3.3 Synthesis of 7-*epi*-clusianone

The details on the synthesis based on this first retrosynthetic strategy can be found in Jayasekara's dissertation, therefore, I am not discussing every aspect of it. However, I will comment on why the route (Scheme 3.3.1) did not succeed, because it was a pertinent question so far as my approach towards the molecule was concerned. He commenced from 1,3-cyclohexanedione, and, after that, successfully synthesized **310d**. There, he faced a roadblock to constructing the bicyclic molecule **310b**: the aldol reaction of **310d** did not

proceed. He reasoned that A<sup>1,2</sup>-strain in **310c1** prevented the enol or enolate from forming, preventing the intramolecular aldol reaction from occurring.

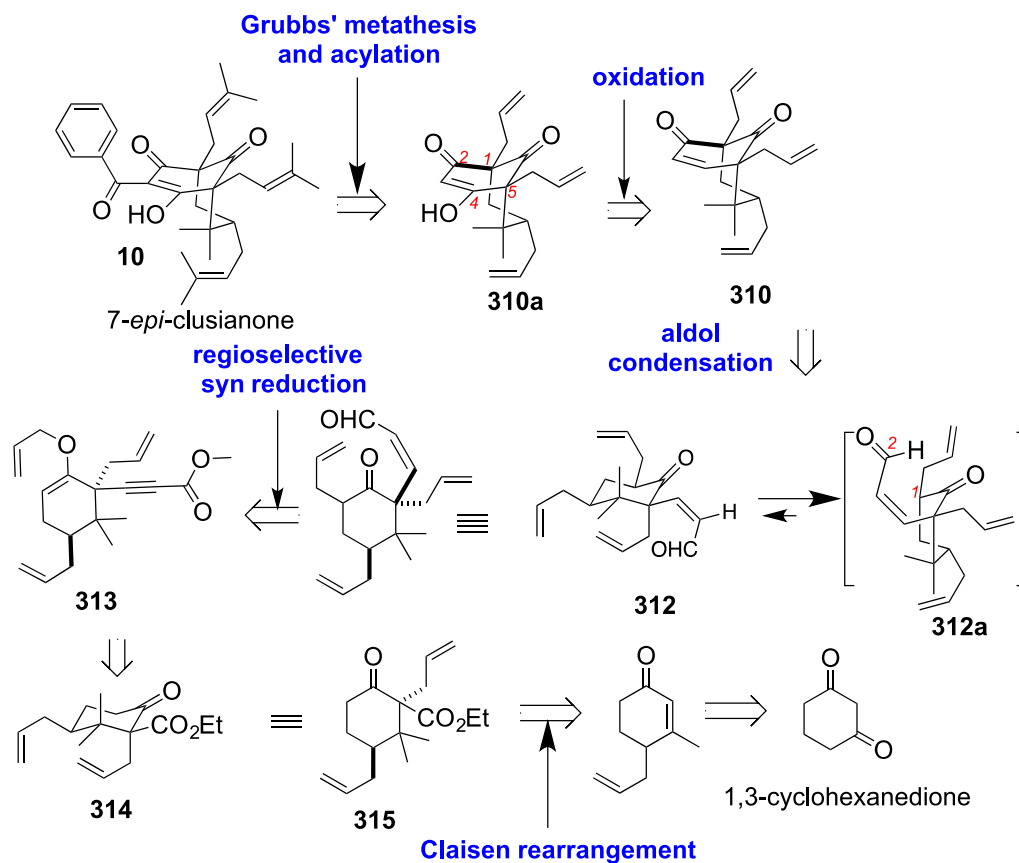


**Scheme 3.3.1. A<sup>1,2</sup>-strain**

### 3.4 Revised retrosynthetic strategy

Realizing that the A<sup>1,2</sup>-strain made the intramolecular aldol of **310d** impossible in the first trial, they pondered over redesigning the retrosynthetic strategy, keeping the overall approach the same. Hence, they decided to disconnect the C1–C2 bond of **10** instead of the C4–C5 bond (Scheme 3.4.1); in that case, there would not be any issue of A<sup>1,2</sup>-strain in the enol or enolate undergoing the key intramolecular aldol reaction. They envisaged that the C4 OH group of **310a** might be introduced into simple alkenone **310**, which, in turn, could be synthesized by an intramolecular aldol reaction of compound **312**. The strategy requires that **312** assume its higher energy conformation, **312a**, before undergoing the reaction. The essential Z-alkenal **312** might be obtained by a stereoselective reduction of alkynoate **313**, which could be prepared by two-carbon homologation from β-keto ester **314**. They planned to make ester **314** from alkenone **315**, which could be

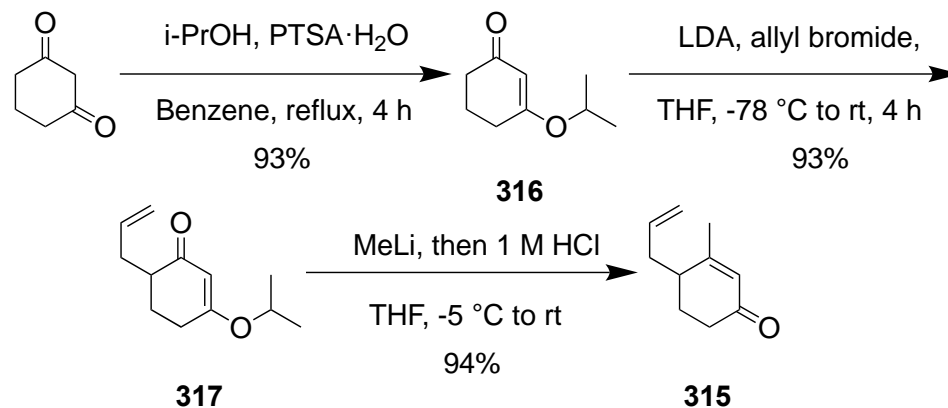
accessed from commercially available 1,3-cyclohexanedione in three steps with good yields. I inherited the scheme, and my research goal was to oxidize the C4 carbon of **310** and then complete the total synthesis, which was three steps away from the target.<sup>53</sup>



**Scheme 3.4.1.** Revised retrosynthetic strategy for *7-epi-clusianone*

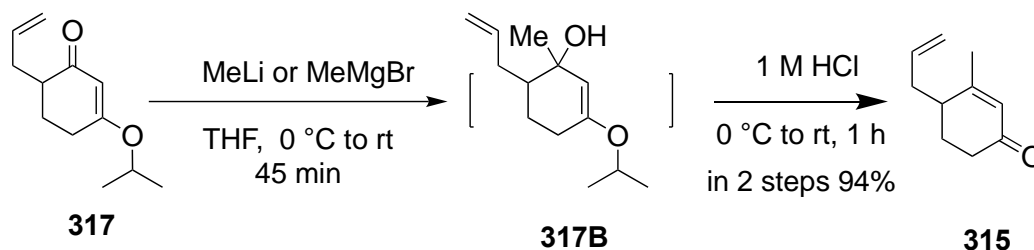
### 3.5 Enol ether formation and allylation followed by methylation

We commenced from commercially available 1,3-cyclohexanedione, and converted it into an isopropyl enol ether **316** in a high yielding reaction (Scheme 3.5.1).<sup>147</sup> Subsequently, compound **316** underwent LDA-mediated allylation and furnished **315** without any purification (93% yield).<sup>148</sup> We were happy to be able to avoid any rigorous column purification in the two initial steps.



**Scheme 3.5.1.** Synthesis of allyl enone **315**

### 3.6 Methylation and hydrolysis



**Scheme 3.6.1.** Methylation and hydrolysis

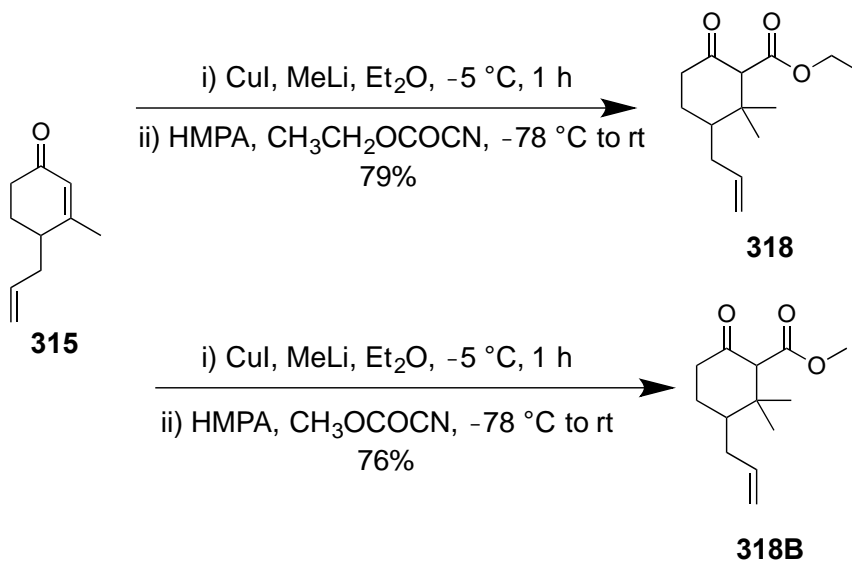
Following the Stoltz protocol for Stork-Danheiser reaction, a nucleophilic addition of MeLi or MeMgBr to the carbonyl carbon of **317** gave allyl alcohol **317B**, and addition of 1 M HCl to **317B** induced a transposition of an allylic double bond to compound **315** in 87% yield after column purification (Scheme 3.6.1).

### 3.7 Synthesis of $\beta$ -keto ester

Compound **315** was treated with lithium dimethylcuprate in the presence of HMPA to add a methyl group across the double bond to construct the C6 quaternary center. The resulting enolate was trapped by methyl or ethyl cyanofornate to furnish  $\beta$ -keto ester, **318B** or **318** with a decent yield ranging from 79% to 76% (Scheme 3.7.1).<sup>149</sup> The yield of the reaction was very sensitive to the amount of HMPA used. We screened several reactions

using 1 to 8 equivalents of HMPA to find the optimum conditions, and the best result was obtained using 7.2 equivalents of HMPA. Less than 6 equivalents of HMPA promoted *O*-acylation rather than *C*-acylation. We tried to replace HMPA with DMPU because of HMPA's carcinogenicity, but the yield was very low in that case.

Both my predecessor and I encountered several challenges in maintaining a good yield while scaling up this reaction. I surmounted this impediment by using mechanical stirring and slow cooling of the reaction to  $-70\text{ }^{\circ}\text{C}$  using a dry ice–isopropanol bath; the slow cooling helped the magnetic stirring. As we scaled up, cost motivated us to prepare our own ethyl or methyl cyanoformate. We prepared them by Webber and Childs' protocol,<sup>150</sup> but the yield was higher when we prepared ethyl cyanoformate in a large amount (59% yield vs. 30%), so thereafter we used ethyl cyanoformate and prepared **318**.



**Scheme 3.7.1.** Synthesis of  $\beta$ -ketoesters **318** and **318B**

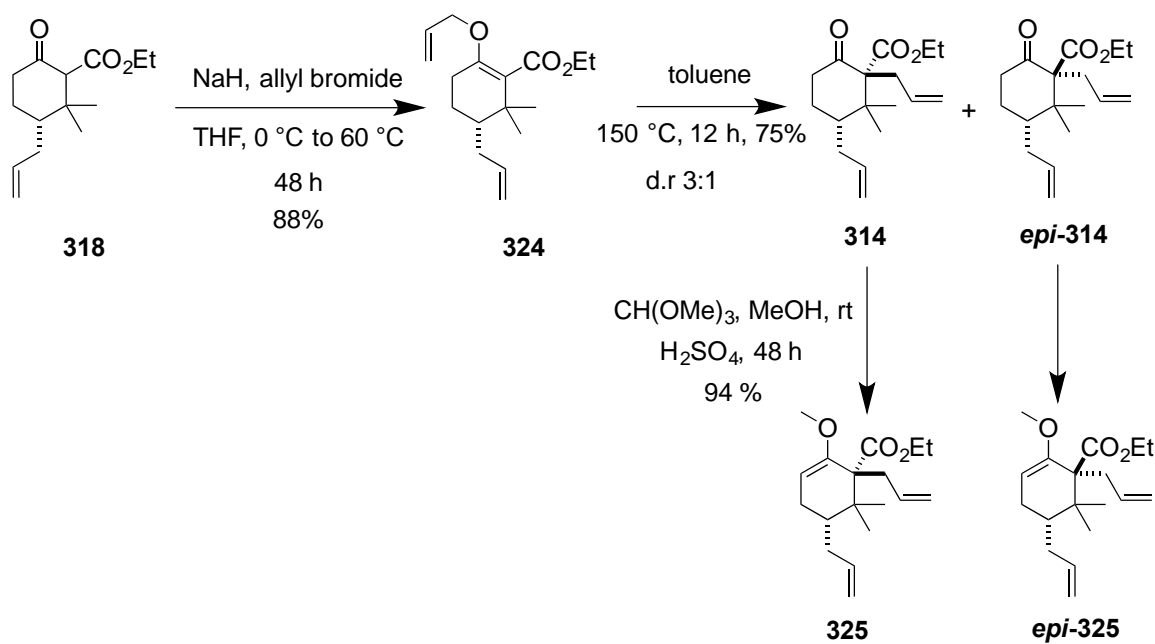
### 3.8 Allylation and enol ether synthesis

The keto ester **318** was converted into *O*-allyl vinyl ether **324** (Scheme 3.8.1) using NaH and allyl bromide with an excellent yield of 88%.<sup>151</sup> The *O*-allyl ether **324** was dissolved in dry toluene and heated in a sealed tube for 12 h at  $150\text{ }^{\circ}\text{C}$ . A [3,3]-sigmatropic



rearrangement yielded two diastereomers, **314** and *epi*-**314**, in a 3:1 ratio and excellent yield.<sup>152</sup>

By examining a transition state model (Figure 3.8.1), we thought that the reaction would more likely to proceed via **TSa**, which had fewer steric interactions than the alternative **TSb**, and we, therefore, believed that **TSa** would produce the major diastereomer; whereas **TSb** would produce the minor diastereomer *epi*-**314**, which was expected to be undesired one. We also expected the major diastereomer to be the desired one. But we did not know yet at this point. We purified the both diastereomers by column chromatography and attempted to confirm our hypothesis by <sup>1</sup>H NMR, COSY, and NOSEY. Unfortunately, overlapping peaks in the <sup>1</sup>H NMR spectra of both diastereomers made it difficult to assign their stereochemistry unambiguously. Therefore, we reserved our judgment on whether the major product was **314** or *epi*-**314** until we could unambiguously assign the structures of downstream intermediates in the synthesis.



**Scheme 3.8.1.** *O*-allylation and Claisen rearrangement and enol ether synthesis

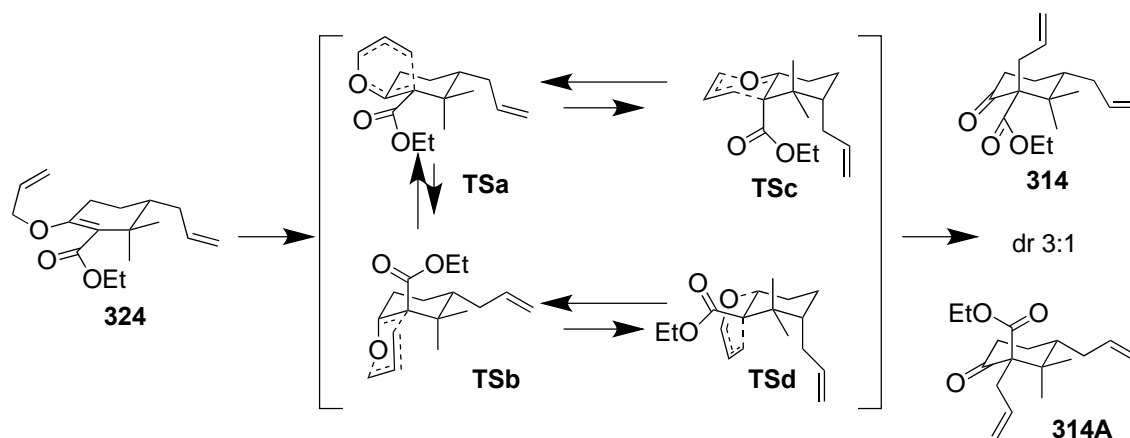


**Figure 3.8.1** Transition state model for the diastereoselectivity

### 3.9 Determination of stereochemistry of major diastereomer

It was necessary to reduce the ester carbonyl in *C*-allylated  $\beta$ -ketoester **314** to an aldehyde to allow us to carry out a two-carbon homologation. Before doing that, we protected the keto group so that we could selectively reduce only the ester group. The reason behind choosing methyl enol ether as a protecting group was not because of the easy synthetic preparative method, but the steric bulk around the quaternary carbon. We previously attempted different protecting groups, like TMS or TBDMS, but in those cases, the alkylation turned out to be very low-yielding, as was also the case when we left the ketone unprotected. Therefore, we selected the methyl enol ether as the optimum protecting group for the ketone, even though the protecting group strategy necessitated an extra step.

We converted the ketone in **314** to methyl enol ether with trimethyl orthoformate and  $\text{H}_2\text{SO}_4$  (cat) in 94% yield. In past, we had trouble converting **314** fully into **325**, especially upon scale-up (from 500 mg to 6 g scale) (Scheme 3.8.1). We tried several acids like PTSA, CSA, and PPTS. At last, we found that a few drops of concentrated  $\text{H}_2\text{SO}_4$  worked the best. We also attempted several equivalents of trimethyl orthoformate, but we found 25 equivalent of  $\text{CH}(\text{OMe})_3$  was essential for the complete conversion, although 25

equivalents sounded like a lot of CH(OMe)<sub>3</sub>. Pleasingly, we did not observe any transesterification in this reaction, although there was a possibility of it because of the presence of an ethyl ester.

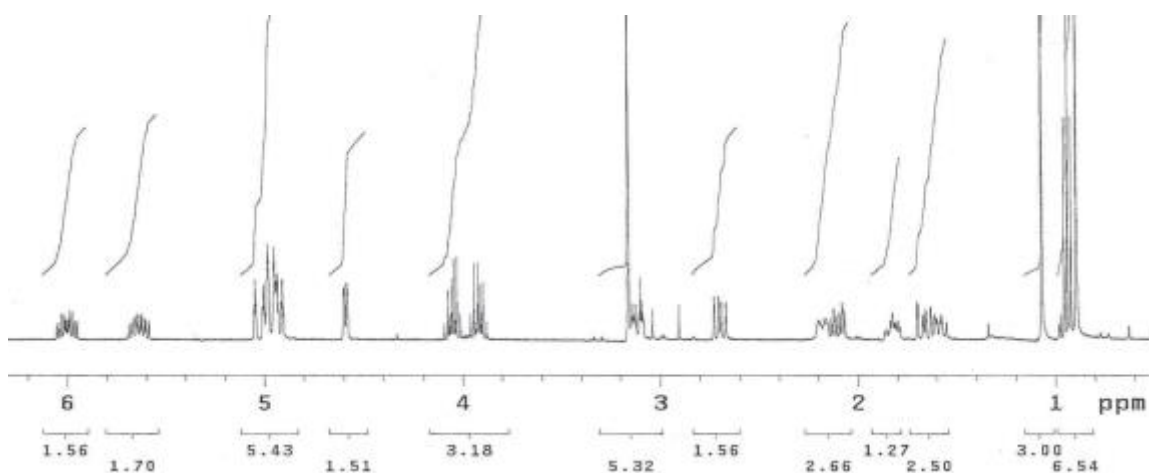
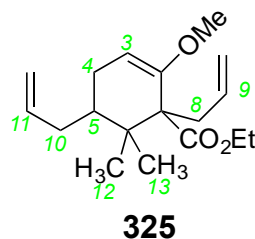


**Figure 3.9.1.** <sup>1</sup>H NMR spectrum of **325** in C<sub>6</sub>D<sub>6</sub>

We had reserved our judgement on the identification of the major diastereomer in the Claisen rearrangement (**314** or **314A**) because of overlapping peaks in its <sup>1</sup>H NMR spectra. Here, in the case of **325** (Figure 3.9.1), <sup>1</sup>H NMR isochrony at 400 MHz did not impede the assignment of the diastereomers. Therefore, we could proceed with a COSY and NOESY analysis. Assignments of peaks in COSY experiment was essential for establishing the trans geometry of the two allyl groups in **325**. Because we needed these correctly assigned protons in NOESY which is the main experiment to assign the geometry. We, here, were using the process of elimination to find a proton which was the key for the whole process; it was H5. We had to assign it.

We assigned the resonance at  $\delta$  4.60 ppm as the enol ether double bond proton H3 because it was quite distinct from the rest and it was vinylic proton, showing a doublet of doublets. However, we had two other vinylic protons but they were further downfield and multiplets. Therefore, neither of them could be H3. Therefore, we found that this resonance correlated with resonances at  $\delta$  2.12 ppm and 1.60 ppm in the COSY spectrum (Figure 3.9.2), which we assigned as H4a and H4b. Due to their chemical shift and multiplicities, we could assign resonances at  $\delta$  2.68 ppm and 3.01 ppm to the two H8 atoms; these resonances showed a correlation in the COSY spectrum to the resonance at  $\delta$  6.00 ppm, which we assigned to H9. This assignment then allowed us to assign the resonance at  $\delta$  5.85 ppm to H11, which in turn allowed us to identify the resonances at  $\delta$  2.20 ppm and 1.86 ppm as H10a and H10b. So, only proton left to assign was H5; and we assigned it. However, identification of H8 and H9 were not important from COSY perspective, but identification of these two peaks led us to assign H5 which was a very important proton to establish the trans geometry of the two-allyl groups in **325**. Finally, we were able to assign the resonance at  $\delta$  1.78 ppm as H5 due to its strong correlations with H10a, H10b, H4a, and H4b in the COSY spectrum.

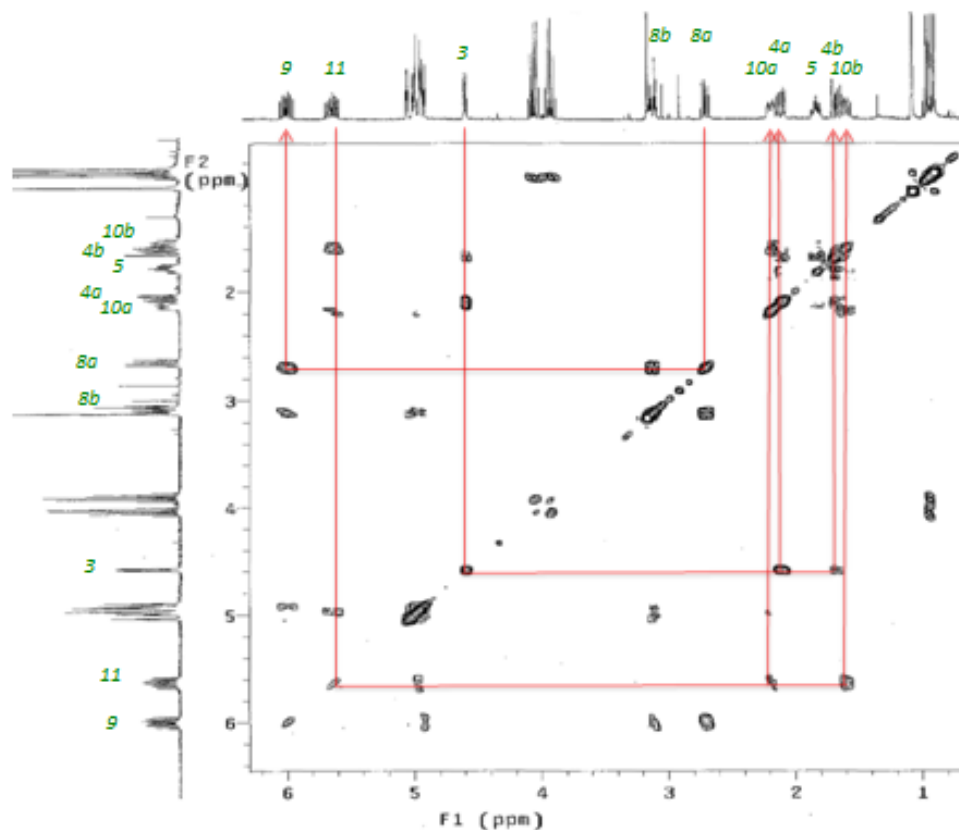


**Figure 3.9.2.** COSY spectrum of **325**

In the NOESY spectrum of **325** (Figure 3.9.3), we observed a strong correlation between resonances due to H5 and one of the H8 atoms, unambiguously establishing the trans geometry of the two allyl groups (Figure 3.9.1, major product). We would not have observed this correlation if the two allyl groups had been cis (Figure 3.9.1, minor product). We also found a strong correlation between peak 12, which was a methyl group, with 4b, and therefore, they must be both axial. On the contrary, we did not observe any correlation of 12 with either of 8a or 8b. These observations unambiguously established the trans geometry of the two allyl groups in **325**. Since **325** was synthesized from **314**, so we concluded that **314** was the major and desired diastereomer.

By contrast, in the NOSEY spectrum, the minor constituent which we assigned *epi-325* correlated H8 and axial CH<sub>3</sub> (identified by correlation to axial which had large JH4-H5 (Figure 3.9.4).

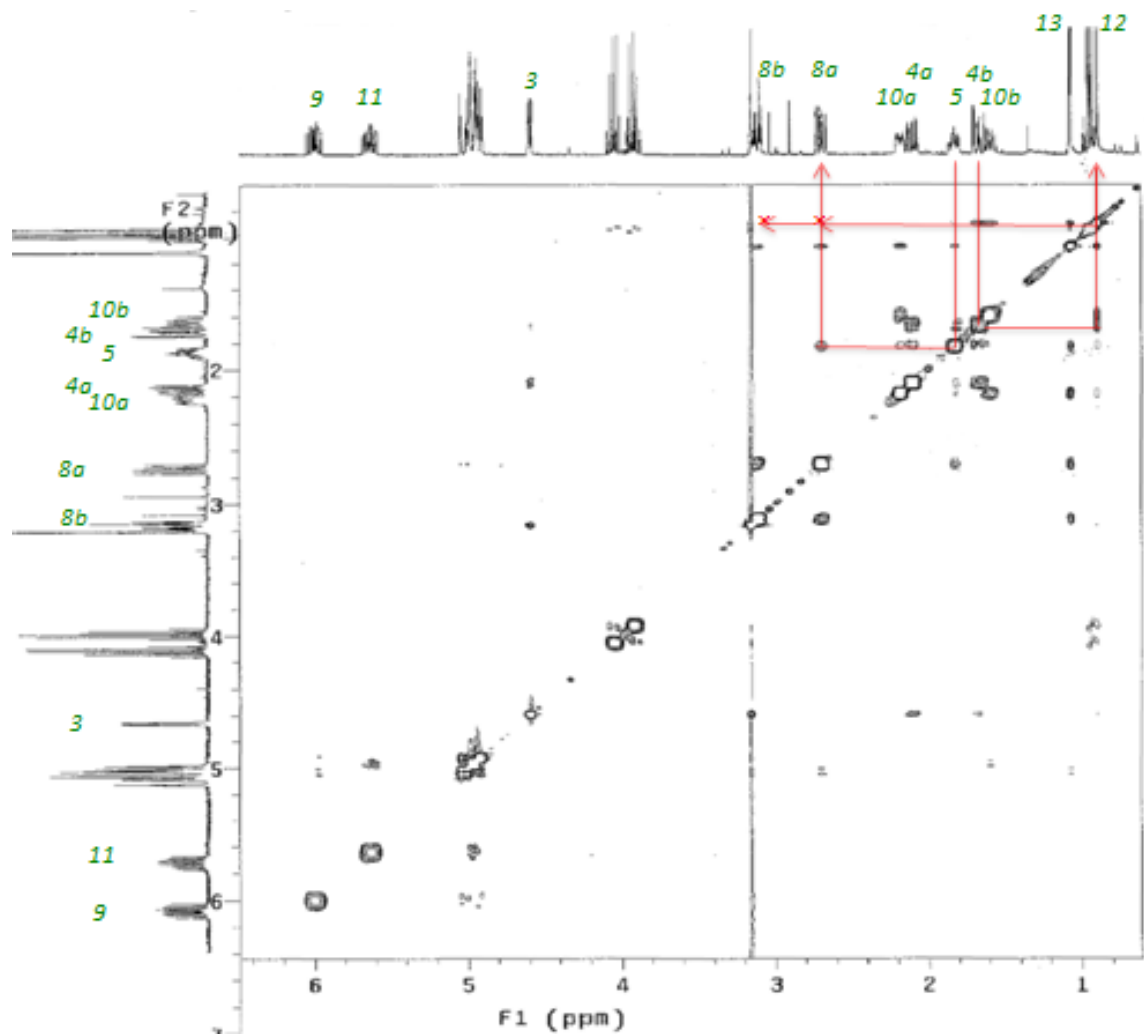


**Figure 3.9.3.** NOESY spectrum of 325

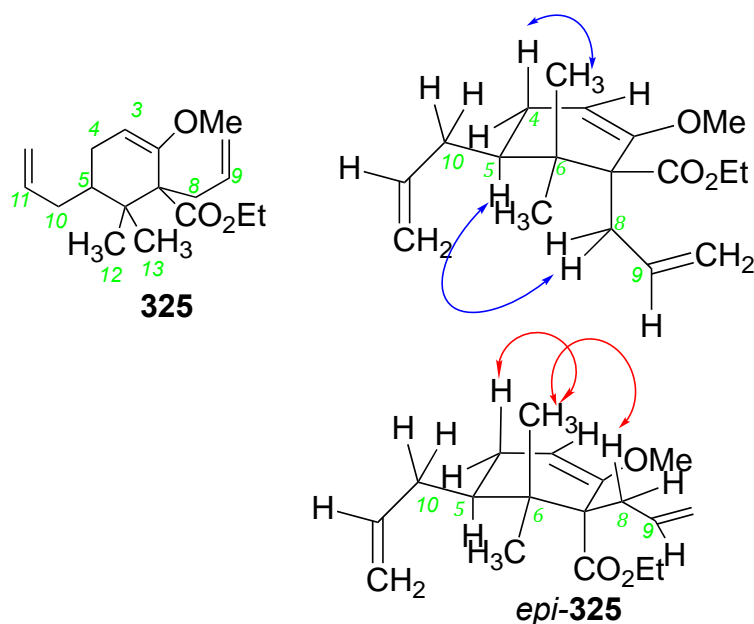
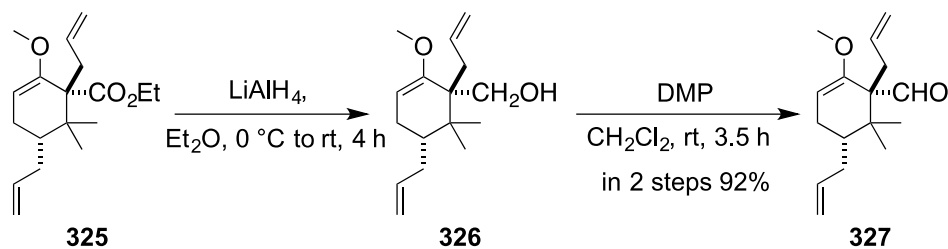


Figure 3.9.4 NOE interactions in **325** and *epi-325*

### 3.10 Conversion of ester to aldehyde

Ester **325** was reduced to alcohol **326** (Scheme 3.10.1) in 87% yield with  $\text{LiAlH}_4$ .<sup>152</sup> We carried this alcohol **326** forward to the next step without any purification. Applying the Dess-Martin periodinane to **326**, the reaction completed within 4 hours. After purification by a short column chromatography, the reaction gave aldehyde **327** in an overall yield of 92% over two steps.<sup>153</sup>

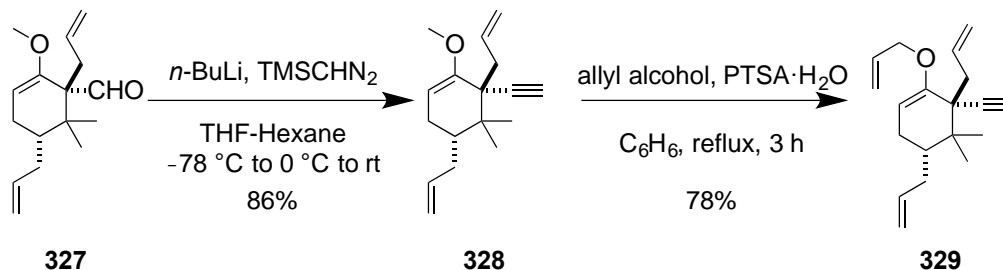


Scheme 3.10.1. Synthesis of aldehyde before alkylation

### 3.11 Alkylation and allyl–methyl exchange

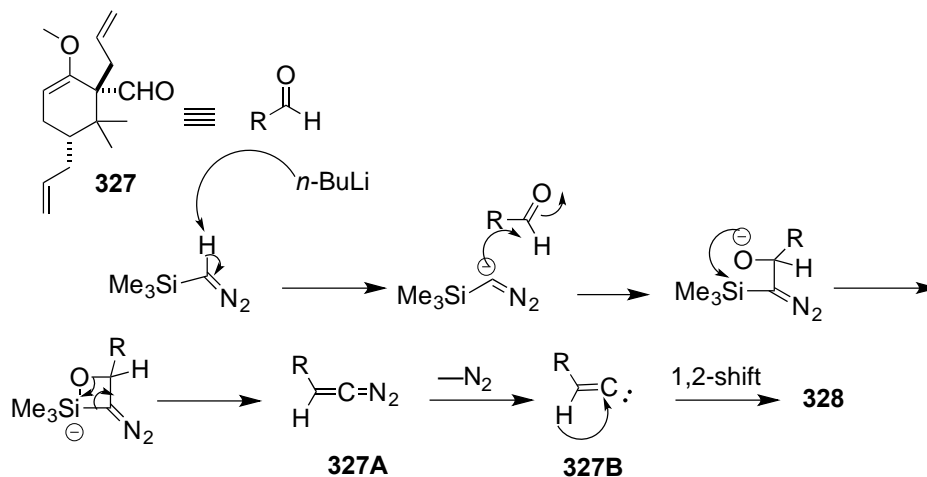
With aldehyde **327** on hand, we concentrated on the most exciting part of the total synthesis, which started with the homologation of one carbon unit. There are several

precedents in the literature about converting an aldehyde into an alkyne.<sup>154</sup> In our case, probably because of the steric bulk around the  $sp^2$  carbon of the aldehyde, we had a poor yield when we used the Corey–Fuchs reaction. However, we obtained an excellent yield when we used a Colvin rearrangement to convert **327** to **328** (Scheme 3.11.1).<sup>155</sup>



**Scheme 3.11.1.** Synthesis of alkyne and *O*-allyl vinyl ether

The mechanism of the Colvin rearrangement (Scheme 3.11.2)<sup>155</sup> starts with the deprotonation of TMSCHN<sub>2</sub> by *n*-BuLi, and the resulting carbanion reacts with aldehyde **327**. The nascent alkoxide undergoes a Peterson olefination-like reaction to generate a carbene intermediate, **327B**, after the expulsion of N<sub>2</sub> from **327A**. Finally, a 1,2-shift furnishes **328**. The Colvin rearrangement of **327** probably proceeds better than the Wittig reaction because of the reduced steric bulk and greater nucleophilicity of the organolithium reagent used in the former reaction.



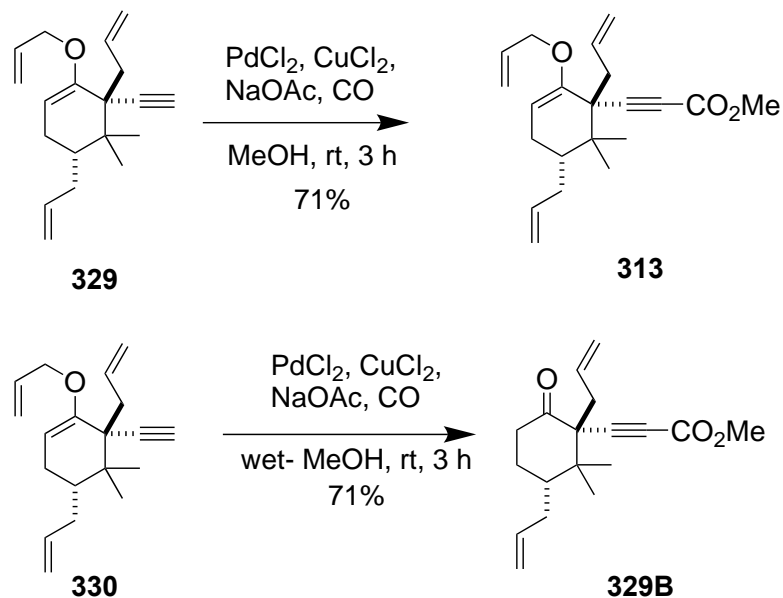
**Scheme 3.11.2.** Mechanism of Colvin rearrangement



At this point in the synthesis, for introducing the third, and the last, allyl group in the molecule, we decided to exchange the *O*-methyl vinyl ether for an *O*-allyl vinyl ether (Scheme 3.11.1). Our idea was to later introduce an allyl group on the C1 carbon by Claisen rearrangement. We applied allyl–methyl exchange reaction to add the allyl group in the molecule **328**, converting it into **329** with a decent yield of 78%. We screened several catalysts, but CSA·2H<sub>2</sub>O gave the best result. Hydrolysis of the enol vinyl ether to the ketone was not a problem under these conditions. Pleasingly, we isolated the product **329** without need for column purification.

### 3.12 Carboxymethylation and reduction

After installation of an alkyne and the allyl group in **329**, the next task was to introduce a CHO group at the terminal alkyne carbon in compound **329**. Alkynes are readily converted into alkynoates,<sup>156</sup> alkynals<sup>157</sup> or propargyl alcohols<sup>158</sup> by treating them with *n*-BuLi followed by an electrophile such as chloroformate, DMF, or paraformaldehyde. We attempted all of these conditions, but, to our surprise, we recovered only the starting material **329**. Therefore, we searched for an alternate route. Thankfully, the alkynoate **313** was synthesized from **329** using CO, MeOH, NaOAc, and CuCl<sub>2</sub> and a catalytic amount of PdCl<sub>2</sub> (Scheme 3.12.1).<sup>159</sup> After column purification, the reaction yielded the alkynoate **313** in 87% yield. The reaction was sensitive to scale-up: the reaction of more than 5 mmol scale failed several times.



**Scheme 3.12.1.** One-carbon homologation–methoxycarbonylation

To our surprise, compound **329B** was a solid. Pleasingly, X-ray crystallographic analysis revealed that both the allyl groups at the C5 and C7 were trans to each other (Figure 3.12.1), which confirmed our stereochemical assignment of **325** and its precursor, **314**.

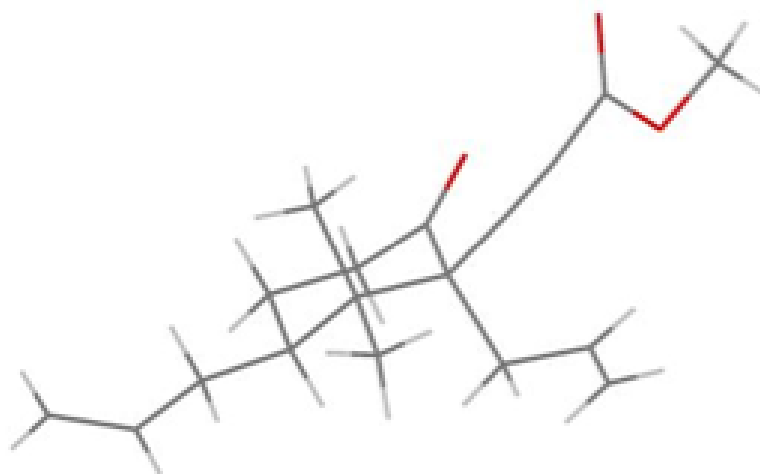


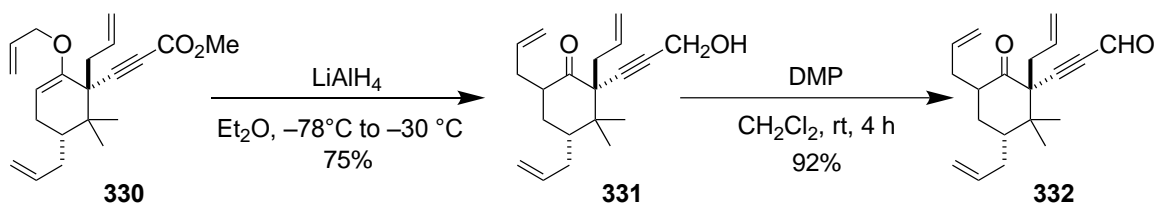
**Figure 3.12.1.** X-ray Structure of **329B**

Next, we reduced alkyanoate **313** to a propargylic alcohol **330** in 87% yield using  $\text{LiAlH}_4$ . The substrate could have been sensitive to further reduction of the triple bond to

the double bond, but we did not observe this overreaction. After column purification, the reaction gave *O*-allyl alkynol **330** in 86% yield.

### 3.13 Claisen rearrangement and oxidation of alcohol

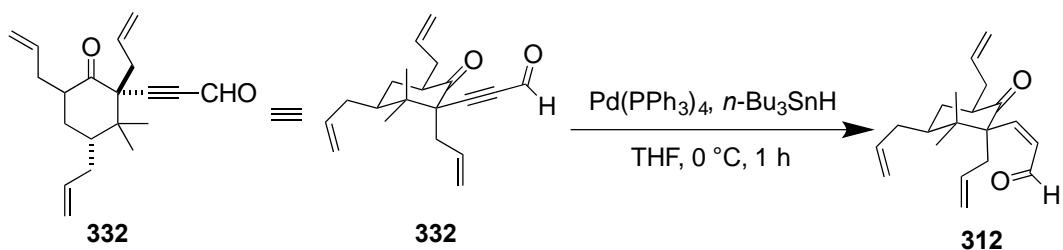
We were now ready to install the last allyl group. Therefore, we subjected compound **330** to Claisen rearrangement (Scheme 3.13.1). After heating compound **330** in a sealed tube for two hours at 150 °C, the reaction yielded **331** as an inconsequential mixture of diastereomers at C1 in nearly 75% yield. We were not concerned with the diastereomers since C1 would shortly undergo deprotonation as part of the aldol condensation. We carried the crude mixture over to the next step, which involved a DMP oxidation, furnishing the alkynal **332** in 92% yield within 4 h.<sup>153</sup>



Scheme 3.13.1. Synthesis of the alkynal

### 3.14 Stereoselective reduction of alkynal to *Z*-alkenal, and intramolecular aldol reaction

We envisaged reducing the  $\text{C}\equiv\text{C}$  triple bond chemoselectively to *Z*-alkenal **312** so that we could make the bicyclo[3.3.1]nonane ring via aldol condensation (Scheme 3.14.1). For years, our lab has been studying the regiospecific syn reduction of alkynals in the presence of isolated double bonds.<sup>5, 118</sup> A catalytic amount of  $\text{Pd}(\text{PPh}_3)_4$  and a stoichiometric amount of  $(n\text{-Bu})_3\text{SnH}$  reduced **332** to cis alkenal **312** in 52% yield.<sup>160</sup> The reaction was clean and finished within 1 hour.



**Scheme 3.14.1.** Reduction of alkyne to cis alkenal

This result was rather surprising to us, because alkynoates generally undergo hydrostannylation under such conditions,<sup>161</sup> but we observed the only syn reduction of the triple bond. We hypothesized that the reaction might proceed via a Pd-stannylketene intermediate **312a**, which could then be protonated on its less hindered face to give the cis double bond in alkenal **312**. There could be another possibility; after the initial 1,4-addition of H<sup>-</sup> to the alkyne **332**, reductive elimination of **312a** could lead to the stannyloxyketene intermediate and then, the protonation led to the formation of the cis double bond in **312** via the same mechanism.

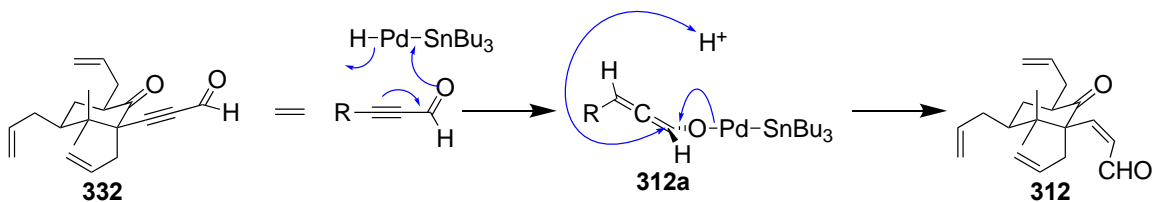


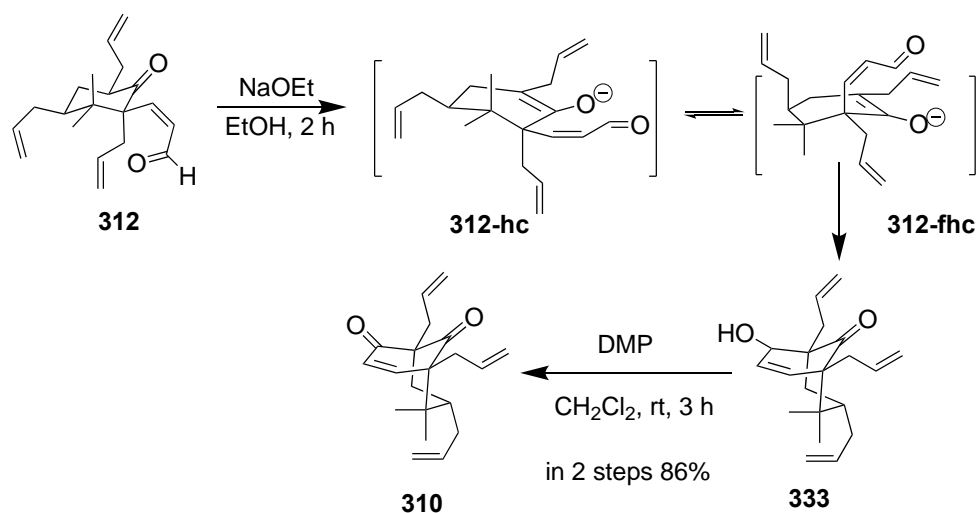
**Figure 3.14.1.** Possible intermediate in syn reduction

Armed with alkenal **312**, we were ready for aldol condensation, for which we used NaOEt in EtOH (Scheme 3.14.2). We envisaged enolate conformers **312-hc**<sup>5</sup> and **312-fhc**<sup>6</sup> in equilibrium. We believed the equilibrium would favor **312-hc** due to a reduced 1,3-diaxial interactions, but we also believed that enough **312-fhc** might be formed to allow

<sup>5</sup> hc = half-chair

<sup>6</sup> fhc = flipped half-chair

the aldol reaction to proceed. Our hope was that the formation of the C–C bond in the product **333** would compensate for the increased steric strain in the bicyclic compound **333** as opposed to **312**. In the event, the aldol reaction finished within 2 hours, giving us two diastereomeric alcohols **333**. Without purification, we used DMP to oxidize the alcohols, and, after column purification, we obtained bicyclic diketone **310** in a solid crystalline form and in 92% yield over the two steps. The crystal structure (Figure 3.14.2) unambiguously established the endo geometry of the bicyclic core of 7-*epi*-clusianone. It was necessary to establish the endo geometry of the bicyclic structure in order to synthesize 7-*epi*-clusianone.



**Scheme 3.14.2.** Synthesis of bicyclo[3.3.1]nonane via aldol reaction

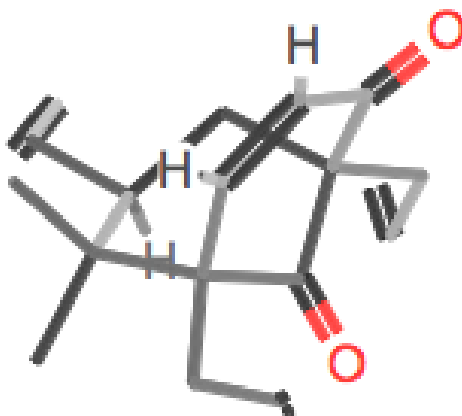
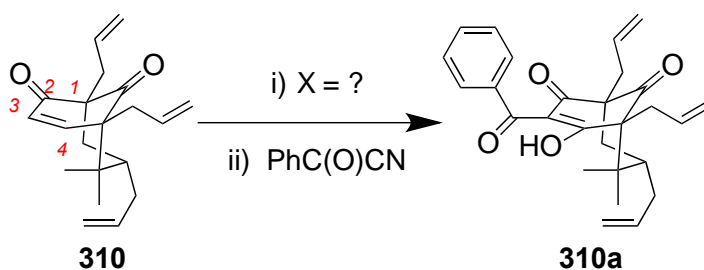


**Figure 3.14.2.** Bicyclic structure of **310**

### 3.15 Oxidation of C4 in bicyclo[3.3.1]nonane: a dilemma or enigma?

With bicyclic compound **310** in hand, we set out to oxidize the C4 carbon in **310** to move closer to the finish line, only three steps away. To the best of our knowledge, no one had ever done a late stage C4 oxidation in a synthesis of a 7-endo type B PPAP, so it would be significant if we could develop a method for this oxidation. My predecessor tried unsuccessfully to oxidize the C4 to advance in the total synthesis.<sup>5</sup> Here, we are not rehashing those results. However, we will be discussing some of his ideas.



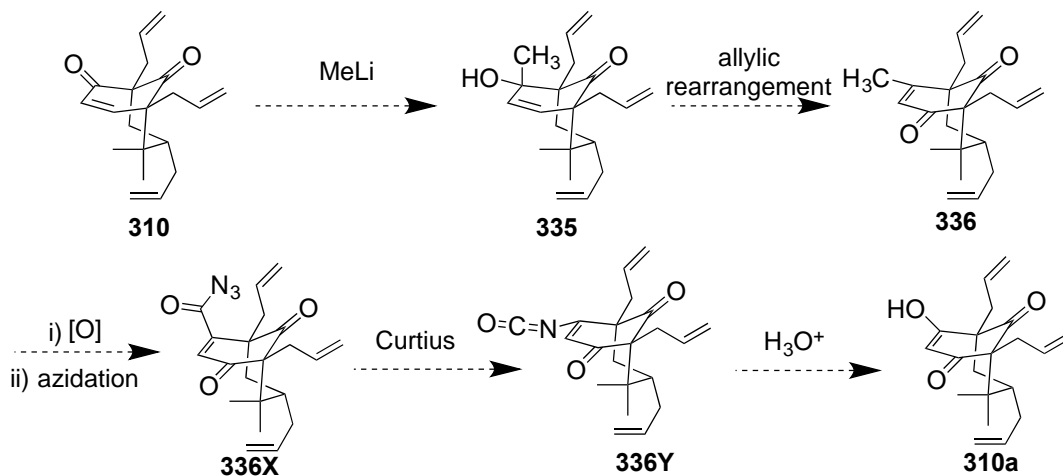
**Scheme 3.15.1.** Ultimate roadblock to the success!

### 3.16 Plan for the oxidation of C4 in **310**

#### 3.16.1 Desaturation followed by oxidation

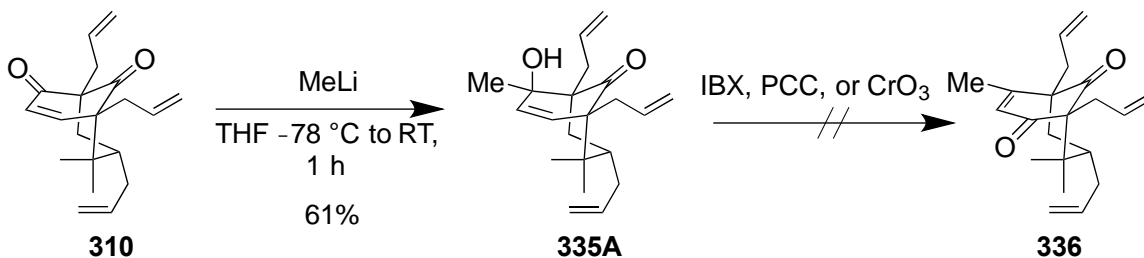
We envisaged that adding MeLi followed by an allylic oxidation would give us a 3-methyl enone (Scheme 3.16.1). We would then oxidize the methyl group to a carboxylic

acid and subsequently form the acid azide **336X**. The resulting acid azide could undergo a Curtius rearrangement to give a 3-isocyanato enone **336Y**. Finally, the hydrolysis of the product from the Curtius rearrangement would give us the 1,3-diketone functionality. If the oxidation of the Me group to a CO<sub>2</sub>H group proved difficult, we could instead use BnOCH<sub>2</sub>Li, which would provide a handle for the oxidation.



**Scheme 3.16.1.** Proposed synthetic scheme for the oxidation of C4 in **310**

With this idea, we allowed MeLi to react with **310** to furnish **335a** (Scheme 3.16.2). The resulting diastereomeric alcohol **335a** was directly subjected to oxidation. Because the alcohol in **335a** was allylic and tertiary, we expected an oxidative allylic transposition to occur. There is a lot of literature precedent for such chemistry.<sup>162, 163</sup> PCC, CrO<sub>3</sub>, and IBX are common oxidants for this type of reaction. However, my predecessor showed that in our case, neither PCC, CrO<sub>3</sub> gave the desired product, leading to either unreacted starting material or the rearrangement into **310**. I further attempted the allylic transposition reaction on **335a** with IBX in DMSO at 60 °C, and disappointingly, we also recovered starting material.



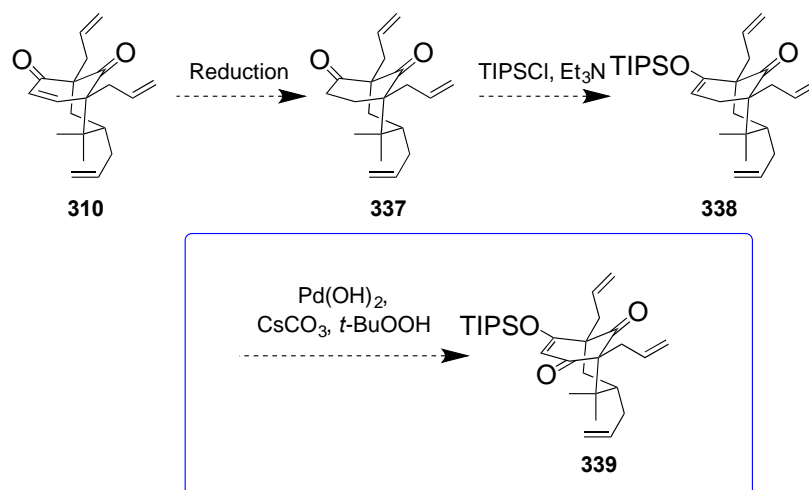
**Scheme 3.16.2.** Failed allylic transposition

The alkyllithium  $\text{LiCH}_2\text{OCH}_2\text{OMe}$  also reacted with **310** to furnish the corresponding tertiary alcohol, but my predecessor showed that treatment of this compound with PCC or  $\text{CrO}_3$  either gave back **310** or did not result in a reaction at all.<sup>118</sup> The reason for the failure was attributed to steric hindrance around the C4 carbon, which made it very resistant to change its hybridization.

### 3.16.2 Reduction and enol ether formation followed by oxidation

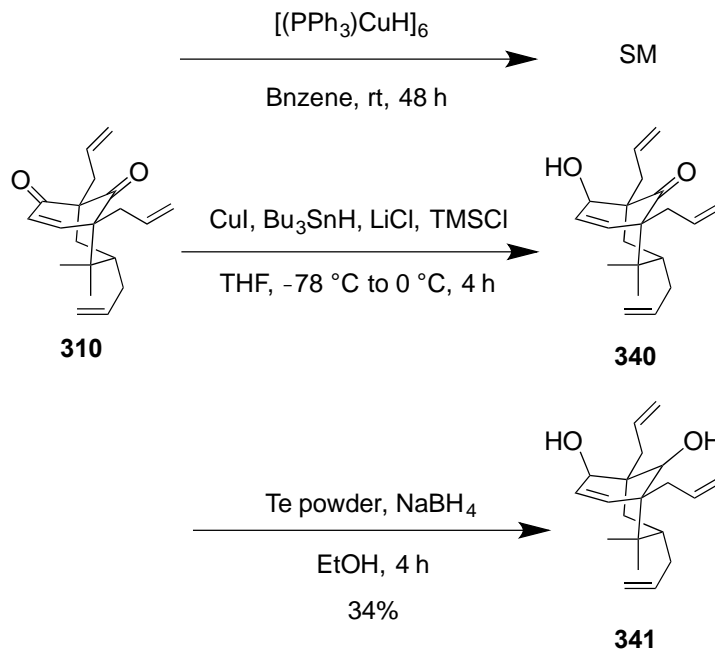
Next, we thought of reducing the double bond of the enone in **310** chemoselectively to diketone **337** (Scheme 3.16.3). Our idea was that ketone **337** could be converted into TIPS-enol ether **338**, which we then might be able to oxidize at C4 with the help of C–H activation. In 2003, Corey and Yu had shown that such an oxidation worked in a bicyclic system.<sup>164</sup> This idea was successfully implemented by Nakata in his hyperforin synthesis.<sup>165</sup> So, we are hopeful that we could try this method of oxidation.





**Scheme 3.16.3.** Strategy for C4 oxidation via Corey-Yu's method

We set off to reduce the conjugate double bond in **310**. The reductions of conjugated double bonds are very common in organic chemistry.<sup>161, 166, 167</sup> Because **310** had three allyl groups, we had to find a chemoselective method of reducing the conjugated double bond. Transition metal hydrides have demonstrated the ability to reduce such conjugated double bonds. Stryker's reagent,  $[(\text{PPh}_3)\text{CuH}]_6$ , is an example of one such metal hydrides. Therefore, we attempted to reduce **310** with Stryker's reagent, but we found that the reagent did not touch the conjugated double bond at all, and we ended up recovering the starting material.<sup>167</sup>



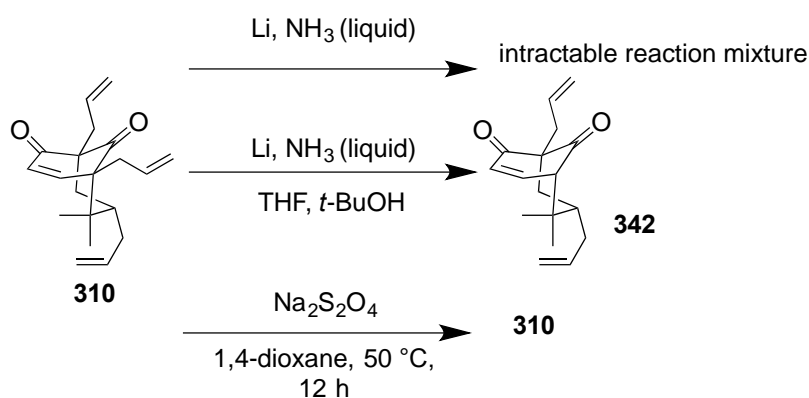
**Scheme 3.16.4.** Attempts to reduce the  $\alpha$ ,  $\beta$ -unsaturated ketone in bicyclic enone **310**

Stryker's reagent, however, is bulky, and because of that, we thought, the delivery of  $H^-$  to the double bond might have been difficult. Therefore, we envisioned generating  $CuH$  in situ, and then we could reduce the conjugated double bond. Accordingly, we attempted to reduce the conjugated double bond in **310** using  $CuH$ , generated in situ from the action of  $CuI$  and  $Bu_3SnH$ , in the presence of  $LiCl$  and  $TMSCl$ . Unfortunately, this reaction furnished the allylic alcohol, leaving the conjugated double bond unreacted (**Scheme 3.16.4**).

Not discouraged by the results, we turned our attention to other metal hydrides.  $TeH$  is also reported to reduce conjugated double bonds.<sup>168</sup> Unfortunately,  $TeH$ , which we generated by the action of  $Te$  powder and  $NaBH_4$ , in ethanol, reduced both ketones in **310**, instead of the conjugated double bond, producing allylic alcohol **341**.

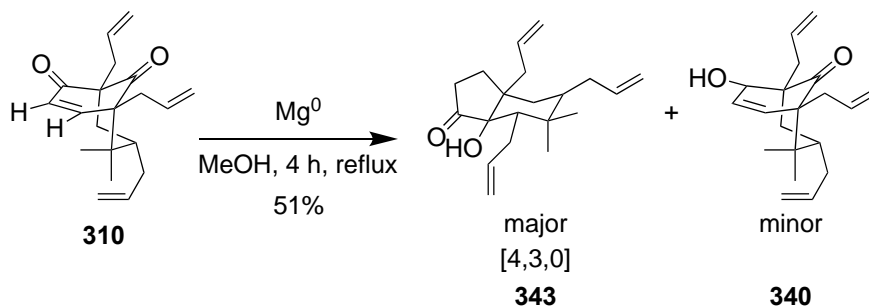
The dissolving metal reduction of  $\alpha,\beta$ -unsaturated ketones has long been utilized in organic synthesis.<sup>169</sup> We were hopeful that the lack of steric demand of the reducing agent

in this reaction would allow our desired reaction to proceed. When **310** was subjected to Li in liquid NH<sub>3</sub> without any cosolvent, however, we obtained an intractable mixture of products, and the NMR spectrum of the crude product indicated that there had been no reduction of the conjugated double bond. The same reaction in the presence of the proton source *t*-BuOH did not reduce the conjugated double bond in **310**, but caused the loss of an allyl group to give **342** (Scheme 3.16.5). Na<sub>2</sub>S<sub>2</sub>O<sub>4</sub> failed to react completely.<sup>170</sup>



**Scheme 3.16.5.** Trials for dissolved metal reduction

We were aware that Hudlicky's group had done a lot of research on chemoselective reduction of a conjugated double bond in  $\alpha,\beta$ -unsaturated esters using Mg/MeOH.<sup>161, 171-173</sup> After allowing **310** to react with Mg in refluxing MeOH for 4 h, we obtained a strange result: the reagent not only reduced the double bond but also promoted the skeletal rearrangement of bicyclo[3.3.1]nonane, leading to the completely unexpected bicyclo[4.3.0]nonane **343** in 51% yield, along with some allylic alcohol (Scheme 3.16.6). X-ray crystallographic analysis established the stereochemistry of **343** without doubt (Figure 3.16.1).



**Scheme 3.16.6.** An unusual reaction of **310** with Mg in methanol

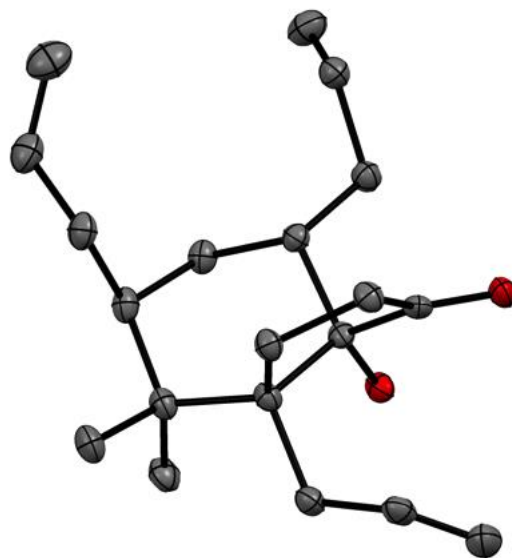
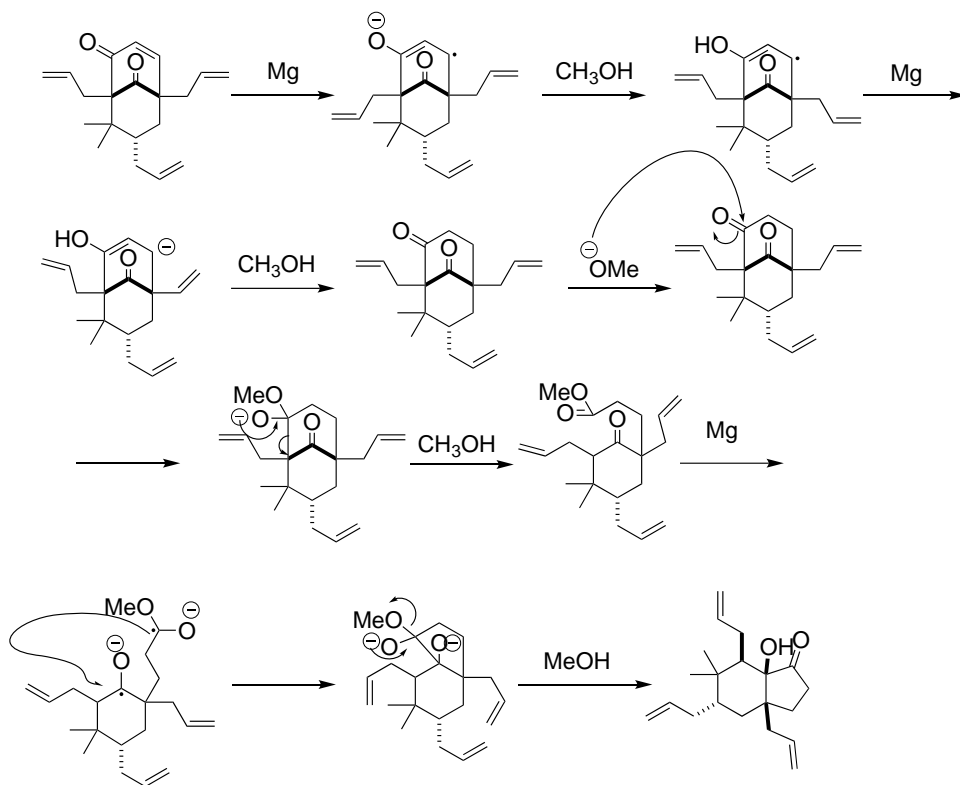


**Figure 3.16.1.** Crystal structure of **343**

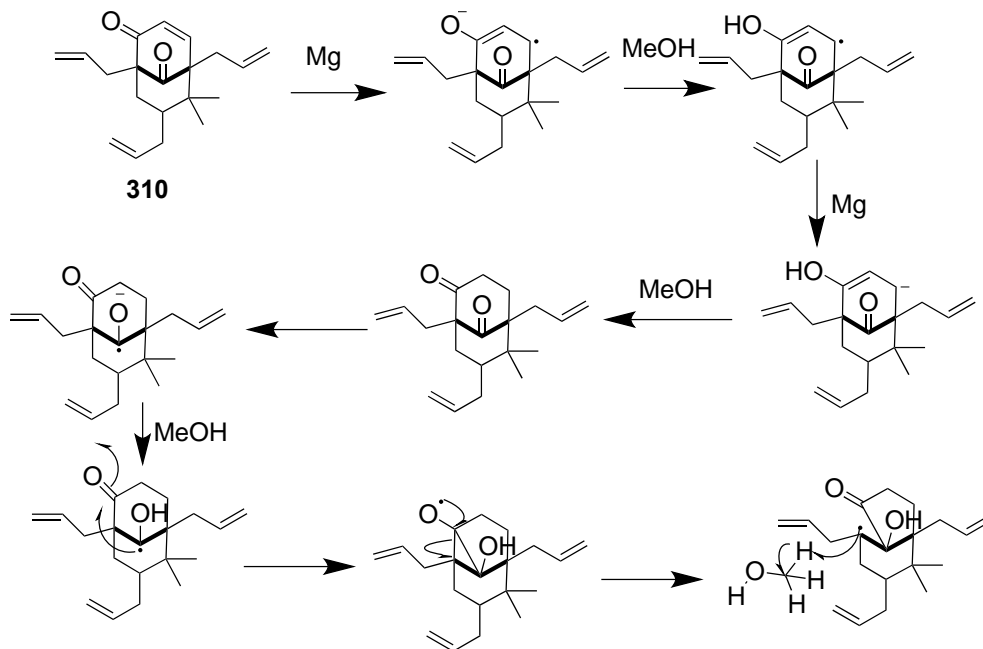
A possible mechanism for the rearrangement is shown here (Scheme 3.16.8). To the best of our knowledge, it was a new kind of reaction where bicyclo[3.3.1]nonane had rearranged to a bicyclo[4.3.0]nonane motif. Unfortunately, though, it did not contribute to a solution to our problem.

The proposed mechanism suggested that the  $\alpha$ ,  $\beta$ -unsaturated ketone of **310** was indeed reduced to the saturated ketone before further reaction occurred. Therefore, we attempted to forestall the rearrangement by using less Mg powder (<10 equivalent), but to no avail. An alternative mechanism for the unusual transformation could be proposed (Scheme 3.16.7). We believed that mechanism in the Scheme 3.16.8 is less likely to

happen because of the formation of cyclopropane intermediate, which is a high in energy.



**Scheme 3.16.7.** An alternate reaction mechanism for the bicyclo[4.3.0]nonane

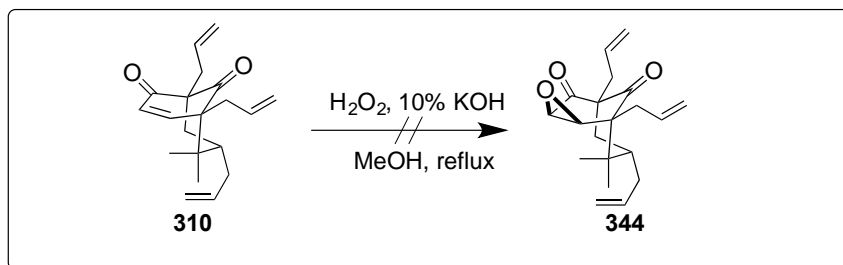
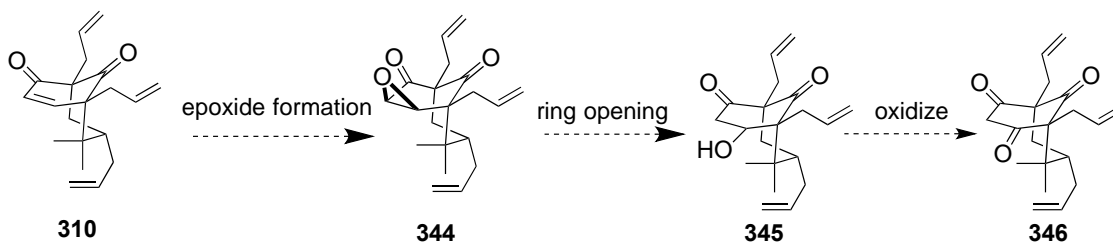


**Scheme 3.16.8.** Mechanistic rationale for an unexpected rearrangement

These failed trials hint us that the C4 carbon of **310** is very resistant to changing its hybridization from  $sp^2$  to  $sp^3$ . Therefore, we need to rethink our strategy to overcome the challenge. A late-stage oxidation strategy may not work here; we need to think about an early stage oxidation.

### 3.16.3 Epoxidation and nucleophilic ring opening

Nucleophilic epoxidation of an enone has been an efficient route for the oxidation of  $\beta$ -carbon of an enone because the resulting epoxide is prone to nucleophilic ring opening (Scheme 3.16.9). Ciochina successfully implemented the strategy—a nucleophilic epoxidation followed by the ring opening—on a model compound in proposing a route for the total synthesis of nemorosone.<sup>5</sup> Therefore, we decided to attempt the strategy on molecule **310**; our plan was to epoxidize the enone **310** to **344**, and then, regioselectively, to open up the epoxide ring in **344** with any less bulky nucleophile. After the ring was opened, the alcohol **345** could then be oxidized to diketone **346**.

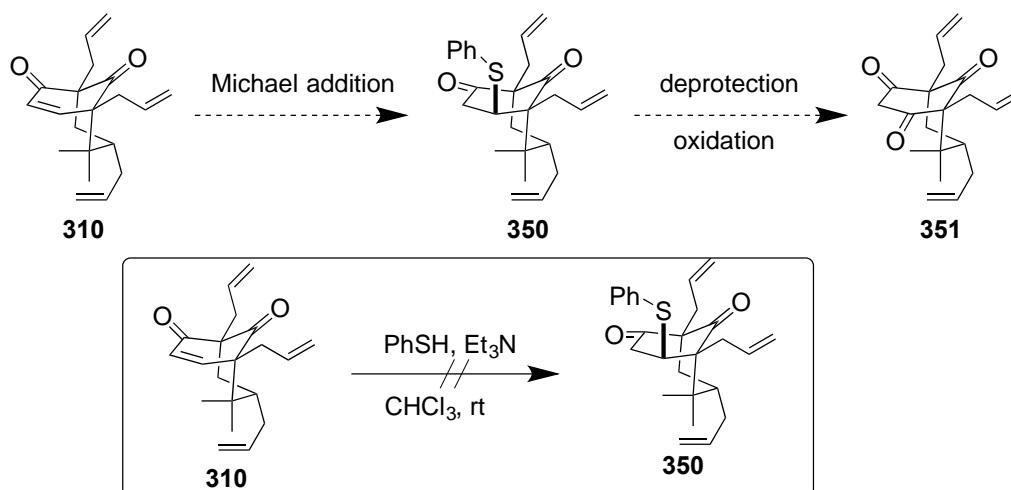


**Scheme 3.16.9.** C4 oxidation: epoxidation and nucleophilic ring opening

Unfortunately, the nucleophilic epoxidation with  $\text{H}_2\text{O}_2$  in the THF and 10% KOH mixture did not touch the double bond of the enone **310**, and we recovered **310**.<sup>174</sup>

### 3.16.4 Conjugate addition–oxidation

We knew that thiols added to enones in a 1,4-fashion. Therefore, we thought of adding thiophenol at the C4 carbon in **310** (Scheme 3.16.10). Our idea was simple; if we could add  $\text{PhS}^-$  to C4 of **310**, we could close the ring, remove the  $\text{PhS}^-$  by oxidizing the sulfur, and subsequently, install OH group at the C4. Accordingly, we attempted to add thiophenol to enone **310**. Not surprisingly, the reaction did not go as per our hope, and we recovered the starting material **310**.



Scheme 3.16.10. Addition of sulfur nucleophile to bicyclic enone

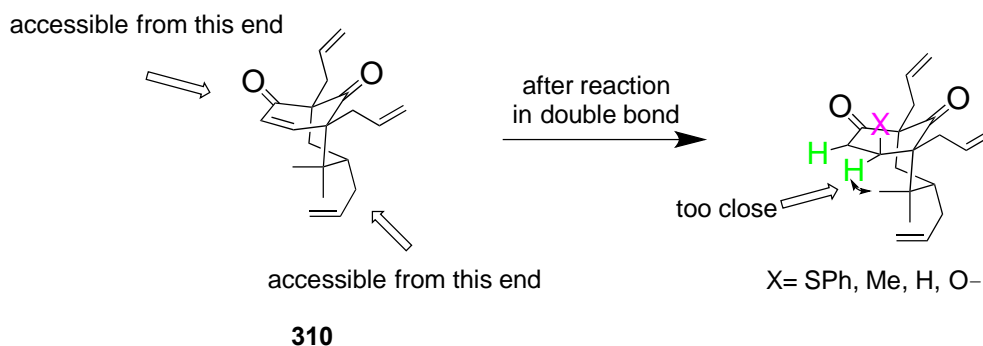
### 3.17 New plan for C4 oxidation

“In solving a problem of this sort, the grand thing is to be able to reason backwards.”

— Sir Arthur Conan Doyle, *A Study in Scarlet*.

The problem of oxidation of C4 in **310**, demanded further deliberation. We reexamined the crystal structure of **310**. Its analysis revealed that the gem-dimethyl groups at the C6 hindered any approach of nucleophile or electrophile from the endo face of the

conjugated double bond. The exo face was still accessible to any approach of Nu<sup>-</sup> or electrophile, but, as the reaction proceeded, the endo H at C4 was forced into an eclipsing position with one of the gem-dimethyl groups, which rendered any reaction virtually impossible (Scheme 3.17.1). Henceforth, we realized that late stage oxidation of the C4 in **310** would not be a viable option, and we needed to think an alternative.



**Scheme 3.17.1.** Rationale for the failure of the oxidation at C4 in **310**

We decided to alter the route, keeping the alkylation-aldol approach intact. We thought if the C4 carbon were in the right oxidation state before the aldol condensation, we could complete the synthesis. This idea led us to a new, revised synthetic scheme.

### 3.18 The revised plan for oxidation of C4

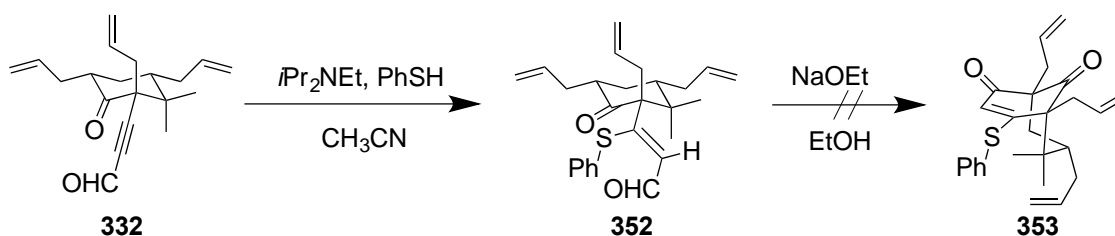
The C4 in **310** was stereochemically and electronically very resistant to change its hybridization from sp<sup>2</sup> to sp<sup>3</sup>, as we learned from a series of failed reactions. Therefore, we envisioned developing a route where the C4 was already in a correct oxidation state before we thought about an aldol reaction to construct the bicyclo[3.3.1]nonane. However, the question remained: at what stage of the synthesis and on which molecule we could perform the oxidation?

With this plan in mind, we realized that if we could add a heteroatom to the β-carbon atom of α,β-unsaturated alkynal **332**, then the β-carbon atom would be in the



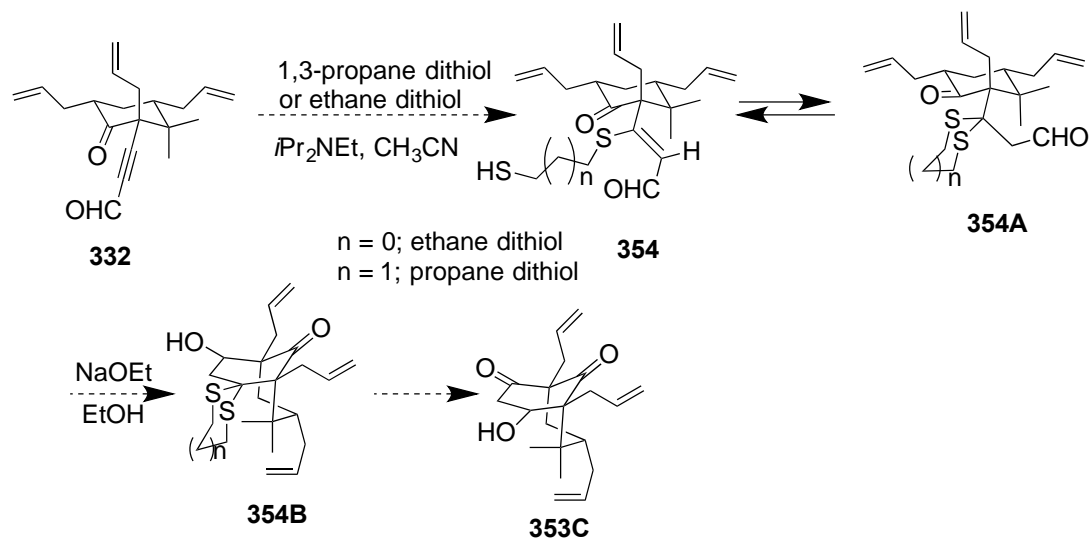
correct oxidation state, and after that we could carry out the aldol condensation (Scheme 3.18.1). Settling with the substrate for the crucial oxidation, we were now in search of a nucleophile that could add to alkyne **332** in a Michael addition fashion.

Thiols have shown such property of adding to a  $\alpha$ ,  $\beta$ -unsaturated aldehyde.<sup>175, 176</sup> Thiophenol is a known to add to  $\beta$  carbon of an alkyne. My predecessor had added a PhS group to the  $\beta$ -carbon of  $\alpha,\beta$ -unsaturated alkyne **332**, but he obtained the *E*-alkyne **352**, which could not undergo aldol condensation.

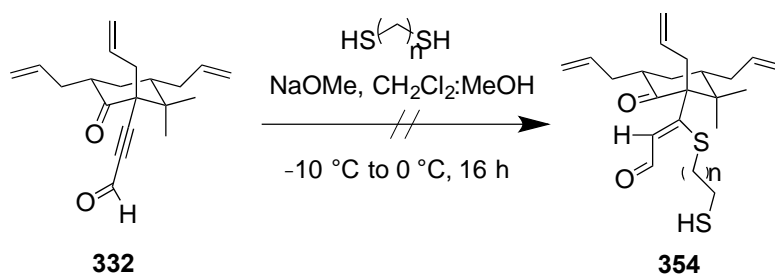


**Scheme 3.18.1.** Addition of PhSH to **332**

The formation of *E*-alkyne **352** from the reaction of thiophenol and alkyne **332** was disappointing. Therefore, we searched for an alternative to thiophenol. Ley showed that 1,2 and 1,3-propanedithiols are nucleophilic towards alkynes and alkynoates, giving a mixture of *E* and *Z* isomers (Scheme 3.18.2).<sup>177</sup> We thought we could apply his methodology on our substrate **332**. Our plan was to affect a Michael addition on **332** to give the aldehyde **354**. However, we knew that we would get a *Z*-alkyne, but, after second Michael addition, there would not be any issue of *E* or *Z*. Therefore, we hoped to get **354A** to avoid any façade of *E* or *Z*- geometry.

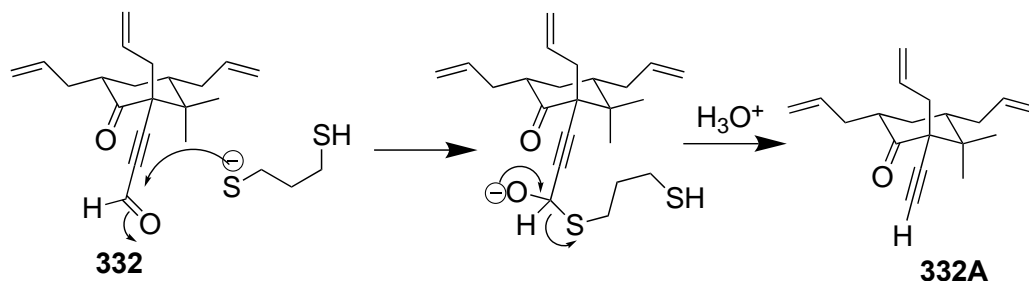


**Scheme 3.18.2.** Strategy for C4 oxidation via propanedithiol reaction



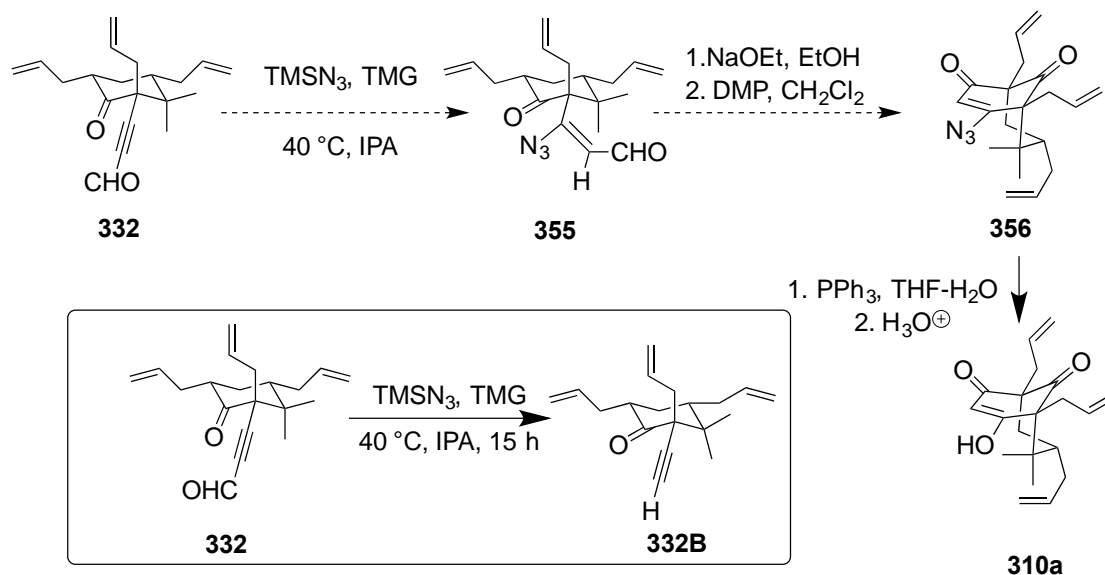
**Scheme 3.18.3.** Addition of 1,2 or 1,3-dithiol to alkyne

With these thoughts in mind, we combined alkyne **332** with 1.1 equivalents of 1,3-propanedithiol in a 1:3 MeOH and THF mixture in the presence of NaOMe (Scheme 3.18.3). We did not see any sign of product formation, **354** or **354A** in the NMR spectrum of the crude material isolated from the reaction mixture. Instead, it appeared that propanedithiol reacted with the aldehyde carbon of **332**, rather than the  $\beta$ -carbon, and, after the hydrolysis, we lost the aldehyde group. We attempted various bases to generate thiolate in situ to add to the  $\beta$ -carbon of **332**, but all the trials were unfruitful, leading only to the deformylation of **332** (Scheme 3.18.4).



**Scheme 3.18.4.** Proposed mechanism for the deformylation of **332**

Small, soft nucleophiles like  $N_3^-$  also add to  $\alpha,\beta$ -unsaturated carbonyl compounds in 1,4-fashion (Scheme 3.18.5). Therefore, we envisioned adding  $N_3^-$  to the  $\beta$ -position of alkyne **332**, converting it to **355**, which could undergo a base-catalyzed aldol reaction, followed by a DMP oxidation, to **356**. Using Staudinger reaction condition, **356** could be reduced to enamine, and after the hydrolysis of enamine, we could get **310a**. The literature suggested that  $Me_3SiN_3$  and tetramethylguanidine hydrochloride would produce tetramethylguanidine azide that could undergo the addition reaction with **332**.<sup>178</sup>



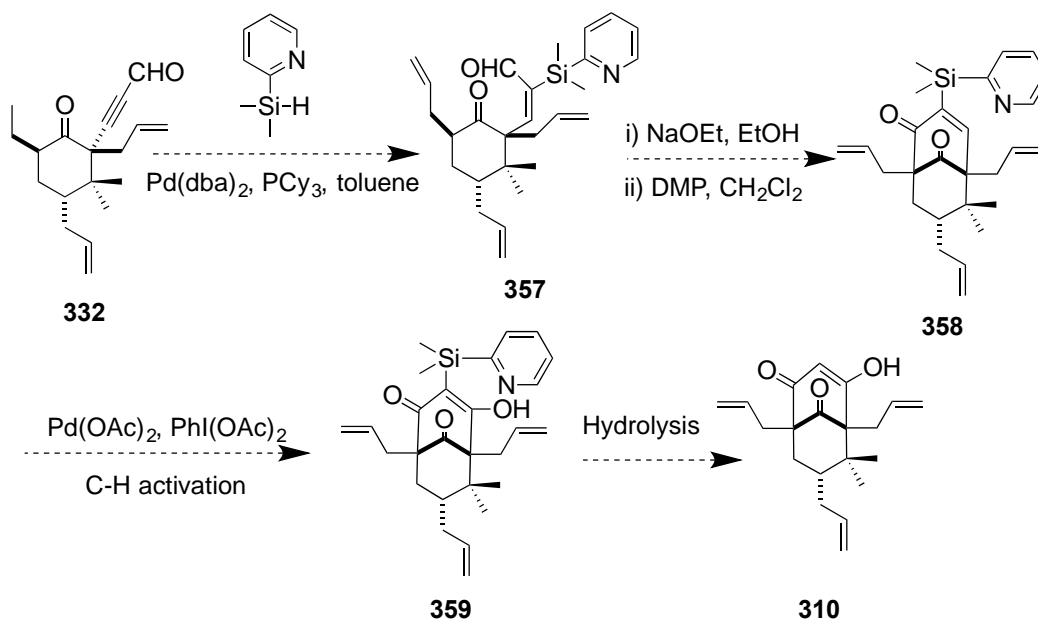
**Scheme 3.18.5.** Azidation and oxidation strategy for C4 oxidation

Accordingly, we performed the reaction with **332** as the substrate. Unfortunately, we did not see any 1,4-addition; instead, we observed loss of the CHO group after the

reaction (Scheme 3.18.5). The result was surprising; we rationalized it with a mechanism similar to the one shown in Scheme 3.18.4.

### 3.18.1 Hydrosilylation and C–H activation

Our next idea was to try to use a C–H activation reaction to functionalize the  $\beta$ -carbon of the bicyclic enone, using a nitrogen heterocycle tethered through a Si atom to the  $\alpha$ -carbon (Scheme 3.18.6). This approach required that we hydrosilylate alkyne **332** with a silane containing a heterocycle, and that the hydrosilylation of **332** would proceed with syn stereochemistry and would direct the silyl group selectively to the  $\alpha$ -carbon and the H to the  $\beta$ -carbon.



**Scheme 3.18.6.** Hydrosilylation–C–H activation route for C4 oxidation

Hydrosilylation of an internal alkyne is not new to organic chemists.<sup>179, 180</sup> Over the last two decades several research groups have been investigating on this topic.<sup>181, 182</sup> There are some advantages of the hydrosilylation; it can reduce a triple bond to an *E*- or *Z*-alkene, depending on the choice of catalysts. Later, the silicon-containing group could be removed

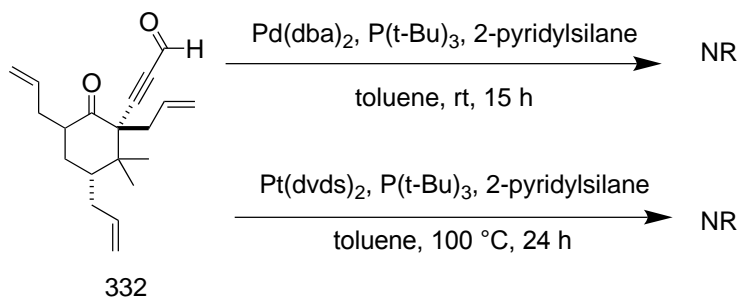
from the substrate via a Tamao–Fleming reaction to carry out further downstream modifications, or one can perform Hiyama coupling on silanes.

The biggest challenge of the hydrosilylation is to control the regio- and stereochemistry of the addition. Our substrate was unsymmetrical alkyne **332**. An unsymmetrical internal alkyne can be hydrosilylated to give four isomers ( $\alpha$ ,  $\beta$ , *E*, and *Z*). Happily, we had already discovered conditions for the hydrosilylation of **332** that gave syn addition across the triple bond and regioselectively placed the silyl group on the  $\alpha$ -carbon and the H on the  $\beta$ -carbon.<sup>183</sup>

After the hydrosilylation, we expected that *Z*-silylated alkenal **357** would undergo the aldol condensation followed by oxidation to **358** (Scheme 3.18.6). We hypothesized if we used 2-pyridyldimethylsilane as a hydrosilylating agent, we could utilize the pyridyl group as a directing group to promote C–H activation at C4 of **358** to give **359**. Then the pyridyl silane group could be removed by hydrolysis, and, hopefully, would provide **310**.

With this idea, we set out to hydrosilylate alkynal **332** with 2-pyridyldimethylsilane. Following Ferreira's method, the hydrosilylation of **332** with PtCl<sub>2</sub> and PySiHMe<sub>2</sub> for more than 24 hours, did not produce **357**;<sup>179</sup> instead, we recovered **332** (Scheme 3.18.7). We also attempted to implement Itami's<sup>184</sup> and Hosoya's<sup>182</sup> reaction

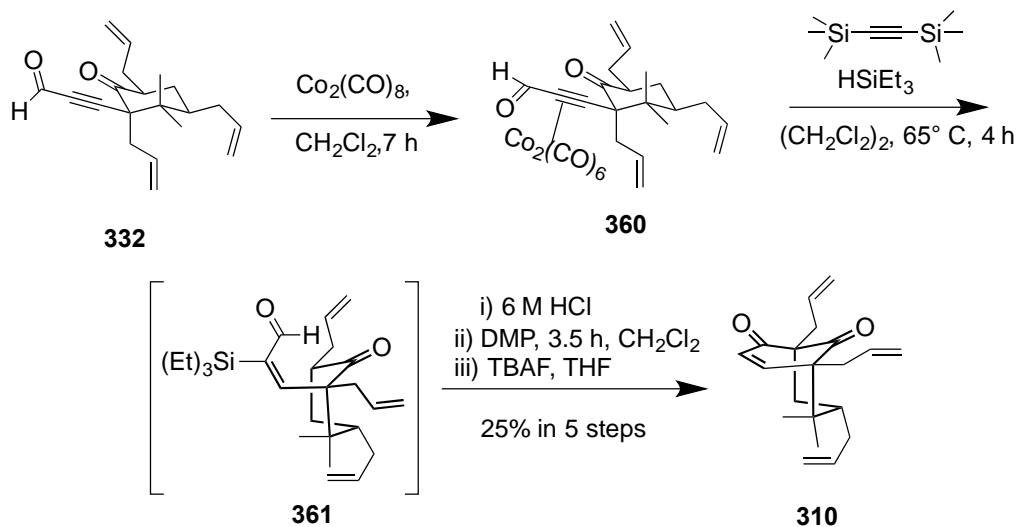
condition separately on **332** (Scheme 3.18.7), but we did not observe hydrosilylation; instead, we recovered starting material.



**Scheme 3.18.7.** Attempts to hydrosilylate **332** with 2-pyridylsilane

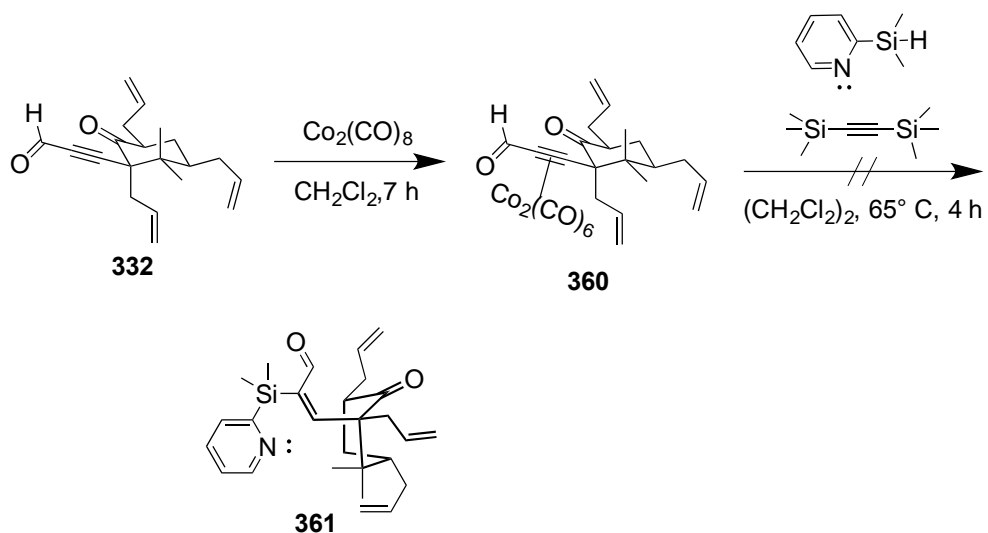
### 3.19 Co-promoted hydrosilylation

Co-promoted hydrosilylation has been used to reduce an  $\alpha,\beta$ -unsaturated alkyne.<sup>185</sup> In 2003, in an effort to develop a model to synthesize nemorosone, Dr. Grossman resorted to a  $\text{Co}_2(\text{CO})_8$ -catalyzed hydrosilylation to reduce an alkyne stereoselectively to *Z*-alkenal.<sup>5</sup> Jayasekara implemented the methodology successfully to synthesize a bicyclo[3.3.1]nonane, **310** (Scheme 3.19.1). We decided to see if the same reaction would work with 2-pyridyldimethylsilane.<sup>53</sup>



**Scheme 3.19.1.** Co-promoted hydrosilylation of alkyne **332** with  $\text{HSiEt}_3$

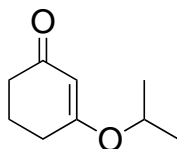
Following the protocol set by Jayasekara, we attempted to reproduce the result with 2-(dimethylsilyl)pyridine. To our disappointment, we did not obtain **361** (Scheme 3.19.2).<sup>184, 186, 187</sup> An attempt at hydrosilylation with (4-methoxyphenyl)dimethylsilane was equally unsuccessful.



**Scheme 3.19.2.** Co-promoted hydrosilylation with 2-pyridyldimethyl silane

## Experimental

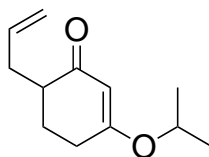
General: All the reactions were done under N<sub>2</sub> atmosphere unless otherwise mentioned. THF, Et<sub>2</sub>O, toluene, and benzene were dried over Na/benzophenone. CH<sub>2</sub>Cl<sub>2</sub> was dried over CaH<sub>2</sub>. Anhydrous MeOH was purchased from Sigma. 1,3-Cyclohexanedione, 2.5 (M) *n*-BuLi, 1.8 (M) MeLi, trimethylsilyldiazomethane, 3 (M) MeMgBr, and PdCl<sub>2</sub> were purchased from Acros organic, and were used without any purification. Allyl alcohol and allyl bromide were distilled before use. Ethyl cyanoformate was synthesized in the lab using Weber-Childs protocol.<sup>150</sup> The reactions were monitored by aluminum backed TLC, and GC. Iodine, KMnO<sub>4</sub>, and *p*-anisaldehyde were used as TLC stains where required. CDCl<sub>3</sub> and C<sub>6</sub>D<sub>6</sub> were used as NMR solvents. NMR spectra were obtained on a 400 MHz Varian instrument. All the chemical shifts were reported in δ ppm with respect to SiMe<sub>4</sub>.



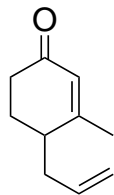
**3-(propan-2-yloxy)cyclohex-2-en-1-one (316):** A 250 mL three-necked round-bottomed flask equipped with a dean stack apparatus was charged with of 1,3-cyclohexanedione (7.50 g, 66.3 mmol) and PTSA·H<sub>2</sub>O (631 mg, 3.31 mmol). Isopropyl alcohol (10 mL, 165 mmol) and benzene (30 mL) were added to the reaction mixture. The resulting light orange solution was refluxed for 4 h. GCMS was monitored to confirm the completion of the reaction. The reaction mixture was cooled to room temperature and the organic solvents were evaporated to red oil. The red oil was dissolved into Et<sub>2</sub>O (100 mL) and then the organic solvent was extracted with Na<sub>2</sub>CO<sub>3</sub> (2×20 mL), NaHCO<sub>3</sub> (2 ×20 mL), and H<sub>2</sub>O (20 mL). The organic layer was finally washed with brine (20 mL). It was dried over anhydrous magnesium sulfate. Finally, the organic solvent was evaporated to red hued yellow oil (9.52



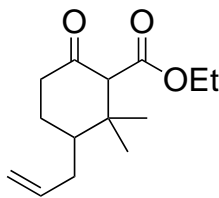
g, 60.0 mmol, yield 93%).  $^1\text{H}$  NMR ( $\text{CDCl}_3$ ):  $\delta$  5.30 (s, 1H), 4.41 (sep, 6.4 Hz, 1H), 2.25 (m, 4H), 2.0 (dd, 13 Hz, 6.5 Hz, 2H), 1.26 (d, 6.4 Hz, 6H).  $^{13}\text{C}$  NMR ( $\text{CDCl}_3$ ):  $\delta$  199.9, 176.9, 102.9, 70.8, 36.6, 29.5, 21.4, 21.1. IR (neat): 2978, 1649, 1379, 1379 1222  $\text{cm}^{-1}$ .



**6-(2-propen-1-yloxy)3-(propan-2-yloxy)cyclohex-2-en-1-one (317):** *n*-BuLi in hexane (2.50 M, 85.5 mL, 213 mmol) was added to a solution of distilled diisopropylamine (23.8 g, 235 mmol) in anhydrous THF (350 mL) under nitrogen at  $-5\text{ }^\circ\text{C}$ . The reaction was stirred for 1 h. The reaction mixture temperature was taken down to  $-78\text{ }^\circ\text{C}$ . In a separate round-bottomed flask, 316 (30.0 g, 200 mmol) was dissolved into dry THF (30 mL) and then added into the previous solution at  $-78\text{ }^\circ\text{C}$  evenly over a period of 10 min. After the addition, the reaction mixture was stirred at  $-78\text{ }^\circ\text{C}$  for 1 h. Allyl bromide (25.8 g, 213 mmol) was dissolved into anhydrous THF (10 mL), and added slowly to the cooled solution. Thereafter, the reaction flask was removed from the dry ice acetone bath, and was allowed to reach at room temperature, and then the reaction mixture was stirred for 3½ h at room temperature. Saturated solution of  $\text{NH}_4\text{Cl}$  (300 mL) was added to the reaction. The organic layer was separated, and the aqueous layer was extracted with  $\text{Et}_2\text{O}$  (4×100 mL). The combined organic solvent was washed with  $\text{H}_2\text{O}$  (2×100 mL) and brine (100 mL), and finally was dried over anhydrous  $\text{MgSO}_4$ . The organic solvent was evaporated under reduced pressure to a light red oil. (34.1 g, 180 mmol, 93%).  $^1\text{H}$  NMR ( $\text{CDCl}_3$ ):  $\delta$  5.80 (m, 1H),  $\delta$ 5.25 (s, 1H), 5.0 (m, 2H), 4.41(sep, 6.2 Hz, 1H), 2.64 (m, 1H), 2.37 (m, 1H), 2.12 (m, 1H), 2.03 (m, 1H), 1.76 (m, 1H), 1.29 (d+m, 5.3 Hz, 6H).  $^{13}\text{C}$ ( $\text{CDCl}_3$ ):  $\delta$  200.6, 140.2, 120, 100, 70, 42, 28, 26, 20, 12. IR (neat): 3050, 2985, 1741, 1447, 1374  $\text{cm}^{-1}$ ;  $m/z$ = 194.

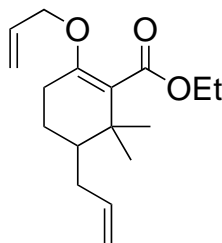


**3-Methyl-4-(2-propen-1-yloxy)cyclohex-2-en-1-one (315):** Compound **317** (6.0 g, 40.0 mmol) was added to an oven dried Schlenk round-bottomed flask and then dry THF (100 mL) was added. The solution was cooled to  $-5\text{ }^{\circ}\text{C}$  under  $\text{N}_2$ . 1.6 M MeLi (1.60 M, 37.5 mL, 60.0 mmol) was added to the cooled solution and it then was stirred at RT for half an hour through GCMS monitoring. Once the starting material vanished, the reaction mixture was cooled to  $0\text{ }^{\circ}\text{C}$ , and 1 M HCl (60 mL) was added slowly (**warning:** vigorous exotherm). The ice bath was removed, and the reaction mixture was stirred for 1 h again at RT. The reaction progress was monitored by GCMS. Next, the reaction mixture was poured into a separatory funnel, and the aqueous layer extracted with  $\text{Et}_2\text{O}$  ( $2 \times 50\text{ mL}$ ). The combined organic layer was washed with water ( $2 \times 50\text{ mL}$ ) and then with brine ( $1 \times 50\text{ mL}$ ). The organic solvent was dried over  $\text{MgSO}_4$ , and evaporated to pale yellow liquid. The reaction yielded **315** (4.33 g, 30.0 mmol, yield 94%) after column chromatography (eluent: petroleum ether: ethyl acetate 5:5).  $^1\text{H NMR}$  ( $\text{CDCl}_3$ ):  $\delta$  5.80-5.60 (s+m, 2H), 5.20-5.00 (m, 2H), 2.50-2.40 (m, 2H), 2.37 (m, 2H), 2.05-1.84 (m+s, 5H).  $^{13}\text{C NMR}$  ( $\text{CDCl}_3$ ):  $\delta$  199.3, 164.9, 135.9, 127.0, 117.3, 39.1, 35.6, 33.7, 26.2, 22.9. IR (neat): 3074, 2928, 1669, 1329, 1251  $\text{cm}^{-1}$ .

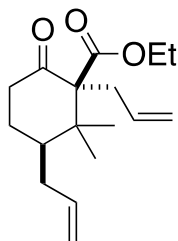


**Ethyl 2,2-dimethyl-6-oxo-3-(2-propen-1-yloxy)cyclohexane-1-carboxylate (318):**

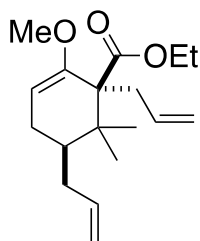
Oven dried CuI (5.25 g, 25.8 mmol) and dry Et<sub>2</sub>O (60 mL) were added to an oven-dried three-necked flask fitted with a mechanical stirrer and N<sub>2</sub> inlet. The suspension was cooled to -5 °C. To this cooled suspension, 1.60 M MeLi (33.0 mL, 51.6 mmol) was slowly added. Soon, the suspension turned into a lime yellow solution, which was stirred for 10 min at -5 °C. Afterwards, enone **315** (2.00 g, 12.9 mmol) was dissolved into dry Et<sub>2</sub>O (10 mL), and was slowly added into the yellow solution over a period of 10 min. After the addition, the reaction mixture was stirred for 1 h at -5 °C. HMPA (10 mL, 55.8 mmol) was added and the reaction mixture was stirred vigorously, and the reaction temperature was taken down slowly to -70 °C by dry ice-methanol bath. 10 min later, ethyl cyanofornate (6.25 g, 51.6 mmol) was dissolved into Et<sub>2</sub>O (10 mL) and added slowly to the previous solution at -70 °C. After the addition, the reaction mixture was allowed to reach room temperature within 1 h. Then, a 1:1 NH<sub>4</sub>OH and saturated solution of NH<sub>4</sub>Cl (100 mL) mixture was added to the reaction mixture and stirred for 30 min. The crude solution was passed through a celite pad to get rid of the fine copper precipitates. The organic phase was separated, and the aqueous layer was extracted with Et<sub>2</sub>O (3×50 mL). The combined organic layers were washed with H<sub>2</sub>O, brine, and dried over MgSO<sub>4</sub>. The organic solvent was evaporated to a pale-yellow liquid that was purified with 10% ethyl acetate in petroleum ether to a colorless oil **318** (3.05 g, 10.0 mmol 76.0%) as a mixture of diastereomers. <sup>1</sup>H NMR (CDCl<sub>3</sub>): δ 5.80 (m, 2H), 5.10 (m, 4H), 4.21 (q, 7.3 Hz, 2H), 3.01 (s, 1H), 2.90 (ddd, 19.3 Hz, 12.1 Hz, 7.1 Hz, 1H), 2.44 (m, 1H), 2.29 (ddd, 15.5 Hz, 9.6 Hz, 6.6 Hz, 1H), 2.00 (m, 1H), 1.90 (ddd, 12 Hz, 10 Hz, 8.2 Hz, 1H), 1.79 (m, 1H), 1.66 (ddd, 14 Hz, 9.0 Hz, 5.8 Hz, 1H), 1.53 (m, 1H), 1.30 (t, 7.3 Hz, 3H), 1.13 (s, 3H), 0.99 (s, 3H). <sup>13</sup>C NMR (CDCl<sub>3</sub>): δ 206.1, 169.0, 137.7, 116.7, 68.8, 60.7, 46.7, 45.9, 41.2, 40.9, 38.9, 34.4, 27.6, 21.9, 14.3. IR (neat): 3423, 2978, 2360, 1712, 1640, 1370, 1228, 1165 cm<sup>-1</sup>



**Ethyl 6,6-dimethyl-5-(prop-2-en-1-yl)-2-(2-propen-1-yloxy)cyclohex-1-ene-1-carboxylate (324):** NaH (1.26 g, 31.5 mmol), which was washed with petroleum ether (3×5 mL), was added to a 250 mL round-bottomed flask and then dry THF (25 mL) was poured into the flask. The suspension was cooled to 0 °C and keto-ester **318** (6.00 g, 25.2 mmol) was dissolved into anhydrous THF (25 mL), and added into the suspension for over 5 min via an addition funnel. After the addition, the suspension was stirred for 1 h at room temperature. Allyl bromide (3.65 g, 30.2 mmol) was dissolved into anhydrous THF (4 mL) and added into the suspension. After this, the suspension was refluxed for 36 h at 60 °C. The reaction mixture was cooled to 0 °C. H<sub>2</sub>O (20 mL) was added followed by extraction with Et<sub>2</sub>O (3 × 40 mL). The combined organic layers were washed with H<sub>2</sub>O (2× 20 mL), brine (20 mL), and dried over MgSO<sub>4</sub>. Finally, the organic solvent was evaporated to a thick yellow liquid, and the thick liquid was purified by column chromatography (eluent: 10 % EtOAc in petroleum ether) to yield a viscous liquid **324** (5.35 g, 20.0 mmol, yield 76%). <sup>1</sup>H NMR (CDCl<sub>3</sub>): δ 5.92 (m, 1H), 5.80 (m, 1H), 5.3 (dd 3.1 Hz, 1.7 Hz, 1H), 5.18 (dd, 3.2 Hz, 1.6 Hz, 1H), 5.06 (m, 2H), 4.27 (m, 4H), 2.36 (m, 1H), 2.19 (m, 2H), 1.86 (m, 1H), 1.74 (m, 1H), 1.48 (m, 1H), 1.3 (t, 7.66 Hz, 3H), 1.10 (s, 3H), 1.02 (s, 3H). <sup>13</sup>C NMR (CDCl<sub>3</sub>): δ 170.3, 152.4, 138.7, 134.7, 122.2, 117.0, 116.5, 115.9, 68.7, 60.4, 43.4, 36.1, 34.0, 27.1, 24.0, 22.4, 22.4, 14.4. IR (neat): 3077, 2972, 2935, 2862, 1714, 1667 cm<sup>-1</sup>.

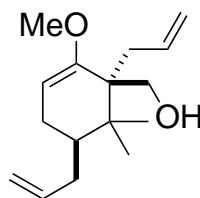


**Ethyl (1R,3S)-2,2-dimethyl-6-oxo-1,3-bis(2-propen-1-yl)cyclohexane-1-carboxylate (314):** *O*-allyl vinyl ether **324** (5.80 g, 20.8 mmol) was dissolved into anhydrous toluene (62 mL) and was heated to 150 °C for 8 hours in a sealed tube. After 8 h, the toluene was evaporated to a red oil and the residue was purified through a column using 5% ethyl acetate in petroleum ether. The reaction furnished required diastereomer **314** (4.40 g, 20.0 mmol, yield 75.0%). <sup>1</sup>H NMR (CDCl<sub>3</sub>): δ 5.80 (m, 2H), 5.08 (m, 4H), 4.21 (q, 7.3 Hz, 2H), 2.74 (m, 2H), 2.44 (m, 1H), 2.29 (ddd, 15.5 Hz, 9.6 Hz, 6.6 Hz, 1H), 2.08 (m, 1H), 1.90 (ddd, 13 Hz, 11 Hz, 8.3 Hz, 1H), 1.79 (m, 1H), 1.66 (ddd, 14 Hz, 9.0 Hz, 5.8 Hz, 1H), 1.30 (t, 7.24 Hz, 3H), 1.13 (s, 3H), 0.99 (s, 3H). <sup>13</sup>C NMR (CDCl<sub>3</sub>): δ 205.5, 170.6, 164.3, 137.8, 134.9, 117.0, 115.8, 67.6, 60.2, 45.0, 43.18, 42.4, 37.4, 35.3, 33.5, 24.7, 21.7, 13.6. IR (neat): 3076, 2973, 2360, 1712, 1640, 1442, 1371 cm<sup>-1</sup>.



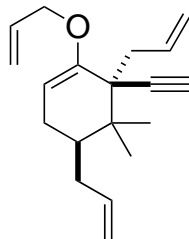
**Ethyl (1R, 5R)-2-methoxy-6,6-dimethyl-1,5-bis(2-propen-1-yl)cyclohex-2-ene-1-carboxylate (325):** Anhydrous CH(OMe)<sub>3</sub> (2.04 mL, 22.7 mmol) and MeOH (1.50 mL, 0.10 mL/mmol) were mixed in a separate round-bottomed flask. Ethyl carboxylate **314** (3.85 g, 15.1 mmol) was added into the previous solution. The reaction was cooled in an ice bath. After that, conc. H<sub>2</sub>SO<sub>4</sub> (40.0 μL, 0.07 mmol) was added, and the reaction mixture

was stirred for 36 h at room temperature. GCMS was checked after 36 hours, and then the reaction mixture was concentrated. The crude mass was dissolved into of Et<sub>2</sub>O (30 mL). The organic layer was washed with a saturated solution of NaHCO<sub>3</sub> (2×20 mL), H<sub>2</sub>O (10 mL), and brine. The organic solvent was dried over anhydrous MgSO<sub>4</sub>. After rotary evaporation and column chromatography by 5% ethyl acetate in petroleum ether, the reaction yielded methyl enol ester **325** (3.70 g, 12.0 mmol, yield 87%). <sup>1</sup>H NMR (CDCl<sub>3</sub>): δ 5.80 (m, 2H), 5.0 (m, 2H), 4.88 (dd, 7.84 Hz, 2.04 Hz, 1H), 4.78 (dd, 6.1 Hz, 2.0 Hz, 1H), 4.22 (m, 2H), 3.41 (s, 3H), 2.81 (m, 1H), 2.54 (dd, 14 Hz, 9.3 Hz, 1H), 2.3 (m, 1H), 2.14 (ddd, 16 Hz, 6.0 Hz, 4.06 Hz, 1H), 1.78 (m, 3H), 1.24 (t, 7.0 Hz, 3H), 1.05 (s, 3H), 0.78 (s, 3H); <sup>13</sup>C NMR (CDCl<sub>3</sub>): δ 173.1, 154.3, 138.2, 137.0, 115.5, 114.6, 95.7, 60.0, 59.2 54.0, 38.8, 38.0, 34.1, 26.6, 22.3, 19.8, 14.2. IR (neat): 3073, 2974, 2946, 2834, 1722, 1671 cm<sup>-1</sup>.



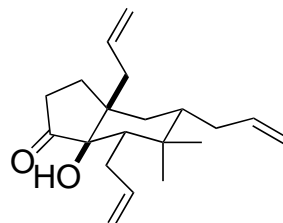
**[(1S,5R)-2-methoxy-6,6-dimethyl-1,5-bis(2-propen-1-yl)cyclohex-2-en-1-yl]methanol (326)**: Ethyl enol ester **325** (3.94 g, 14.1 mmol) was dissolved in dry Et<sub>2</sub>O (150 mL) and cooled to 0 °C. LiAlH<sub>4</sub> (927 mg, 22.5 mmol) was added to the cold solution of enol ester **325** at 0 °C, and stirred for 3½ h at RT. H<sub>2</sub>O (1 mL) and 1 M NaOH (1 mL) were added to the reaction mixture. A few minutes later, H<sub>2</sub>O (3 mL) was added to it. Diethyl ether (100 mL) was added to the slurry and stirred under nitrogen for 20 min at room temperature. The organic solvent was decanted carefully, dried over anhydrous MgSO<sub>4</sub>, and evaporated to a thick white liquid (3.02 g, 10.0 mmol, 86%). <sup>1</sup>H NMR

(CDCl<sub>3</sub>): δ 5.90 (m, 2H), 5.04 (m, 4H), 4.77 (dd, 5.37 Hz, 2.31 Hz, 1H), 3.81 (dd, 11 Hz, 6.5 Hz, 1H), 3.71 (dd, 11 Hz 8.1 Hz, 1H), 3.48 (s, 3H), 2.54 (dd, 8.0 Hz, 6.1 Hz, 1H), 2.32 (m, 2H), 2.18 (dt, 11 Hz, 5.3 Hz, 1H), 1.89 (m, 3H), 0.98 (s, 3H), 0.82 (s, 3H). <sup>13</sup>CNMR (CDCl<sub>3</sub>): δ 157.1, 138.4, 137.9, 115.3, 114.7, 95.5, 65.8, 65.2, 53.8, 49.5, 38.9, 38.1, 34.2, 26.9, 21.8, 17.6, 15.2. IR (neat): 3435, 3073, 2969, 2934, 2832, 1672 cm<sup>-1</sup>.



**(4R, 6R)-6-ethynyl-5,5-dimethyl-4,6-bis(2-propen-1-yl)-1-(2-propene-1-yloxy)cyclohex-1-ene (329):** Allyl alcohol (5 mL, 0.07 mmol), CSA·H<sub>2</sub>O (14.3 mg, 0.06 mmol) and benzene (15 mL) were added in a 50 mL round-bottomed flask, fitted with dean stack apparatus, and the reaction mixture was heated to reflux for an hour. The solution was allowed to reach room temperature and then alkyne **328** (300 mg, 1.22 mmol), dissolved in anhydrous benzene (5 mL), was added to the previous solution. The reaction mixture was refluxed for 2½ h. The reaction mixture was cooled to room temperature and the organic layer was diluted with 20 mL of Et<sub>2</sub>O. The organic solvent was extracted with Na<sub>2</sub>CO<sub>3</sub> (2 × 10 mL), NaHCO<sub>3</sub> (2 × 10 mL) and brine. The organic layer was dried over anhydrous MgSO<sub>4</sub> and was evaporated to dryness. The residue was eluted with 5% ethyl acetate in petroleum ether to furnish *O*-allyl-alkyne **329** (276 mg, 0.01 mmol, yield 78%). <sup>1</sup>H NMR (CDCl<sub>3</sub>): δ 6.03 (m, 1H), 5.98 (m, 1H), 5.8 (m, 1H), 5.38 (ddd, 17 Hz, 3.7 Hz, 2.1 Hz, 1H), 5.18 (ddd, 10 Hz, 3.4 Hz, 1.8 Hz, 1H), 5.04 (m, 4H), 4.58 (dd, 5.1 Hz, 2.8 Hz, 1H), 4.26 (ddt, 13 Hz, 5.4 Hz, 1.8 Hz, 1H), 4.08 (ddt, 13 Hz, 5.4 Hz, 1.8 Hz, 1H), 2.56 (ddt, 13.4 Hz, 6.8 Hz, 2.02 Hz, 1H), 2.44 (dd, 13, 7.8 Hz, 1H), 2.34 (dd, 9.3 Hz, 5.5 Hz,

1H), 2.22 (s, 1H), 2.19 (dt, 9.8 Hz, 5.0 Hz, 1H), 1.78 (m, 2H), 1.68 (m, 1H), 1.42 (s, 3H), 1.0 (s, 3H). <sup>13</sup>C NMR (CDCl<sub>3</sub>): δ 153.3, 138.0, 136.9, 133.6, 128.3, 116.0, 115.6, 114.6, 94.3, 85.4, 71.7, 67.5, 49.8, 42.8, 39.4, 36.9, 35.1, 29.6, 27.1, 23.1, 19.1. IR (neat): 3075, 2955, 2923, 2855, 2150, 1639 cm<sup>-1</sup>



**(3aR, 6R, 7aR)-7a-hydroxy-5,5-dimethyl-2,3a,6-tris(2-propen-1-yl)-octahydro-1H-inden-1-one (343)**: Mg powder (30.0 mg, 1.27 mmol) was added in an oven dried round-bottomed Schlenk flask. Enone **310** (19.0 mg, 0.06 mmol) was dissolved into anhydrous MeOH (3.00 mL) in a separate round-bottomed flask, and then was added to the Schlenk flask. The reaction mixture was refluxed for 3 h, and then the reaction mixture was cooled to room temperature. The reaction mixture was treated with 1 M HCl (2 mL). The reaction mass was extracted with Et<sub>2</sub>O (3×5 mL) and then, H<sub>2</sub>O (1×10 mL). The combined organic layer was dried over anhydrous MgSO<sub>4</sub>. The organic solvent was evaporated under reduced pressure, and the residue was chromatographed (eluent 7:3 petroleum ether: EtOAc) to afford **343** (8.35 mg, 0.04 mmol, yield 51%). <sup>1</sup>H NMR (CDCl<sub>3</sub>): δ 5.8-5.6 (m, 3H), 5.0 (m, 6H), 3.6 (s, 1H), 2.80-2.40 (m, 8H), 1.10 (s, 3H), 1.00 (s, 3H). <sup>13</sup>C NMR (CDCl<sub>3</sub>): δ 219.7, 139.3, 136.7, 136.0, 117.7, 116.2, 115.6, 83.6, 50.1, 47.5, 37.4, 35.2, 33.2, 32.4, 31.2, 28.5, 23.9, 23.5, 23.3.



## Conclusion

7-*epi*-Clusianone is an important molecule because of its broad range of biological activity, namely, vasorelaxant, antimalarial, cytotoxic. These properties have inspired us to devise a scheme for a total synthesis of the molecule and, later, propose a general scheme for other endo or exo PPAPs. We have not succeeded in finishing the synthesis; however, we have a couple of feats in this project that has offered more satisfaction than conceiving a solution.

We developed a robust method of a 1,4-addition followed by an acylation even on a large scale (Scheme 3.7.1). Establishing a method for synthesis of methyl enol ether from a  $\beta$ -keto ester without transesterification is worth mentioning here (Scheme 3.8.1). We established a robust method for constructing a bicyclo [3.3.1] nonane using alkynylation followed by aldol approach. The strategy has viability with a board substrate scope including silanes, although the yield was not impressive.

We observed an interesting rearrangement of a carbon skeleton into another when we tried to reduce a  $\alpha$ ,  $\beta$ -bond in bicyclic enone (**310**) to a saturated ketone. As far as our knowledge goes, it was a first of its kind of reaction, where a bicyclo [3.3.1] nonane rearranged to a bicyclo [4.3.0] nonane (**Scheme 3.16.6**). Currently, we are writing the manuscripts to publish the result.

Finally, we have realized that the oxidation of C4 carbon has been a bottleneck for the overall scheme of the total synthesis. The gem-dimethyl at C6 has been at the root of the problem. Therefore, we need to devise a scheme where C4 is in the correct oxidation state before we think about the constructing the quaternary center at C6.



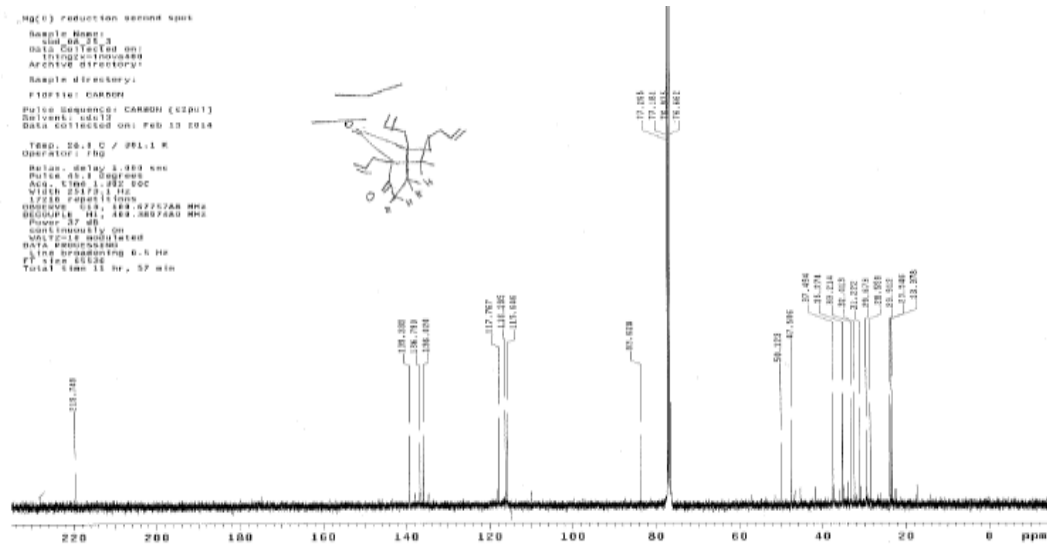
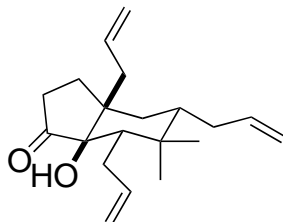


Figure 3.19.2. C NMR of 343

Table 3.2. Crystal data and structure refinement for **343**.

Empirical formula	C <sub>20</sub> H <sub>30</sub> O <sub>2</sub>
Formula weight	302.44
Temperature	90.0(2) K
Wavelength	1.54178 Å
Crystal system, space group	Triclinic, P -1
Unit cell dimensions	
a	6.6628(2) Å
α	78.1350(11) °
b	11.2157(3) Å
β	76.4840(12) °
c	12.1836(3) Å
γ	84.0060(12) °
Volume	864.81(4) Å <sup>3</sup>
Z, Calculated density	2, 1.161
Mg/m <sup>3</sup>	
Absorption coefficient	0.561 mm <sup>-1</sup>
	F(000)
	332
Crystal size (mm)	0.200 x 0.080 x 0.025
θ range for data collection (°)	3.799 to 68.211
Limiting indices	-3 ≤ h ≤ 8
•	13 ≤ k ≤ 13
	14 ≤ l ≤ 14
Reflections collected / unique	11768 / 3080
[Rint = 0.0351]	
Completeness to	θ = 67.679 98.4%
Absorption correction	Semi-empirical from equivalents
Max. and min. transmission	0.956 and 0.871
Refinement method	Full-matrix least-squares on F <sup>2</sup>
Data / restraints / parameters	3080 / 0 / 201
Goodness-of-fit on F <sup>2</sup>	1.077
Final R indices [I > 2σ(I)]	R1 = 0.0371, wR2 = 0.0953

R indices (all data)      R1 = 0.0411, wR2 = 0.0981

Extinction coefficient    0.0023(5)

Largest diff. peak and hole 0.261 and -0.198 e<sup>-</sup> Å<sup>-3</sup>

Table 3.3. Atomic coordinates (x 104) and equivalent isotropic displacement parameters (Å<sup>2</sup> x 103) for 343.

U (eq) is defined as one third of the trace of the orthogonalized U<sub>ij</sub> tensor.

x	y	z	U (eq)	
O(1)	4505 (1)	8253 (1)	6162 (1)	18 (1)
O(2)	7748 (1)	9497 (1)	4492 (1)	20 (1)
C(1)	6948 (2)	8677 (1)	7236 (1)	16 (1)
C(2)	8119 (2)	8604 (1)	5187 (1)	16 (1)
C(3)	10161 (2)	7883 (1)	5159 (1)	19 (1)
C(4)	9690 (2)	6708 (1)	6052 (1)	18 (1)
C(5)	7297 (2)	6674 (1)	6453 (1)	16 (1)
C(6)	6579 (2)	5959 (1)	7722 (1)	18 (1)
C(7)	6811 (2)	6679 (1)	8655 (1)	19 (1)
C(8)	5901 (2)	7989 (1)	8409 (1)	18 (1)
C(9)	6586 (2)	8060 (1)	6270 (1)	15 (1)
C(10)	6213 (2)	10037 (1)	7088 (1)	19 (1)
C(11)	7165 (2)	10695 (1)	7776 (1)	21 (1)
C(12)	6134 (2)	11200 (1)	8641 (1)	29 (1)
C(13)	6468 (2)	6063 (1)	5620 (1)	20 (1)
C(14)	7365 (2)	6441 (1)	4357 (1)	21 (1)
C(15)	6303 (2)	7001 (1)	3597 (1)	29 (1)
C(16)	8970 (2)	6664 (1)	8922 (1)	22 (1)
C(17)	8843 (2)	7106 (1)	10019 (1)	27 (1)
C(18)	9681 (2)	8083 (2)	10105 (2)	35 (1)
C(19)	7754 (2)	4702 (1)	7900 (1)	23 (1)
C(20)	4263 (2)	5722 (1)	7965 (1)	23 (1)

--

Table 3.5 Anisotropic displacement parameters (A<sup>2</sup> x 10<sup>3</sup>) for 343. The anisotropic displacement factor exponent takes the form:

$$2 \pi^2 [h^2 a^2 U_{11} + \dots + 2 h k a^* b^* U_{12}]$$

	U11	U22	U33	U23	U13	U12
O(1)	14(1)	15(1)	24(1)	-1(1)	-7(1)	0(1)
O(2)	26(1)	14(1)	18(1)	-1(1)	-6(1)	-1(1)
C(1)	16(1)	16(1)	17(1)	-2(1)	-5(1)	-1(1)
C(2)	20(1)	14(1)	17(1)	-5(1)	-6(1)	-3(1)
C(3)	17(1)	18(1)	20(1)	-2(1)	-2(1)	-2(1)
C(4)	17(1)	16(1)	19(1)	-2(1)	-3(1)	1(1)
C(5)	17(1)	14(1)	18(1)	-1(1)	-4(1)	0(1)
C(6)	18(1)	16(1)	20(1)	1(1)	-3(1)	-1(1)
C(7)	17(1)	20(1)	16(1)	1(1)	-2(1)	0(1)
C(8)	17(1)	20(1)	16(1)	-2(1)	-3(1)	1(1)
C(9)	12(1)	15(1)	17(1)	-2(1)	-5(1)	-1(1)
C(10)	22(1)	17(1)	18(1)	-3(1)	-5(1)	0(1)
C(11)	23(1)	18(1)	23(1)	-3(1)	-7(1)	-2(1)
C(12)	31(1)	31(1)	28(1)	-12(1)	-11(1)	1(1)
C(13)	22(1)	14(1)	22(1)	-3(1)	-6(1)	-2(1)
C(14)	26(1)	16(1)	24(1)	-7(1)	-4(1)	-2(1)
C(15)	40(1)	24(1)	25(1)	-5(1)	-10(1)	-4(1)
C(16)	21(1)	23(1)	21(1)	-1(1)	-7(1)	3(1)
C(17)	25(1)	34(1)	23(1)	-2(1)	-9(1)	0(1)
C(18)	27(1)	45(1)	37(1)	-13(1)	-10(1)	-2(1)
C(19)	26(1)	17(1)	24(1)	2(1)	-4(1)	0(1)
C(20)	20(1)	21(1)	24(1)	2(1)	-2(1)	-6(1)

Table 3.6 Hydrogen coordinates ( $\times 104$ ) and isotropic displacement parameters ( $\text{\AA}^2 \times 103$ ) for 343.

	x	y	z	U (eq)
H(10)	4254	8996	5910	27
H(1A)	8469	8621	7199	20
H(3A)	11164	8348	5360	22
H(3B)	10742	7692	4385	22
H(4A)	10316	6704	6715	22
H(4B)	10268	5986	5708	22
H(7A)	5906	6281	9388	23
H(8A)	4404	7976	8442	22
H(8B)	6060	8423	9010	22
H(10A)	6589	10421	6265	23
H(10B)	4688	10112	7339	23
H(11A)	8623	10750	7571	25
H(12A)	4675	11164	8871	34
H(12B)	6850	11602	9035	34
H(13A)	6719	5168	5831	23
H(13B)	4952	6237	5751	23
H(14A)	8800	6262	4089	25
H(15A)	4864	7194	3834	35
H(15B)	6975	7212	2811	35
H(16A)	9608	5822	8986	27
H(16B)	9865	7190	8281	27
H(17A)	8095	6642	10708	33
H(18A)	10442	8573	9437	42
H(18B)	9527	8300	10836	42
H(19A)	7282	4277	8693	35
H(19B)	9240	4811	7750	35
H(19C)	7487	4219	7370	35
H(20A)	3827	5277	8754	34
H(20B)	4039	5234	7427	34
H(20C)	3453	6502	7867	34

Table 3.7 Torsion angles [ $^{\circ}$ ] for **343**.

O(2)-C(2)-C(3)-C(4)	-167.61 (12)
C(9)-C(2)-C(3)-C(4)	14.64 (13)
C(2)-C(3)-C(4)-C(5)	8.84 (13)
C(3)-C(4)-C(5)-C(13)	87.13 (12)
C(3)-C(4)-C(5)-C(9)	-27.83 (12)
C(3)-C(4)-C(5)-C(6)	-151.28 (10)
C(4)-C(5)-C(6)-C(19)	-49.88 (14)
C(13)-C(5)-C(6)-C(19)	71.43 (13)
C(9)-C(5)-C(6)-C(19)	-166.34 (10)
C(4)-C(5)-C(6)-C(20)	-167.72 (10)
C(13)-C(5)-C(6)-C(20)	-46.40 (13)
C(9)-C(5)-C(6)-C(20)	75.83 (13)
C(4)-C(5)-C(6)-C(7)	73.93 (13)
C(13)-C(5)-C(6)-C(7)	-164.76 (10)
C(9)-C(5)-C(6)-C(7)	-42.53 (14)
C(19)-C(6)-C(7)-C(8)	172.69 (10)
C(20)-C(6)-C(7)-C(8)	-72.53 (12)
C(5)-C(6)-C(7)-C(8)	48.07 (13)
C(19)-C(6)-C(7)-C(16)	44.05 (15)
C(20)-C(6)-C(7)-C(16)	158.83 (11)
C(5)-C(6)-C(7)-C(16)	-80.58 (13)
C(10)-C(1)-C(8)-C(7)	-171.99 (10)
C(9)-C(1)-C(8)-C(7)	62.80 (13)
C(16)-C(7)-C(8)-C(1)	73.64 (13)
C(6)-C(7)-C(8)-C(1)	-59.11 (13)
O(2)-C(2)-C(9)-O(1)	29.15 (16)
C(3)-C(2)-C(9)-O(1)	-153.06 (10)
O(2)-C(2)-C(9)-C(1)	-92.45 (13)
C(3)-C(2)-C(9)-C(1)	85.34 (11)
O(2)-C(2)-C(9)-C(5)	150.17 (11)
C(3)-C(2)-C(9)-C(5)	-32.04 (12)
C(8)-C(1)-C(9)-O(1)	70.94 (12)
C(10)-C(1)-C(9)-O(1)	-53.00 (13)
C(8)-C(1)-C(9)-C(2)	-165.96 (9)
C(10)-C(1)-C(9)-C(2)	70.10 (12)



C (8) -C (1) -C (9) -C (5)	-54.73 (13)
C (10) -C (1) -C (9) -C (5)	-178.67 (10)
C (4) -C (5) -C (9) -O (1)	157.78 (10)
C (13) -C (5) -C (9) -O (1)	42.81 (13)
C (6) -C (5) -C (9) -O (1)	-79.70 (12)
C (4) -C (5) -C (9) -C (2)	35.70 (11)
C (13) -C (5) -C (9) -C (2)	-79.27 (11)
C (6) -C (5) -C (9) -C (2)	158.22 (10)
C (4) -C (5) -C (9) -C (1)	-76.97 (12)
C (13) -C (5) -C (9) -C (1)	168.06 (10)
C (6) -C (5) -C (9) -C (1)	45.55 (13)
C (8) -C (1) -C (10) -C (11)	74.57 (13)
C (9) -C (1) -C (10) -C (11)	-161.74 (10)
C (1) -C (10) -C (11) -C (12)	-115.65 (15)
C (4) -C (5) -C (13) -C (14)	-43.30 (14)
C (9) -C (5) -C (13) -C (14)	67.33 (13)
C (6) -C (5) -C (13) -C (14)	-167.14 (10)
C (5) -C (13) -C (14) -C (15)	-116.66 (15)
C (8) -C (7) -C (16) -C (17)	65.85 (14)
C (6) -C (7) -C (16) -C (17)	-165.35 (11)
C (7) -C (16) -C (17) -C (18)	-117.10 (16)

Table 3.8. Hydrogen bonds for 343 [ $\text{\AA}$  and  $^\circ$ ]

D-H...A	d (D-H)	d(H...A)	d(D...A)	$\angle$ (DHA)
O(1)-H(10)...O(2)#1	0.84	2.09	2.8635(12)	152.6

Symmetry transformations used to generate equivalent atoms:

#1  $-x+1, -y+2, -z+1$

Table 3.9. Crystal data and structure refinement for 329B.

Identification code 329B  
 Empirical formula C18 H24 O3  
 Formula weight 288.37  
 Temperature 90.0(2) K  
 Wavelength 1.54178 Å  
 Crystal system, space group Orthorhombic, P2(1)2(1)2(1)  
 Unit cell dimensions  
 a 7.6532(3) Å  
 α 90 °  
 b 13.3427(6) Å  
 β 90 °  
 c 15.7225(7) Å  
 γ 90 °  
 Volume 1605.49(12) Å<sup>3</sup>  
 Z, Calculated density 4, 1.193 Mg/m<sup>3</sup>  
 Absorption coefficient 0.634F (000) 624(mm<sup>-1</sup>)  
 Crystal size 0.270 x 0.250 x 0.200 mm  
 Θ range for data collection 4.346 to 68.064 °  
 Limiting indices -9<=h<=3 -15<=k<=15  
 18<=l<=18  
 Reflections collected / unique 20802 / 2912  
 [R (int) = 0.0439]  
 Completeness to Θ = 67.679 99.9 %  
 Absorption correction Semi-empirical from equivalents  
 Max. and min. transmission 0.929 and 0.721  
 Refinement method Full-matrix least-squares on F<sup>2</sup>  
 Data / restraints / parameters 2912 / 0 / 193  
 Goodness-of-fit on F<sup>2</sup> 1.089  
 Final R indices [I>2σ(I)] R1 = 0.0324, wR2 = 0.0908  
 R indices (all data) R1 = 0.0334, wR2 = 0.0916  
 Absolute structure parameter 0.43(6)  
 Extinction coefficient n/a  
 Largest diff. peak and hole 0.167 and -0.128 (e. Å<sup>-3</sup>)

Table **3.10** Atomic coordinates ( $\times 10^4$ ) and equivalent isotropic displacement parameters ( $\text{Å}^2 \times 10^3$ ) for 329B.

U (eq) is defined as one third of the trace of the orthogonalized

U<sub>ij</sub> tensor.

	x	y	z	U (eq)
O (1)	6612 (2)	5826 (1)	7472 (1)	39 (1)
O (2)	-73 (2)	5426 (1)	8711 (1)	37 (1)
O (3)	2182 (2)	4376 (1)	8919 (1)	40 (1)
C (1)	6668 (2)	6724 (1)	7565 (1)	30 (1)
C (2)	8269 (3)	7337 (2)	7369 (1)	33 (1)
C (3)	8743 (2)	8063 (2)	8086 (1)	31 (1)
C (4)	7176 (2)	8694 (1)	8367 (1)	26 (1)
C (5)	5613 (2)	8029 (1)	8648 (1)	26 (1)
C (6)	5065 (2)	7323 (1)	7883 (1)	27 (1)
C (7)	4305 (3)	7929 (2)	7115 (1)	30 (1)
C (8)	3807 (3)	7298 (2)	6366 (1)	38 (1)
C (9)	4447 (3)	7414 (2)	5595 (1)	46 (1)
C (10)	7698 (2)	9465 (2)	9049 (1)	31 (1)
C (11)	9236 (3)	10095 (2)	8799 (1)	32 (1)
C (12)	10543 (3)	10316 (2)	9295 (2)	40 (1)
C (13)	6106 (3)	7366 (2)	9408 (1)	31 (1)
C (14)	4050 (2)	8688 (2)	8903 (1)	30 (1)
C (15)	3738 (2)	6602 (1)	8171 (1)	30 (1)
C (16)	2700 (3)	5998 (2)	8415 (1)	32 (1)
C (17)	1615 (3)	5177 (2)	8708 (1)	30 (1)
C (18)	-1241 (3)	4617 (2)	8955 (2)	40 (1)

Table 3.12. Anisotropic displacement parameters ( $A^2 \times 10^3$ ) for 329B.

The anisotropic displacement factor exponent takes the form:

$$\bullet \frac{2 \pi^2}{\sqrt{h^2 a^2 U_{11} + \dots + 2 h k a^* b^* U_{12}}} ]$$

	U11	U22	U33	U23	U13	U12
O(1)	40(1)	28(1)	49(1)	-6(1)	1(1)	1(1)
O(2)	29(1)	36(1)	47(1)	5(1)	2(1)	-4(1)
O(3)	38(1)	33(1)	48(1)	2(1)	5(1)	-2(1)
C(1)	31(1)	29(1)	30(1)	-2(1)	-2(1)	1(1)
C(2)	29(1)	31(1)	39(1)	-4(1)	4(1)	3(1)
C(3)	25(1)	32(1)	37(1)	-2(1)	2(1)	-1(1)
C(4)	24(1)	26(1)	27(1)	1(1)	0(1)	0(1)
C(5)	25(1)	27(1)	27(1)	2(1)	0(1)	1(1)
C(6)	25(1)	27(1)	29(1)	1(1)	0(1)	-1(1)
C(7)	28(1)	32(1)	31(1)	3(1)	-3(1)	1(1)
C(8)	38(1)	37(1)	38(1)	2(1)	-8(1)	-5(1)
C(9)	56(1)	47(1)	36(1)	-4(1)	-6(1)	-1(1)
C(10)	30(1)	30(1)	32(1)	-2(1)	-1(1)	-1(1)
C(11)	33(1)	29(1)	33(1)	0(1)	-1(1)	-2(1)
C(12)	36(1)	40(1)	45(1)	4(1)	-6(1)	-7(1)
C(13)	32(1)	31(1)	31(1)	6(1)	-3(1)	-3(1)
C(14)	28(1)	31(1)	32(1)	0(1)	3(1)	1(1)
C(15)	29(1)	31(1)	28(1)	0(1)	-3(1)	-1(1)
C(16)	31(1)	33(1)	31(1)	-1(1)	-2(1)	-4(1)
C(17)	32(1)	31(1)	27(1)	-5(1)	1(1)	-6(1)
C(18)	32(1)	41(1)	47(1)	1(1)	4(1)	-11(1)

Table 5. Hydrogen coordinates ( $\times 10^4$ ) and isotropic displacement parameters ( $\text{Å}^2 \times 10^3$ ) for 329B.

	x	y	z	U(eq)
H(2A)	8065	7723	6840	40
H(2B)	9267	6880	7267	40
H(3A)	9187	7678	8579	37
H(3B)	9689	8514	7890	37
H(4A)	6782	9082	7858	31
H(7A)	3261	8302	7310	36
H(7B)	5185	8428	6931	36
H(8A)	2975	6780	6453	45
H(9A)	5282	7924	5486	55
H(9B)	4073	6986	5147	55
H(10A)	6688	9909	9163	37
H(10B)	7977	9107	9583	37
H(11A)	9258	10354	8236	38
H(12A)	10568	10072	9862	48
H(12B)	11472	10721	9089	48
H(13A)	6525	7788	9875	47
H(13B)	7030	6898	9239	47
H(13C)	5077	6988	9595	47
H(14A)	4247	8964	9472	46
H(14B)	2983	8282	8905	46
H(14C)	3923	9237	8494	46
H(18A)	-2447	4801	8815	60
H(18B)	-1144	4498	9569	60
H(18C)	-920	4006	8647	60

Table 3.13. Torsion angles [ $^{\circ}$ ] for 329B.

O(1)-C(1)-C(2)-C(3)	-131.8(2)
C(6)-C(1)-C(2)-C(3)	49.3(2)
C(1)-C(2)-C(3)-C(4)	-50.6(2)
C(2)-C(3)-C(4)-C(10)	-176.47(16)
C(2)-C(3)-C(4)-C(5)	56.5(2)
C(3)-C(4)-C(5)-C(13)	61.1(2)
C(10)-C(4)-C(5)-C(13)	-65.34(19)
C(3)-C(4)-C(5)-C(14)	-178.50(16)
C(10)-C(4)-C(5)-C(14)	55.1(2)
C(3)-C(4)-C(5)-C(6)	-58.25(19)
C(10)-C(4)-C(5)-C(6)	175.33(15)
O(1)-C(1)-C(6)-C(15)	10.0(3)
C(2)-C(1)-C(6)-C(15)	-171.04(16)
O(1)-C(1)-C(6)-C(7)	-107.4(2)
C(2)-C(1)-C(6)-C(7)	71.5(2)
O(1)-C(1)-C(6)-C(5)	129.8(2)
C(2)-C(1)-C(6)-C(5)	-51.3(2)
C(13)-C(5)-C(6)-C(15)	51.8(2)
C(14)-C(5)-C(6)-C(15)	-66.29(19)
C(4)-C(5)-C(6)-C(15)	172.88(15)
C(13)-C(5)-C(6)-C(1)	-67.01(19)
C(14)-C(5)-C(6)-C(1)	174.95(15)
C(4)-C(5)-C(6)-C(1)	54.11(19)
C(13)-C(5)-C(6)-C(7)	172.52(16)
C(14)-C(5)-C(6)-C(7)	54.5(2)
C(4)-C(5)-C(6)-C(7)	-66.35(19)
C(15)-C(6)-C(7)-C(8)	-60.0(2)
C(1)-C(6)-C(7)-C(8)	57.1(2)
C(5)-C(6)-C(7)-C(8)	178.55(17)
C(6)-C(7)-C(8)-C(9)	-122.2(2)
C(3)-C(4)-C(10)-C(11)	51.9(2)
C(5)-C(4)-C(10)-C(11)	178.48(15)
C(4)-C(10)-C(11)-C(12)	-135.9(2)
C(18)-O(2)-C(17)-O(3)	-3.1(3)
C(18)-O(2)-C(17)-C(16)	176.89(16)



## References

1. Butler, M. S., The role of natural product chemistry in drug discovery. *J. Nat. Prod.* **2004**, *67*, 2141-53.
2. All natural. *Nat. Chem. Biol.* **2007**, *3*, 351-51.
3. Berlinck, R. G. S., Review of natural product chemistry for drug discovery. *J. Nat. Prod.* **2012**, *75*, 1256-56.
4. Dias, D. A., et al., A historical overview of natural products in drug discovery. *Metabolites* **2012**, *2*, 303-36.
5. Ciochina, R., Studies toward synthesis of polycyclic polyprenylated acylphloroglucinols **2006**.
6. Bart, H.-J. ö. r., Extraction of natural products from plants – an introduction. **2011**.
7. Ciochina, R.; Grossman, R. B., Polycyclic polyprenylated acylphloroglucinols. *Chem. Rev.* **2006**, *106*, 3963-86.
8. Alavijeh, M. S., et al., Drug metabolism and pharmacokinetics, the blood-brain barrier, and central nervous system drug discovery. *NeuroRx* **2005**, *2*, 554-71.
9. Crystal, G. J.; Salem, M. R., The bainbridge and the “reverse” bainbridge reflexes: History, physiology, and clinical relevance. *Anesthesia & Analgesia* **2012**, *114*, 520-32.
10. Chakravarti, R. N., Stories and history of finalization of structure of strychnine: *J. Inst. Chem. (India)* **1994**, *66*, 121-66.
11. Kingston, D. G. I., Recent advances in the chemistry of taxol. *J. Nat. Prod.* **2000**, *63*, 726-34.
12. Patridge, E., et al., An analysis of fda-approved drugs: Natural products and their derivatives. *Drug Discovery Today* **2016**, *21*, 204-07.
13. Newman, D. J.; Cragg, G. M., Natural products as sources of new drugs from 1981 to 2014. *J. Nat. Prod.* **2016**.
14. Zhao, J., et al., Recent advances regarding constituents and bioactivities of plants from the genus hypericum. *Chemistry & Biodiversity* **2015**, *12*, 309-49.
15. Marti, G., et al., Antiplasmodial benzophenone derivatives from the root barks of symphonia globulifera (clusiaceae). *Phytochemistry (Elsevier)* **2010**, *71*, 964-74.
16. Gustafson, K. R., et al., The guttiferones, hiv-inhibitory benzophenones from symphonia globulifera, garcinia livingstonei, garcinia ovalifolia and clusia rosea. *Tetrahedron* **1992**, *48*, 10093-102.
17. Mennini, T.; Gobbi, M., The antidepressant mechanism of hypericum perforatum. *Life Sciences* **2004**, *75*, 1021-27.

18. Salatino, A., et al., *Evidence-Based Complement. Alternat. Med.* **2005**, *2*, 33.
19. Bankova, V. S., et al., *Apidologie* **2000**, *31*, 3.
20. Diaz-Carballo, D., et al., The contribution of plukenetione a to the anti-tumoral activity of cuban propolis. *Bioorg. Med. Chem.* **2008**, *16*, 9635-43.
21. Naito, Y., et al., Antiinflammatory effect of topically applied propolis extract in carrageenan-induced rat hind paw edema. *Phytotherapy Research* **2007**, *21*, 452-56.
22. de Castro Ishida, V. F., et al., A new type of brazilian propolis: Prenylated benzophenones in propolis from amazon and effects against cariogenic bacteria. *Food Chemistry* **2011**, *125*, 966-72.
23. Patel, M., et al., Anxiolytic activity of aqueous extract of garcinia indica in mice. *International Journal of Green Pharmacy* **2013**, *7*, 332.
24. Zhang, J.-J., et al., 1,9-seco-bicyclic polyprenylated acylphloroglucinols from hypericum uralum. *J. Nat. Prod.* **2015**, *78*, 3075-79.
25. Yang, X.-W., et al., Skeleton reassignment of type c polycyclic polyprenylated acylphloroglucinols. *J. Nat. Prod.* **2016**.
26. Kuramochi, A., et al., Total synthesis of ( $\pm$ )-garsubellin a. *J. Am. Chem. Soc.* **2005**, *127*, 14200-01.
27. Xu, J., et al., Neurotrophic natural products: Chemistry and biology. *Angew. Chem. Int. Ed.* **2014**, *53*, 956-87.
28. Wanka, L., et al., The lipophilic bullet hits the targets: Medicinal chemistry of adamantane derivatives. *Chem. Rev.* **2013**, *113*, 3516-604.
29. Fan, Y.-M., et al., Two unusual polycyclic polyprenylated acylphloroglucinols, including a pair of enantiomers from garcinia multiflora. *Org. Lett.* **2015**, *17*, 2066-69.
30. Pedraza-Chaverri, J., et al., Medicinal properties of mangosteen (garcinia mangostana). *Food and Chemical Toxicology* **2008**, *46*, 3227-39.
31. Murakami, M., Über die konstitution des mangostins. *Justus Liebigs Annalen der Chemie* **1932**, *496*, 122-51.
32. Rao, B. S., 176. Morellin, a constituent of the seeds of garcinia morella. *Journal of the Chemical Society (Resumed)* **1937**, 853-55.
33. Kartha, G., et al., The constitution of morellin. *Tetrahedron Lett.* **1963**, *4*, 459-72.
34. Karanjgoakar, C. G., et al., The constitution of xanthochymol and isoxanthochymol. *Tetrahedron Lett.* **1973**, *14*, 4977-80.
35. Dreyer, D. L., Xanthochymol from clusia rosea (guttiferae). *Phytochemistry* **1974**, *13*, 2883-84.
36. Blount, J., Revised structure by xanthochymol. *Tetrahedron Lett.* **1976**, *17*, 2921-24.

37. Piccinelli, A. L., et al., Structural revision of clusianone and 7-epi-clusianone and anti-hiv activity of polyisoprenylated benzophenones. *Tetrahedron* **2005**, *61*, 8206-11.
38. Monache, F. D., et al., Prenylated benzophenones from clusia sandiense. *Phytochemistry* **1991**, *30*, 2003-05.
39. de Oliveira, C. M. A., et al., *Tetrahedron Lett.* **1996**, *37*, 6427.
40. dos Santos, M. H., et al., Complete assignment of the <sup>1</sup>h and <sup>13</sup>c nmr spectra of the tetraisoprenylated benzophenone 15-epiclusianone. *Magn. Reson. Chem.* **2001**, *39*, 155-59.
41. Winkelmann, K., et al., New phloroglucinol derivatives from hypericum papuanum. *J. Nat. Prod.* **2000**, *63*, 104-8.
42. Heilmann, J., et al., Studies on the antioxidative activity of phloroglucinol derivatives isolated from hypericum species. *Planta. Med.* **2003**, *69*, 202-6.
43. Ioset, J. R., et al., Antifungal xanthenes from roots of marila laxiflora. *Pharmaceutical Biology* **1998**, *36*, 103-06.
44. Bokesch, H. R., et al., *J. Nat. Prod.* **1999**, *62*, 1197.
45. Grossman, R. B.; Jacobs, H., On the structures of plukenetiones b, d, and e and their relationships to other polycyclic polyprenylated acylphloroglucinols. *Tetrahedron Lett.* **2000**, *41*, 5165-69.
46. Cuesta-Rubio, O., et al., *J. Nat. Prod.* **1999**, *62*, 1013.
47. Cuesta-Rubio, O., et al., *J. Nat. Prod.* **2001**, *64*, 973.
48. Herath, K., et al., *J. Nat. Prod.* **2005**, *68*, 617.
49. Wu, S.-B., et al., Structural diversity and bioactivities of natural benzophenones. *J. Nat. Prod.* **2014**, *31*, 1158-74.
50. Trost, B. M.; Debieu, L., Palladium-catalyzed trimethylenemethane cycloaddition of olefins activated by the sigma-electron-withdrawing trifluoromethyl group. *J. Am. Chem. Soc.* **2015**, *137*, 11606-9.
51. Winkelmann, K., et al., *J. Nat. Prod.* **2001**, *64*, 701.
52. Jambou, R., et al., Resistance of plasmodium falciparum field isolates to in-vitro artemether and point mutations of the serca-type pfatpase6. *The Lancet* *366*, 1960-63.
53. Jayasekara, S. Progress towards the synthesis of type b polycyclic polyprenylated acylphloroglucinols. 2010.
54. Zhou, Y., et al., Qualitative and quantitative analysis of polycyclic polyprenylated acylphloroglucinols from garcinia species using ultra performance liquid chromatography coupled with electrospray ionization quadrupole time-of-flight tandem mass spectrometry. *Anal. Chim. Acta* **2010**, *678*, 96-107.

55. Xia, Z.-X., et al., Bioassay-guided isolation of prenylated xanthenes and polycyclic acylphloroglucinols from the leaves of *garcinia nuijiangensis*. *J. Nat. Prod.* **2012**, *75*, 1459-64.
56. Xu, G., et al., Cytotoxic acylphloroglucinol derivatives from the twigs of *garcinia cowa*. *J. Nat. Prod.* **2010**, *73*, 104-08.
57. Hernandez, I. M., et al., *J. Nat. Prod.* **2005**, *68*, 931.
58. Cottet, K., et al., Polycyclic polyprenylated xanthenes from *symphonia globulifera*: Isolation and biomimetic electrosynthesis. *J. Nat. Prod.* **2015**, *78*, 2136-40.
59. Li, D. Y., et al., Two new adamantyl-like polyprenylated acylphloroglucinols from *hypericum attenuatum choisy*. *Tetrahedron Lett.* **2015**, *56*, 1953-55.
60. Li, D., et al., Hyperatennins a-i, bioactive polyprenylated acylphloroglucinols from *hypericum attenuatum choisy*. *RSC Adv.* **2015**, *5*, 5277-87.
61. Albernaz, L. C., et al., Spiranthenones a and b, tetraprenylated phloroglucinol derivatives from the leaves of *spiranthera odoratissima*. *Planta. Med.* **2012**, *78*, 459-64.
62. Carroll, A. R., et al., Guttiferones o and p, prenylated benzophenone mapkapk-2 inhibitors from *garcinia solomonensis*. *J. Nat. Prod.* **2009**, *72*, 1699-701.
63. Marti, G., et al., Antiplasmodial benzophenones from the trunk latex of *moronobea coccinea* (clusiaceae). *Phytochemistry (Elsevier)* **2009**, *70*, 75-85.
64. Baggett, S., et al., *J. Nat. Prod.* **2005**, *68*, 354.
65. Lyles, J. T., et al., In vitro antiplasmodial activity of benzophenones and xanthenes from edible fruits of *garcinia* species. *Planta. Med.* **2014**, *80*, 676-81.
66. Marti, G., et al., Antiplasmodial benzophenone derivatives from the root barks of *symphonia globulifera* (clusiaceae). *Phytochemistry* **2010**, *71*, 964-74.
67. Fu, W., et al., Prenylated benzoylphloroglucinols and biphenyl derivatives from the leaves of *garcinia multiflora champ.* *RSC Advances* **2015**, *5*, 78259-67.
68. Hartati, S., et al., A novel polyisoprenyl benzophenone derivative from *garcinia eugeniaefolia*. *J. Asian. Nat. Pro. Res.* **2008**, *10*, 509-13.
69. Gao, X.-M., et al., Novel polyisoprenylated benzophenone derivatives from *garcinia paucinervis*. *Tetrahedron Lett.* **2010**, *51*, 2442-46.
70. Xiao, Z. Y., et al., Polyisoprenylated benzoylphloroglucinol derivatives from *hypericum sampsonii*. *J. Nat. Prod.* **2007**, *70*, 1779-82.
71. Marti, G., et al., Antiplasmodial benzophenones from the trunk latex of *moronobea coccinea* (clusiaceae). *Phytochemistry* **2009**, *70*, 75-85.
72. Carne, B., et al., Unexpected trend in chemosensitivity of *plasmodium falciparum* in brazzaville, congo. *The Lancet* **1991**, *338*, 582-83.

73. Sang, S., et al., Chemical studies on antioxidant mechanism of garcinol: Analysis of radical reaction products of garcinol and their antitumor activities. *Tetrahedron* **2001**, *57*, 9931-38.
74. Matsumoto, K., et al., Cytotoxic benzophenone derivatives from *Garcinia* species display a strong apoptosis-inducing effect against human leukemia cell lines. *Biological and Pharmaceutical Bulletin* **2003**, *26*, 569-71.
75. Sarli, V.; Giannis, A., Selective inhibition of cbp/p300 hat. *Chemistry & Biology* **2007**, *14*, 605-06.
76. Tian, Z., et al., Cambogin is preferentially cytotoxic to cells expressing pdgfr. *PLOS ONE* **2011**, *6*, e21370.
77. Stark, T. D., et al., Antioxidative compounds from *Garcinia buchananii* stem bark. *J. Nat. Prod.* **2015**, *78*, 234-40.
78. Tchakam, P. D., et al., Antimicrobial and antioxidant activities of the extracts and compounds from the leaves of *Psorospermum aurantiacum* Engl. and *Hypericum lanceolatum* Lam. *BMC Complementary and Alternative Medicine* **2012**, *12*, 136.
79. Wang, M., et al., Amelioration of experimental autoimmune encephalomyelitis by isogarcinol extracted from *Garcinia mangostana* L. Mangosteen. *J. Agri. Food Chem.* **2016**, *64*, 9012-21.
80. Rouger, C., et al., Prenylated polyphenols from Clusiaceae and Calophyllaceae with immunomodulatory activity on endothelial cells. *PLOS ONE* **2016**, *11*, e0167361.
81. Masullo, M., et al., Direct interaction of garcinol and related polyisoprenylated benzophenones of *Garcinia cambogia* fruits with the transcription factor stat-1 as a likely mechanism of their inhibitory effect on cytokine signaling pathways. *J. Nat. Prod.* **2014**, *77*, 543-49.
82. Monzote, L., et al., Role of mitochondria in the leishmanicidal effects and toxicity of acyl phloroglucinol derivatives: Nemorosone and guttiferone A. *Parasitology* **2015**, *142*, 1239-48.
83. Fromentin, Y., et al., Synthesis of novel guttiferone A derivatives: In-vitro evaluation toward *Plasmodium falciparum*, *Trypanosoma brucei* and *Leishmania donovani*. *Eur. J. Med. Chem.* **2013**, *65*, 284-94.
84. Li, X., et al., The natural compound guttiferone F sensitizes prostate cancer to starvation induced apoptosis via calcium and JNK elevation. *BMC Cancer* **2015**, *15*, 1-24.
85. Nunez-Figueroa, Y., et al., Neuroprotective action and free radical scavenging activity of guttiferone-A, a naturally occurring prenylated benzophenone. *Arzneim. Forsch.* **2012**, *62*, 583-89.

86. Kolodziejczyk, J., et al., Effects of garcinol and guttiferone k isolated from *Garcinia cambogia* on oxidative/nitrative modifications in blood platelets and plasma. *Platelets* **2009**, *20*, 487-92.
87. Duan, Y.-h., et al., *Chemical and Pharmaceutical Bulletin* **2011**, *59*, 231-34.
88. Wu, S. B., et al., Structural diversity and bioactivities of natural benzophenones. *Natural Product Reports* **2014**, *31*, 1158-74.
89. Sales, L., et al., Anticancer activity of 7-epiclusianone, a benzophenone from *Garcinia brasiliensis*, in glioblastoma. *Bmc Complementary and Alternative Medicine* **2015**, *15*, 8.
90. Ionta, M., et al., 7-epiclusianone, a benzophenone extracted from *Garcinia brasiliensis* (Clusiaceae), induces cell cycle arrest in G1/S transition in A549 cells. *Molecules (Basel, Switzerland)* **2015**, *20*, 12804-16.
91. Santa-Cecilia, F. V., et al., 7-epiclusianone, the natural prenylated benzophenone, inhibits superoxide anions in the neutrophil respiratory burst. *J. Med. Food* **2012**, *15*, 200-05.
92. Murata, R. M., et al., Inhibitory effects of 7-epiclusianone on glucan synthesis, acidogenicity and biofilm formation by *Streptococcus mutans*. *FEMS Microbiol Lett.* **2008**, *282*, 174-81.
93. Coelho, L. P., et al., 7-epiclusianone, a tetraprenylated benzophenone, relaxes airway smooth muscle through activation of the nitric oxide-cGMP pathway. *Journal of Pharmacology and Experimental Therapeutics* **2008**, *327*, 206-14.
94. Almeida, L. S. B., et al., Antimicrobial activity of *Rheedia brasiliensis* and 7-epiclusianone against *Streptococcus mutans*. *Phytomedicine* **2008**, *15*, 886-91.
95. Neves, J. S., et al., Antianaphylactic properties of 7-epiclusianone, a tetraprenylated benzophenone isolated from *Garcinia brasiliensis*. *Planta. Med.* **2007**, *73*, 644-49.
96. Ionta, M., et al., 7-epiclusianone, a benzophenone extracted from *Garcinia brasiliensis* (Clusiaceae), induces cell cycle arrest in G1/S transition in A549 cells. *Molecules* **2015**, *20*, 12804.
97. Pereira, I. O., et al., Leishmanicidal activity of benzophenones and extracts from *Garcinia brasiliensis* Mart. fruits. *Phytomedicine* **2010**, *17*, 339-45.
98. Cruz, A. J., et al., Vascular effects of 7-epiclusianone, a prenylated benzophenone from *Rheedia gardneriana*, on the rat aorta. *Phytomedicine* **2006**, *13*, 442-45.
99. Lankford, T., et al., Analysis of state obesity legislation from 2001 to 2010. *J. Public Health Manag. Pract.* **2013**, *19*, S114-S18.
100. Moreira, M. E. d. C., et al., Bacupari peel extracts (*Garcinia brasiliensis*) reduce high-fat diet-induced obesity in rats. *Journal of Functional Foods* **2017**, *29*, 143-53.

101. Reis, F. H. Z., et al., Clusianone, a naturally occurring nemorosone regioisomer, uncouples rat liver mitochondria and induces hepg2 cell death. *Chem.-Biol. Interact.* **2014**, *212*, 20-29.
102. Zhang, L.-J., et al., Cytotoxic polyisoprenyl benzophenonoids from *Garcinia subelliptica*. *J. Nat. Prod.* **2010**, *73*, 557-62.
103. Jantan, I.; Saputri, F. C., Benzophenones and xanthenes from *Garcinia cantleyana* var. *Cantleyana* and their inhibitory activities on human low-density lipoprotein oxidation and platelet aggregation. *Phytochemistry* **2012**, *80*, 58-63.
104. Roux, D., et al., *J. Nat. Prod.* **2000**, *63*, 1070.
105. Fromentin, Y., et al., *Symphonia globulifera*, a widespread source of complex metabolites with potent biological activities. *Planta. Med.* **2015**, *81*, 95-107.
106. Lokvam, J., et al., *Phytochemistry* **2000**, *55*, 29.
107. Inuma, M., et al., Antibacterial activity of some *Garcinia* benzophenone derivatives against methicillin-resistant *Staphylococcus aureus*. *Biological & Pharmaceutical Bulletin* **1996**, *19*, 311-14.
108. Mulzer, J., Trying to rationalize total synthesis. *J. Nat. Prod.* **2014**, *31*, 595-603.
109. Lindermayr, K.; Plietker, B., The bidirectional total synthesis of sampsonione p and hyperibone i. *Angew. Chem. Int. Ed.* **2013**, *52*, 12183-86.
110. Nicolaou, K. C., et al., Synthesis of the fully functionalized bicyclic core of garsubellin a. *J. Am. Chem. Soc.* **1999**, *121*, 4724-25.
111. Siegel, D. R.; Danishefsky, S. J., *J. Am. Chem. Soc.* **2006**, *128*, 1048.
112. Tsukano, C., et al., Differentiation of nonconventional "carbanions"-the total synthesis of nemorosone and clusianone. *Angew. Chem. Int. Ed.* **2007**, *46*, 8840-44.
113. Shimizu, Y., et al., Catalytic asymmetric total synthesis of ent-hyperforin. *Angew. Chem. Int. Ed.* **2010**, *49*, 1103-06.
114. Richard, J. A., et al., The chemistry of the polycyclic polyprenylated acylphloroglucinols. *Angew. Chem. Int. Ed.* **2012**, *51*, 4536-61.
115. Ting, C. P.; Maimone, T. J., Total synthesis of hyperforin. *J. Am. Chem. Soc.* **2015**, *137*, 10516-19.
116. Sparling, B. A., et al., Enantioselective total synthesis of hyperforin. *J. Am. Chem. Soc.* **2013**, *135*.
117. Biber, N., et al., The total synthesis of hyperpapuanone, hyperibone l, epclusianone and oblongifolin a. *Nat. Chem.* **2011**, *3*, 938-42.
118. Jayasekara, S.; Grossman, R. B. In *Progress towards the total synthesis of 7-epi-clusianone* 2010 American Chemical Society; pp ORGN-446.

119. Bhat, B. A., et al., Annulation reactions of allenyl esters: An approach to bicyclic diones and medium-sized rings. *J. Org. Chem.* **2014**, *79*, 9402-07.
120. Schmitt, S., et al., A metathesis–acylation approach to the bicyclic core of polycyclic poly-prenylated acylphloroglucinols. *Synlett.* **2014**, *25*, 2025-29.
121. Boyce, J. H., et al., Syntheses of (+)-30-epi-, (–)-6-epi-, (±)-6,30-epi-13,14-didehydroxyisogarcinol and (±)-6,30-epi-garcimultiflorone a utilizing highly diastereoselective, lewis acid-controlled cyclizations. *J. Am. Chem. Soc.* **2016**, *138*, 14789-97.
122. Qi, J., et al., Catalytic enantioselective alkylative dearomatization-annulation: Total synthesis and absolute configuration assignment of hyperibone k. *J. Am. Chem. Soc.* **2010**, *132*, 13642-44.
123. Qi, J.; Porco, J. A., Rapid access to polyprenylated phloroglucinols via alkylative dearomatization–annulation: Total synthesis of (±)-clusianone1. *J. Am. Chem. Soc.* **2007**, *129*, 12682-83.
124. Zhang, Q.; Porco, J. A. In *Development of a unified synthetic strategy to the polyprenylated acylphloroglucinols* 2010 American Chemical Society; pp ORGN-39.
125. Boyce, J. H., et al., Syntheses of (+)-30-epi-, (–)-6-epi-, (±)-6,30-epi-13,14-didehydroxyisogarcinol and (±)-6,30-epi-garcimultiflorone a utilizing highly diastereoselective, lewis acid-controlled cyclizations. *J. Am. Chem. Soc.* **2016**.
126. Garnsey, M. R., et al., Development of a strategy for the asymmetric synthesis of polycyclic polyprenylated acylphloroglucinols via n-amino cyclic carbamate hydrazones: Application to the total synthesis of (+)-clusianone. *Org. Lett.* **2010**, *12*, 5234-37.
127. Bellavance, G.; Barriault, L., Total syntheses of hyperforin and papuaforins a-c, and formal synthesis of nemorosone through a gold(i)-catalyzed carbocyclization. *Angew. Chem. Int. Ed.* **2014**, *53*, 6701-04.
128. Huang, H., et al., Recent advances in the gold-catalyzed additions to c–c multiple bonds. *Beilstein Journal of Organic Chemistry* **2011**, *7*, 897-936.
129. Kaldas, S. J., et al., Indole functionalization via photoredox gold catalysis. *Org. Lett.* **2015**, *17*, 2864-66.
130. McGee, P., et al., Synthesis and isolation of organogold complexes through a controlled 1,2-silyl migration. *Chem. Eur. J.* **2015**, *21*, 9662-65.
131. McCallum, T., et al., Light-mediated deoxygenation of alcohols with a dimeric gold catalyst. *Eur. J. Org. Chem.* **2015**, *2015*, 81-85.
132. Grise, C. M.; Barriault, L., Gold-catalyzed synthesis of substituted tetrahydronaphthalenes. *Org. Lett.* **2007**, *8*, 5905-08.



133. Poulin, J., et al., Pericyclic domino reactions: Concise approaches to natural carbocyclic frameworks. *Chem. Soc. Rev.* **2009**, *38*, 3092-101.
134. Hayes, C. J.; Simpkins, N. S., Bridgehead enolate or bridgehead organolithium? Dft calculations provide insights into a difficult bridgehead substitution reaction in the synthesis of the polycyclic polyprenylated acylphloroglucinol (ppap) nemorosone. *Org. Biomol. Chem.* **2013**, *11*, 8458-62.
135. Simpkins, N. S., et al., Synthesis of nemorosone via a difficult bridgehead substitution reaction. *Synlett* **2010**, 639-43.
136. Simpkins, N. S., Adventures in bridgehead substitution chemistry: Synthesis of polycyclic polyprenylated acylphloroglucinols (ppaps). *Chem. Comm.* **2013**, *49*, 1042-51.
137. Plietker, B., A highly regioselective salt-free iron-catalyzed allylic alkylation. *Angew. Chem. Int. Ed* **2006**, *45*, 1469-73.
138. Matsuhisa, M., et al., *J. Nat. Prod.* **2002**, *65*, 290.
139. Horeischi, F., et al., The total syntheses of guttiferone a and 6-epi-guttiferone a. *J. Am. Chem. Soc.* **2014**, *136*, 4026-30.
140. Socolsky, C.; Plietker, B., Total synthesis and absolute configuration assignment of mrsa active garcinol and isogarcinol. *Chem. Eur. J.* **2015**, *21*, 3053-61.
141. Ciochina, R.; Grossman, R. B., A new synthetic approach to the polycyclic polyprenylated acylphloroglucinols. *Org. Lett.* **2003**, *5*, 4619-21.
142. Richard, J.-A., Chemistry and biology of the polycyclic polyprenylated acylphloroglucinol hyperforin. *Eur. J. Org. Chem.* **2014**, *2014*, 273-99.
143. Chrea, B., et al., Nature's antidepressant for mild to moderate depression: Isolation and spectral characterization of hyperforin from a standardized extract of st. John's wort (*hypericum perforatum*). *J. Chem. Ed.* **2014**, *91*, 440-42.
144. Zhang, Q.; Porco, J. A., Total synthesis of ( $\pm$ )-7-epi-nemorosone. *Org. Lett.* **2012**, *14*, 1796-99.
145. Alves, T. M., et al., Biological activities of 7-epiclusianone. *J. Nat. Prod.* **1999**, *62*, 369-71.
146. Neves, J. S., et al., Antianaphylactic properties of 7-epiclusianone, a tetraprenylated benzophenone isolated from *garcinia brasiliensis*. *Planta. Med.* **2007**, *73*, 644-49.
147. Meng, J., et al., Samarium diiodide mediated intramolecular cyclisation of mixed enone-enoate systems: A simple preparation of spirocyclic ethers. *Tetrahedron Lett* **2011**, *52*, 928-31.
148. Varseev, G. N.; Maier, M. E., Formal total synthesis of platencin. *Angew. Chem. Int. Ed.* **2009**, *48*, 3685-88.

149. Laval, G., et al., A short and efficient enantiospecific synthesis of (+)-(2r,6s)-cis- $\gamma$ -irone via a highly diastereoselective protonation. *J. Org. Chem.* **2000**, *65*, 3551-54.
150. Childs, M. E.; Weber, W. P., Preparation of cyanofornates. Crown ether phase transfer catalysis. *J. Org. Chem.* **1976**, *41*, 3486-87.
151. Magatti, C. V., et al., Total synthesis of dehydroambliol-a and its unnatural z isomer. *J. Org. Chem.* **1991**, *56*, 3102-08.
152. Nystrom, R. F.; Brown, W. G., Reduction of organic compounds by lithium aluminum hydride. I. Aldehydes, ketones, esters, acid chlorides and acid anhydrides. *J. Am. Chem. Soc.* **1947**, *69*, 1197-99.
153. Dess, D. B.; Martin, J. C., Readily accessible 12-i-5 oxidant for the conversion of primary and secondary alcohols to aldehydes and ketones. *J. Org. Chem.* **1983**, *48*, 4155-56.
154. Habrant, D., et al., Conversion of carbonyl compounds to alkynes: General overview and recent developments. *Chem. Soc. Rev.* **2010**, *39*, 2007-17.
155. Colvin, E. W.; Hamill, B. J., A simple procedure for the elaboration of carbonyl compounds into homologous alkynes. *J. Chem. Soc., Perkin Tran. 1* **1977**, 869-74.
156. Köster, F., et al., Electrochemical selective incorporation of co<sub>2</sub> into terminal alkynes and diynes. *Eur. J. Org. Chem.* **2001**, *2001*, 2507-11.
157. Marshall, J. A.; Yanik, M. M., *J. Org. Chem.* **2001**, *66*, 1373-79.
158. Li, K., et al., Construction of the basic skeleton of ophiobolin a and variecolin. *Organic & Biomolecular Chemistry* **2013**, *11*, 7550-58.
159. Crimmins, M. T.; DeLoach, J. A., Intramolecular photocycloaddition-cyclobutane fragmentation: A highly stereoselective total synthesis of (+-)-pentalenic acid. *J. Org. Chem.* **1984**, *49*, 2076-77.
160. Cochran, J. C., et al., Palladium(0) catalysis in hydrostannation of carbon-carbon triple bonds. *Tetrahedron Lett.* **1990**, *31*, 6621-24.
161. Trost, B. M., *Selectivity, strategy & efficiency in modern organic chemistry comprehensive organic synthesis*. 1991; Vol. 8.
162. Baran, P. S.; Zhong, Y.-L., Selective oxidation at carbon adjacent to aromatic systems with ibx. *J. Am. Chem. Soc.* **2001**, *123*, 3183-85.
163. Shibuya, M., et al., Oxidative rearrangement of cyclic tertiary allylic alcohols with ibx in dmsO. *Org. Lett.* **2004**, *6*, 4303-06.
164. Qian, H.; Widenhoefer, R. A., Mechanism of the palladium-catalyzed intramolecular hydroalkylation of 7-octene-2,4-dione. *J. Am. Chem. Soc.*, *125*, 2056-57.

165. Uetake, Y., et al., Enantioselective approach to polycyclic polyprenylated acylphloroglucinols via catalytic asymmetric intramolecular cyclopropanation. *J. Org. Chem.* **2015**, *80*, 1735-45.
166. Lipshutz, B. H., et al., Analyses of anionic cu(i) complexes via electrospray mass spectrometry. *J. Am. Chem. Soc.* **1996**, *118*, 6796-97.
167. Lipshutz, B. H.; Servesko, J. M., Cuh-catalyzed asymmetric conjugate reductions of acyclic enones. *Angew. Chem. Int. Ed.* **2003**, *115*, 4937-40.
168. Yamashita, M., et al., Selective reduction of alpha, beta unsaturated carbonyl compounds by sodium hydrotelluride. *Chem. Lett.* **1980**, *9*, 847-48.
169. Fortunato, J. M.; Ganem, B., Lithium and potassium trialkylborohydrides. Reagents for direct reduction of .Alpha.,.Beta.-unsaturated carbonyl compounds to synthetically versatile enolate anions. *J. Org. Chem.* **1976**, *41*, 2194-200.
170. Louis-Andre, O.; Gelbard, G., Exclusive 1-4 reduction of conjugated ketones by sodium dithionite. *Tetrahedron Lett.* **1985**, *26*, 831-32.
171. Hudlicky, T., et al., Selective reduction of  $\alpha,\beta$ -unsaturated esters in the presence of olefins. *Tetrahedron Lett.* **1987**, *28*, 5287-90.
172. Hudlisky, M., Reductions in organic chemistry. **1984**.
173. Zarecki, A.; Wicha, J., Magnesium in methanol selective reduction of a conjugate double bond in an  $\alpha,\beta$ -unsaturated ester related to pregnadiene. *Synthesis* **1996**, *1996*, 455-56.
174. Münchmeyer, C. J., et al., Epoxidation of olefins with molecular catalysts in ionic liquids. In *Topics in Organometallic Chemistry* 2015; Vol. 51, pp 185-236.
175. Porter, M. J., et al., Unusual oxidation behaviour of a propargylic alcohol. *Tetrahedron Lett.* **2004**, *45*, 6541-43.
176. Teiber, M.; Muller, T. J. J., Rapid consecutive three-component coupling-fiesselmann synthesis of luminescent 2,4-disubstituted thiophenes and oligothiophenes. *Chem. Comm.* **2012**, *48*, 2080-82.
177. Sneddon, H. F., et al., Double conjugate addition of dithiols to propargylic carbonyl systems to generate protected 1,3-dicarbonyl compounds. *J. Org. Chem.* **2006**, *71*, 2715-25.
178. Brown, D. J.; Waring, P., Simple pyrimidines. Xvi. A synthetic route to some 2-(pyrimidin-2'-yl)acetic acids and esters. *Aust. J. Chem.* **1977**, *30*, 621-27.
179. Rooke, D. A., et al., An analysis of the influences dictating regioselectivity in platinum-catalyzed hydrosilylations of internal alkynes. *Tetrahedron* **2014**, *70*, 4232-44.
180. Cheng, C.; Hartwig, J. F., Catalytic silylation of unactivated c-h bonds. *Chem. Rev.* **2015**, *115*, 8946-75.

181. Miller, Z. D., et al., Regiodivergent and stereoselective hydrosilylation of 1,3-disubstituted allenes. *Angew. Chem. Int. Ed.* **2015**, *54*, 9088-91.
182. Sumida, Y., et al., Palladium-catalyzed regio- and stereoselective hydrosilylation of electron-deficient alkynes. *Org. Lett.* **2012**, *14*, 1552-55.
183. Ojima, I., et al., Recent advances in the hydrosilylation and related reactions. In *Patai's chemistry of functional groups*, John Wiley & Sons, Ltd 2009.
184. Itami, K., et al., Metal-catalyzed hydrosilylation of alkenes and alkynes using dimethyl(pyridyl)silane. *J. Org. Chem.* **2002**, *67*, 2645-52.
185. Sun, J.; Deng, L., Cobalt complex-catalyzed hydrosilylation of alkenes and alkynes. *ACS Catalysis* **2016**, *6*, 290-300.
186. Kira, K., et al., Mechanistic studies on the hydrosilylation of an acetylene cobalt complex; trapping an active catalyst  $\text{Co}_2(\text{CO})_6$  causing olefin-isomerization and osilylation. *Tetrahedron* **2002**, *58*, 6485-92.
187. Jayasekara, S., Progress towards the synthesis of type b polycyclic polyprenylate. **2010**.

## Vita

### Shubhankar Dutta

#### Education

University of Kentucky, Lexington, KY	2017 August
Research Title: Towards the Total Synthesis of 7- <i>epi</i> -Clusianone	
Advisor: Dr. Robert B. Grossman	
University of Kalyani, West Bengal, India	2005 July
Master of Science, Organic Chemistry	
Krishnagar Govt. College, West Bengal, India	2003 June
Bachelor of Science (Hons), Chemistry	

#### Awards

Best Teaching Awards in Organic Chemistry	2015
---	------

#### Research Experience

Ph.D. candidate University of Kentucky	2009-present
Synthesized several intermediates to complete the total synthesis	
Transition metal catalyzed organic synthesis	
Purified several compounds by distillation, column chromatography, and crystallization	
Glove-Box and Schlenk techniques: handling sensitive reaction	
Low temperature reactions	
High pressure reactions	
GCMS, LCMS, NMR, IR techniques to elucidate structures of several key intermediates	
Chemdraw, Mestronova, ACD-lab, <i>i</i> -NMR (NMR processing tool), MS office	
Co-op intern in GlaxoSmithKline, PA, USA	July 2016-Jun 2017

#### Leadership and Mentorship

University of Kentucky, Chemistry Department	
Teaching assistant organic chemistry laboratory	Fall 2009-Fall 2015
Super Teaching Assistant organic chemistry laboratory	Spring & Fall 2105
NMR Manager	Jan 2016-Jun 2016
CHO (Chief Hygiene officer) of CP325	fall 2011-Jun 2016
Trained undergraduate and graduate students	

### **Selected Presentation and Publications**

“Progress Toward the Total Synthesis of 7-epi-Clusianone.” 50, NOS 2015, College Park, MD.

“Progress Toward the Total Synthesis of 7-epi-Clusianone.” Natural Product Symposium 2015, College of Pharmacy, University of Kentucky, Lexington, KY.

“Progress Toward the Total Synthesis of 7-epi-clusianone.” Naff Symposium 2014, University of Kentucky, Lexington, KY.

“Progress Toward the Total Synthesis of 7-epi-Clusianone.” 247 ACS National Meeting & Exposition 2014, Dallas, TX, ORG-475.

“Progress Toward the Total Synthesis of 7-epi-Clusianone.” Naff Symposium 2013, University of Kentucky, Lexington, KY.

“An Approach Toward the Total Synthesis of 7-epi-Clusianone, a Type B endo Polyprenylated Acylphloroglucinols.” The manuscript is under preparation.

### **Professional Membership**

Member of the American Chemical Society 2011-present

Member of the American Chemical Society of organic division 2011-present